



---

**Forschungszentrum Karlsruhe**  
in der Helmholtz-Gemeinschaft

---

**Wissenschaftliche Berichte**  
FZKA 6748

# **Plutonium Biokinetics in Human Body**

**A. Luciani**

Hauptabteilung Sicherheit

Oktober 2002



**Forschungszentrum Karlsruhe**

in der Helmholtz-Gemeinschaft

Wissenschaftliche Berichte

FZKA 6748

**PLUTONIUM BIOKINETICS IN HUMAN BODY**

Andrea Luciani

Hauptabteilung Sicherheit

Von der Fakultät für Elektrotechnik und Informationstechnik  
der Universität Fridericiana Karlsruhe genehmigte Dissertation

Forschungszentrum Karlsruhe GmbH, Karlsruhe  
2002

Für diesen Bericht behalten wir uns alle Rechte vor

Forschungszentrum Karlsruhe GmbH  
Postfach 3640, 76021 Karlsruhe

Mitglied der Hermann von Helmholtz-Gemeinschaft  
Deutscher Forschungszentren (HGF)

ISSN 0947-8620

# **PLUTONIUM BIOKINETICS IN HUMAN BODY**

Zur Erlangung des akademischen Grades eines  
Doktor-Ingenieurs

bei der Fakultät für Elektrotechnik und Informationstechnik  
der Universität Fridericiana Karlsruhe

vorgelegte  
DISSERTATION  
von  
Andrea Luciani  
aus Ferrara (Italien)

Tag der mündlichen Prüfung: 14. Mai 2002

Hauptreferent: Prof. Dr. Olaf Doessel  
Korreferenten: Dr. Hans-Richard Doerfel und Prof. Scott Miller



The biokinetic model presented by the International Commission on Radiological Protection (ICRP) in the Publication 67 represents one of the basic tools for evaluating the risk following an exposure to an internal contamination from Plutonium. However it is characterized by some assumptions that have no clear physiological explanation, but that were introduced to have a closer fit to the available data from studies on humans, particularly in relation to the urinary excretion at long time after exposure. Such assumptions are not only a correction of model's prediction of Plutonium urinary excretion, but it was shown that they are the leading process in determining the urinary excretion after already 100 days post intake. Yet, even with such corrections, this biokinetic model still shows difficulties in describing the metabolism of Plutonium in human body.

In recent years, as data relating to the urinary excretion of Plutonium at long time after exposure become more and more available, an enhancement of the urinary excretion long after intake was observed in some contaminated subjects. The application of the original model on these actual cases would result in a significant overestimation of the dose, with important consequences not only from a scientific, but even from a legal point of view.

Owing to these considerations the biokinetic model from ICRP was further developed. Particular attention was paid to the predictions of the urinary excretion, because this is the most common and feasible technique for monitoring the risk after an internal contamination of Plutonium. The ICRP model was modified on the basis of the available data from studies of Plutonium metabolism in humans in order to get accurate predictions of the urinary excretion without the ICRP assumptions that can't be physiologically supported. The optimized model obtained from this analysis predicts also values for the fecal excretion and blood retention of Plutonium that agree better to the available data than ICRP model does.

Dose coefficients and analytical expressions that approximate the urinary excretion of Plutonium predicted by the optimized model were calculated in order to allow an easy implementation of the model into the monitoring routine of radiation protection.

Furthermore a sensitivity analysis was carried out with respect to the transfer rates of the model in order to point out the most significant parameters in determining the urinary excretion of Plutonium and, to a smaller extent, the fecal excretion and the blood retention.

On the basis of the results of the sensitivity analysis an uncertainty analysis was also carried out to evaluate the range of variation of the model transfer rates that would reproduce the variability of the urinary excretion observed in humans. It is therefore possible to have an indication about the possible values of the transfer rates that can be assumed for a specific subject of the population.

The optimized model was finally used to describe the urinary excretion of an actual case of contamination. This subject is today one of the most known and studied worldwide because a great number of data are available since his contamination in 1983. Furthermore he represents one the most significant examples of enhancement of the urinary excretion of Plutonium at long time after exposure.

In occasion of the present work a complete set of measurements was carried out in the Forschungszentrum Karlsruhe in order to assess the urinary and fecal excretion and blood retention of Plutonium at the present time. Whole body counter and alpha-spectrometry techniques were adopted for performing *in vivo* and *in vitro* measurements on organs and bioassay samples, respectively. The measurements have confirmed the enhancement of Plutonium urinary excretion observed in occasion of previous investigations of the same subject. The application of the information about the possible inter-subjectual variation of the

model transfer rates obtained from the uncertainty analysis has allowed describing the Plutonium metabolism in this subject by means of the optimized model. Particularly the enhancement of the urinary excretion was modelled by assuming subject-specific transfer rates with values in the calculated range of variation for a population of healthy subjects.



Das von der Internationalen Strahlenschutzkommission (ICRP) in Publikation 67 vorgestellte biokinetische Modell bildet eine wesentliche Grundlage für die Abschätzung des Risikos durch Inkorporationen von Plutonium. Allerdings wird das Modell von einigen Hilfsannahmen geprägt, die keinen physiologischen Hintergrund haben, sondern die nur eingeführt wurden, um eine bessere Übereinstimmung mit der Beobachtung zu erzielen, insbesondere in Hinblick auf die langfristige Aktivitätsausscheidung im Urin. In der vorliegenden Arbeit wird gezeigt, dass die Hilfsannahmen nicht nur eine Korrektur des Modells darstellen, sondern dass sie von zentraler Bedeutung für die Aktivitätsausscheidung im Urin sind. So wird die Ausscheidungsrate bereits 100 Tage nach der Aktivitätszufuhr nahezu ausschließlich von den Hilfsannahmen bestimmt. Allerdings werden dadurch die generellen Schwierigkeiten bei der Modellierung des Stoffwechsels von Plutonium im Menschen nicht behoben.

In jüngster Zeit sind in vermehrten Maße Messdaten der langfristigen Aktivitätsausscheidung von Plutonium im Urin verfügbar geworden, die auf eine Erhöhung der Ausscheidungsrate bei länger zurückliegenden Expositionen hinweisen. Die Anwendung des ICRP Modells in der ursprünglichen Form würde in diesen Fällen zu einer signifikanten Überschätzung der Dosis mit möglicherweise erheblichen beruflichen und rechtlichen Konsequenzen führen.

Aufgrund dieser Überlegungen wurde das ICRP Modell im Rahmen der vorliegenden Arbeit weiterentwickelt. Besonderes Augenmerk wurde dabei auf die Aktivitätsausscheidung im Urin gelegt, weil sie die Grundlage für die Inkorporationsüberwachung auf Plutonium bildet. Auf der Basis der verfügbaren Studien des Metabolismus von Plutonium wurde das Modell so modifiziert, dass die auf die von der ICRP eingeführten Hilfsannahmen ohne physiologischen Hintergrund nicht mehr erforderlich sind, um eine hinreichend genaue Vorhersage der Ausscheidungsrate im Urin zu erzielen. Mit dem derart optimierten Modell kann auch die Aktivitätsausscheidung im Stuhl sowie die Aktivitätskonzentration im Blut besser modelliert werden als mit dem ursprünglichen ICRP Modell.

Zur Vereinfachung der Implementierung des optimierten Modells in die routinemäßige Inkorporationsüberwachung wurden im Rahmen der vorliegenden Arbeit die Dosiskoeffizienten und die Funktionen zur Beschreibung der Aktivitätsausscheidung im Urin berechnet. Außerdem wurde eine Empfindlichkeitsanalyse durchgeführt, um diejenigen Modellparameter zu identifizieren, die den größten Einfluss auf die Urinausscheidungsrate sowie auf die Stuhlausscheidungsrate und die Aktivitätskonzentration im Blut haben. Auf der Basis der Empfindlichkeitsanalyse wurde eine Fehleranalyse durchgeführt, um die Variationsbreite dieser Modellparameter aufgrund der am Menschen beobachteten Variationsbreite der Aktivitätsausscheidung zu quantifizieren. Mit Hilfe dieser Fehleranalyse können nun die bei einer bestimmten Person im Einzelfall möglichen Übergangswahrscheinlichkeiten genauer eingegrenzt werden.

Im experimentellen Teil der vorliegenden Arbeit wurde das optimierte Modell zur Beschreibung der Aktivitätsausscheidung im Urin am Beispiel eines konkreten Inkorporationsfalls angewendet. Dieses Beispiel stellt den zur Zeit weltweit am besten dokumentierten Inkorporationsfall dar. Außerdem repräsentiert dieser Fall ein eindrucksvolles

Beispiel für die langfristige Erhöhung der Plutonium-Ausscheidungsrate im Urin. Zur Bestimmung des aktuellen Status des Falles wurden im Forschungszentrum Karlsruhe umfangreiche *in vivo* und *in vitro* Messungen zur Bestimmung der aktuellen Aktivität in den Organen, der Aktivitätsausscheidung in Urin und Stuhl und der aktuellen Aktivitätskonzentration im Blut der betreffenden Person durchgeführt. Die Messungen bestätigten die erhöhte Aktivitätsausscheidung im Urin, die bereits bei früheren Untersuchungen ermittelt wurde. Bei Berücksichtigung der aus der Fehleranalyse gewonnenen Informationen über die individuelle Schwankungsbreite der Modellparameter ist es möglich, die ermittelten Messwerte mit dem optimierten biokinetischen Modell qualitativ und quantitativ zu beschreiben. So kann insbesondere auch die langfristig erhöhte Aktivitätsausscheidung durch geeignete Wahl von personenspezifischen Modellparametern im Rahmen des bei gesunden Personen ermittelten Schwankungsbereichs modelliert werden.

INDEX OF SYMBOLS .....	3
Chapter 1 INTRODUCTION.....	5
1.1 PROBLEM DEFINITION.....	7
1.2 PLUTONIUM.....	9
1.2.1 Physical characteristics .....	9
1.2.2 Chemical properties .....	11
1.2.3 Toxicology .....	13
1.2.4 Uses of Plutonium .....	14
1.3 PRINCIPLES OF INTERNAL DOSIMETRY.....	17
1.3.1 Paths and modes of intake.....	17
1.3.2 Dose assessments .....	19
1.3.3 Measurement techniques.....	21
1.4 THE ICRP 67 MODEL FOR PLUTONIUM .....	25
1.4.1 Description of the ICRP 67 model.....	25
1.4.2 Comments on the ICRP 67 model.....	28
Chapter 2 DATA AND MEASUREMENTS.....	31
2.1 AVAILABLE INFORMATION ON PLUTONIUM METABOLISM .....	33
2.1.1 Experiments on humans .....	34
2.1.1.1 <i>Langham's study and relating works</i> .....	34
2.1.1.2 <i>Further experimental investigations</i> .....	35
2.1.2 Empirical curves.....	36
2.1.3 Occupational exposures .....	40
2.2 A DESCRIPTION OF THE CONTAMINATION CASE.....	43
2.2.1 The contamination event.....	43
2.2.2 Available measurements .....	44
2.3 ACTIVITY MEASUREMENTS IN ORGANS.....	47
2.3.1 Basic measurement principles.....	47
2.3.1.1 <i>Shielding</i> .....	47
2.3.1.2 <i>Detectors</i> .....	48
2.3.1.3 <i>Geometry</i> .....	52
2.3.1.4 <i>Energy calibration</i> .....	53
2.3.1.5 <i>Efficiency calibration</i> .....	55
2.3.1.6 <i>Minimum Detectable Activity</i> .....	57
2.3.2 Materials and Methods.....	59
2.3.2.1 <i>Description of the devices</i> .....	59
2.3.2.2 <i>Performances</i> .....	63
2.3.2.3 <i>Measurements execution</i> .....	67
2.3.3 Results of the measurements.....	68
2.4 ACTIVITY MEASUREMENTS IN BIOASSAYS .....	72
2.4.1 Basic measurement principles.....	72
2.4.1.1 <i>Sample collection</i> .....	72
2.4.1.2 <i>Sample preparation</i> .....	72

2.4.1.3	<i>Chemical separation</i> .....	73
2.4.1.4	<i>Source preparation</i> .....	74
2.4.1.5	<i>Alpha spectrometry</i> .....	74
2.4.2	Materials and Methods .....	76
2.4.2.1	<i>Description of the devices</i> .....	76
2.4.2.2	<i>Performances</i> .....	79
2.4.2.3	<i>Measurements execution</i> .....	79
2.4.3	Results of the measurements .....	79
Chapter 3	INVESTIGATION ON PLUTONIUM METABOLISM .....	81
3.1	BIOKINETIC MODELLING.....	83
3.1.1	Mathematical tools .....	83
3.1.1.1	<i>Solution of a compartmental model</i> .....	83
3.1.1.2	<i>Target function for data vs. model comparison</i> .....	85
3.1.2	Analysis of the ICRP 67 model.....	87
3.1.2.1	<i>The reference data set</i> .....	87
3.1.2.2	<i>Model predictions compared to reference data</i> .....	92
3.1.3	Modification of the ICRP 67 model.....	97
3.1.3.1	<i>New concepts of skeletal remodelling</i> .....	97
3.1.3.2	<i>Optimization of the parameters</i> .....	101
3.1.4	Verification of the optimized model (Model-b).....	111
3.1.5	Characterization of the optimized model (Model-b).....	114
3.1.5.1	<i>Dose coefficients</i> .....	114
3.1.5.2	<i>Analytical functions for the urinary excretion</i> .....	118
3.1.5.3	<i>Sensitivity analysis</i> .....	121
3.1.5.4	<i>Uncertainty analysis</i> .....	128
3.2	APPLICATION OF THE OPTIMIZED MODEL (MODEL-B) TO A CASE OF CONTAMINATION	137
3.2.1	Harmonization of the activity measurements in bioassays .....	137
3.2.2	Classification of the available measurements .....	137
3.2.3	Analysis of the set of reliable measurements .....	139
3.2.4	Analysis of the set of less reliable measurements .....	145
3.2.5	Plutonium urinary excretion enhancement.....	147
3.2.5.1	<i>The effect of the uncertainty of the transfer rates</i> .....	147
3.2.5.2	<i>The research of the best fitting individual parameters</i> .....	149
3.2.6	Dose assessments .....	152
	CONCLUSIONS.....	153
ANNEX	QUANTITIES USED IN RADIOLOGICAL PROTECTION AND INTERNAL DOSIMETRY .....	155
	BIBLIOGRAPHY.....	161
	OWN PUBLICATIONS RELATED TO THE SUBJECT .....	175

## INDEX OF SYMBOLS

---

Here a short glossary of the most common symbols and abbreviations used in the present work is given.

ET1	First region of the extrathoracic section comprising the anterior nose.
ET2	Second region of the extrathoracic section comprising the posterior nasal passages, larynx, pharynx and mouth.
ET2 <sub>seq</sub>	Compartment of the extrathoracic region ET2 modelling the fraction of deposited particles retained ( <i>sequestered</i> ) in the airway walls.
BB1	Bronchial region of the thoracic section comprising the airway generation 0 through 8 (trachea through the bronchi) where the deposited particles are removed by the mucociliary action.
BB2	Compartment of the bronchial region modelling the fraction of deposited particles with slow clearance rates.
BB2 <sub>seq</sub>	Compartment of the bronchial region modelling the fraction of deposited particles retained ( <i>sequestered</i> ) in the airway walls.
bb1	Bronchiolar region of the thoracic section comprising airway generation 9 through 15 where the deposited particles are removed by the mucociliary action.
bb2	Compartment of the bronchiolar region modelling the fraction of deposited particles with slow clearance rates.
bb2 <sub>seq</sub>	Compartment of the bronchiolar region modelling the fraction of deposited particles retained ( <i>sequestered</i> ) in the airway walls.
AI1	Compartment of the alveolar-interstitial region with high clearance rate.
AI2	Compartment of the alveolar-interstitial region with intermediate clearance rate.
AI3	Compartment of the alveolar-interstitial region with slow clearance rate.
LNET	Lymph nodes of the extrathoracic section.
LNTN	Lymph nodes of the thoracic section.
s <sub>p</sub>	Initial dissolution rate for modelling the absorption into blood of the particles in the initial state.
s <sub>pt</sub>	Transformation dissolution rate for modelling the transformation of particles from the initial state into the transformed state.

$s_t$	Final dissolution rate for modelling the absorption into blood of the particles in the transformed state.
Type S	Type of absorption (S, slow) of a radionuclide from the respiratory tract into the blood. The default values of the corresponding parameters $s_p$ , $s_{pt}$ and $s_t$ are 0.1, 100 and $0.0001 \text{ d}^{-1}$ , respectively.
Type M	Type of absorption (M, moderate) of a radionuclide from the respiratory tract into the blood. The default values of the corresponding parameters $s_p$ , $s_{pt}$ and $s_t$ are 10, 90 and $0.005 \text{ d}^{-1}$ , respectively.
Type F	Type of absorption (F, fast) of a radionuclide from the respiratory tract into the blood. The default values of the corresponding parameters $s_p$ , $s_{pt}$ and $s_t$ are 100, 0 and $0 \text{ d}^{-1}$ , respectively.
$f_1$	Fraction of a radionuclide reaching the blood following an ingestion.
AMAD	Activity Median Aerodynamic Diameter, commonly expressed in micrometers [ $\mu\text{m}$ ]. It is the median of an aerosol activity distribution with respect to particles aerodynamic diameter.
$eu(t)$	Percentage daily urinary excretion at time $t$ for a certain radionuclide.
$ef(t)$	Percentage daily fecal excretion at time $t$ for a certain radionuclide.
$e_u(t)$	Fractional daily urinary excretion at time $t$ for a certain radionuclide.
$I$	Intake, i.e. amount of activity of a certain radionuclide introduced into the body.
$E(50)$	Committed effective dose for a certain radionuclide (see Annex).
$H_T(50)$	Committed equivalent dose for a certain radionuclide (see Annex).
MDA	Minimum Detectable Activity, characterizing the sensitivity performances of a certain techniques of activity measurement.

Matrices and vectors are named with capital and small bold letters, respectively: e.g. matrix **M** and vector **v**.

Chapter 1  
Introduction





Probably there is no single element in the periodic table with a history of discovery, development and use covering such a short time period of less than two generations. Since its discovery in the forties, Plutonium was extensively used in military and civilian activities, but the control of occupational exposure and the limitation of the risk of Plutonium incorporation is still one of the most difficult tasks in the radiation protection practice [1]. Two main constraints characterize the monitoring of an internal contamination from Plutonium isotopes: On one hand their high radiotoxicity results in very low acceptable limits of intake; on the other hand they are hardly detectable in the human body if amounts of activity comparable to the limits of intake have to be measured. At present the monitoring of the internal contamination of Plutonium is carried out mainly on the basis of bioassay, because the non-penetrating alpha-radiation cannot escape from the human body to be directly detected. Commonly samples of urine are collected and dose estimations are carried out, but in specific cases when more thorough investigations are needed, feces or blood samples can be also analyzed. The interpretation of these bioassay data in terms of organ burdens and radiation doses to sensitive tissues requires an accurate knowledge of the metabolism of Plutonium.

Up to now several compartmental models were developed to represent the biokinetics of Plutonium in the human body. Particularly the International Commission on Radiological Protection (ICRP) has successively published various models with increasing degrees of complexity. The latest version, issued a few years ago [2], which is based on an extensive review of available data, can be considered to embody the current knowledge of Plutonium metabolism in humans. Therefore it presently represents the main tool for evaluating the risk from the intake of Plutonium. Unfortunately this model is blemished by some assumptions, that have no clear physiological explanation but were simply introduced to obtain closer fits to existing data. Yet, even with these assumptions the model still has difficulties in describing the Plutonium biokinetics in the different organs and bioassay. Particularly in recent years it was found that the model is not able to explain the enhancement of the urinary excretion of Plutonium long after intake. This was observed in different subjects, whose contamination dates back up to 20 years. The application of the ICRP model on these subjects results in a significant overestimation of the intake and, consequently, of the actual exposure to ionizing radiations. This ensues important consequences, beyond strictly scientific issues of model accuracy. First of all, if intakes and radiation doses exceed the limits set for radiation protection purposes, it is likely that the responsible authorities will prohibit the continuation of the worker's activity and request his/her employment in other areas. This usually remains in effect until an explanation of the exceeding of limits is found: In this case important problems in the organization of working activities are foreseeable which could entail some economic disadvantages. Secondly the involved subject and likely his co-workers too could be subject to an unjustified state of psychological stress, due to the erroneous idea of an important failure in the system of radiological protection. At a third level serious consequences could occur from a legal point of view. The increased enhancement of Plutonium excretion, if considered as an unexplained deviation from the model, could suggest that systematic errors likely occur for all the evaluations based on the same model, undermining the whole concept of monitoring of internal exposure. On the other hand, if the deviation between a model's predictions and experimental measurements are viewed as caused by further events of contamination, the final radiation doses calculated could be significantly higher than the limits set by the authorities. This in turn would suggest that systematic failures occur in the execution of working procedures. The last two aspects are particularly important in relation to

the duties of the Department for Radiation Protection of the Forschungszentrum Karlsruhe, which acts as official regional center for the monitoring of internal exposure from occupational activities.

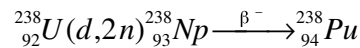
In order to correctly explain the bioassays from occupationally contaminated subjects, the available ICRP model for Plutonium metabolism in humans must be further developed. Particular care will be taken for the model's ability to predict the activity in urine, because this is the most common and feasible technique in the radiation protection practice in case of Plutonium exposure. To this end all relevant data and investigations on Plutonium metabolism and excretion rates available in the scientific literature will be assembled and used in the analysis below.

An occupationally exposed subject, characterized by a well documented scenario of contamination, will be also considered. Measurements on this subject have already been carried out since the first event of contamination, providing an extensive set of data on Plutonium metabolism, covering almost two decades. The data obtained in recent years show a significant enhancement of the urinary excretion compared to earlier assays. In the present work further measurements will be carried out providing simultaneously the amounts of activity both in bioassays and different organs.

Starting from the available ICRP model, the final goal is to develop a biokinetic model that accurately describes the Plutonium metabolism by avoiding any assumption that can't be supported by known physiological processes. Also procedures such as sensitivity and uncertainty analysis, rarely applied in modeling projects of internal dosimetry, will be applied to interpret phenomena like urinary excretion enhancement at long times after exposure. As a by-product, a deeper and more complete understanding of the internal workings of the new model will be obtained.

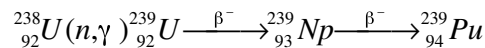
## 1.2.1 PHYSICAL CHARACTERISTICS

Plutonium (Pu, Z = 94) belongs to the actinide series, which starts with Actinium (Ac, Z = 89) and ends with Lawrencium (Lr, Z = 103). It is a silvery-white metal that melts at 639.5 °C and boils at 3235 °C, and its density at 25 °C is 19.737 gcm<sup>-3</sup> [3]. The first synthesized Plutonium isotope was <sup>238</sup>Pu, produced by bombarding Uranium with 16-MeV deuterons at the University of California cyclotron, and was identified on 23 February, 1941 [4]. The reaction was:



*reaction 1.2.1*

Later a second isotope was produced, <sup>239</sup>Pu, obtained by neutron capture of <sup>238</sup>U. The neutrons were generated from a (d,n) reaction using a cyclotron:



*reaction 1.2.2*

It was soon found that <sup>239</sup>Pu is more readily fissionable by slow neutrons than <sup>235</sup>U. This discovery stimulated intensive studies of the properties of Plutonium and its compounds. Prolonged irradiation of Uranium by slow neutrons, carried out during the years 1941-1943, made it possible to prepare and isolate in pure forms micrograms and later ever increasing amounts of the <sup>239</sup>Pu isotope. All the neutron deficient isotopes of Plutonium from 232 to 238 were produced by irradiation with charged particles. Some of the heavier isotopes were also produced in a similar way.

At present Plutonium is mainly produced in nuclear reactors based on the Uranium-Plutonium cycle [5], normally as result of (n,γ) neutron captures in <sup>238</sup>U and to a lesser extent through (n,2n) reactions. The isotopes 240, 241, 242 and 243 are formed from successive neutron captures. The short half life of <sup>243</sup>Pu essentially limits the production of Plutonium isotopes in reactors with <sup>242</sup>Pu. Plutonium may be produced from <sup>238</sup>U in a reactor with any type of neutron energy spectrum, from thermal to fast. Indeed the yield of the various ratio of Plutonium isotopes differs according to the large variation of the neutron cross sections of the various Plutonium isotopes with neutron energies. Generally, fissions are more likely with fast neutrons than with intermediate or thermal neutrons [4].

Even if the Plutonium is regarded as one of the typically anthropogenic elements, it is constantly produced in nature in Uranium ores according to reaction 1.2.2. The neutrons necessary for the (n,γ) reaction of <sup>238</sup>U are provided by spontaneous fission and alpha-neutron reactions. The resulting <sup>239</sup>Pu was observed in pitchblende and monazite ores. Yet the concentrations due to this natural source are very small: The Uranium to Plutonium ratio is approximately 10<sup>11</sup>:1 [6]. The possibility of finding other Plutonium radioisotopes in nature due to the primordial processes of earth formation depends on the halftime of the

radionuclide. Therefore only isotopes with long halftimes are likely to be found, such as  $^{244}\text{Pu}$ , that was found in the rare-earth mineral bastnasite [6].

At present 20 isotopes are known, from  $N = 228$  to  $N = 247$ , but only for 17 isotopes, from  $N = 231$  to  $N = 247$ , the halftimes are known [7]. In Table 1.2.1 the physical characteristics of the most important Plutonium isotopes with their respective half-time, type of decay and specific activity are given. Most of the Plutonium isotopes are unstable to alpha emission [8]. Alpha decays energies are frequently used to identify heavy nuclei. However some Plutonium isotopes can be hardly distinguished with current energy analysis. For example the main alpha transitions of  $^{239}\text{Pu}$ , one of the most important isotopes for industrial application, have alpha-energies close to those of  $^{240}\text{Pu}$ . So it is extremely difficult to separate these two isotopes by alpha- spectrometry. Other isotopes with  $N = 241$ , 243 and from 245 to 247 are unstable to beta decay.  $^{241}\text{Pu}$  also decays by alpha emission, but the alpha half-time is around 40,000 times that of the betas. Spontaneous fission can also occur with different probabilities for Plutonium isotopes, with even  $N$  values from 236 to 244 and for the odd atomic mass number 239. For other radioisotopes such decay is less significant.

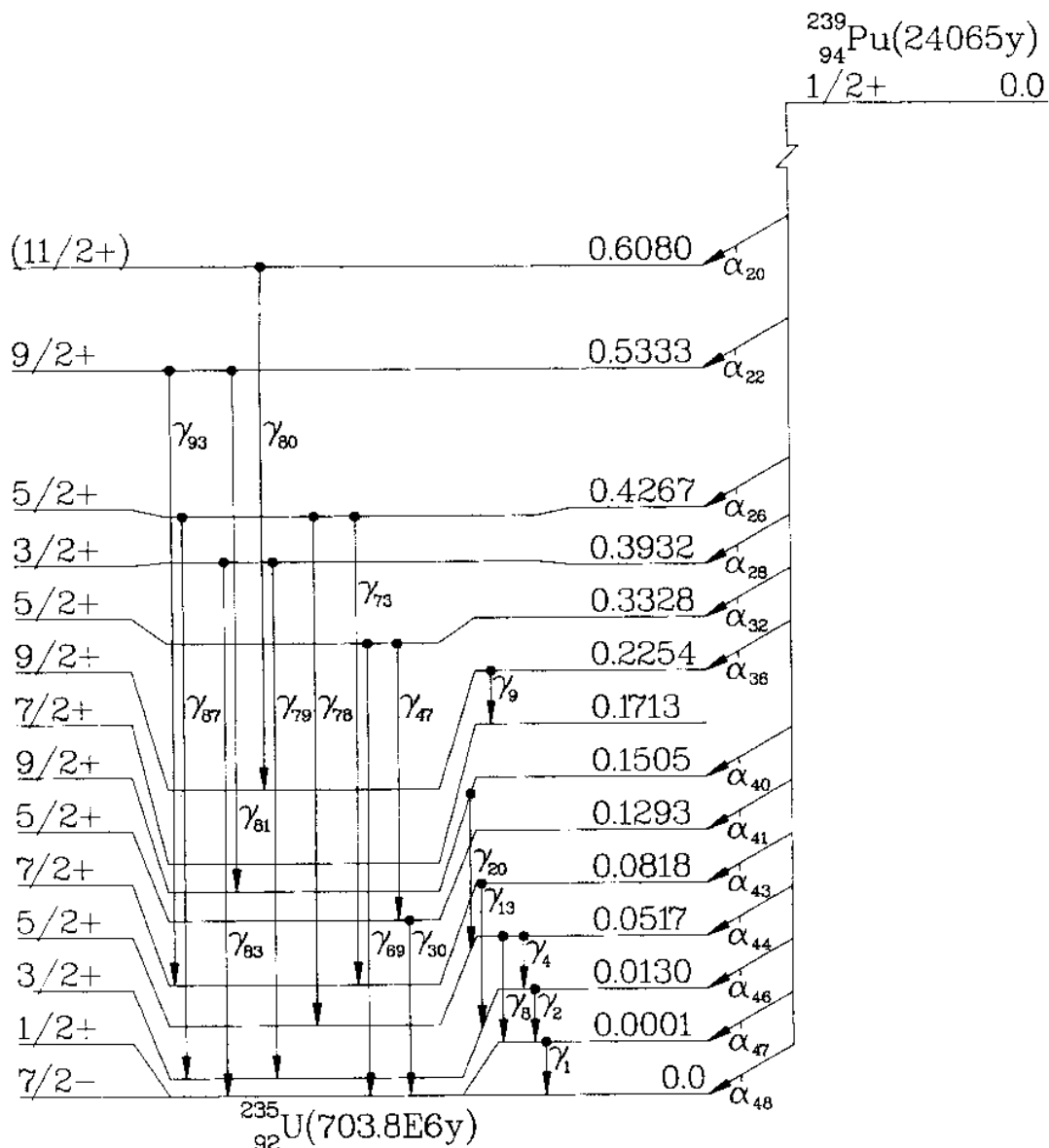
Among all these radioisotopes the most common and extensively used is  $^{239}\text{Pu}$ . Its complete decay scheme is given in Figure 1.2.1 [9].

**Table 1.2.1** Physical characteristics of major Plutonium isotopes (only the main emissions are given).

Isotopes	Half time [years]	Type of decay, (yield [%] - energy [Mev])	Specific activity [ $\text{Bqg}^{-1}$ ]
$^{238}\text{Pu}$	87.74	$\alpha$ (71.6 - 5.499) (28.3 - 5.456) sf <sup>(a)</sup>	$6.34 \cdot 10^{11}$
$^{239}\text{Pu}$	$2.410 \cdot 10^4$	$\alpha$ (73.8 - 5.157) (15.2 - 5.144) (10.7 - 5.105) sf <sup>(a)</sup>	$2.30 \cdot 10^9$
$^{240}\text{Pu}$	6563	$\alpha$ (73.4 - 5.168) (26.5 - 5.124) sf <sup>(a)</sup>	$8.40 \cdot 10^9$
$^{241}\text{Pu}$	14.35	$\beta$ (100 - 0.02 <sup>(b)</sup> ) $\alpha$ ( $2.04 \cdot 10^{-3}$ - 4.897)	$3.83 \cdot 10^{12}$

<sup>(a)</sup> spontaneous fission.

<sup>(b)</sup> maximum energy.



Legenda =  $\alpha_i$ ,  $\gamma_i$ : alpha particles (or gamma rays) where  $i$  is a sequential index ordered according to increasing alpha-particle (or gamma rays) energy; nuclear spin and energy levels are also given.

**Figure 1.2.1** Decay scheme of  $^{239}\text{Pu}$ .

## 1.2.2 CHEMICAL PROPERTIES

A wide range of possible oxidation states characterizes many elements of the actinides series. Particularly Plutonium exhibits all oxidation states from three (Pu(III)) to seven (Pu(VII)) [10]. All the oxidation states from three to six can co-exist in the same aqueous solution [10, 11]. In mammalian fluids, such as blood plasma, lung fluids, bile, urine and in tissues liquids, the Pu(IV) oxidation state is predominant, because most endogenous ligands

stabilise the +4 oxidation state [11]. A great number of Plutonium compounds have been studied up to the present [12], but here Plutonium compounds of potential importance from a radiation protection point of view will be mainly considered.

The oxidized form is probably the most important chemical form. Examples are the dioxide,  $\text{PuO}_2$ , which is the most common, the monoxide,  $\text{PuO}$ , and the sesquioxide,  $\text{Pu}_2\text{O}_3$ . They can occur in pure form or in non-stoichiometric mixtures with other metal oxides (Uranium, Potassium, Sodium), and they may have been formed at either very high temperature (above 1500 °C) or relatively low temperatures up to ambient ones [11]. The composition and formation temperature of Plutonium oxides determines their solubility and thus their metabolic behaviour. In relation to the former aspect, oxides of other metals that can occur in mixed Plutonium oxides are often more soluble, enhancing the solubility of Plutonium oxides itself. The latter aspect is of interest with regard to the Plutonium in the fall-out from nuclear weapon testing. This represents the main source of public exposure, in comparison with other anthropogenic sources [13, 14]. The fall-out Plutonium is partially composed by oxides which were formed at very high temperatures during the explosion phase, whereas the greatest fraction is due to the reaction  $^{238}\text{U}(n,\gamma)^{239}\text{U}$  and subsequent decay of  $^{239}\text{U}$  through  $^{239}\text{Np}$  to  $^{239}\text{Pu}$ . The latter is a low temperature process generating Plutonium oxides of high solubility, if compared to oxides produced at high temperatures [11].

Other possible forms of Plutonium are halogen compounds, nitrates, nitrides, sulphates, phosphates, oxalates but they are less important from a radiation protection point of view.

In aqueous solution Plutonium ions, particularly Pu(IV) undergo significant hydrolysis owing to their high ionic charge and relatively small radius [10]. Hydrolytic reactions depend on many factors, such as concentration of the metal in the solution, temperature, pH and presence of anions and cations, the latter producing the competing phenomena of complex formation. Particularly hydrolytic reactions occur more readily at high pH. As in mammalian systems the pH is about 7, it is quite unlikely that Plutonium ions can exist without undergoing hydrolytic reactions.

Complex formation too plays an important role in the solution chemistry of Plutonium, particularly for the Pu(IV) oxidation state, e.g. Plutonium complexes with inorganic ions (sulphate, nitrate, chloride, carbonate), with acetate, lactate and citrate. The latter is particularly interesting, because it is the form used in biokinetic studies with intravenously injected Plutonium in human subjects and animals. Plutonium complexes with citrate are characterized by very stable binding [10]. Complex formation between Plutonium and heavier molecules are also important, e.g. with polyaminopolycarboxylic acids for the recovery of Plutonium from process waste streams [12] and for the treatment of contaminated subjects. Particularly diethylenetriaminepentaacetic acid (DTPA) is known as one of the most important chelating agents [15]. This compound firmly binds to circulating Plutonium enhancing the normal excretion from the body, but toxic effects can accompany its action [16].

Summarising with regard to the ionic forms of Plutonium entering human body, three main types of reaction may be expected to occur:

- Hydrolysis yielding polymeric or colloidal species;
- Complexing with proteins or other biological macromolecules;
- Complexing with small molecular weight components, as acid organic and inorganic anions.

In case of an intravenous injection of Plutonium, the second process is likely the predominant reaction. At the other hand, if Plutonium enters directly in contact with a tissue, such as muscle in case of a contamination through a wound, or through an intramuscular injection, the first or the third process is expected to be occur with higher probability [10].

Complexing reactions occur with different high molecular weight components. Since the first investigations, transferrin was supposed to be the predominant transport protein for Plutonium in blood plasma [17]. This is a glycoprotein where Plutonium binds to the same sites as those which bind Iron, involving the same binding ligands. The binding of Plutonium to other proteins, such as ferritin, was also observed, even in recent studies [18, 19; 20]. Binding of Plutonium to bone proteins is particularly interesting, because of its role as a bone-seeking radionuclide. Complexing reactions with bone sialoprotein, bone glycoproteins and soluble collagen were observed [21, 22, 23].

Plutonium complexes with small molecular weight components are expected to play an important role in vivo. In this context binding with citrate is the most important, because of its ubiquity in human tissues. This complex shows high chemical stability, but as the complexing ligand is readily metabolised, they are likely of low stability in vivo. This was supported by experiments on animals showing that most of the Plutonium injected as citrate was later bound to plasma proteins, mainly transferrin [24].

### 1.2.3 TOXICOLOGY

The biologic effects of incorporated Plutonium isotopes are mainly due to the energy transferred to the tissue and organs by the alpha particles produced during nuclear decay [25]. The absorption of the energy released by ionizing radiations can cause two kinds of effects, named stochastic and non-stochastic (or deterministic) effects [26]. For the former a release of energy causes an increase of the probability of neoplastic or theratogenic events. For the latter the effect occurs only when a certain limit of energy (i.e. dose) is exceeded and the seriousness of such effects is proportional to the amount of released energy. As body burdens in the order of several kilobecquerel can cause deterministic effects and a few becquerel per gram of tissue can produce stochastic effects, it is quite unlikely that chemical effects of the type familiar to the pharmacologists and toxicologists can occur after an internal contamination of Plutonium [25]. Yet the chemical properties briefly described below are still important in determining the radiological toxicity of Plutonium, because they are important factors influencing the distribution of Plutonium within tissues and organs.

The radiological effects of Plutonium incorporated by animals and men have been widely studied [27, 28, 29, 30, 31]. Evidence of cancers and other neoplastic pathologies with different levels of morbidity have been found in experimental studies on animals. Deposition of inhaled Plutonium oxides in the respiratory tract of animals can deliver high doses from alpha radiation to the deeper airways and lung regions, where the gaseous exchange takes place. Acute tissue inflammation and a progressive fibrosis can occur [32]. The frequency of different types of cancer such as squamous cell carcinoma, adenocarcinoma and oat cell carcinoma appears to be dose dependent. Inhalation of soluble compounds of Plutonium seems to be least effective in causing stochastic effects to the respiratory tract, because of the fast transfer from the lung to the blood and to other organs. Systemic absorption of soluble compounds can cause bone tumours. Leukaemia has been also observed in strains of mouse injected with Plutonium nitrate [33]. Bile duct cancers and lymph node tumours are other confirmed pathologies.

Stochastic effects unequivocally attributable to the intake of Plutonium isotopes have not been clearly established in humans. This is due to the numerous confounding factors in groups of humans subject to occupational or public exposures. Yet epidemiological studies have been carried out on Plutonium workers employed in different nuclear weapons and fuel reprocessing plants. One of the best known studies considers the workers of the Rocky Flats plant [34, 35]. A mortality study of a cohort of 5400 white males was carried out even though factors such as individual expositions to other external radiations and low sensitivity

techniques adopted in the early phase of the study doesn't allow pointing out the possible effect of incorporated Plutonium. In comparison with the natural frequencies of the various cancers in the US no excess of cancer mortality could be confirmed for the whole cohort of workers in Plutonium facilities. But when the cohort was divided in two groups having low and high body content of Plutonium, a statistically significant excess of lymphopietic tumours for the highest contaminated group was observed, if a latency period of five years was assumed in the calculations. No significant differences were found if other latency periods were assumed. In another study twenty-six workers at the Los Alamos laboratories employed for the Manhattan Project were investigated. They were exposed to high airborne Plutonium concentrations at the early phases of the project and have been followed up for about fifty years [36]. Body burdens up to a few kBq were estimated for some workers, and by 1990 seven individuals died because of lung and bone cancer. But confounding factors such as smoking and the limited number of stochastic effects does not allow attributing the observed pathologies to Plutonium intakes. Similar studies were carried out on workers of Sellafield (UK) and in the Mayak Radiochemical Plant (former USSR). In the latter case 2300 workers were studied and an excess of lung cancer deaths was observed mainly in a cohort of workers that received an equivalent dose to the lung greater than 4 Sv [37]. Also in this case smoking habits can be a determinant in the interpretation of the epidemiological data. Recently studies of deterministic effects also have been carried out [38]. In a random sample of 221 workers, who were employed in a cohort of 8,055 workers at Mayak PA, 96 cases of chronic radiation sickness, 14 cases of acute radiation syndrome and 13 cases of Plutonium pneumosclerosis were observed [39].

Epidemiological studies carried out on cohorts of members of the public are even more difficult in revealing stochastic effects. Several events have caused releases of Plutonium activity to the environment [40] following activities now discontinued, as testing of nuclear weapons in atmosphere, or still continuing, as reprocessing of irradiated fuel from nuclear power reactors. Doses due to the global fallout [41], or to accidental releases from nuclear power production, as occurred in Sellafield (UK) and Cap de la Hague (France) [42], are negligible. More significant is the public exposure of the population around the Mayak reprocessing plant, which resulted in the release of relevant quantities of Plutonium and other radioisotopes into the near-by Techa river. A recent study estimated a body content of adult inhabitants up to thirty times higher than the average global levels [43], and investigations on cancer occurrence and morbidity are still under work [44].

#### 1.2.4 USES OF PLUTONIUM

Plutonium played and still plays a very important role in the nuclear industry where fission reactions of heavy elements are used to generate electrical power. Other applications of minor importance are ship propulsion, generation of process heat and research. Such applications are based on the use of a nuclear reactor where the break-up of the nucleus of heavy atoms (nuclear fission) occurs in a controlled and self-sustained manner with an energy release that is millionfold greater than the energy obtained from chemical reactions. In a nuclear reactor, two isotopes of Uranium,  $^{233}\text{U}$  and  $^{235}\text{U}$ , and one Plutonium isotope  $^{239}\text{Pu}$  represent the main constituents of the "nuclear fuel", because of their large absorption cross section for slow neutrons and their successive significant probability for decay by fission [6]. Therefore those isotopes are called "fissile materials". Of these isotopes only  $^{235}\text{U}$  occurs in nature, although only in quantities one hundred times less than  $^{238}\text{U}$ , the main constituent of natural Uranium. The other two fissionable isotopes are artificially produced:  $^{239}\text{Pu}$  as previously presented by neutron capture in  $^{238}\text{U}$ ;  $^{233}\text{U}$  by neutron capture in  $^{232}\text{Th}$ . Conventionally the former reaction is referred as Uranium-Plutonium cycle, the latter as



Uranium-Thorium cycle [5]. For their capacity of producing fissile materials,  $^{238}\text{U}$  and  $^{232}\text{Th}$  are therefore called “fertile materials”.

The use of a mixture of fissionable and fertile materials in a nuclear reactor can help in reducing the rate of depletion of nuclear fuel, because the excess of neutrons not necessary for the maintenance of the fission reaction can be used for converting the fertile materials into fissile materials. Thus, for the specific case of Uranium-Plutonium cycle, the  $^{235}\text{U}$  can be burned and the surplus of neutrons produce Plutonium  $^{239}\text{Pu}$  from the fertile  $^{238}\text{U}$ . This kind of nuclear reactor is called converter reactor [6]. The efficiency of this process of production of new fuel depends on the extent of neutron losses. If these losses are kept small by controlling and limiting undesirable neutron absorption or neutron leakage, even more fuel can be produced than that burned. Moreover  $^{239}\text{Pu}$  can be used as a fuel in place of the original  $^{235}\text{U}$ . Reactors that burn  $^{239}\text{Pu}$  (or  $^{233}\text{U}$  in the Uranium-Thorium cycle) and produce as much, or more, fuel as is consumed, are called breeder reactors. This kind of reactor is characterized by a particularly high efficiency in breeding Pu by fast neutrons (fast breeder reactors).

In this frame Plutonium is first of all and more commonly a by-product of fission reactions used in the nuclear power industry, because of the ubiquitous presence of  $^{238}\text{U}$  in nuclear fuels. Plutonium is used only in small amounts on its own to fuel reactors, mainly for the development of fast breeder reactors. In fact, even if the breeder reactors technology has given the possibility of using  $^{239}\text{Pu}$  as fuel, high capital cost, operational difficulties and doubts over safety have limited the application of this technology, particularly with regard to the commercially unfavourable process of treatment of spent reactor fuel elements to recover Plutonium [45]. At present Plutonium is more commonly used blended with natural or depleted Uranium in so-called mixed-oxide fuels (MOX) for light-water thermal reactors. In 1998 about 20 reactors in five countries (Belgium, France, Germany, Japan and Switzerland) were loaded with MOX fuel, but the number is expected to rise in the next years because the use of MOX fuels reduces the inventory of separated Plutonium, thereby reducing the problems of safe Plutonium storage, even if extensive handling of Plutonium is still necessary. However the multiple recycling in light-water reactors degrades Plutonium, limiting the number of times it can be recycled to two or three [46]. After such use and without the possible following application of Plutonium as fuel for fast breeder reactors, spent MOX fuel ends up in a final depository or in storage facilities.

Beside the civilian applications, Plutonium was extensively used for military purposes for manufacturing nuclear explosives. An explosive fission reaction can be generated with Plutonium by two different procedures: Bringing together rapidly two chunks of fissile material, each with subcritical mass, to achieve a supercritical mass (“gun” technique) or compressing a sphere of Plutonium by application of concentrated high explosives (implosion technique) [47]. The Plutonium used in nuclear warheads is produced with dedicated production reactors. The spent fuel from power reactors contains a large amount of  $^{238}\text{U}$ , and some  $^{235}\text{U}$ ,  $^{239}\text{Pu}$ ,  $^{240}\text{Pu}$  and  $^{241}\text{Pu}$ . If this “reactor grade” Plutonium is chemically separated and made into a weapon, the presence of neutrons from the spontaneous fission of  $^{240}\text{Pu}$  will cause premature detonation and an inefficient explosion. Therefore specific reactors were designed and operated to produce “weapon grade” Plutonium with high concentration of the fissile  $^{239}\text{Pu}$  and lower concentrations of the other isotopes, notably  $^{240}\text{Pu}$ . Usually the Plutonium for military purposes contains less than seven per cent of  $^{240}\text{Pu}$ .

The nuclear power production in the civilian area and the weapons manufacture in the military sector are the main applications of Plutonium and consequently the main sources of inventoried Plutonium. Estimates for inventories of Plutonium at the end of 1990 in these two fields of application are shown in Table 1.2.2 [modified from 48]. Of the total inventoried Plutonium (911 tons), 72 % comes from civilian inventories (654 tons) and of this 83 % is

present in spent and MOX reactor fuel. The remaining 28 % of Plutonium comes from military applications. As to the Plutonium from spent fuel, more recent data gave a worldwide production of 75 tons in 1997. It is estimated that the annual production figure will remain more or less the same until 2010. The cumulative amount of Plutonium in spent fuel from nuclear power reactors worldwide is predicted to increase to about 1700 tons by 2010 [46]. In the last years increasing amounts of Plutonium are expected to be removed from military programs, owing to the dismantling of thousands of US and Russian warheads on the basis of the START-I and START-II treaties. At least 50 tons of Plutonium from each side are expected.

**Table 1.2.2** Estimates for inventories of Plutonium at the end of 1990.

Application	Tonnes
<i>Civilian sources</i>	
in spent and MOX reactor fuel	545
separated in store	72
in fast reactor fuel	<u>37</u>
<i>Total</i>	654
<i>Military sources</i>	
in warheads	178
weapon-grade outside warheads	56
others	<u>23</u>
<i>Total</i>	257

Besides the application based on controlled (civilian) and explosive (military) fission reactions, Plutonium has been widely used as a thermo-electric generator: By means of thermoelectric couples, the heat produced by the nuclear decays is converted into electric power and used to supply energy to low-power control and communication equipment. This kind of power source has many advantages such as lightness and compactness (to fit within a spacecraft), resistance to ambient conditions (low temperatures, radiation and meteorites) and independence from sunlight (permitting explorations of distant planets). For such purposes  $^{238}\text{Pu}$  has been widely used, because its high energy alpha particles (5.499 Mev) and the relatively short half-life (87.74 y) result in a high specific activity ( $6.34 \cdot 10^{11} \text{ Bqg}^{-1}$ ) and a favorable power to weight ratio, quoted to be  $0.57 \text{ Wg}^{-1}$  [47].

## 1.3.1 PATHS AND MODES OF INTAKE

In the human body different radioisotopes are commonly present as a consequence of the dietary intake and respiratory exchanges (Table 1.3.1). The most common natural radionuclides are:  $^3\text{H}$ ,  $^7\text{Be}$  and  $^{14}\text{C}$  originating from cosmic ray interactions with the terrestrial atmosphere;  $^{40}\text{K}$ ,  $^{87}\text{Rb}$  and  $^{138}\text{La}$  since primordial ages in the lithosphere; the natural series of  $^{238}\text{U}$ ,  $^{235}\text{U}$  and  $^{232}\text{Th}$  with their progenies [49]. Additional radionuclides come from the global fallout following the numerous atomic weapon tests in the atmosphere carried out in the sixties and seventies. All of these radionuclides and others of minor importance are introduced into the body in relation to the environmental and geological conditions of the area where the subjects are used to live and to its dietary habits. Activities of radionuclides normally present in adult human subjects are given in [50]. Human technologies which involve the use of radioactive materials, such as nuclear power and related procedures (mining, transports, fuel production and reprocessing, waste management), applications in the conventional industries, scientific research, medical applications, etc. can be a source of additional exposure for the population and the workers involved.

**Table 1.3.1** Indicative values of human body content of main natural radioisotopes.

Radionuclides	Amount [Bq]	Origin
$^3\text{H}$	30	global fallout and natural
$^{14}\text{C}$	$10^2 - 10^3$	“
$^{40}\text{K}$	$4 - 5 \cdot 10^3$	natural
$^{87}\text{Rb}$	700	“
$^{226}\text{Ra}$	1 - 10	“
$^{228}\text{Ra}$	0.4	“
$^{214}\text{Pb}$ , $^{214}\text{Bi}$	40	“
$^{235,238}\text{U}$	1.5	“
$^{137}\text{Cs}$	100	global fallout
$^{90}\text{Sr}$ - $^{90}\text{Y}$	30	“
$^{239,240}\text{Pu}$	0.4	“

Substances can enter the human body through essentially five pathways: Inhalation, ingestion, injection, wound and absorption through skin. The quantity of activity entering the body is conventionally named *intake*. The phase of the contamination in which the activity is not yet absorbed into fluids (as in the early phases of inhalation or ingestion) is named pre-systemic phase. A scheme of the possible paths of intake with a general overview of the main transfers in the body is presented in Figure 1.3.1 (modified from [51]).

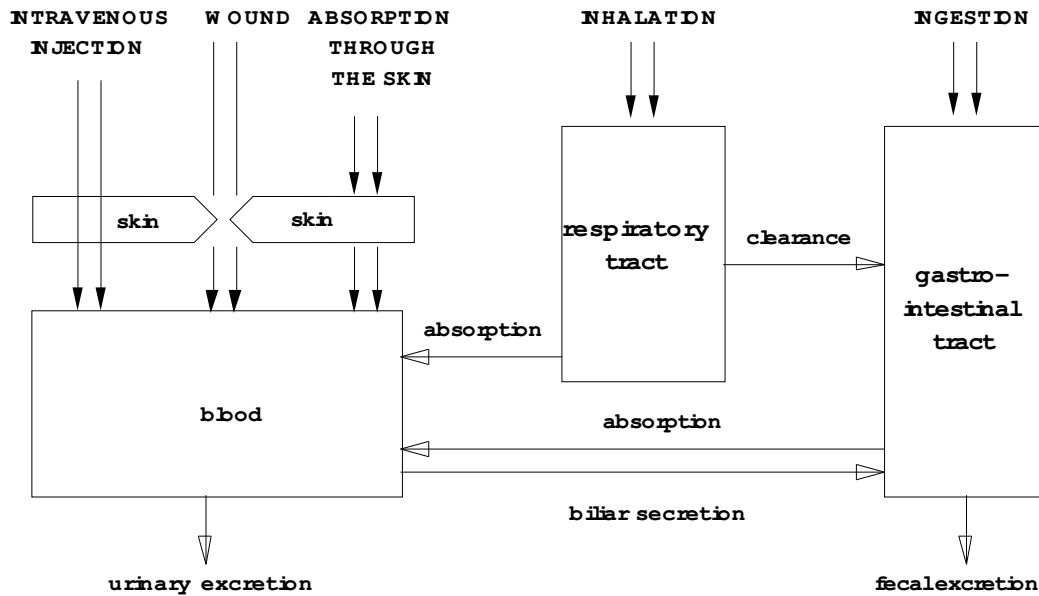


**Figure 1.3.1** Main route for internal contamination.

After the introduction into the body, a proportion of the activity is absorbed to blood. This absorption of activity is named *uptake*. Activity reaching body fluids (transfer compartments) is named systemic activity. Both in the pre-systemic and systemic phase of the contamination, the activity undergoes various and complex transfers which determine its distribution within the body and its route and rate of excretion. The distribution of systemic activity in the body can be homogeneous, as for tritium, or localized in specific organs or tissues, such as iodine in thyroid, alkaline earth metals in bone or Plutonium in bone and liver [52].

A contamination via inhalation is the most likely way of intake in case of a subject's exposure to an environment with radioactive vapours or aerosols. The former are partially absorbed directly in the body fluids by means of gaseous exchange phenomena. The latter are partially deposited on the airway walls by three main mechanisms: Sedimentation, impaction and diffusion. Electrostatic deposition and interception are generally less important mechanisms of deposition in the respiratory tract [53]. A contamination by inhalation can occur for both occupationally exposed subjects and members of the general population.

The contamination of food and drinking water can cause introductions of radioactivity by ingestion. This is the typical pathway for the contamination of the general population. Yet workers too can be exposed to a risk of contamination via ingestion by means of the transfer of activity to the mouth following a contamination of the hands (typically because of using faulty or broken gloves).

Injection too has to be considered as a path of internal contamination, even if it is a consequence of a planned action and not of an accidental event. Intravenous injections of radiopharmaceuticals are with increasing frequency used for therapeutic and diagnostic purposes in nuclear medicine and metabolic therapy [54].

A contamination via wound can also be considered a systemic contamination, because the activity is directly transferred to the blood stream. Yet it differs from the simple case of injection, because the activity is partially retained in the wound edge and successively

released to the bloodstream with varying rates. A fraction of this activity, particularly in case of insoluble compounds, can be also transferred to regional lymph nodes as a consequence of lymphatic clearance [55].

Intact skin is normally a good barrier against the entry of substances into the body. However a few elements are transferred, sometimes rapidly, to the blood after a skin contamination, such as tritiated water and to a lesser extent iodine [55]. Skin can be contaminated by the deposition of aerosols or by contact with liquids or surfaces contaminated with radionuclides. This path of intake is typical for occupationally exposed subjects.

Intakes can differ also with regard to the time pattern. Three main modalities can be distinguished: Acute, repeated and chronic [50]. In case of an acute intake the radionuclide is introduced during a time interval that can be considered short in comparison with the time of retention in the body (instantaneous intake). Moreover the intake is not followed by any further introduction of the same radionuclide before it is completely cleared or decayed. On the contrary a repeated intake occurs if an introduction of a radionuclide is followed by subsequent intakes before the activity due to the previous introduction is cleared. Finally, a chronic intake is characterized by a continuous introduction of radionuclides that lasts for a time period comparable or longer than the overall body retention. In this case when the intake and excretion of activity are in equilibrium, the accumulation of activity in the body can reach an equilibrium value and then remain constant. The time necessary to reach the equilibrium level depends on the decay time of the radionuclide and on the biological retention time in the body. For example in case of an intake of  $^{131}\text{I}$ , the necessary time is a few weeks, for  $^{137}\text{Cs}$  it is 1.5 years, for  $^{90}\text{Sr}$  it is about 50 years. Because of the long physical half life (24,065 years) and biological half life of  $^{239}\text{Pu}$  (50-100 years), equilibrium conditions are never reached, even for intakes lasting for the whole human life.

### 1.3.2 DOSE ASSESSMENTS

The potential risk associated with an internal contamination is evaluated by calculating the effective dose. This is a radiation protection quantity based on physical properties of the interaction of radiation with matter (energy released per unit mass of the biological target), subsequently weighted by some dimensionless factors to take into account two modifications:

- The effectiveness in causing damage to a certain biological target in relation to the type and energy of the absorbed radiation (radiation weighting factor,  $w_R$ );
- The different radiosensitivity of the various biological targets, when irradiated with the same type and energy of the radiation (tissue weighting factor,  $w_T$ ).

The dosimetric and radiation protection quantities are explained in details in the Annex.

After an intake, cells, tissues and organs are normally non-uniformly irradiated with regard to time, type and energy of radiations. Whereas in case of exposure to an external source of radiations the dose can be directly measured using properly placed dosimeters, internal doses following an intake of radioactive materials can only be inferred indirectly from measured quantities such as body or organ activity, excretion rates in bioassay samples and environmental monitoring [55].

Doses are generally calculated by means of a two-step procedure: Evaluation of the intake and calculation of the dose by multiplying the intake by a suitable dose coefficient (dose per unit of intake).

The intake is evaluated by using biokinetics models that allow quantifying the concentrations of the radionuclides in the organism in time. Retention and excretion

functions, defined as retained and excreted activity per unit activity of intake, respectively, are calculated. On the basis of the measurements the intake can be assessed. In case of environmental monitoring, such as surface or air contamination measurements, assumptions on resuspension factor and breathing habits of exposed subject are made to infer a hypothetical intake. The intake assessment is strictly related to the scenario of contamination such as time of intake, compound, path of intake, etc.

In the second step a dose coefficient, commonly taken as committed effective dose (see Annex) per unit activity of intake, can be derived on the basis of the biokinetic model. The same biokinetic model adopted in the phase of intake estimation, must be adopted also in calculating dose coefficients.

Multiplying the estimated intake by the calculated dose coefficient, the dose is finally obtained.

Biokinetic studies have been carried out since many years to describe the time-dependent distribution, both after the introduction of a radioactive compound via a specific pathway, and after the direct uptake into the blood. For this purpose models for the pre-systemic and systemic phases of the contamination were developed, respectively. In internal dosimetry the relevant organs and/or tissues are represented by distinct compartments, and generally it is assumed that the radionuclide is transported from one compartment to another at a rate which is proportional to the amount present in the feeding compartment. This type of behaviour is named *first order kinetics* [56]. Compartmental models are a general tool for modelling the behaviour of material obeying first order kinetics, whether radioactive or stable. For the specific case of radioactive materials, processes of biological transport are conveniently separated from radioactive decay. Thus biokinetic models normally treat materials as stable and consequently the transfer rates specified in the model represent only the biological transport. The effect of radioactive decay is taken into account separately by considering for each compartment an exit pathway with rate equal to the physical decay constant.

ICRP has developed models for the pre-systemic phase of the contamination to represent the behaviour of radionuclides that have entered the human body via inhalation and ingestion, and also systemic models for the metabolism of the radionuclides after the uptake into the blood.

The ICRP model for the respiratory tract [57] distinguishes five regions:

- Extrathoracic airways, divided in anterior nasal passage (ET1) and posterior nasal-oral passage (ET2), including also pharynx and larynx.
- Thoracic airways divided in bronchial (BB), bronchiolar (bb) and alveolar-interstitial (AI) regions.

Lymphatic tissues (LNET and LNTH) are associated with extrathoracic and thoracic airways, respectively. Deposition in each region of the respiratory tract is determined by the aerosol particle size and breathing parameters. The clearance from the respiratory tract is treated as two competing processes: Particle transport (by mucociliary clearance and translocation to lymph nodes) and absorption to blood. Particle transport is a function of the deposition site in the respiratory tract and of particle size. The mechanical transport being time dependent, most regions are subdivided into several compartments with different clearance rates. Absorption to the blood is treated as a function of the deposition site in the respiratory tract and of the physicochemical form of the radionuclide. Specific dissolution rates are normally recommended. But if no specific information is available, default absorption parameters are given for three dissolution types, namely type F (fast), M (moderate) and S (slow). In case of the inhalation of vapours, the respiratory tract deposition is material specific. Values are given

for three default classes, namely SR-0, SR-1 and SR-2, which characterize different solubility and reactivity features of inhaled compounds.

The ICRP model describing the behaviour of ingested radionuclides is given in Publication 30 [58]. It is composed of four compartments describing the kinetics in the stomach, small intestine, upper large intestine and lower large intestine. The uptake into blood takes place from the small intestine and is quantified by a transfer factor (even called gut uptake factor),  $f_1$ , that specifies the fraction of activity in the small intestine transferred to blood. Its value is related to the chemical properties of the ingested compounds.

For other routes of intake, such as absorption through the intact skin or wound, less information is available. Thus no general model has been developed, although some attempts for modelling a contamination via wound were made [59, 60].

Systemic models are also proposed by ICRP for modelling the metabolism of radionuclides after the uptake into blood. These models are used in connection with the above intake models in case of a contamination via inhalation or ingestion, but they are applied also directly in case of a systemic contamination (e.g. by injection or skin contamination from tritiated water). Specific models are given for each radionuclide or for groups of chemically similar radionuclides. As the Plutonium kinetics is the main subject of this work, a detailed description of the related ICRP systemic model is given in the last section of this first chapter.

### 1.3.3 MEASUREMENT TECHNIQUES

The individual monitoring for internal dosimetry purposes may be carried out by means of body and organ activity measurements (named also *in vivo* or direct measurements), bioassay measurements (named also *in vitro* or indirect measurements), environmental sampling, or a combination of these techniques.

The choice of the suitable measurement technique depends on several factors such as type and energy of emitted radiations, biokinetic behaviour of the contaminant taking into account its retention/excretion and radioactive decay, sensitivity, availability and convenience of the technique [55]. For some radionuclides, only one measurement technique may be feasible, such as urine excreta analysis for a contamination with tritiated water, whereas for other radionuclides a combination of techniques might be preferable if difficulties of measurements and interpretation of data occur, as is the case with a Plutonium contamination.

When different methods of similar and adequate sensibility are available, the order of preference with regard to the accuracy of dose assessment is: Direct measurements, indirect measurements and environmental measurements [52]. The advantages of direct measurements in comparison with indirect measurements are: More accurate determination of intake activity; insoluble materials that are not excreted can be detected; fast execution; body or organ activities can be determined without using metabolic models; the body contents of multiple radionuclides can be determined simultaneously. On the other hand, the disadvantages in comparison with indirect measurements are a higher detection limit, external and not removable contamination cannot be discriminated by an internal contamination, dedicated and often more expensive facilities are generally required [61]. Particular care should be taken when environmental measurements, as air or surface contamination, are used for a quantitative determination of intake. Air concentrations and above all surface contamination measurements are often difficult to relate to intake; the former because the suspended activity can significantly differ from the inhaled activity, particularly when it results from the worker's own actions and movements; the latter because the resuspension factors determining the fraction of activity released in air and then inhaled are hardly determinable [62]. Thus, they should be used mainly to complement hard information about

the contamination event, of such as aerosol size distribution, chemical form, time of accidental release, likely path of introduction. For these and other reasons direct and indirect techniques of measurements will be considered in the following.

Direct measurement are feasible only for those radionuclides, whose emitted radiations can escape from the body. Therefore from a theoretical point of view this technique can reveal radionuclides emitting X- or  $\gamma$ -radiation, positron through the annihilation of photons, energetic  $\beta$ -particles due to the bremsstrahlung radiation generated,  $\alpha$ -emitters because of the characteristic X-rays [63]. In practical situations the usefulness of these measurement techniques are limited because of the poor sensitivity and the consequent high detection limits for several radionuclides. The activity is detected with a detector positioned at specific locations around the body, usually with at least partial shielding of the detector and/or the subject, to reduce the interference from ambient external sources. With regard to the radionuclide distribution throughout the body (uniform distribution or concentration in particular organs), several geometries have been studied to provide the greatest sensibility. Furthermore a variety of detection systems have been developed which were optimized with respect to the energy of the radiation escaping from the body.

In the specific case of a Plutonium intake via inhalation, a direct measurement of the activity in lungs can be attempted. This technique is based on the detection of low energy photons (e.g. X-rays at 17.0 and 20.4 keV for  $^{239}\text{Pu}$ ). Thin NaI(Tl) crystals can be used as detectors, which have a similar detection efficiency as large crystals, but a much lower background. The use of a phoswich detector, composed of a NaI(Tl) crystal coupled with anti-coincidence circuits to a Cs(Tl) crystal, improves significantly the sensitivity by eliminating the contribution of high energy photons. Single crystals or an array of solid state detectors (particularly High Purity Germanium detector, HPGe) are today the best available facilities due to their high resolution and low background [55].

Independently of the applied technique, for Plutonium it is essential to account for the photon attenuation in tissues overlaying the lungs, when low energy photons have to be detected. Thus it is important to estimate the chest wall thickness of the subject. This can be calculated by means of anthropometric functions based on the subject's weight and height, or measured directly with ultrasound or magnetic resonance [64, 65, 66].

Even with the latest developments in direct measurement techniques, the sensitivity for Plutonium detection is still poor if activities below the annual limit of intake have to be detected. Direct measurement can be more useful, if the contamination from Plutonium is associated with other radionuclides and the isotopic composition of the contaminant is known. This typically occurs in actual cases of contamination from industrial sources, where a mixture of Plutonium isotopes with  $^{241}\text{Am}$  ingrown from  $^{241}\text{Pu}$  is present [52]. This isotope of Americium emits 59.5 keV  $\gamma$ -rays with 46% intensity and thus is easier to detect than Plutonium. Therefore it can be a useful tracer of an internal contamination by Plutonium. In Table 1.3.2 indicative values for the detection limit of direct measurements of  $^{239}\text{Pu}$ , based on X-ray spectrometry are provided [52]. Detection limits for  $^{239}\text{Pu}$  for a real whole body counter based on  $^{241}\text{Am}$  measurements are also given for various isotopic compositions [67]. These values have to be compared with the expected activity in lung, as predicted by ICRP models, at different times after intake. An intake giving an effective dose of 20 mSv, the annual average dose limit for an occupationally exposed worker [26, 68]) was assumed. The inadequacy of the sensitivity for the detection of pure  $^{239}\text{Pu}$  is clearly to be seen. Only Plutonium detection via tracer Americium has an adequate sensitivity, and only in case of a slow absorption type compound and for a short time after inhalation.

Indirect measurements on biological samples are commonly based on the determination of radioactivity in excreta (urine and feces), but rarely in blood. Other sampling



techniques such as nose blow, nose swabs, sweat, hair and breath are used just for metabolic studies of particular radionuclides or for specific investigations. Breath analysis is commonly used for  $^{226}\text{Ra}$  and  $^{228}\text{Th}$  whose decay chains include gases that can be exhaled. Blood is sampled in case of suspected high level contamination or dedicated metabolic studies [52]. However because of the lack of experimental studies and observations, biokinetic models don't describe how the human metabolism cumulates the radionuclides in these uncommon samples. Therefore the interpretation of these measurements can be extremely difficult. For research purposes the analysis of tissue samples is carried out post-mortem in specimens collected at autopsy.

Urine sampling is the most common technique. The excreted activity is due to the introduced activity that has reached the blood stream and depends on the transferability of the compound (the capability of reaching the blood in case of contamination via inhalation or ingestion). Generally a 24 h collection is preferred to limit the variability during the day, but a collection over several days is carried out when adequate sensitivity must be achieved [52]. Fecal samples are also used but they are more difficult to analyze because of the large daily fluctuations in fecal excretion. The activity excreted in the feces comes from two contributions: The activity in the gastrointestinal tract, that was not absorbed into the blood, and the activity absorbed into the blood that has reached the gastrointestinal tract through the biliar secretion.

Whatever the bioassay technique, the sample must be prepared isolating the radionuclide to be investigated from the matrix material. Generally different phases can be identified[69]: Sample preparation (wet and/or dry ashing), chemical separation (by means of ion-exchange resin or solvent extraction), source preparation (in function of the measuring technique). The most common measuring techniques are  $\alpha$ -spectrometry,  $\beta$ -counting, liquid scintillation counting and  $\gamma$ -spectrometry. Fluorimetry, neutron activation analysis, inductively coupled plasma - mass spectrometry (ICP-MS), and fission track analysis can be also applied but they are not extensively used.

In the particular case of Plutonium,  $\alpha$ -spectrometry is one of the most common measuring techniques. Indicative values for the detection limit of indirect measurements of  $^{239}\text{Pu}$ , based  $\alpha$ -spectrometry, are provided Table 1.3.2 [52]. For good energy resolution, very thin sources are needed. Therefore particular care is taken for source preparation, using techniques such as direct evaporation or electrodeposition. Detection limits around one  $\text{mBql}^{-1}$  or fraction can be achieved [70]. Lower limits of detection can be accomplished by fission track analysis [71, 72], but this measuring technique requires sophisticated infrastructures and procedures. ICP-MS is also a very sensitive technique for Plutonium measurements [70, 73] and its big advantages are that almost no treatment of samples is required and results can be obtained in a few minutes of measurement.

The typical detection limits for *in vivo* measurements and *in vitro* measurements based  $\alpha$ -spectrometry techniques, provided in Table 1.3.2, can be compared with the expected values of  $^{239}\text{Pu}$  activity in lungs and bioassays, calculated by means of ICRP models: the respiratory tract model from ICRP 66 [57] and the systemic model from ICRP 67 [74]. In the evaluations an intake determining a reference committed effective dose of 20 mSv was assumed. Such value is the annual average dose suggested by the ICRP as limit for the professionally exposed workers [26]. The conditions of exposure (scenario of contamination) were assumed according to the standard parameters (breathing rate, diameters of inhaled particles, absorption from the gut tract into the blood) suggested by ICRP in case of inhalation and ingestion. In comparison with *in vivo* measurements the analysis of excreta by means of  $\alpha$ -spectrometry is generally more adequate. In fact the detection limits for  $\alpha$ -spectrometry analysis of excreta allows detecting a Plutonium contamination in a large number of contamination scenarios and for extended time intervals after intake.

**Table 1.3.2** Indicative  $^{239}\text{Pu}$  detection limits for in vivo and in vitro techniques.

Technique	In vivo measurements	In vitro measurements	
	X-ray spectrometry	$\alpha$ -spectrometry	
organ or sample	lung	urine	feces
typical detection limits [52]	2000 Bq	0.001 Bq $l^{-1}$	0.001 Bq
<i>detection limit of a real whole body counter [67]</i>			
<i>17.0 and 20.4 keV x-rays from pure <math>^{239}\text{Pu}</math></i>	<i>3000 Bq</i>		n.a.
<i>59.5 keV <math>^{241}\text{Am}</math> tag with 15:1 <math>^{239}\text{Pu}/^{241}\text{Am}</math> ratio</i>	<i>90 Bq</i>		n.a.
<i>59.5 keV <math>^{241}\text{Am}</math> tag with 5:1 <math>^{239}\text{Pu}/^{241}\text{Am}</math> ratio</i>	<i>33 Bq</i>		n.a.

**Table 1.3.3** Expected  $^{239}\text{Pu}$  in lung and bioassay samples at four time intervals after intake and for different scenarios of contamination. An intake giving an effective dose of 20 mSv $y^{-1}$  was assumed.

Scenario of intake	Organ or sample	Time [d]			
		10 [d]	180 [d]	1 [y]	10 [y]
<i>Inhalation</i>					
absorption type M	lung [Bq]	31	8.0	2.5	<
	urine [Bq $l^{-1}$ ]	0.0094	0.0034	0.0024	0.00069
	feces [Bq]	0.36	0.011	0.0034	0.00028
absorption type S	lung [Bq]	140	77	65	8.2
	urine [Bq $l^{-1}$ ]	0.00053	0.00039	0.00040	0.00029
	feces [Bq]	1.6	0.089	0.053	0.0021
<i>Ingestion</i>					
$f_i = 5.0 \cdot 10^{-4}$	urine [Bq $l^{-1}$ ]	0.014	0.0028	0.0020	0.00072
	feces [Bq]	18	0.0014	0.0010	0.00028
$f_i = 1.0 \cdot 10^{-4}$	urine [Bq $l^{-1}$ ]	0.014	0.0031	0.0018	0.00068
	feces [Bq]	83	0.0013	0.0010	0.00026
$f_i = 1.0 \cdot 10^{-5}$	urine [Bq $l^{-1}$ ]	0.008	0.0017	0.0012	0.00044
	feces [Bq]	490	0.00076	0.00062	0.00017

### 1.4.1 DESCRIPTION OF THE ICRP 67 MODEL

The most recent and updated biokinetic model for Plutonium was presented in 1994 [74]. This model can also describe the metabolism of Americium and Neptunium with some modifications. It was developed from a previous model [75] with two main goals:

1. To introduce specific pathways for the urinary excretion in order to evaluate the effective dose to the urinary bladder, explicitly considered in the ICRP's new list of tissue weighting factors [26];
2. To implement the new information on the biokinetics of Plutonium in soft tissue that seems to suggest a greater retention of Plutonium in soft tissues at long times after exposure than thought previously.

The model is depicted in Figure 1.4.1. The compartments of the gastrointestinal tract affected in case of a systemic contamination are also given. The systemic model for Plutonium biokinetics is characterized by a mamillary compartmental structure with a "central" compartment, the blood, connected to all the other organs and tissues: Liver, soft tissues, skeleton, gonads, kidneys and the urinary bladder. Each organ or tissue is represented by one or more compartments. Except for the urinary bladder, all the compartments represent the kinetics of Plutonium, once it is absorbed in the tissues. The urinary bladder compartment instead represents an empty organ and is used here to describe the kinetics of Plutonium in the content of the organ, i.e. the urine.

The general structure was derived from an age-specific biokinetic model for Americium developed in the early nineties [76]. A second liver compartment was added for Plutonium. It was introduced mainly on kinetic rather than biological reasons in order to represent better the long-term retention of Plutonium in the liver. From a physiological point of view, this second liver compartment can be associated to the reticulo-endothelial system. The activity from the blood is transferred to the first liver compartment that represents the short-time hepatic retention. From there the activity is removed to both the gastrointestinal tract via biliary excretion and to the second liver compartment. The second liver compartment clears to the blood.

The kinetics of Plutonium in the soft tissues is modelled using three compartments, ST0, ST1 and ST2. The first, a soft tissue pool including also extracellular fluids and the fast exchange of Plutonium with blood, represents the early build-up and clearance of material in soft tissues. The compartments ST1 and ST2 are used to describe the intermediate (up to 2 years) and long term retention (many years), respectively, in those solid soft tissues such as muscle, skin, subcutaneous fat etc., not explicitly represented in the model.

The skeleton is represented by separate cortical and trabecular parts. In each part Plutonium kinetics is described using three compartments: Bone surfaces, bone volume and bone marrow. The activity first reaches the bone surface and then is subsequently transferred to bone marrow by bone resorption and to bone volume by bone formation. The activity in the bone volume is also transferred to bone marrow by resorption processes. From the bone marrow the activity reaches the blood, where then it is again re-distributed among all the organs and tissues.

The gonads compartment is used to describe the kinetics of Plutonium in testes (male subjects) and ovaries (female subjects). The activity from blood is transferred to the gonads with gender specific transfer rates, while it is removed from the gonads with the same rate for male and female.

The kinetics of Plutonium in the kidneys is modelled by two compartments: One represents the kidney tissue exchanging activity with the blood, and another describing the urinary path through which the Plutonium reaches the urinary bladder.

The activity accumulated in the urinary bladder is excreted with the urine. Three paths contribute to the activity in this compartment: The direct transfer from the blood, the blood contribution through the urinary path and the transfer of activity from the soft tissue compartment ST1.

The fecal excretion of Plutonium is also modelled. The systemic activity is transferred to the gastrointestinal tract via two pathways: From the first liver compartment to the small intestine (biliary secretion), and from the blood to the upper large intestine. These paths describe the contribution to the fecal excretion of Plutonium at short and long times after exposure.

The model is appropriate to simulate the metabolism of Plutonium both in male and female subjects. As mentioned before, gender specific transfer rates are given only for the gonads (testes and ovaries). Age specific transfer rates are defined by ICRP for six age classes: 3 months, 1, 5, 10 and 15 years and adults. Here an adult is a person at least 25 years old, whereas in previous publications of the ICRP concerning the biokinetics of other radionuclides, an adult was defined as at least 20 years old. The 25-rule is also used here for the development of new models, because the skeletal transfer rates are equated with bone formation rates, which are still elevated with respect to the mature skeleton at the beginning of the third decade of life. The transfer rates for an adult subject, useful for the monitoring of an internal contamination from an occupational exposure, are given in Table 1.4.1.

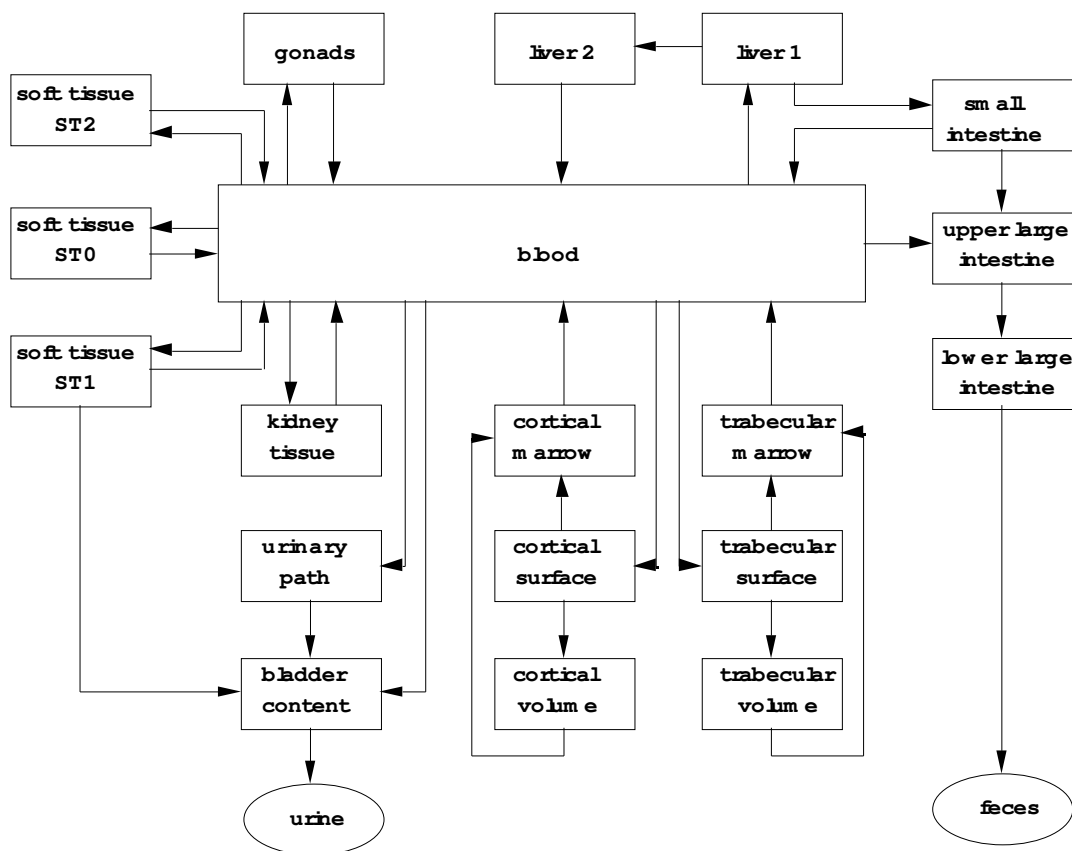


*Figure 1.4.1 The ICRP systemic model for Plutonium biokinetics. The affected gastrointestinal compartments are also shown.*

**Table 1.4.1** Transfer rates for the ICRP biokinetic model for Plutonium.

Compartments	Transfer rates [d <sup>-1</sup> ]
Blood to liver	0.1941
Blood to cortical surface	0.1294
Blood to trabecular surface	0.1941
Blood to urinary bladder content	0.0129
Blood to urinary path	0.00647
Blood to other kidney tissue	0.00323
Blood to ULI contents	0.0129
Blood to testes	0.00023
Blood to ovaries	0.000071
Blood to ST0	0.2773
Blood to ST1	0.0806
Blood to ST2	0.0129
ST0 to blood	0.693
Urinary path to urinary bladder content	0.01386
Other kidney tissue to blood	0.00139
ST1 to blood	0.000475
ST1 to urinary bladder content	0.000475
ST2 to blood	0.000019
Trabecular surface to volume	0.000247
Trabecular surface to marrow	0.000493
Cortical surface to volume	0.0000411
Cortical surface to marrow	0.0000821
Trabecular volume to marrow	0.000493
Cortical volume to marrow	0.0000821
Cortical marrow to blood	0.0076
Trabecular marrow to blood	0.0076
Liver 1 to Liver 2	0.00177
Liver 1 to Small Intestine	0.000133
Liver 2 to Blood	0.000211
Gonads to blood	0.00019

#### 1.4.2 COMMENTS ON THE ICRP 67 MODEL

The ICRP 67 model was designed mainly for dosimetry purposes. It allows to calculate dose coefficients considering explicitly the dose to the urinary system and bladder as suggested in the 1990 recommendations of the ICRP [26]. Activities in urine and feces can be also estimated and directly compared with the measurements of bioassay samples, normally collected after any Plutonium exposure. However, the modelling of Plutonium excretion, particularly in urine, seems to be plagued by some shortcomings. This may be suspected from the assumed transfer of activity from one of the soft tissue compartment (ST1) directly to the urinary bladder. This pathway was introduced in order to account for “...an apparent increase with time in fractional clearance of circulating plutonium...”, as explicitly stated in the publication where the model was presented [74]. Some considerations are given here in relation to this assumption.

The assumed transfer of activity from the soft tissue compartment to the urinary bladder content allows one to obtain good fits to empirical data, particularly at long times, for which it was expressively introduced, but lacks justification by any known physiological process. The same ICRP, commenting this assumption doesn't provide an idea of a physiological phenomenon that could justify this hypothesis. As the soft tissue compartment ST1 represents the retention of Plutonium in solid soft tissues (as muscle, fat, etc.), it is difficult to imagine a physiological process where a transfer of materials from such tissues to the urine occurs by-passing the blood.

Furthermore it is important to underline that the aforementioned assumption is not a marginal correction of the model, but plays a significant role in its ability to predict the urinary excretion. This is well pointed out in Figure 1.4.2.

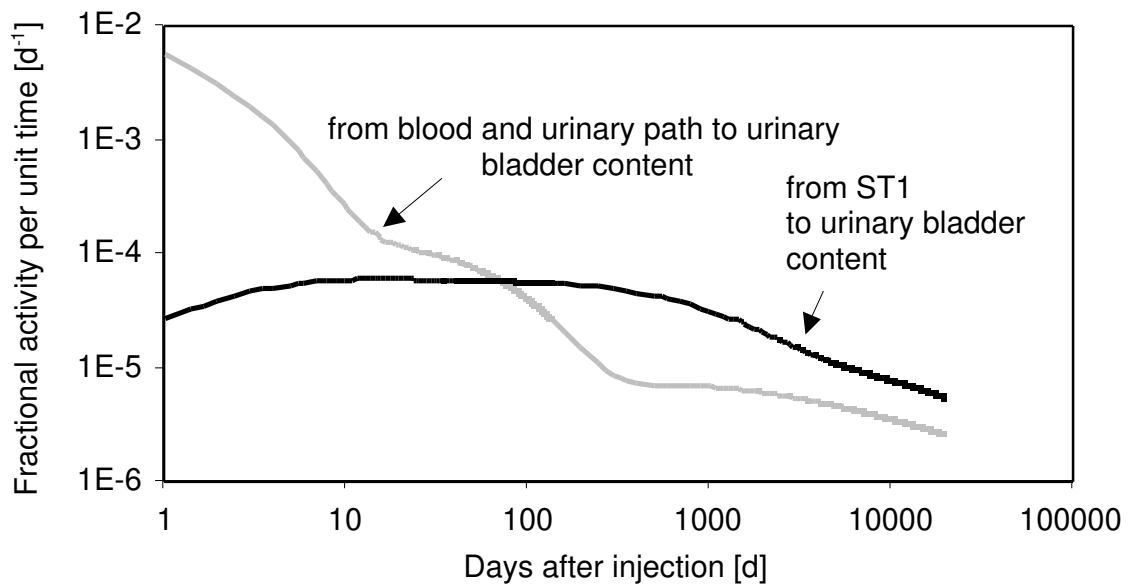


**Figure 1.4.2** Daily transfer of Plutonium activity to the urinary bladder from the soft tissue compartment ST1 and from blood (directly and through the urinary path compartment).

Here an acute systemic contamination (injection) due to an injection of Plutonium was assumed and the Plutonium transferred per unit time from blood, directly and through the urinary path, and from the ST1 soft tissue compartment to the urinary bladder was calculated.

The plot reveals that the contribution of the latter dominates the former by up to a factor of five after 100 days post injection. In other words, the urinary excretion in the ICRP model is mainly governed by a postulated fictional excretion pathway and the truly physiological mechanism of kidney clearance only plays a minor role. This is particularly important for the urinary excretion at long times, where the phenomenon of excretion enhancement is observed, and which available models fail to explain.





## Chapter 2

### Data and measurements



## 2.1 AVAILABLE INFORMATION ON PLUTONIUM METABOLISM

---

From a general point of view the study of the metabolism of a chemical element in humans is based on a combination of different kind of observations in relation to the considered element (the element itself or one of its surrogates) and to the organism (the man itself or other species) [77]. Therefore four kind of observation can be picked out: studies on the behaviour of the element in human subjects (H1) or on other mammalian species (A1), studies on the behaviour of surrogates of the element of interest in human subjects (H2) or on other mammalian species (A2). Besides these four primary sources of information, basic physiological data for the main human body functions are often taken into account.

For modelling purposes H1 data can be considered to be the most reliable data. Unfortunately H1 data are not often sufficient for characterizing completely the biokinetic behaviour of an element, even in case of specifically designed experiments, because of the limited number of involved subjects in the studies and the generally short time range of observation. If the H1 data are derived from not specifically designed experiments, for instance investigations on members of the public that incidentally introduced the element, further difficulties could occur. Examples are uncertainty in amount and pattern of introduced activity, atypical observed subjects (for age, health conditions) for radiation protection purposes of occupationally exposed subjects, uncertainty in the time of the intake. For these reasons other kinds of observations such as A1, H2 and A2 are often considered in order to complete the information that H1 data can't provide. Yet less confidence can be placed on these data for evaluating the metabolism of interest in humans.

Use of A1 data implicitly supposes that similarities in mammalian species, in relation to biochemistry, structure and function of cells and organs, can be translated in an analogous similarity in relation to the metabolism of elements. However quantitative differences in metabolism of elements were pointed out when qualitatively similar mammalian species were compared, even if data are scaled to take into account the most macroscopic differences as body size or known metabolic rates. Sometimes species can be reasonably considered human-like not from a general point of view but only for a well defined physiological process. All these reasons limit the cases in which confidence can be placed in the use of interspecies extrapolation data for modelling purposes.

The use of H2 is based on the evidence that chemically similar elements exhibit partially analogous physiological behaviour (e. g. Strontium and Calcium, Radium and Barium, Curium and Americium, Potassium and Rubidium). However only few elements are almost completely interchangeable regarding their biokinetic (e.g. Sodium and Potassium). More often some elements cumulate in the same organs and tissues following the same pattern but they show different kinetics (e.g. Potassium and Caesium). For the specific case of Plutonium, Hafnium was suggested as a possible surrogate [78], but there are always doubts on the suitability of using surrogates (a lanthanide as in this case) for studying the metabolism of actinide elements [79].

The use of A2 data is even more problematic because it requires an interspecies extrapolation on the basis of data obtained with elements chemically analogue to the element of interest.

In the specific case of studying the biokinetics of radioactive elements, effects of physical decay on the biokinetic were sometimes observed. For instance some studies attest different dissolution rates for  $^{238}\text{Pu}$  and  $^{239}\text{Pu}$  isotopes [11]. Animals exposed to aerosols of  $^{238}\text{PuO}_2$  exhibited an enhanced translocation from the lung and a lower accumulation in liver and skeleton as compared with animals exposed to aerosols of  $^{239}\text{PuO}_2$ . This process seems due to the specific activity of  $^{238}\text{Pu}$ , about two hundred and fifty times more than of  $^{239}\text{Pu}$ .

Therefore the radiolysis process, more significant for the latter radionuclide, generates small fragments of particles, thereby increasing the surface area and so the dissolution rate [11].

In the frame of developing a biokinetic model of Plutonium in humans, the use of H1 data, when available, is particularly recommendable. In the following three subparagraphs (2.1.1, 2.1.2 and 2.1.3) the most important studies based on both specifically designed experiments and uncontrolled events of contamination will be presented. Experiments based on intravenous injection of volunteers will be particularly considered because such studies can provide direct information on systemic biokinetic of Plutonium avoiding interference from Plutonium biokinetic in other organs and tissues relating to the pattern of intake (e.g. respiratory or gastrointestinal tracts). Investigations providing data and information relating to Plutonium activity in biological samples, particularly in urine, will be mainly considered as "in vitro techniques" are the most suitable for monitoring an internal contamination of Plutonium.

## 2.1.1 EXPERIMENTS ON HUMANS

### 2.1.1.1 Langham's study and relating works

The study carried out by Langham [80] and co-workers is one of the most famous and important investigations about metabolism and excretion of Plutonium in humans, thanks to the number of analyzed subjects and the long period of observation available up to the present. Between April 1945 and July 1946 twelve subjects were injected intravenously with known amounts of soluble plutonium  $^{239}\text{Pu}(\text{IV})$  in a citrate complex. The selection of the subjects was mainly based on their life expectancy: as a rule the chosen subjects were past forty-five years of age and suffering from chronic pathologies such that survival for ten years was highly improbable. Of twelve subjects, ten were past the age of forty-five. The group was composed of eight men and four women, coded from HP-1 to HP-12. In about two years five subjects died of their diagnosed illness. Urine samples were collected in 24-hour period except on the day the Plutonium was given. The first day 12-hours urinary samples were collected. Fecal samples were pooled during intervals of four days, except immediately after the Plutonium administration when the first two stools were collected separately. Blood samples too were collected but generally a smaller amount of data is available in comparison to the other bioassays. Tissue samples were obtained at autopsy on few dead subjects. In Langham's study further four subjects too were considered, coded Cal-I [81], Chi-1, Chi-2 and Chi-3 [82, 83, 84, 85, 86, 87]. The first was injected with  $^{238}\text{Pu}$  in a nitrate compound with Pu(VI) oxidation state. The latter subjects were injected with  $^{239}\text{Pu}$ , Pu(VI) oxidation state. These subjects too were terminally ill. Plutonium measurements carried out on their samples are mainly related to urinary excretion.

On the basis of the aforementioned data, relating to the first 138 days post-injection, a percentage daily urinary excretion function after an acute intake of plutonium was calculated:

$$eu(t) = 0.23t^{-0.77}$$

equation 2.1.1

A percentage daily fecal excretion was calculated as well:

$$ef(t) = 0.63t^{-1.09}$$

equation 2.1.2

The expression (equation 2.1.1) for the urinary excretion through 138 days was then adjusted by including data collected in the frame of the monitoring control of occupational exposure in Los Alamos Laboratory. Three subjects were considered. They accumulated significant amounts of Plutonium during wartime operations and Plutonium measurements in urine were available up to about five years (1750 days) after their last possible exposure. This last set of data is not analogous to the previous data from volunteers because the individuals received unknown amounts of Plutonium over an indefinite time period and via likely inhalation route. However Langham and co-workers made an attempt to use these data: they approximated a chronic variable intake in term of an effective single intake occurred at a certain effective time between the probable limits of exposure. This was carried out using the aforementioned urinary excretion function on the short time urinary excretion data. Then the experimental urinary excretion curve was fitted again extending it to 1750 days. The resulting expression for the percentage urinary excretion was:

$$eu = 0.20t^{-0.74} \qquad \text{equation 2.1.3}$$

Two subjects of Langham's study, a male and a female patient (HP-3 and HP-6), survived to their illness. Therefore further data on Plutonium biokinetics at long time after injection became available. Samples of urine, feces and blood were collected at about 10,000 days (around 27 years) after the injection [88, 89, 90, 91, 92,]. A review of the original injection experimental records was later carried out and additional data were found [93]. In this work it was evident that the data reported by Langham's group were not corrected for chemical recovery losses. Starting from this observation all the original data for the urinary excretion rate of Plutonium from Langham's study (Chi-3 and from HP-1 to HP12) were reviewed [94]. Through a literary research recovery correction factors of 90% for samples collected at 0-526 days post injection and of 67.4% at 1610-1648 days were adopted. No correction factors were necessary for samples collected at later time.

### 2.1.1.2 Further experimental investigations

In the last decade further studies were carried out in order to investigate Plutonium biokinetics in humans. New experiments based on intravenous injection of Plutonium isotopes into healthy volunteers were designed. Yet,  $^{239}\text{Pu}$ , the most important isotope in the radiation protection practice from Plutonium exposure, would have delivered a prohibitive radiation dose if injected into healthy subjects in the amount required for such studies. Therefore the use of other Plutonium isotopes was considered.  $^{237}\text{Pu}$  resulted as one of the best candidates. Studies in rats and beagles showed  $^{237}\text{Pu}$  can be a suitable metabolic tracer for other Plutonium isotopes with longer half time [95, 96].  $^{237}\text{Pu}$ , with 45.3 d half life and radioactive decay mainly due to electron capture (>99.99 %), delivers an effective dose significantly smaller than  $^{239}\text{Pu}$ , limiting the radiotoxicological effects for the same administered amounts. For instance in case of ingestion of  $^{237}\text{Pu}$  with any  $f_1$  values the effective dose per unit of intake is from 90 up to 2500 times smaller than  $^{239}\text{Pu}$  [97]. Moreover the x rays emitted during its decays would allow to study the patterns of organ uptake with direct measurement techniques. Even though all these characteristics, making  $^{237}\text{Pu}$  a suitable tracer for biokinetics studies, were known since long time, it was not previously used because of difficulties in producing it sufficiently free of other Plutonium isotopes potentially delivering much larger effective doses.

Recent technologic developments in Plutonium isotopes production made available amounts of  $^{237}\text{Pu}$  with increasing levels of isotopes purity. Metabolism of Plutonium was investigated following intravenous injection of  $^{237}\text{Pu}$  as Pu(IV) citrate in two healthy male volunteers [98, 99]. Excreta and blood samples were collected at intervals during the first 21 days and measurements of their Plutonium content were carried out. The patterns of hepatic and skeletal uptake too were monitored up to 153 days after injection with an external scintillation counter located close to liver, sacrum, knees and skull. Yet, these measurements provided only a limited information on organs uptake because of the difficulties in discriminating the contributions from activity in adjacent tissues and blood.

Following the same experimental methodology, ten further volunteers were intravenously injected with  $^{237}\text{Pu(IV)}$  [100]. Larger amounts of Plutonium were administered in order to detect it in bioassays for a longer time after injection. Moreover six women were included in the studied groups of volunteers and sex-related differences in Plutonium metabolism, particularly in the excreta, were investigated and considerations were extended also to other actinides [101]. Samples of urine, feces and blood were collected and measured at intervals for the first 21 days after injection. Further samples were collected and analyzed at around 40 and 90 days post injection. Measurements of hepatic uptake and gonads deposition were also carried out [102, 103].

## 2.1.2 EMPIRICAL CURVES

The original data set from Langham's subjects has been used and re-evaluated numerous times over the years by various researchers. This confirms the importance and originality of these first experiments that were for different decades the only source of direct knowledge about Plutonium biokinetics. One of the first modifications of Langham's urinary excretion curve was proposed by Beach and Dolphin [104] to distinguish two phases in the Plutonium excretion: an initial rapid excretion of the injected Plutonium in the citrate form and the lower excretion rate of metabolized plutonium. This approach yielded a non-integrable equation for which a graphical solution was provided.

As a result of the developments in computer programming slight discrepancies were observed between Langham's function and the functions calculated by minimization routine with computer. On this basis the following function for the percentage daily urinary excretion was calculated by Robertson and Cohn [105] with the Brookhaven Merlin computer:

$$eu(t) = 0.193t^{-0.721}$$

*equation 2.1.4*

Yet the most important and interesting re-evaluation of Langham's subjects data set was carried out at the beginning of seventies by Durbin [106]. A meticulous re-examination of the original data was carried out particularly considering the physiological and health status of the investigated subjects and integrating the available data with occupational exposure and laboratory animals' data. The need of a Plutonium urinary excretion curve representative of an adult human being in good health was pointed out. Therefore only the data from those subjects without abnormal kidney function or abnormal plasma Plutonium binding due to anaemic status were considered, because irregular Plutonium urinary excretion rates were observed for subjects characterized by such pathologies. Moreover differences in biokinetics of Pu(IV) and Pu(VI) were pointed out, particularly for the early urinary excretion. As the Pu(IV) oxidation state was deemed likely to be the chemical form of Plutonium commonly

encountered in occupational exposure cases, Pu(VI) injection cases of Langham's studies were omitted. The long term excretion rates were determined on the basis of one of Langham's subjects and four occupational exposed persons. A five exponential terms function was finally calculated for the percentage daily urinary excretion:

$$eu(t) = 0.41e^{-0.578t} + 0.12e^{-0.126t} + 0.013e^{-0.0165t} + 0.003e^{-0.00231t} + 0.0012e^{-0.000173t}$$

*equation 2.1.5*

The main difference of Durbin's function from Langham's one (equation 2.1.3) is represented by long term excretion components. However attention must be paid in using it because of the limited number of long term excretion data on which Durbin's function is based.

A function for the Plutonium excretion in feces was also provided, but the small number of data obliged to consider data from laboratory experiments on animals, particularly for calculating the long term excretion rates when almost no human data were available. Also in this case only subjects in reasonably good health conditions for fecal excretion modelling purposes were considered. Therefore only subjects with liver and digestive tract function presumed to be within normal limits were included. The calculated function for the percentage daily fecal excretion of Plutonium is:

$$ef(t) = 0.60e^{-0.347t} + 0.16e^{-0.105t} + 0.012e^{-0.0124t} + 0.002e^{-0.00182t} + 0.0012e^{-0.000173t}$$

*equation 2.1.6*

Over the years the underestimation of long term Plutonium urinary excretion was identified as one of the most significant deficiency in Langham's model that, even in Durbin's analysis, was not completely cured, although long term excretion components were introduced. This was pointed out for the first time by Hempelmann and co-workers in their 27-years follow-up of selected groups of Manhattan Project workers [107] and partially quantified in the following studies based on measurements from occupationally exposed subjects [108]. A better quantification of the underestimation of long term urinary excretion of Plutonium was possible when the results of a follow-up study of few of the Langham's original injection cases, who survived their illness, were made available [88]. It resulted that the urinary excretion rates at 10,000 days post injection were approximately of an order of magnitude greater than predicted by Langham's or Durbin's functions.

An attempt of curing the underestimation of Plutonium long term excretion predicted by the available functions was carried out by Parkinson and Henley [109]. They calculated a new excretion function by estimating the long term urinary excretion using the contemporary metabolic model recommended by ICRP [110]. The short term urinary excretion used in the fitting procedure was estimated by means of equation 2.1.1 from Langham's study. It must be noted that this is the function proposed by Langham before introducing any correction on the basis of long term excretion data from Los Alamos occupational exposure cases. The percentage daily urinary excretion function calculated by Parkinson and Henley is:

$$eu(t) = 0.19e^{-0.272t} + 0.023e^{-0.0237t} + \\ + 0.0052e^{-0.00303t} + 0.00086e^{-0.0000190t}$$

*equation 2.1.7*

The data for long term Plutonium excretion from those subjects of Langham's study who survived their illness [88] were for the first time expressively considered for function fitting purposes by Jones [111]. In his study he considered only those urinary excretion data judged in Durbin's review to be representative of persons in normal health and intravenously injected with Plutonium in the form Pu(IV). A four component exponential function was calculated:

$$eu(t) = 0.475e^{-0.558t} + 0.0239e^{-0.442t} + \\ + 0.00855e^{-0.00380t} + 0.00142e^{-0.0000284t}$$

*equation 2.1.8*

A good description of the long term urinary excretion, better than Langham's function does, was pointed out already after 100 days post injection. This function was validated by studies on a number of occupational exposure cases from Sellafield nuclear site. The author also pointed out a more realistic estimate for long term Plutonium retention when compared to autopsy data.

Langham's function was later empirically corrected to avoid the underestimation of long term urinary excretion by Leggett and Eckerman [112]. A time dependent correction factor was introduced in the form  $1+kt$  where  $k$  is a suitable constant and  $t$  is the number of days after injection. By comparing the observed long term data and predictions based on Langham's function the authors estimated the value of  $k$  and obtained the following function:

$$eu(t) = 0.2(1 + 0.0008t)t^{-0.74}$$

*equation 2.1.9*

In recent years data of Plutonium excretion following a contamination event through wound were also considered for excretion modelling purposes. Data obtained over 6,500 days post incident were considered. Long term systemic excretion rates were evaluated by assuming that no significant long term transfer of Plutonium to blood from either the wound site or the lymphatic system occurred. On the basis of both these data and revised Langham's injection data [94] for evaluating long and short urinary excretion, respectively, a new percentage daily excretion function was calculated [113]:

$$eu(t) = 0.569e^{-0.658t} + 0.0405e^{-0.0961t} + \\ + 0.0137e^{-0.00751t} + 0.00277e^{-0.0000405t}$$

*equation 2.1.10*



A verification of the function was also carried out by comparing the estimated systemic retention of Plutonium to post mortem data available for this contamination case via wound. A good agreement between function predictions and experimental data was observed.

The data collected from occupational exposed workers contaminated via paths as inhalation and ingestion were recently considered for modelling Plutonium excretion in order to evaluate a systemic excretion function as in the previous injection studies.

One of the most important attempts in this field was carried out considering the large data set of the occupationally exposed workers from Mayak radiochemical plant [114]. Data from 130 workers were included, aged from 38 to 73 years at the time of urine collection for analysis and with different levels of health impairment. An excretion factor ( $K_s$ ), as the fraction of the overall systemic content of the radionuclide excreted daily in urine, was calculated. It was exactly defined as the ratio of mean  $^{239,240}\text{Pu}$  level in daily volume of urine by the retained systemic body burden. The latter one was estimated by post mortem radiochemical analysis of organs and tissues of the same individual. Sums of five exponential terms were adopted for describing urinary and fecal excretion of Plutonium. The parameters of the fifth summand describing long term excretion in urine were estimated on the basis of the excretion factor  $K_s$  calculated for a sub-group of workers resulted without significant health impairment. Leggett's ratio of Plutonium in daily excreted urine and feces [115] was used to evaluate the same parameters for the fecal excretion. The parameters of the first four summands describing the early and intermediate excretion in urine and feces were directly taken from Durbin's equations (equation 2.1.5 and equation 2.1.6): actually only slight discrepancies probably due to rounding process can be pointed out among Khokhryakov's and Durbin's parameters. The calculated function for the percentage daily urinary excretion of Plutonium is:

$$eu(t) = 0.41e^{-0.56t} + 0.12e^{-0.126t} + 0.013e^{-0.0165t} + 0.003e^{-0.00231t} + 0.0013e^{-0.00002t}$$

*equation 2.1.11*

For the fecal excretion of Plutonium the relating function is:

$$ef(t) = 0.60e^{-0.35t} + 0.16e^{-0.105t} + 0.012e^{-0.0124t} + 0.002e^{-0.00182t} + 0.00052e^{-0.00002t}$$

*equation 2.1.12*

The aforementioned functions are useful to predict systemic excretion in practically normal individuals at any time between 1 day and 40 years following a systemic uptake. The authors pointed out that the new function for the urinary excretion roughly coincides with the estimates obtained with Jones's function (equation 2.1.8) in spite of the different forms of the equations. They also stressed that excretion rates in individuals with impaired health may increase by factors of 1.7 to 2.6 depending on the gravity of the disease, as compared with that in practically normal individual.

The last significant contribution to the knowledge about systemic excretion of Plutonium is due to Sun' and Lee's study [116]. A four compartments model was developed describing Plutonium retention in four organs: blood, bone, liver and other generic tissues. On the basis of Leggett's systemic whole body retention function [115] the single retention

function for each of the considered organs was calculated. The urinary and fecal excretion functions were then calculated multiplying the retention functions in liver and blood by the relative excretion transfer rates, respectively. The calculated function for the percentage daily urinary excretion is:

$$eu(t) = 0.8344e^{-0.693t} + 0.06587e^{-0.03t} + 0.003870e^{-0.0028t} + 0.001254e^{-0.0000216t}$$

*equation 2.1.13*

For the fecal excretion of Plutonium the calculated function is:

$$ef(t) = -0.002811e^{-0.693t} - 0.005870e^{-0.03t} + 0.007936e^{-0.0028t} + 0.0007450e^{-0.0000216t}$$

*equation 2.1.14*

It should be stressed that negative coefficients resulted for the fecal excretion function.

### 2.1.3 OCCUPATIONAL EXPOSURES

Over the years the numerous applications of Plutonium and other transuranium elements in civil and military field has determined an increasing number of workers exposed to the risk of an internal contamination. The monitoring of contaminated workers has enabled to collect several data relating to Plutonium in bioassays after occupational exposures. Most of these data are today available in scientific literature. Even if these cases relate to expositions through not only systemic path, they were recently used also for determining systemic biokinetics of Plutonium, as in the aforementioned study of Khokhryakov and co-workers [114]. Yet it is often difficult to extrapolate information on the systemic behaviour of a radionuclide from such kind of observations.

Data sets based on the results from the monitoring of occupational exposed workers are more commonly and easily used for checking models. Yet, even for verification purposes, some minimal characteristics are required:

- Complete information on the scenario of the contamination is given, such as working activities carried out by the subjects, protection facilities adopted, commonly manipulated compounds and their chemical form;
- Multiple kinds of data are available for the same contamination event as activity in different bioassay samples, direct measurements when feasible, workplace monitoring measurements;
- The data set covers a significantly long time period after the contamination event;
- An exhaustive information about health impairments occurred in subject's life are given, with particular care to those illnesses that could significantly influences the radionuclide biokinetics.

Information on the scenario of the contamination should firstly enable to make realistic assumptions about the most probable path of intake that, in case of an occupational exposure, will be basically inhalation, ingestion or introduction through wound. The path of intake plays a particular role because of its strong influence on the biokinetics of a

radionuclide. For instance discrepancies in dose assessments of several orders of magnitude are possible between via inhalation or ingestion hypotheses of intake [97]. Accidental events such as damage on radiation protection facilities or errors in the manipulation activities can provide information on the most probable time of intake. When such events can't be determined, a continuous and constant rate of intake can be realistically assumed.

Path of intake and time modality can be better established if the information on the scenario of the contamination is integrated with available workplace monitoring measurements. For instance anomalous level of air radioactivity concentration can suggest a probable contamination via inhalation. Furthermore if multiple stage impactors are used to sample the air in the working area, aerosol size distribution can also be determined and condition of exposure can be realistically quantified. Sometimes nose wipe measurements can be a useful way of discriminating a prevalent contamination via inhalation. Information on chemical form of contaminating compound can also be obtained from air or surface monitoring measurements.

Availability of multiple kinds of measurements on contaminated subjects such as direct and indirect measurements is extremely useful because they provide information on model accuracy in describing the numerous physiological processes and on the truthfulness of initial assumptions.

Information strictly related to the health status of the subjects are also important because it was already observed that pathologies and illnesses can significantly change the biokinetic of a radionuclide in human body. Examples were already given in Durbin' and Khokhryakov's studies [106, 114] where significant enhancement of Plutonium urinary excretion was observed in subjects with different health impairments.

Finally data sets must cover a time period comparable with the effective half life of the radionuclide in human body. In fact the shorter is time series of available measurements, the greater the possibility of fitting them with different models or the same model but with different initial assumptions (time or path of intake, chemical and physical characteristics, etc.). In the specific case of Plutonium and other long-lived radionuclides time series from several years up to decades could be necessary.

Unfortunately few data sets relating to Plutonium occupational exposures comply all the aforementioned conditions. Among those ones available in scientific literature, two main data sets should be considered: Manhattan Project Workers (MPW) and United States Transuranium and Uranium Registries (USTUR) data sets. The former is composed by the results of the monitoring of twenty-five male subjects who worked with Plutonium at what is now the Los Alamos National Laboratory (Los Alamos, New Mexico, US) in the days of the Manhattan Project during World War II. They were engaged in different activities under extraordinarily cruel working conditions and therefore with high risk of Plutonium exposure, mainly from recovery operations. They have been monitored for a long time and, for some of these subjects, medical follow-up and bioassay measurements are available up to recent years [107, 108, 117, 118, 119, 120]. The second data set relates to workers generally engaged in Plutonium industries [121], even if the societies or laboratories where they carried out their activities are less clearly stated. Some of the subjects included in this data set can also be found in Manhattan Project workers data set under different codes.

Among all the contamination cases reported in these two data sets, a further selection should be carried out in order to facilitate the use of them for verification purposes of Plutonium urinary excretion predicted by a model.

Firstly, measurements of urinary excretion should be available because other kind of bioassays (feces or blood) or direct measurements of activity in organs and tissues offer only indirect information on urinary excretion. The measurements should be always higher than

the minimum detectable activity of the adopted measuring technique because of difficulties in fitting model with values “less than” a certain quantity. The contamination event should be characterized by a unique path of intake because of the difficulties in evaluating the contributions to the urinary excretion from different intake patterns. Furthermore the time modality of intake should be acute or approximately analogous in order to avoid the uncertainty due to hardly verifiable hypothesis on constant rates of intake, or times of repetitive singles intakes. Finally patients subjected to chelating therapy (as with DTPA) should be avoided too because of the enhancement of Plutonium urinary excretion observed in such subjects.

Complying the aforementioned conditions nine contamination cases were extracted from the Manhattan Project Workers and United States Transuranium and Uranium Registries data sets. In Table 2.1.1 they are shortly presented, together with the number of urine samples suitable for checking model’s predictions of urinary excretion. In fact in the present work for each considered subject those urine samples collected and analyzed before 1957 were disregarded because only after this year corrections were systematically determined and applied for chemical and physical analysis [121]. As for all the selected cases the most significant intakes occurred in the period 1945-1946 and in any case before 1950, the long period between the intake and the chosen measurements assures also that the same measurements are not significantly influenced by the actual time modalities of intake. Therefore these cases of contamination can be reasonably considered as due to an acute intake.

**Table 2.1.1** Occupational contamination cases selected from Manhattan Project Workers (MPW) and United States Transuranium and Uranium Registries (USTUR) data sets.

Subject’s code	Data set	Birth year	Number of useful samples of Pu urinary excretion
242	USTUR	1909	107
193*	USTUR	1920	105
4	MPW	1919	105
208	USTUR	1915	64
25	MPW	1918	21
10	MPW	1912	21
18	MPW	1922	20
7	MPW	1907	10
21	MPW	1924	8

\* it is also present in MPW under the code “27”.

## 2.2 A DESCRIPTION OF THE UPDATED CONTAMINATION CASE

---

The contamination incident investigated in the present work is one of the best documented cases of a single intake of transuranium elements worldwide ( $^{238}\text{Pu}$ ,  $^{239}\text{Pu}$ ,  $^{240}\text{Pu}$ ,  $^{241}\text{Pu}$ , and  $^{241}\text{Am}$ ). This contamination case complies quite well the requirements previously described for using a data set of occupational exposure for model verification purposes. Furthermore it shows two important aspects:

- The measurements carried out in recent years in occasion of dose assessments intercomparisons showed a significant enhancement of Plutonium urinary excretion, particularly at long time after contamination. This was already pointed out, but at a lesser extent, in other contaminated subjects [122];
- The Plutonium mixture introduced by the subject contains  $^{241}\text{Am}$  too, giving the possibility of carrying out direct measurements of organs activity burden, otherwise hardly detectable in case of a contamination of pure Plutonium.

For such characteristics it was already proposed as a case study in different intercomparisons on dose assessment. It is present as “Case 8” in the IAEA intercomparison [123] and it is the base for “Case 6” in the 3<sup>rd</sup> European intercomparison [124]. At the time of the intercomparisons there was already a set of excretion and organ burden data from the first day after the intake up to almost ten years [125]. Since 1983 direct measurements of Americium burden in different organs were carried out also in Forschungszentrum Karlsruhe [126]. In the frame of the present work in 1999 a complete follow-up of this case was carried out in Forschungszentrum Karlsruhe and new data for the Plutonium and Americium amounts in bioassays (urine, feces and blood) and for the Americium organs burdens were obtained. The results of these direct and indirect measurements are extensively presented in the two paragraphs 2.3.3 and 2.4.3, respectively.

### 2.2.1 THE CONTAMINATION EVENT

The working area where the contamination event occurred was a radiochemical laboratory for the development of advanced nuclear fuel in a nuclear research centre. In the laboratory nuclear fuels microspheres had been produced in a glove box using a special gelling technique. The waste water resulting from this technique was routinely collected and evaporated in the box. The residual waste water deriving from this process was transferred into a second glove box for further evaporation and successive disposal.

The subject (male, 26 years old at that time, 91 kg weight, 179 cm height) was working at the first glove box where the fuel microspheres were produced. On 24.05.83 at 4:15 PM an explosion occurred in the second glove box during the evaporation of three litres waste water as a consequence of a unexpected exothermic reaction. The subject left the laboratory immediately after the explosion, yet he resulted strongly contaminated at face, hairs and clothes. He was immediately decontaminated in the radiation protection unit of the research centre and nose swabs with bronchial slime samples were collected.

In the glove boxes the washing water contained Plutonium and Uranium in a mixture of hydroxide gel with 10 % of ammonium nitrate and about 3.5 % of hexamethylentetramine. The  $\alpha$  activity composition of the substance causing the internal contamination of the subject was 9 %  $^{238}\text{Pu}$ , 55 %  $^{239}\text{Pu}$ , 26 %  $^{240}\text{Pu}$  and 10 %  $^{241}\text{Pu}$ . The  $^{241}\text{Pu}$  activity was 750 % of the total  $\alpha$  activity. Size distribution analysis of dust samples collected in the laboratory was also carried out by means of scanning electron microscope exposures and x ray analyses. The diameter of the particles containing Plutonium resulted to be between 3 and 40  $\mu\text{m}$ .

## 2.2.2 AVAILABLE MEASUREMENTS

Immediately after the accident samples of nasal swab and bronchial slime were collected and  $^{239}\text{Pu}+^{240}\text{Pu}$  activity of  $5.5\cdot 10^{-3}$  and  $1.4\cdot 10^{-3}$  Bq were measured, respectively. The other measurements [123, 124, 126] are given in the following tables. The first available data for direct measurements of  $^{241}\text{Am}$  burden in lung are given in Table 2.2.1. In recent years direct measurements of activity in lungs and other organs were carried contemporarily by two different laboratories and the results are presented in Table 2.2.2. The data for the measurements carried out on bioassays (urine and feces) are given in Table 2.2.3 and Table 2.2.4 for urine and feces, respectively.

**Table 2.2.1**  $^{241}\text{Am}$  burden in lungs for the contaminated subject.

Time post intake [d]	Lung burden of $^{241}\text{Am}$ [Bq]	Uncertainty [%]	Time post intake [d]	Lung burden of $^{241}\text{Am}$ [Bq]	Uncertainty [%]
0	390	25	44	230	25
1	310	25	160	220	25
3	230	25	164	230	25
6	240	25	357	220	25
15	230	25	1077	240	25
34	230	25	2925	180	25
38	260	25			

**Table 2.2.2**  $^{241}\text{Am}$  burden in lungs and other organs for the contaminated subject. The measurements were carried out by two different laboratories (PNL, Pacific North-West Laboratory and FZK, Forschungszentrum Karlsruhe).

Time post intake [d]	Laboratory	Organ	Burden of $^{241}\text{Am}$ [Bq]	Uncertainty [%]
3724	PNL	Lymph node	26	14
3724	PNL	Lung	120	13
3724	PNL	Bone	69	12
3724	PNL	Liver	57	16
3828	FZK	Lymph node	72	29
3828	FZK	Lung	120	21
3828	FZK	Bone	65	12
3828	FZK	Liver	24	33
5110	FZK	Lymph node	76	11
5110	FZK	Lung	133	10
5110	FZK	Bone	95	11
5110	FZK	Liver	17	30

**Table 2.2.3** Daily urinary excretion of  $^{241}\text{Am}$ ,  $^{238}\text{Pu}$ ,  $^{239}\text{Pu}$  and  $^{240}\text{Pu}$  for the contaminated subject.

Time post intake [d]	Daily urinary excretion [Bq d <sup>-1</sup> ]	Uncertainty [%]	Daily urinary excretion [Bq d <sup>-1</sup> ]	Uncertainty [%]
	$^{239}\text{Pu}+^{240}\text{Pu}$		$^{241}\text{Am}+^{238}\text{Pu}$	
1	$1,10\cdot 10^{-2}$	30	$1,10\cdot 10^{-1}$	30
2	$4,10\cdot 10^{-2}$	30	$1,00\cdot 10^{-1}$	30
14	$4,70\cdot 10^{-3}$	50	$1,60\cdot 10^{-2}$	30
21	$3,70\cdot 10^{-3}$	50	$1,10\cdot 10^{-2}$	30
31	$3,70\cdot 10^{-3}$	50	$5,60\cdot 10^{-3}$	50
37	$5,60\cdot 10^{-3}$	50	$5,60\cdot 10^{-3}$	50
43	$3,70\cdot 10^{-3}$	50	$5,20\cdot 10^{-3}$	50
181	$3,70\cdot 10^{-3}$	50	$4,60\cdot 10^{-3}$	50
368	$3,50\cdot 10^{-3}$	50	$4,00\cdot 10^{-3}$	50
607	$2,90\cdot 10^{-3}$	40	$3,40\cdot 10^{-3}$	37
1075	$3,70\cdot 10^{-3}$	50	$2,70\cdot 10^{-3}$	50
1922	$5,90\cdot 10^{-3}$	36	$4,70\cdot 10^{-3}$	34
2090	$6,20\cdot 10^{-3}$	33	$3,80\cdot 10^{-3}$	32
3902	$3,40\cdot 10^{-3}$	18	$2,60\cdot 10^{-3}$	15
	$^{238}\text{Pu}+^{239}\text{Pu}+^{240}\text{Pu}$		$^{241}\text{Am}$	
2528	$6,70\cdot 10^{-3}$	17	$4,30\cdot 10^{-3}$	20
2923	$4,60\cdot 10^{-3}$	23	$2,30\cdot 10^{-3}$	22

**Table 2.2.4** Daily fecal excretion of  $^{241}\text{Am}$ ,  $^{238}\text{Pu}$ ,  $^{239}\text{Pu}$  and  $^{240}\text{Pu}$  for the contaminated subject.

Time post intake [d]	Daily fecal excretion [Bq d <sup>-1</sup> ]	Uncertainty [%]	Daily fecal excretion [Bq d <sup>-1</sup> ]	Uncertainty [%]
	$^{239}\text{Pu}+^{240}\text{Pu}$		$^{241}\text{Am}+^{238}\text{Pu}$	
1	$5,20\cdot 10^{+3}$	15	$1,50\cdot 10^{+3}$	15
2	$3,00\cdot 10^{+3}$	15	$7,40\cdot 10^{+2}$	15
3	$4,40\cdot 10^{+2}$	15	$7,40\cdot 10^{+2}$	15
13	$6,70\cdot 10^{-1}$	20	$1,60\cdot 10^{-1}$	50
21	$7,20\cdot 10^{-1}$	20	$1,50\cdot 10^{-1}$	50
30	$6,70\cdot 10^{-1}$	20	$1,20\cdot 10^{-1}$	50
37	$2,50\cdot 10^{-1}$	20	$7,80\cdot 10^{-2}$	50
44	$2,10\cdot 10^{-1}$	20	$5,90\cdot 10^{-2}$	50
181	$4,20\cdot 10^{-1}$	24	$9,40\cdot 10^{-2}$	50
369	$2,60\cdot 10^{-1}$	44	$5,90\cdot 10^{-2}$	50
607	$2,60\cdot 10^{-1}$	50	$7,50\cdot 10^{-2}$	50
	$^{238}\text{Pu}+^{239}\text{Pu}+^{240}\text{Pu}$		$^{241}\text{Am}$	
1075	$7,00\cdot 10^{-2}$	50	$1,80\cdot 10^{-2}$	41
1922	$9,50\cdot 10^{-2}$	50	$2,50\cdot 10^{-2}$	50
2527	$3,40\cdot 10^{-2}$	15	$1,20\cdot 10^{-2}$	17
2923	$1,30\cdot 10^{-2}$	19	$5,60\cdot 10^{-3}$	29



## 2.3 ACTIVITY MEASUREMENTS IN ORGANS

---

In the following section basic principles relating to direct measurements of activity in organs are presented. The presentation is limited to those principles and techniques adopted specifically for carrying out measurements of Americium activity on the aforementioned case of contamination. The relative results are presented in the last part of this section.

Particular care is taken in presenting those aspects characterizing a direct measurement of transuranium elements in human body by low energy photon emissions in comparison to indirect measurement of alpha particles emissions from bioassay samples, the technique described in the last section. Therefore shieldings, detectors physics, detector-source configuration and calibration procedures were emphasized, whereas for electronic devices (preamplifier, amplifier, multichannel analyzer and signal elaboration), common to *in vivo* and *in vitro* measurements and to other kind of radiation spectroscopy applications, one should refer to the available scientific literature.

### 2.3.1 BASIC MEASUREMENT PRINCIPLES

#### 2.3.1.1 *Shielding*

In order to perform direct measurements of low level x and gamma emitters in organs the background radiation must be limited. The main radiation sources are:

- natural radioactivity in detectors materials;
- cosmic radiation;
- natural radioactivity in building materials;
- radioactive gas and dust naturally present in the area of measurements.

The detector and mounting materials normally contain natural radionuclides sometimes in significant amount. For example NaI(Tl) detector contains also a homologue element of Sodium, the Potassium, with its radioactive isotope  $K^{40}$  [127]. The presence of radionuclides and the amounts of their activity in detecting materials can be controlled and limited only at the moment of detector design and production.

Primary cosmic radiation is mainly given by protons, helium nuclei and other nuclei. The interaction with atmosphere elements produces secondary cosmic radiation composed by charged particles, mesons and neutrons with fluxes of about  $0.01 \text{ particles.cm}^{-2}\text{s}^{-1}\text{sr}^{-1}$ . These indicative values are strongly dependent on the atmospheric pressure. For instance a decrease of 1 cm Hg of atmospheric pressure, decrease neutron flux of about 10 % [127]. The interaction of secondary cosmic radiation with detectors and surrounding materials generates further radiations with decreasing energies distribution towards low energy.

Radioactive elements too present in the building materials contribute to enhance background radioactivity. Radionuclides as  $^{40}\text{K}$  and others from natural radioactive series of  $^{232}\text{Th}$ ,  $^{235}\text{U}$  and  $^{238}\text{U}$  give the main contribution. Other elements from radioactive fall-out can also be present. An example of activity concentration in building materials for few common natural radionuclides is given in Table 2.3.1.

The most common way of decreasing the interference from cosmic radiation and natural radioactivity in building material is based on shielding construction. The detection system is surrounded by shielding barriers or often is directly located in shielded rooms. Lead or steel is normally used because their high Z atomic number assures the absorption of mostly high energetic radiations. When available pre-World War II naval plate steel is preferred because much steel made since the war contains radionuclides from global fall-out and  $^{60}\text{Co}$  used in the steel manufacturing process [67]. After the interaction with such shielding

elements the spectral distribution of background radiations shows a preponderance at low energies which is due to the degradation of  $\gamma$  photons by multiple Compton scattering in the shield. The interaction of natural radiation with Lead shield reduces background below 250 keV but adds lead fluorescence x rays of about 80 keV. To reduce this component further layers are used in decreasing order of Z (e.g. Lead, Cadmium and Copper) to absorb the characteristic x rays emitted by the preceding shield layer. Therefore a covering with Cadmium ( $Z=48$ ) absorbs Lead x rays but add its own fluorescence x rays of about 22 keV. Thus, a final covering with Copper is used to absorb Cadmium fluorescence x rays. Copper fluorescence x rays of about 8 keV can be neglected because they fall below the energy region, even for low energy photon measurements [61].

Contributions to the natural background from gas and dust are due to  $^{222}\text{Rn}$  and  $^{220}\text{Rn}$ , daughters of  $\text{Ra}^{226}$  and  $\text{Th}^{232}$ , together with their progenies that can diffuse in the air from the building materials and the ground. This source of radioactivity is normally limited with ventilation system filtering the air introduced in the shielded rooms where the detection system is located.

**Table 2.3.1** Activity concentration in building materials for few common natural radionuclides.

Material	Country	Average activity concentration [ $\text{Bqkg}^{-1}$ ]		
		$^{226}\text{Ra}$	$^{232}\text{Th}$	$^{40}\text{K}$
<i>Natural Origin</i>				
granite	Germany	100	80	1200
granite	Russia	110	170	1500
tuff	Italy	130	120	1500
pumice stone	Germany	130	130	1100
concrete with alum	Sweden	1500	70	850
<i>Industrial Origin</i>				
phosphorite chalk	Germany	600	< 5	110
phosphate chalk	Great Britain	800	20	70
calcium silicate	Canada	2150	-	-
calcium silicate	USA	1400	-	-
red mud brick	Germany	280	230	330
ash	Germany	210	130	700
aggregate of coal, ash and concrete	Finland	100	70	190

### 2.3.1.2 Detectors

Different kinds of detectors are available for direct measurements of activity in human organs. For the particular case of detecting low energy photon emitters two kinds of detecting

systems were used in the frame of the present work: a phoswich scintillation detector system and a semiconductor detector system.

The “phoswich” detector (from “phosphor sandwich”) is based on the scintillation mechanism occurring in some inorganic crystals when exposed to a field of ionizing radiations [128].

The luminescence of inorganic scintillators can be explained on the basis of allowed and forbidden energy bands of a crystal. In an atom the electronic energy states are composed by discrete energy levels that are usually represented with an energy level diagram composed by single lines. In a crystal composed by numerous atoms, the single atomic energy levels merge to form a band of allowed energy states. In the ground state of the crystal, the uppermost allowed band that contains electrons, called valence band, is completely filled whereas the next allowed band, called conduction band, is empty. The two bands are separated by a forbidden energy band where, in case of an ideal pure crystal, electrons can never be found. Absorption of energy produces the elevation of an electron from its normal position in the valence band into the conduction band, consequently forming a hole in the valence band. In case of a pure crystal the return of the electron from the conduction to the valence band is an inefficient mechanism of luminescence production. In fact the typical energy gap determines too high energetic photon to lie in the visible range, where the optoelectronic devices work more efficiently.

In order to enhance the probability of visible photon emissions, small amounts of impurities are commonly added to inorganic scintillators forming energy states between valence and conduction band. These impurities are called activators and their energy states may exist at a ground and excited level. Transition among these levels can efficiently produce scintillation visible photons.

An ionizing radiation crossing a crystal produces charged particles that will form a large number of electron-hole pairs by elevating electrons from the valence to the conduction band. The positive hole will drift to the location of an activator site ionizing it while the electron will migrate through the crystal until it encounters an ionized activator. The electron can so drop in the impurity site creating a neutral impurity configuration with its own energy states in the forbidden gap of the crystal. If the activator state is in an excited configuration a transition will occur quickly and with high probability with the emission of a photon in the visible range. The time gap between the absorption of the radiation and the photon emission depends on the decay time constant, specific for each scintillating material.

The use of the scintillation detectors would be impossible without the availability of devices to convert the extremely weak light output of a scintillation pulse into the corresponding electrical signal [128]. This is carried out by a photomultiplier that can be considered a fast amplifier. It consists of an evacuated glass tube with a photocathode at its entrance and several dynodes in the interior part. The photocathode serves to convert the incident light photons produced in the scintillating material into low energy electrons. Because only few hundred electrons may be produced, their charge is still too small to be used as a detectable electrical signal. Therefore the electrons emitted by the photocathode are guided, with the help of an electric field, into the electron multiplier section of the photomultiplier. The electrons are guided to the first dynode that is coated with a substance that emits secondary electrons when primary electrons impact on it. The secondary electrons emitted by the first dynode are then focused in direction to the successive dynode where they impact producing other electrons that will move to a third dynode and so on. The production of secondary electrons by the successive dynodes results in a final amplification of the number of electrons up to  $10^7$ - $10^{10}$  electrons for a typical scintillation pulse, sufficient to easily serve as a charge signal for the original scintillation event. This charge is normally collected at the anode of the multiplier section.

The phoswich detector is based on two different scintillators coupled together and mounted on a single photomultiplier tube (see Figure 2.3.1) [129]. It is used for detecting low level radiation in presence of significant background. The scintillating detectors composing the phoswich have different decay constants. In such way the shape of the output pulse from the multiplier is dependent on the relative contribution of scintillation light from the two scintillators. Differences in the pulse output are used to distinguish events that have occurred in only one scintillator from those that occur in both. Typical scintillation crystal used for this purpose are Sodium and Caesium iodide, both with Thallium as activator, NaI(Tl) and CsI(Tl), because of their different decay constants (about 0.25 and 1.1  $\mu$ s, respectively). Lightly penetrating radiations can be stopped almost completely in the first scintillator, i.e. NaI(Tl), giving a fast pulse as output because they will not reach the slow pulse generator crystal, i.e. CsI(Tl). More penetrating radiations will reach both scintillators with a pulse shape modified because of the different decay constants of the crystals. The two crystals in the phoswich detector are commonly used for Compton interactions reduction purposes: a Compton interaction delivers a signal in both detectors that can be discriminated by the a full energy absorption event detected only in the first detector.

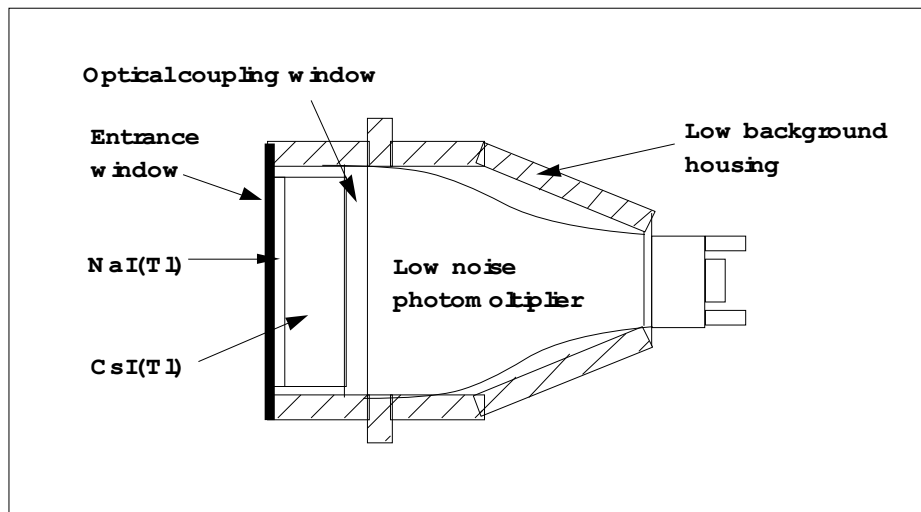


**Figure 2.3.1** The basic elements of a phoswich detector.

Similarly to the case of a scintillation crystal, a semiconductor detector structure too can be described with conduction and valence energy bands [128]. The bands are separated by a band gap of forbidden energy states, the size of which determines whether the material is a semiconductor or insulator. In the absence of thermal excitation both insulator and semiconductor have a configuration in which the valence band is completely full and the conduction band is empty. Therefore neither would show any electrical conductivity. In a metal the high energy band is not completely occupied and therefore metals are always characterized by high electrical conductivity. At any nonzero temperature thermal energy is shared among the electrons of a semiconductor and therefore there is the possibility for a valence electron to reach the conduction band. As a consequence of this process a vacancy (hole) is created in the valence band. In a completely pure semiconductor all electrons and vacancies will result from thermal excitation. This configuration is named *intrinsic*. If impurities are present the properties of the material are mainly determined by them. Actually controlled amounts of impurities are introduced by a process called doping, which increases the conductivity of the material by orders of magnitude. Two types of doping can be

produced. The impurity is called donor when it creates energy levels located very close to conduction band. Semiconductor with donor atoms has a large number of electrons and a small number of holes. Therefore its conductivity is mainly due to the electrons and the semiconductor is called *n-type*. On the other hand when the impurity creates energy levels located very close to valence band, such impurity is called acceptor. Semiconductor with acceptor atoms has a large number of holes and a small number of electrons and consequently it is called *p-type*. For instance Phosphorus impurity in Silicon crystal creates donor states, whereas Boron creates acceptor states.

When n-type and p-type semiconductors are joined together (n-p junction ) electrons and holes undergo to migration because of two reasons: for diffusion, moving from areas of high concentrations to areas of low concentrations; under the influence of the electric field that will move them because of their charge in opposite direction. When the concentration of charge carriers has reached equilibrium, an imbalance charge is determined over a region, called depletion region that extends into both the p and the n sides of the junction. The depleted region exhibits some very attractive properties as a medium for the detection of radiation. The electric field of this area causes any electrons created in or near the junction to be swept toward the n-type part, and any holes toward to p-type part. Yet, this junction without any applied external electric field will be a detector with very poor performance because of recombination processes. But if the p side of the junction is made negative with respect to the n side, the junction is reversibly biased. Now the potential difference from one side of the junction to the other is enhanced and the depletion region is significantly expanded. Under this circumstances the charge carriers created by a radiation interaction within the depleted region are quickly and efficiently collected: this configuration of the semiconductor becomes a useful device for ionizing radiation detecting purposes. Yet, because a semiconductor has a relatively low band gap, they must be cooled in order to reduce thermal generation of charge carriers (leakage current). Otherwise, noise induced by the leakage current would degrade the resolution performance of the detector.

Different techniques are used to produce detectors based on n-p junction principle [128]. Examples are surface barrier detectors, and diffused junction detectors. These detectors are characterized by a sensitive region useful for detecting purposes with a depth upper limit of about 2 mm. This limitation affects the maximum energy of radiation that can be measured. Depletion region can be significantly increased if the semiconductor is doped with an ion drifting process. Starting from a p-type material, donor atoms are added to generate the desired compensation. Alkali metals such as Lithium, Sodium and Potassium tend to form interstitial donors in crystals of Germanium and Silicon. Actually only Lithium can be introduced into Silicon or Germanium in sufficient concentration to serve as a practical compensating impurity. Typical examples are the so-called Lithium drifted Silicon or Germanium detectors, Si(Li) and Ge(Li) respectively. A practical disadvantage of Lithium drifted detectors is that Lithium spatial distribution becomes unstable at room temperature. This phenomenon is particularly important for Ge(Li) because Lithium has a higher mobility in Germanium at room temperature determining an undesirable redistribution of the Lithium at such temperature. Therefore these detectors are not only used, but also continuously stored at reduced temperature, typically by means of a bulky liquid nitrogen dewar.

The use of a hyperpure Germanium detector (HPGe) represents the last important step in the development of semiconductor detector for detection purposes. This is based on the present availability of Germanium in a very high state of purity. In such material impurity concentration can be reduced to a very low level. Therefore the resistivity of the material and consequently the depth of the depleted area is increased [129]. It is possible to obtain active regions that are comparable with those for Ge(Li), for instance, but without any Lithium compensation. The resulting detector can be stored at room temperature, whereas it is cooled only in the measurement phase to prevent excessive leakage current.

HPGe crystals are produced in cylindrical shape (called coaxial) for the detection of high energy photon emitters (typically for energy higher than 100 keV): their large volume enhances the probability of interaction of the penetrating energetic photons with the crystal. For the detection of low energy photon emitters (typically for energy lower than 100 keV) planar shaped Germanium detectors are normally used because low penetrating photons have high probability of interacting, i.e. of being detected, already with thin Germanium crystals. At FZK coaxial and planar HPGe detectors are coupled: a coaxial detector is placed back to the planar detector in order that high energy photons cross the planar detector and can be detected by the coaxial detector. They can operate as a anticoincidence guard for background suppression purposes of high energy photons, in the same way as a phoswich detector. Both the detectors are cooled by means of a cooling rod with an extremity dipped in the liquid nitrogen contained in a dewar (see Figure 2.3.2).

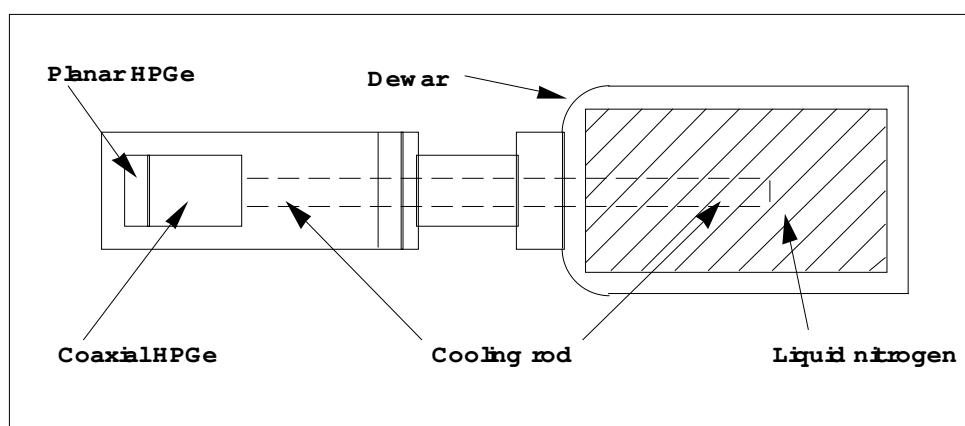


**Figure 2.3.2** The basic elements of a coaxial and planar germanium detectors assembly with the dewar for the cooling.

### 2.3.1.3 Geometry

Geometry is defined as the detector-source configuration, where the source is given by the distribution of photon emitting radionuclides in human body. The direct measurements systems can be divided in two different types: geometry independent and geometry dependent systems, often named whole body and partial body counters, respectively.

Whole body counters can be efficiently used when radionuclides can be reasonably assumed as uniformly distributed within human body without particular concentration in organs and tissues. Typical photon emitters for which such system can be used are  $^{137}\text{Cs}$  or  $^{60}\text{Co}$ . The most common example of such geometry is the tilting chair, introduced for the first time by Marinelli [130]. The subject was sitting in a chair tilted about  $45^\circ$  backwards and a large scintillation detector was placed above the abdomen. The result of a measurement relates to the activity diffused within the whole body.

Partial body counter is characterized by detectors positioned close to the subject, in order to view a specific organ or tissue. Therefore the results refer to the activity in such organ. The advantages of such geometry are a higher efficiency (the detector is closer to the source of radiation) and better detection capabilities (background radioactivity is shielded by the same subject body too). Geometry dependent configuration is extremely important in measuring low energy photons, where the efficiency of the system must be maximized. On

the other hand calibration and measurements must be carried out for each geometry distribution of radionuclides, making the use of such configuration particularly time spending.

Other geometries were developed to a smaller extent. They are based on scanning devices where the detector, by moving above the subject, reveals the real distribution of the radionuclide within the body. Yet calibration procedures for such systems are hardly performed.

In the case of direct measurements performed in the frame of the present work, transuranium elements must be detected in a contaminated subject. Low level activity and affinity for specific organs generally characterize contamination from transuranium elements. Therefore Partial body counters are more efficiently applied. According to their biokinetics, measurements of activity in liver and skeleton should be carried out. For cases of contamination via inhalation, particularly for insoluble compounds, measurements of activity in lung can be efficiently performed too.

#### 2.3.1.4 Energy calibration

The purpose of the energy calibration is to associate an energy value to the respective channel of a multichannel analyzer (MCA). Calibration sources are normally used with certified amounts of activity of one or more radionuclides. The detection of the emitted radiations provides a complex spectrum due to the different kind of radiation-material interactions, basically photoelectric, Compton and pair production interactions. For calibration purposes the full energy peak, due to the total energy absorption of the photon interacting with the detecting materials, is considered. The full energy peak is generally due to the photoelectric interaction but, at a lesser extent, Compton and, to a smaller extent, pair production interactions too can contribute to the full energy peak if the detector is large enough to virtually absorb all the secondary radiations produced through such effects [128].

Several methods have been developed for the automatic identification of the full energy peaks in the spectrum. One is based on second derivative analysis of the spectrum, as the second derivative of a smooth symmetric peak has a large negative excursion at the center of the peak. Other methods are based on filter functions that approximate the shape of the peak, and they operate by identifying those structures of the spectrum that can be assimilated to the filter function, mainly Gaussian. Even if these methods provide good results, a visual location procedure should be always performed for verification purposes. Particularly visual location is easily performed in energy calibration phase when simple spectra with few peaks from known calibrated sources are available. After the location of the full energy peak, its center (called centroid) is evaluated with different methods. Generally it can be calculated by means of a weighted mean of the counts of the peak channels. When the filter function method is applied, the centroid is calculated as a central parameter of the filter function.

The possibility of locating single full energy peaks that don't derive from a convolution of two or more peaks depends on the detecting system capacity of distinguishing full energy peaks of photons with different energy. This is quantified by the energy resolution of the system, based on the width of the full energy peak for the spectrum of a monoenergetic photon. The width is measured at half of the maximum and is named FWHM (Full Width Half Maximum) and the energy resolution ( $R(E_0)$ ) is calculated as the ratio of FWHM by the photon energy  $E_0$ :

$$R(E_0) = \frac{FWHM}{E_0}$$

*equation 2.3.1*

This quantity is normally expressed as a percentage. The main important factors affecting the energy resolution are:

- the statistical fluctuations in the number of charge carriers (i.e. electron-hole pair) produced in the detector;
- the electronic noise in the detector itself, the preamplifier and the amplifier;
- the incomplete collection of the charge carriers.

Such factors are generally present in any kind of detecting system. For a scintillation detector further factors affect the energy resolution because the initial electric sign is firstly converted into light and then converted again into an electric one. Such further factors are the emission of the luminescence, the collection of photons on the photocathode and the emission of photoelectrons.

The energy ( $w$ ) spent by a radiation interacting with a detecting materials to create one electron-hole pair (as in the semiconductor detectors) is actually greater than the energy gap ( $E_g$ ) between valence and conduction bands. For instance for a Germanium detector the mean energy required for creating a pair is 2.96 eV whereas the energy gap is only about 0.67 eV at 300 K. This difference between  $w$  and  $E_g$  reveals that part of the energy is dissipated into processes that don't generate charge carriers. Therefore if the energy  $E$  is deposited in the detector, the average number of charge carriers is given by  $E/w$  and in case of a pure Poisson statistical process the standard deviation of the number of pairs should be just the square root of such ratio. Yet, the experience has shown that the fluctuations are smaller. A factor, called Fano factor ( $F$ ), is therefore introduced and the standard deviation of the number of charged carriers is more realistically given by:

$$\sigma = \sqrt{\frac{FE}{w}}$$

*equation 2.3.2*

The two extreme values of  $F$  are 0 and 1. The former means there are no statistical fluctuations and all the energy is spent for generating charged carriers. The latter means that the number of produced pairs is governed by Poisson statistics. If the distribution of an energy spectrum relating to a monoenergetic source with energy  $E$  is described with a Gaussian function, the FWHM results as following [129]:

$$FWHM = 2\sqrt{2\ln(2)w\sigma} = 2\sqrt{2\ln(2)wFE}$$

*equation 2.3.3*

It results that the FWHM and so the energy resolution decreases with decreasing values of  $w$ .

On the basis of such considerations a semiconductor detector is expected to have the best energy resolution, thanks to its low energy threshold for an electron-hole pair production. Single full energy peaks even separated by few keV energies can be easily identified in the spectrum. In case of scintillation detectors full energy peaks can be still located and the centroid calculated, but the lower energy resolution doesn't allow sometimes to distinguish photons with energy closer than some ten keV.

When single full energy peaks are present energy calibration is easily performed. The centroids of the full energy peaks are associated to the energy of the emitted radiations, known from the decay characteristics of the radionuclides. A fitting is normally performed using a polynomial function to calculate the energy value of each channel of the MCA. On the basis of the energy calibration the energy of any further full energy peak can be evaluated and the relative radionuclide identified.



### 2.3.1.5 Efficiency calibration

The purpose of the efficiency calibration of a direct measurement system is to evaluate the fraction of photons from a radioactive source located within the body that are actually detected and thus converted in pulses. The efficiency will depend on several factors such as:

- source-detector geometry due to source distribution and source-detector distance;
- elemental composition and density of all the materials traversed by the photons
- photons attenuation coefficients of these materials;
- energy and angle-dependent cross sections of the detector material for the various photon interactions.

In principle the detector efficiency for a certain radionuclide distributed in the human body could be typically calculated by means of Monte Carlo simulations. Yet, this procedure is time expensive and often not all the input information necessary for simulating the source-detector configuration is likely available. Therefore efficiency calibration is normally performed by measuring known amounts of activity of a radionuclide. The radionuclide is present in a source characterized by materials and geometry simulating the actual conditions of measurement on contaminated subjects. Therefore the source used for efficiency calibration of in vivo detecting system, named *phantom*, is given by one or more radionuclides dispersed throughout a volume of materials simulating in elemental composition, density and shape the whole human body or some particular organs.

For radionuclides that are roughly uniformly distributed in human body as Caesium or Cobalt and for which whole body counters are used, the phantom is easily built by assembling bottles filled by aqueous solution with known amount of activity. The bottles are then arranged for simulating a human body. A famous example of such phantom is the so-called BOMAB (Bottle Manikin Absorption) [131].

For low energy photons emitters that concentrate in specific organs or tissue of human body and that are detected with partial body counters, the physical and geometric characteristics of the part of the body where the radionuclide is deposited must be accurately reproduced in calibration phase. Therefore anthropomorphic phantoms are used with tissue equivalent materials for the different organs and tissues. This is the case of Iodine that accumulates in thyroid, transuranium elements as Americium and Plutonium that accumulate in liver and skeleton, or other radionuclides inhaled in insoluble form that concentrate in lung.

The efficiency is normally calculated according to Deutsches Institut für Normung (DIN) methodology [132]. A spectrum of a certain calibration phantom is acquired and the full energy absorption peak is separated for each radionuclide within the phantom. The spectrum region around the peak is divided in five parts, as in Figure 2.3.3.

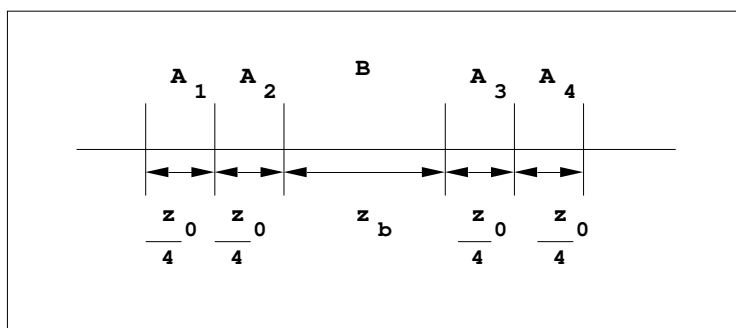


**Figure 2.3.3** Partitioning of the full energy peak area for efficiency calculation purposes according to DIN methodology (see the text for the meaning of the symbols).

The peak is located in the region B (length  $z_b$ ) and the other four regions ( $A_1, A_2, A_3$  and  $A_4$ , total length  $z_0$ ) are set to evaluate the contribution of background in the B area of the peak. If  $N_i$  is the number of counts in the region  $A_k$  ( $k$  from 1 to 4), two quantities are defined in the time of measurement  $t_M$ :

$$M_o = N_1 + N_2 + N_3 + N_4 \quad \text{equation 2.3.4}$$

that is the sum of the counts in the regions around the peak;

$$M_I = N_1 - N_2 - N_3 + N_4 \quad \text{equation 2.3.5}$$

that is used for evaluating a non linear contribution of the background in the region of interest B. The background contribution to the counts in the peak area is therefore calculated as:

$$N_o = qM_o - rM_I \quad \text{equation 2.3.6}$$

where:

$q$  is  $z_b/z_0$ , i.e. the ratio of the B area length by the total length of the four regions  $A_k$ ;  
 $r$  is a factor that depends on whether the background can be considered linear in this region of the spectrum; in case of linearity  $r=0$ . Otherwise  $r$  is defined as:

$$r = q \frac{\left( \frac{5}{4} + 4q + \frac{8}{3}q^2 \right)}{1 + 2q} \quad \text{equation 2.3.7}$$

If  $N_b$  is the gross number of counts in the B area of the peak, the net number of counts is therefore calculated as:

$$N_n = N_b - N_o \quad \text{equation 2.3.8}$$

The efficiency factor  $\epsilon$  is finally calculated by means of the certified activity ( $A$ ) of the radionuclides within the calibration phantom as:

$$\epsilon = \frac{N_n}{At_M y} \quad \text{equation 2.3.9}$$

where  $y$  is the yield, i.e. the probability of emission of the considered radiation per nuclear transformation and  $t_m$  is the time of measurement.

For each full energy peak of one or more radionuclides an efficiency factor can be calculated. A curve is normally fitted on these points to calculate the efficiency for all the energy values of the spectrum. Yet the efficiency calibration curve is characterized by rapid variation, particularly in the low energy range as for the transuranium elements emissions. Therefore calibration phantoms containing the radionuclides that must be measured in the actual situations are normally used. Thus, the efficiency factors are determined exactly for the full energy peaks of these radionuclides instead of extrapolating them from an efficiency

calibration curve. As the same energy line is used in phase of efficiency calibration and of measurement, the yield correction  $y$  in the efficiency factor (equation 2.3.9) can be neglected.

### 2.3.1.6 Minimum detectable activity

A complete characterization of a system for activity measurements requires an evaluation of its sensitivity. This is particularly important in radiation measurements because the samples are always measured in presence of background radiation limiting the detectability of the sample contribution. Two quantities are normally introduced:

- 1 decision threshold that allows to establish if there is a contribution of the sample in the measured counts;
- 2 detection limit that allows to evaluate the smallest contribution from the sample that can be reliably detected.

These concepts were firstly addressed by Currie [133] and were furtherly developed by national and international standardization authorities [132, 134]. Basically the determination of the decision threshold and detection limit is based on testing statistical hypotheses about the equality of distributions of sample and background counts [135].

If  $N_0$  is the background counts number,  $N_b$  the sample counts number,  $N_n = N_b - N_0$  the net counts number, then the decision threshold  $L_C$  is defined as the critical value of a statistical test of null hypothesis,  $H_0: \nu_0 = \nu_b$ . The critical value of the statistical test,  $L_C$ , is defined as the probability  $P(N_n > L_C) = \alpha$  where  $\alpha$  is a pre-selected test level (with  $0 < \alpha < 1$ ) calculated on the background counts distribution. If a measured counts number  $N_n$  is larger than  $L_C$  the null hypothesis is rejected concluding that there is a contribution from the sample. The probability that the null hypothesis is wrongly rejected (error of the first type) is  $\alpha$  (see Figure 2.3.4). The decision threshold is also named *a posteriori* limit because a performed measurement is usually judged on the basis of this limit to establish if it is statistically evident a contribution greater than the background.

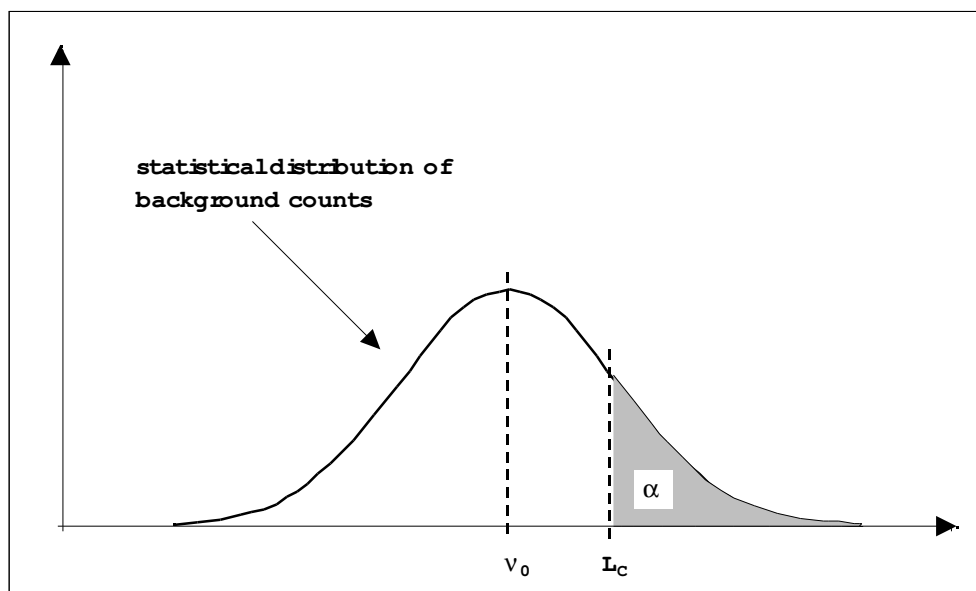


**Figure 2.3.4** Definition of the decision threshold ( $L_C$ ).  $\nu_0$ : expected value of the background counting distribution;  $\alpha$ : pre-selected test level.

To introduce the second quantity, the detection limit ( $L_D$ ), let's consider the null hypothesis is wrongly accepted. This means that there is a contribution from the sample but it is decided that there is none. This is an error of second type, the probability of which shall be denoted as  $\beta$ . On the basis of this kind of error the detection limit is defined as the smallest expected value of the counts number for which, with a decision threshold as above defined, the probability of an error of the second type is equal to a predefined value  $\beta$ :  $P(N_n < L_D) = \beta$ . Thus, if  $N_n$  exceeds  $L_D$ , the probability of wrongly rejecting an existing contribution from the sample will be  $\beta$  (see Figure 2.3.5). On the basis of the previous definition, the detection limit is also named *a priori* limit because it characterizes the capability of the system of detecting a source in the sample before that the measurements is actually performed.

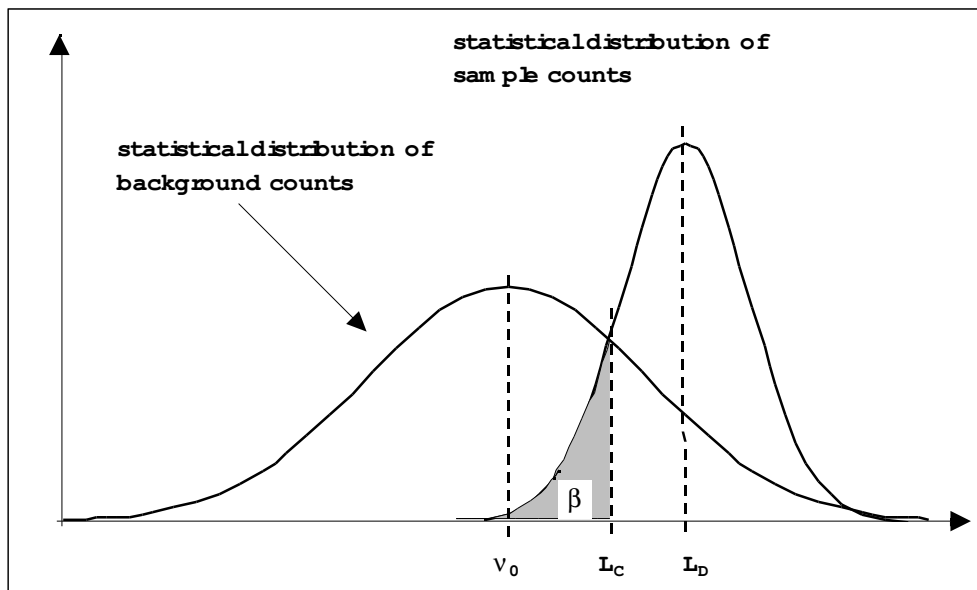


**Figure 2.3.5** Definition of the detection limit ( $L_D$ ).  $v_0$ : expected value of the background counting distribution;  $\beta$ : pre-selected test level.

According to DIN methodology [132] the empirical variance of the background  $s_0^2$  in the peak area of the spectrum is given by:

$$s_0^2 = (q^2 + r^2) M_0 - 2 q r M_1 \quad \text{equation 2.3.10}$$

The decision threshold and the detection limit,  $L_C$  and  $L_D$ , are calculated in DIN report and expressed as:

$$L_C = \frac{1}{2} k_{1-\alpha}^2 + k_{1-\alpha} \sqrt{N_0 + s_0^2 + \frac{1}{4} k_{1-\alpha}^2}$$

equation 2.3.11

$$L_D = \frac{1}{2} \left( k_{1-\alpha} + k_{1-\beta} \right)^2 + \left( k_{1-\alpha} + k_{1-\beta} \right) \sqrt{N_0 + s_0^2 + \frac{1}{4} \left( k_{1-\alpha} + k_{1-\beta} \right)^2}$$

equation 2.3.12

The minimum detectable activity (MDA) characterizes the system before performing any measurements, therefore it is defined on the basis of the detection limit. It is calculated as:

$$MDA = \frac{L_D}{t_M \epsilon y}$$

equation 2.3.13

where:

$t_M$  is the time of measurement;

$y$  is the yield, i.e. the probability of emission of the considered radiation per nuclear transformation;

$\epsilon$  is the efficiency factor.

In case of direct measurements of activity in organs or whole body as considered in the aforementioned equations, “background” has a particular meaning because it is a “not contaminated subject”. However the person’s background is determined by the radionuclides that are naturally present within body and that can significantly change from subject to subject. The MDA calculated on the basis of its background spectrum will be characteristic for such person. In order to have a more general description of MDA capability of a detecting system, a general background spectrum is normally calculated as average of background spectra of a reference group of not contaminated persons. The evaluations of MDA are then carried out on this average spectrum.

DIN methodology is not applied to a phoswich detecting system. For such detector the MDA is calculated by substituting the  $L_D$  with 2 times the standard deviation of the net counts rate in the region of interest in the spectrum [136]. The spectrum is evaluated by subtraction of four reference person’s background spectra with similar body proportions and potassium content. From the resulting differences the standard deviation is calculated.

## 2.3.2 MATERIALS AND METHODS

### 2.3.2.1 Description of the devices

The direct measurements of activity in organs and tissues were performed with both HPGe and phoswich detecting systems. Both systems are located in a shielded room with approximately inner dimensions: height 2.25 m; width 2.25 m; length 4.20 m. The room is accessible through a pneumatically moved steel door and shielded with four different layers. In decreasing order of Z they are: Steel (15 cm), Lead (3 mm), Tin (1.5 mm) and Copper (0.5 mm). The room is also equipped with a double ventilation system operating at 292 cm<sup>3</sup>h<sup>-1</sup> and

117 cm<sup>3</sup>h<sup>-1</sup> for the incoming and outgoing flux, respectively. Therefore a difference of pressure between the environment inside and outside of the shielded room is produced.

During the measurement the subject lays in supine position on a stretcher. The detecting systems are assembled on their own trolleys electrically moved on tracks fixed on the shielded room ceiling. Furthermore the trolleys are equipped with supports hosting each detector allowing to regulate the orientation. The mobile trolley and supports allow to locate each detecting systems over the supine subject lying on the stretcher, according to the best geometry for each kind of measurement, e.g. lung, liver, head.

The HPGe detecting system consists of four planar n-type hyper pure Germanium crystals thick 10 mm. Each planar detector is assembled with a 50 mm thick coaxial hyper pure Germanium detector (see Figure 2.3.6). Both planar and coaxial detectors have a diameter of 50 mm. A dewar of 1.5 litre assures the cooling of detectors.



**Figure 2.3.6** *The HPGe detecting system for direct measurements of body activity available at the Forschungszentrum Karlsruhe.*

The phoswich detecting system is composed by two detectors NaI(Tl) and CsI(Tl), 20 cm diameter, 1 and 50 mm thick respectively. The entrance window is given by a Beryllium layer 0.25 mm thick (see Figure 2.3.7). A third detector with the same characteristics of the aforementioned ones is added when measurements of activity deposited in head are carried out.

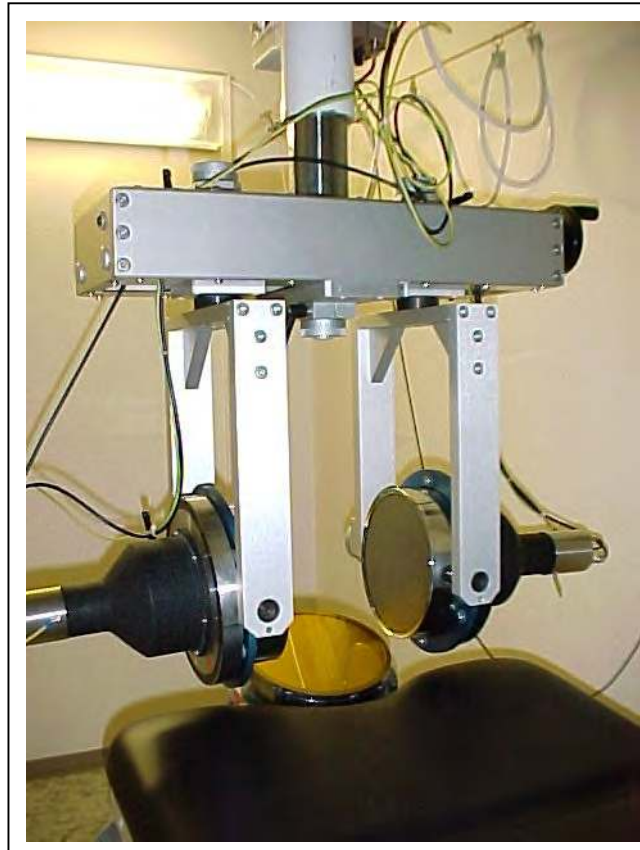


*Figure 2.3.7 The phoswich detecting system for direct measurements of body activity available at the Forschungszentrum Karlsruhe.*

Two phantoms were used for the efficiency calibration of the detecting systems: the Lawrence Livermore National Laboratory (LLNL) phantom and the United States Transuranium and Uranium Registries (USTUR) phantom.

LLNL torso phantom [131] allows to simulate the distribution of a radionuclide in the liver, lymph nodes and lungs. It is designed to represent the human male thorax from approximately the level of the fifth cervical vertebra to the twelfth thoracic vertebra (Figure 2.3.8). The phantom is composed by polyurethane loaded with varying amounts of calcium carbonate to increase the effective atomic number in order to represent the photon attenuation properties of human tissues. The core phantom has the attenuation properties of human muscle tissues and structures of bone equivalent materials are inserted to represent the spinal column, ribs and sternum. The internal organs of the thorax are removable in several blocks. Such organs are the heart, the two lungs, the liver, the tracheo-bronchial lymph nodes and the muscle equivalent tissue filling the volumes among the organs. Lungs, made by foamed polyurethane, liver and lymph nodes made by muscle equivalent polyurethane, are provided loaded with certified amounts of Americium or Plutonium. Set of blank organs is also available. As the detection efficiency of low energy photons is deeply influenced by the thickness of material that the photons must cross, this phantom is supplied with overlays of different thickness in order to reproduce different subject sizes. These overlays are also available representing different percentage composition of fat and muscle tissues.

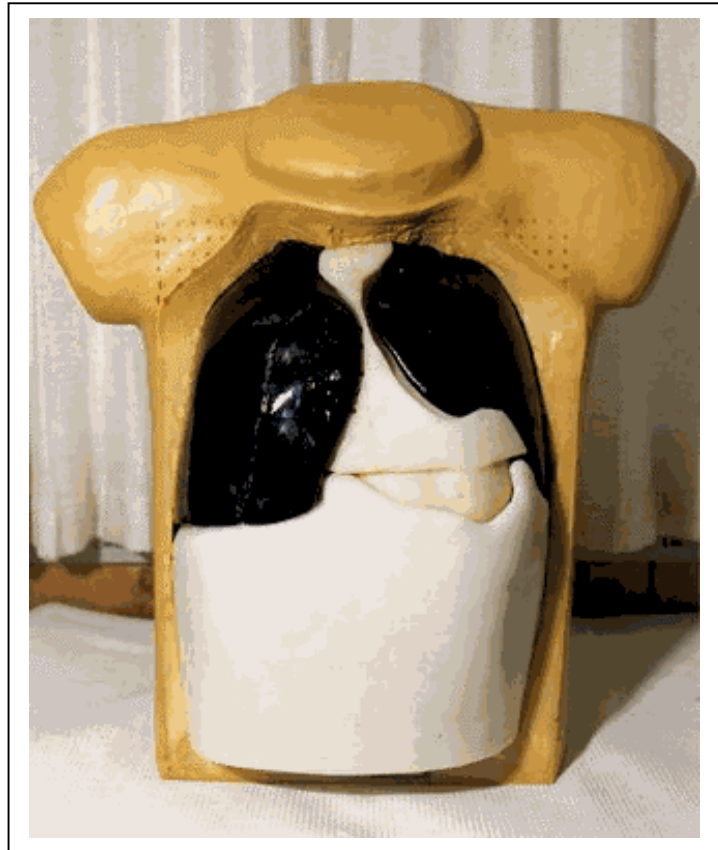


*Figure 2.3.8 The Lawrence Livermore National Laboratory phantom.*

The USTUR phantom incorporates a half skeleton from a voluntary donor to the USTUR [131]. The donor was a 49 years old male Caucasian radiochemist who died for metastatic melanoma in 1979. He was presumably contaminated via wound when he used an unsealed  $^{241}\text{Am}$  source in his doctoral research. The soft tissue and about one half of the skeleton were radiochemically analyzed for  $^{241}\text{Am}$  content [137]. The other half of the skeleton was used for the construction of the phantom, composed by four parts: head, torso, left leg and left arm. Polyurethane based materials were used for simulating the tissue equivalent parts of the body. The phantom is represented in Figure 2.3.9.

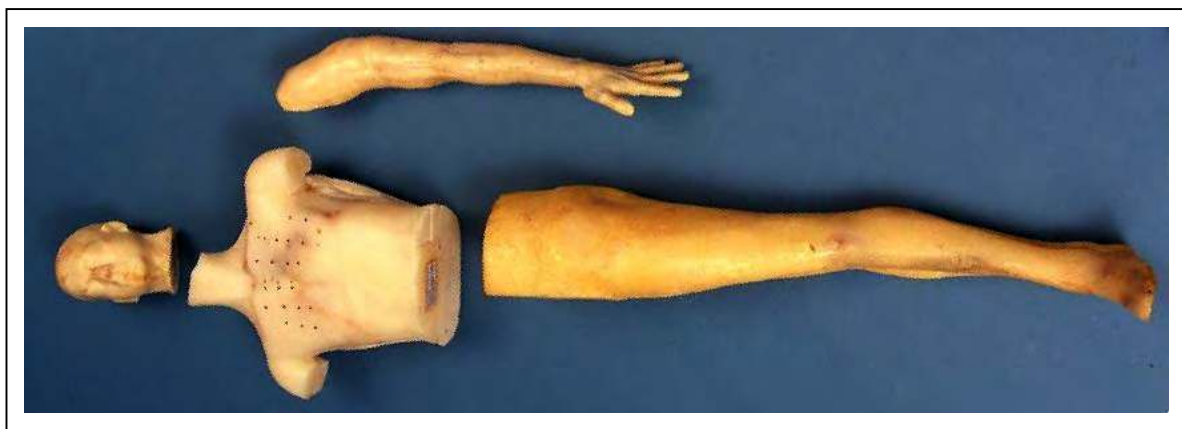


*Figure 2.3.9 The United States Transuranium and Uranium Registries phantom.*



### 2.3.2.2 Performances

Energy resolution of the HPGe and phoswich detecting systems are evaluated for  $\gamma$  59.5 keV energy peak of  $^{241}\text{Am}$ , the radionuclide of interest for the direct measurements performed on the contaminated subject. The results for the energy resolution R of the two detecting systems expressed as percentage are given in Table 2.3.2.

**Table 2.3.2** Energy resolution (R) of each detector of the HPGe and Phoswich detecting systems for 59.5 keV energy peak of  $^{241}\text{Am}$ .

Detecting system	Detector	R [%]
HPGe	D 1	1.1
	D 2	1.2
	D 3	0.9
	D 4	1.0
Phoswich	D 1	29
	D 2	24
	D 3	23

It can be pointed out the two detecting systems are characterized by significantly different energy resolution performances. Therefore different energy calibration methods were applied.

The energy calibration of HPGe detecting system in the low energy range of the spectrum was carried out using two point sources of  $^{241}\text{Am}$  and  $^{57}\text{Co}$  of 40 and 1 kBq activity, respectively. They were located at about 25 cm distance from the detectors on the symmetry central axis of the whole detecting system. Three full energy peaks of  $^{241}\text{Am}$  were considered: 13.9, 26.4 and 59.5 keV. For  $^{57}\text{Co}$  the 121 keV peak was considered. The choice of such peaks allowed to uniformly cover the energy range of interest. The spectrum from the energy calibration sources was acquired using Silena IMCA Plus programme for spectroscopy [138] and the peaks were visually located. The centroid of each peak is calculated by the acquisition programme on the basis of a Gaussian filter for the fitting of spectrum peaks. Each Germanium detector was singularly calibrated using a 3<sup>rd</sup> degree polynomial curve to fit the considered energy peaks. A minimum least square fitting procedures was applied for this purpose.

The poor energy resolution of phoswich detecting system doesn't allow to individuate each single peak as for the HPGe detectors. Therefore a proper energy calibration curve was not calculated, but a spectrum for just  $^{241}\text{Am}$  was acquired and the channels for delimiting the region of interest for the 59.5 peak energy were fixed.

The efficiency calibration of both the detecting systems were carried out by acquiring the spectra of Americium loaded calibration phantoms. In the actual conditions of measurements, HPGe detecting system was used for thorax measurements, and phoswich detectors for measurements of activity in lungs, liver, head and knee. In Figure 2.3.10 the measurement positions of the detecting systems in respect of subject are presented. In case of measurements on the skull with the phoswich detecting system (measurement position: Head),

three detectors are used. Two detectors are located on both side of subject's head: in Figure 2.3.10 they are depicted according to a lateral prospective. The third detector is located under the subject's head and therefore not visible.

Both detecting systems were calibrated, for their own measurement positions, using the whole USTUR phantom to evaluate the efficiency factors in case of activity distribution in the skeleton. Furthermore both detecting systems were calibrated using LLNL phantom to evaluate the efficiency factor in case of activity distribution in lungs, liver and lymph nodes. For such calibration issue, efficiency factors relating to different chest wall thickness were evaluated using the different overlays available for the LLNL phantom.

As phoswich is even used for measurement of activity in head, efficiency factors for activity distribution in lungs, liver and lymph nodes were evaluated using the LLNL phantom to evaluate their contribution for measurements performed on head. In this case, owing to their low contributions, only a LLNL phantom overlay was used (29 mm, one of the two central values).

The efficiency factors of the detecting systems for 59.5 keV energy peak of  $^{241}\text{Am}$  are given in Table 2.3.3 and Table 2.3.4 under different measurements positions of detectors (MP) and activity distribution (AD) of the radionuclide in the body. For LLNL phantom efficiency factors relate to overlays with 50%/50% fat/muscle ratio.

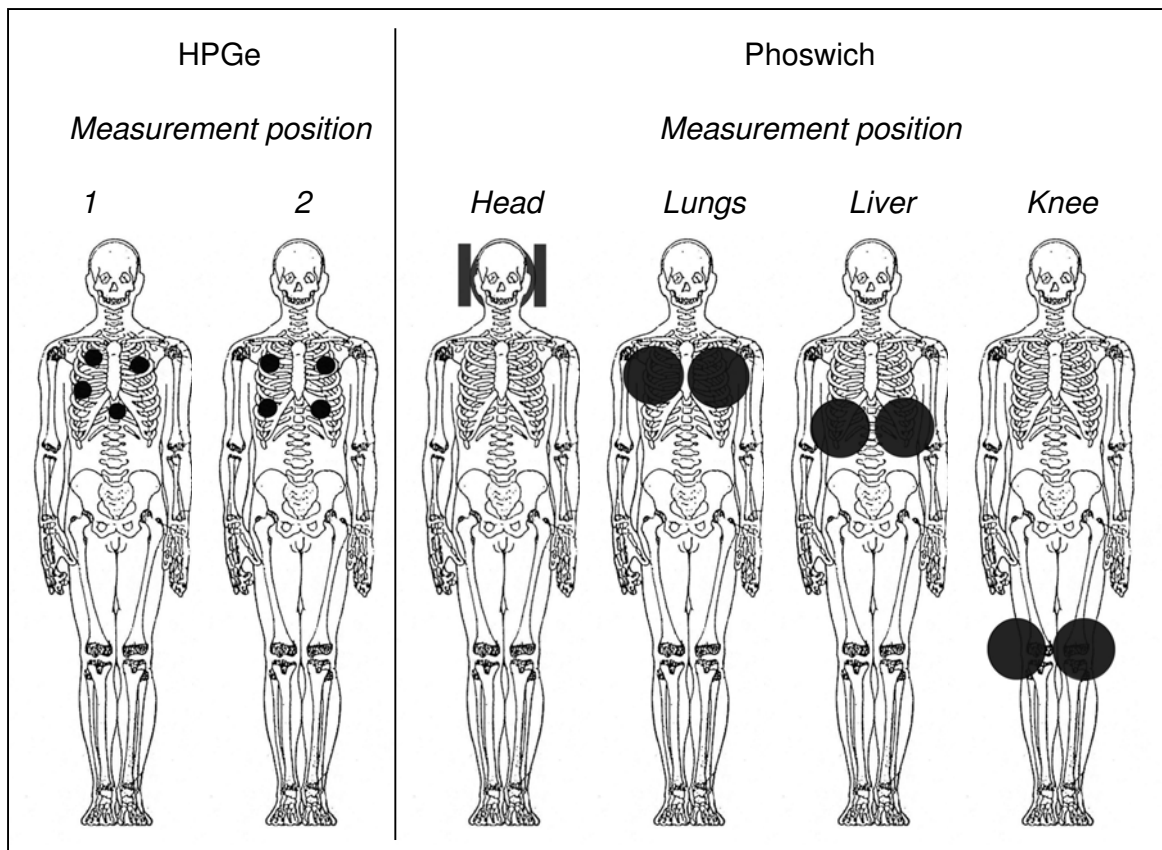


**Figure 2.3.10** The measurement positions (MP) of HPGe and phoswich detectors in respect of the subject.

**Table 2.3.3** Efficiency factors of HPGe detecting system for 59.5 keV energy peak of  $^{241}\text{Am}$  under different measurements positions (MP) and activity distribution (AD) of radionuclides using LLNL and USTUR phantoms (time of measurement,  $t_M$ , 3000 and 2000 s, respectively).

MP - AD	Detector	Efficiency factors in impulse/ $t_M$ per Bq of $^{241}\text{Am}$ in the respective organ			
		<i>Overlays [mm] for LLNL phantom</i>			
		19	25	29	36
1 - Lung	D 1	1.18	0.93	0.78	0.60
	D 2	1.77	1.43	1.26	0.95
	D 3	1.56	1.34	1.14	0.86
	D 4	0.22	0.19	0.18	0.16
1 - Liver	D 1	0.06	0.05	0.05	0.04
	D 2	0.19	0.15	0.14	0.11
	D 3	0.47	0.41	0.37	0.31
	D 4	2.29	1.88	1.51	1.12
1 - Lymph node	D 1	0.61	0.49	0.43	0.33
	D 2	0.94	0.75	0.66	0.49
	D 3	0.46	0.37	0.32	0.25
	D 4	0.04	0.04	0.03	0.03
2 - Lung	D 1	1.18	0.96	0.80	0.60
	D 2	1.54	1.28	1.07	0.79
	D 3	0.43	0.38	0.36	0.29
	D 4	0.09	0.08	0.08	0.08
2 - Liver	D 1	0.06	0.06	0.06	0.05
	D 2	0.17	0.15	0.16	0.11
	D 3	1.70	1.41	1.49	0.92
	D 4	1.67	1.36	0.91	0.88
2 - Lymph node	D 1	0.42	0.34	0.29	0.27
	D 2	0.61	0.50	0.43	0.35
	D 3	0.06	0.06	0.05	0.06
	D 4	0.03	0.03	0.02	0.03
		<i>USTUR phantom</i>			
1 - Skeleton	D 1		0.025		
	D 2		0.035		
	D 3		0.019		
	D 4		0.0037		
2 - Skeleton	D 1		0.025		
	D 2		0.029		
	D 3		0.0029		
	D 4		0.0026		

**Table 2.3.4** Efficiency factors of phoswich detecting system for 59.5 keV energy peak of  $^{241}\text{Am}$  under different measurement positions (MP) and activity distributions (AD) of the radionuclide using LLNL and USTUR phantoms (time of measurement,  $t_M$ , 2000 s).

MP - AD	Detector	Efficiency factors in impulse/ $t_M$ per Bq of $^{241}\text{Am}$ in the respective organ			
		<i>Overlays [mm] for LLNL phantom</i>			
		19	25	29	36
Lung - Lung	D 1	34.0	30.1	26.6	23.6
	D 2	56.4	48.2	44.8	37.4
Lung - Liver	D 1	14.6	14.1	12.9	12.0
	D 2	32.2	29.0	26.9	23.5
Lung - Lymph node	D 1	23.3	21.6	18.6	16.7
	D 2	35.8	31.4	29.0	24.5
Liver - Lung	D 1	11.7	10.1	9.5	8.2
	D 2	5.0	5.0	4.8	4.6
Liver - Liver	D 1	71.7	65.2	58.7	50.1
	D 2	32.0	28.9	26.7	23.9
Liver - Lymph node	D 1	6.2	5.5	5.4	4.4
	D 2	3.7	3.4	3.1	2.9
		<i>USTUR phantom</i>			
Lung - Skeleton	D 1	2.14			
	D 2	2.46			
Liver - Skeleton	D 1	1.35			
	D 2	1.55			
Knee - Skeleton	D 1	7.00			
	D 2	8.00			
Head - Skeleton	D 1	7.70			
	D 2	8.90			
	D 3	5.60			
		<i>LLNL phantom</i>			
Head - Lung	D 1	1.09			
	D 2	1.20			
	D 3	1.50			
Head - Liver	D 1	0.25			
	D 2	0.28			
	D 3	0.15			
Head - Lymph node	D 1	1.09			
	D 2	1.21			
	D 3	1.12			

Examples of MDA values of HPGe and phoswich detecting systems are presented in Table 2.3.5 and Table 2.3.6 for some measurement positions of detectors and activity distributions of Americium. Particularly for MDA values calculated with LLNL phantom efficiency factors, the thicker overlays are, the smaller efficiency factors and therefore the higher the MDA values are. The MDA values are given for the whole detecting systems and therefore are calculated using the sum of the efficiency factors of each detector.

**Table 2.3.5** MDA values of HPGe detecting system for 59.5 keV energy peak of  $^{241}\text{Am}$  under different measurement positions of detectors (MP) and activity distributions (AD) of the radionuclide using LLNL phantom ( $t_M = 3000$  s).

MP - AD	MDA [Bq]			
	<i>Efficiency factors from LLNL phantom overlays [mm]</i>			
	19	25	29	36
1 - Lung	4.4	5.4	6.3	8.2
1 - Liver	7.0	8.4	10	13
2 - Lung	6.5	7.8	9.1	12
2 - Liver	5.8	7.1	8.0	11

**Table 2.3.6** MDA values of phoswich detecting system for 59.5 keV energy peak of  $^{241}\text{Am}$  under different measurement positions of detectors (MP) and activity distributions (AD) of the radionuclide using LLNL phantom ( $t_M = 2000$  s).

MP - AD	MDA [Bq]			
	<i>Efficiency factors from LLNL phantom overlays [mm]</i>			
	19	25	29	36
Lung - Lung	4.4	5.1	5.6	6.6
Lung - Liver	8.5	9.3	10.0	11.3
Liver - Lung	26.9	29.8	31.6	35.3
Liver - Liver	4.3	4.8	5.3	6.1

### 2.3.2.3 Measurements execution

The direct activity measurements on the subject were carried out in one day. As he is not anymore engaged in manipulating unsealed sources, no particular procedures must be followed for removing skin contamination that could contaminate the room of measurements affecting the accuracy of the internal activity evaluation. Therefore the procedure normally applied for routine monitoring was applied: he was made to undress of his clothes and to dress an overall. The measurements series was planned considering some constraints:

- the limited whole time of availability of the subjects;

- the necessity of performing measurements with both detecting systems and under different geometry configurations for which the efficiency factors are known;
- the necessity of limiting the measurement time in order to minimize the time that the subject was obliged to remain in the shielded room;
- the statistical significance of impulse counted by each detector in the region of interest of Americium.

A measurement time of 2000 seconds seemed to satisfy all the aforementioned requirements. In order to decrease the whole time necessary for carrying out the series of measurements with both detecting systems and for different geometry, when possible simultaneous acquisitions from both detecting systems were carried out. Yet, as the trolleys supporting the detecting systems move on the same track, not all the combinations in the measurement positions were possible to simultaneously perform with both detecting systems. Typically measurements of activity on lung with HPGe detecting system and on knee with phoswich detecting system were simultaneously performed. Similarly measurements of activity on lung with phoswich detecting system and on knee with HPGe detecting system were simultaneously performed too. As the phoswich detecting system has a better geometric efficiency, the measurement time was reduced to 1500 seconds, when measurements with HPGe detectors were not simultaneously carried out.

Unfortunately some days before performing measurements on the contaminated subject one of the HPGe detectors was damaged. Therefore in the following part the results of the measurements performed with the other three germanium crystals are presented. This had a limited implication on the final evaluation of subject's organs burden activity. The measurements with phoswich were carried out in normal way.

### 2.3.3 RESULTS OF THE MEASUREMENTS

Examples of the spectra acquired from the subject with HPGe and phoswich systems positioned on the lung region are shown in Figure 2.3.11 and Figure 2.3.12, respectively.

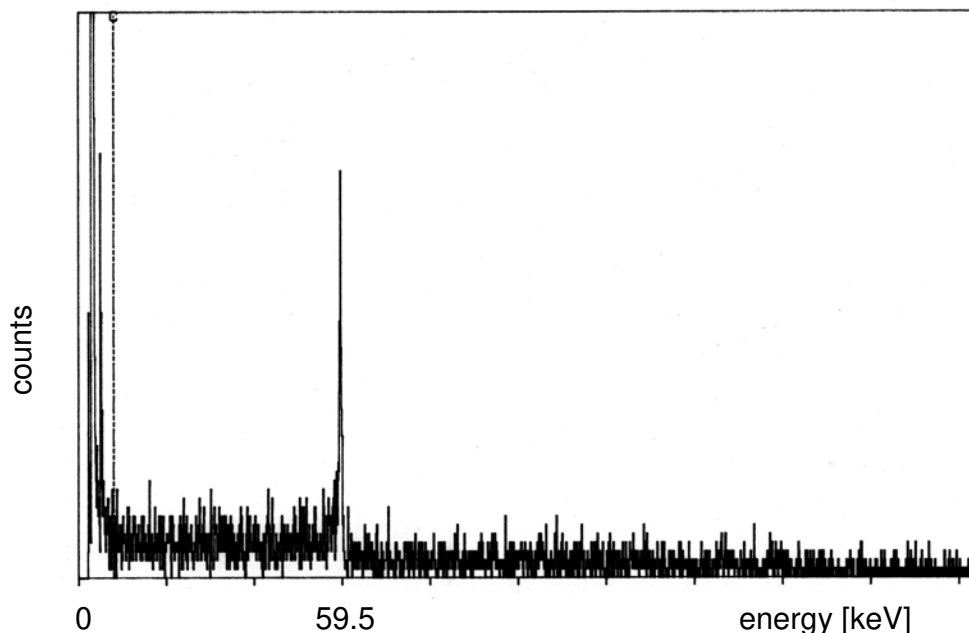


**Figure 2.3.11** The spectrum acquired with the HPGe detecting system positioned on the lung (measurement position 1) of the contaminated subject. The full energy peak is given by  $^{241}\text{Am}$  (59.5 keV).

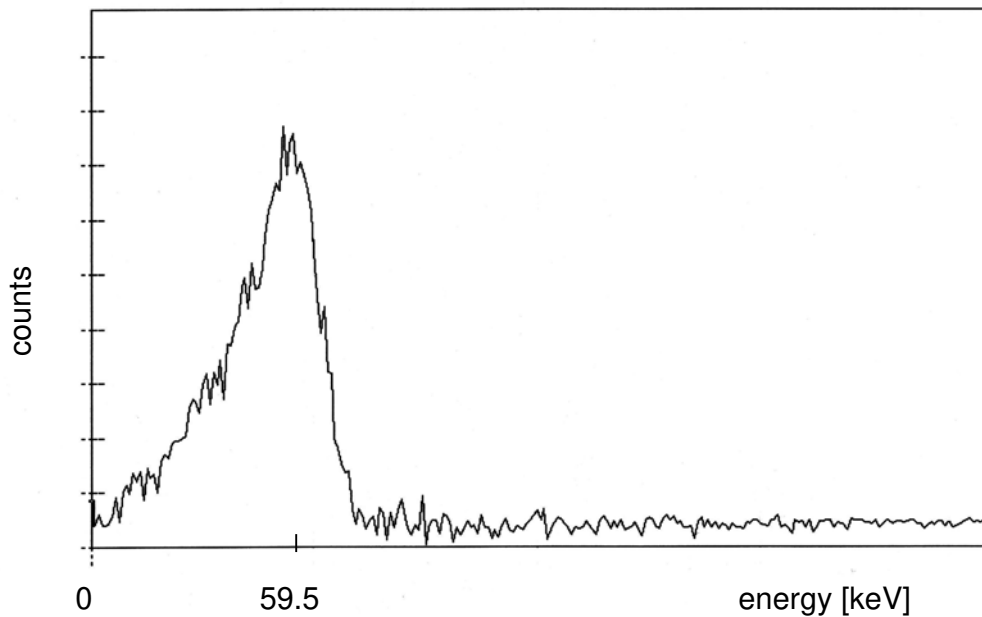


**Figure 2.3.12** The spectrum acquired with the phoswich detecting system positioned on the lung of the contaminated subject. The full energy peak is given by  $^{241}\text{Am}$  (59.5 keV).

The measurements provided a first set of raw data given by the impulses counted by each detector of the phoswich and HPGe detecting systems in each measurement position geometry, i.e. lung, liver knee and head for the phoswich and positions 1 and 2 for the HPGe detectors. The results of the measurements are given in Table 2.3.7 and Table 2.3.8.

The counts values in Table 2.3.7 and Table 2.3.8 were converted to activity (Bequerel) of  $^{241}\text{Am}$  by means of a weighted multiple linear regression [139] using the efficiency factors given in Table 2.3.3 and Table 2.3.4. Such efficiency factors were corrected for the actual chest wall thickness according by linear interpolation. The subject's actual chest wall thickness was evaluated by means of the following expression:

$$\text{CWT}[\text{cm}] = 4.57 \cdot \frac{\text{Weight}[\text{kg}]}{\text{Height}[\text{cm}]} + 0.44$$

*equation 2.3.14*

Such expression was evaluated on the basis of different empirical formula [140, 141, 142, 143] available in literature to calculate the chest wall thickness on the basis of the weight and height of a subject. Such empirical curves were used to evaluate the chest wall thickness for a group of seven subjects with different values of weight and height. The average of the calculated chest wall thickness values were then fitted and the expression given in equation 2.3.14 was finally obtained.

The final results relating to the activity in the main organs with respect to the adopted measurement geometry are given in Table 2.3.9.

**Table 2.3.7** Impulses in the measurement time for the contaminated subject as acquired with the HPGe detecting system for different measurement positions (MP).

MP	Detector	Measurement time [s]	Counts	Standard deviation
1	D 1	2000	93.9	10.32
	D 2	2000	-	-
	D 3	2000	72.29	9.2
	D 4	2000	14.11	4.73
2	D 1	2000	62.85	8.69
	D 2	2000	-	-
	D 3	2000	26.94	5.86
	D 4	2000	3.34	3.52

**Table 2.3.8** Impulses in the measurement time for the subject of study as acquired with the phoswich detecting system for different measurement positions (MP).

MP	Detector	Measurement time [s]	Counts	Standard deviation
Lung	D 1	2000	4505	126
	D 2	2000	6007	169
Liver	D 1	1500	765	80
	D 2	1500	619	65
Head	D 1	1500	516	36
	D 2	1500	549	39
	D 3	1500	599	42
Knee	D 1	2000	825	71
	D 2	2000	695	59

In a first attempt the linear regression analysis (Table 2.3.9) pointed out that the calculated linear model can well describe the activity measurements in the considered organs: a coefficient of multiple determination  $R^2 = 0.99$  was obtained. Furthermore the F test analysis on the ratio between the regression variance and the variance due to residual variation has pointed out that the observed correlation among the independent (measurements) and dependent variables (efficiency factors) in the regression model is not randomly occurred ( $P=0.05$ , one tail,  $v_1=4$  and  $v_2=6$ ). The t-test on the regression coefficients



(activity burden in considered organs) allowed pointing out that the liver is not a significant organ in the regression model.

On the basis of such last consideration a new regression model (second attempt in Table 2.3.9) was assessed without taking into account the liver. Also for this regression model the coefficient of multiple determination and the F and analysis confirmed the quality of the regression analysis. The regression coefficients practically agree with the values obtained on the basis of the previous regression model, confirming that the liver activity burden may be neglected. Therefore the results of the second regression analysis were considered as base for the analysis of the contamination case in Chapter 3.

**Table 2.3.9** Activity and standard deviation ( $A$  and  $\sigma_A$ , expressed in Bq) of  $^{241}\text{Am}$  evaluated for the considered organs by multiple regression analysis.

	Skeleton	Lymph nodes	Liver	Lung
<i>First attempt</i>				
A	96	104	-2	69
$\sigma_A$	6	29	2	19
<i>Second attempt</i>				
A	95	114	-	61
$\sigma_A$	6	27	-	17

## 2.4 ACTIVITY MEASUREMENTS IN BIOASSAYS

---

In this section basic principles relating to measurements of activity in bioassays are presented. As for the direct measurements of activity in organs, principles and techniques adopted for carrying out measurements on the aforementioned case of contamination were specifically pointed out. Particular care is taken in presenting those aspects specifically characterizing a measurement of transuranium elements in bioassays through the alpha particles emissions. Therefore particular attention was paid to manipulation and preparation of the samples, that is the most sensitive phase in this kind of technique in comparison with activity measurements itself. The measurements were carried out by the Toxicological Laboratory of the Medical Department of the Forschungszentrum Karlsruhe. The results of the bioassays analysis are presented in the last part of this section.

### 2.4.1 BASIC MEASUREMENT PRINCIPLES

#### 2.4.1.1 *Sample collection*

For accurate results in bioassays analysis the subject should be provided with an appropriate protocol and vials kit for the collection of excreta. It is a good practice to collect the samples far from the area of potential exposure in order to avoid any contamination of the sample itself from radioactive pollutants present on clothes, on subject's hands or suspended in the air [41]. These considerations are particularly applied in case of excreta samples collection because they are directly collected by the subjects and contamination from external pollutants is a possible risk. For other bioassays, as blood sample for the case of the subject in this study, risks of contamination from external sources are less relevant.

The samples must be collected in vials with relatively small tendency to absorb traces of elements of interest and easily washed with a single acid wash, if a re-use is planned. For such purposes vials of polyethylene are commonly used. Volume vials are determined by the amounts that must be collected. For urine 24 hours samples should be collected for limiting the daily variability in urinary excretion. For feces a single whole voiding is normally collected. Sometimes cumulative samples related to the voiding on two or more consecutive days are collected.

For liquid bioassays, as urine, if the time between the sample collection and the analysis is likely to be more than few days, it is important to add some percentage by volume of chloridric or nitric acid, to avoid precipitations and biological growth [144].

#### 2.4.1.2 *Sample preparation*

This procedure is performed to homogenize and prepare the sample for the successive chemical processing. In fact each bioassay contains a very small amount of the radionuclide of interest, normally bound within a complex matrix of other chemical constituents [41]. For an accurate measurement of the radionuclide amount it is necessary to remove it from this matrix that could interfere in the following radiochemical analysis. Different procedures can be applied in relation to the different kinds of bioassays. Generally most of the biological samples are wet ashed in acid solutions with nitric acid, sometimes adding few amounts of oxygenate water. In case of feces samples a dry ashing is previously performed, firstly by drying at low temperatures and then by heating at more than 400 °C. After this phase wet ashing is performed as for the other biological samples. The residues of the wet and dry ashing procedures of any biological samples should be finally dissolved in appropriate

concentration of acid solution, as nitric or chloridric acid, depending on the specific radiochemical procedures to be employed.

The result of sample preparation phase is a liquid sample in acid solution where the radionuclide of interest has been released from the sample organic matrix. The liquid sample is then concentrated by various co-precipitation techniques in order to separate the radionuclide of interest from the bulk of inorganic materials. The selection of the co-precipitation technique depends upon the successive chemical separation techniques to be applied. This can be considered as an initial purification step, as many common elements are left behind in the process. Yet, the chemical purification is massively carried out in the successive phase of the radiochemical process.

The numerous manipulations carried out on the sample lead to an inevitable partial loss of the radionuclide of interest that is almost impossible to evaluate *a priori*. Therefore known amounts of an appropriate radioactive tracer are added to the sample as early in the process as is feasible in order to provide means to correct for these losses [144]. The tracer is typically added before any procedure of the sample preparation phase. At the end of the analytical procedure, when the sample activity will be measured, the determination of the residual tracer activity will indicate how much of the radionuclide loss occurred. Thus the measurement for the radionuclide of interest will be accordingly adjusted.

#### 2.4.1.3 Chemical separation

Once the radionuclide of interest has been released from the sample matrix, purification processes are carried out to separate it from other chemical impurities that are present in the biological samples and from other radionuclides which otherwise might interfere in the activity measurement phase. As the radionuclide is a very small fraction of the total sample mass, multiple purification steps are usually required to achieve the desired purity. Different techniques can be applied for chemical separation purposes such as solvent extraction (also named liquid-liquid extraction), ion-exchange separation or extraction chromatography.

For the samples collected from the subject studied in the present work, solvent extraction technique was applied as it is the current technique used in FZK Toxicological Laboratory. The liquid sample resulted from the preparation phase is placed in a separating funnel [145]. Several compounds, normally of organic nature as amines, can be used as extracting agent, in relation to the nature of the sample and to the chemical properties of the radionuclide of interest. Chemical separation is based on the application of Nerst equation that gives the repartition constant  $K$  of a certain substance in two different solvents:

$$K = \frac{C_1}{C_2}$$

*equation 2.4.1*

where:

$C_1$  is the concentration of substance in the solvent 1;

$C_2$  is the concentration of substance in the solvent 2;

The appropriate extracting agent for the radionuclide of interest will maximize the  $K$  values by favouring the concentration of the radionuclide in one of the phases. Practically the radionuclide of interest will concentrate in an organic phase while the other radionuclides will remain in the aqueous solution. The radionuclide is then back extracted from the organic phase by reducing agents.

If more than one radionuclide is matter of interest, chemical separation with other extracting agents can be successively performed on the organic phase resulting from the use of the first extracting agent. This was carried out on the samples from the subject studied in the present work in order to separate and measure Plutonium and Americium isotopes.

#### 2.4.1.4 *Source preparation*

Once purified, the sample must be prepared in a suitable form for measuring the activity of the radionuclide of interest. Different techniques are available for such measurements. In case of the present work alpha spectrometry analysis was performed. Alpha particles are heavy charged particles that lose energy readily in materials because of ionization and excitation processes induced by the interacting materials[129]. These attenuation characteristics determine for example a complete absorption of alpha from already few micrometers of biological tissues or few centimetres of air. Therefore alpha particles emitted by the radionuclide in the sample will interact with the materials within the sample itself and with any material between the sample and the detector active area. Any interaction will decrease the number of particles that will reach the detector causing a loss of efficiency of the detecting system. Furthermore, the particle interacting with materials before reaching the detector will show a degradation in the energy spectrum, causing a characteristic tailing in the alpha peak that will tend to have an asymmetric shape instead of the typical gaussian. This will affect the resolution performance of the alpha spectrometer.

For such reasons it is necessary to produce from the sample resulting from the chemical separation phase, a thin, flat uniform deposit [144] to be successively measured. Ideally the source should have a monatomic layer of the alpha emitter with no extraneous matter above this layer that could attenuate the alpha radiation. Furthermore the source should be handled without excessive problems, chemically stable and all the traces of solvent and acid must be easily removed to prevent damage to counting chambers and detectors. Finally, as alpha spectrometry will be executed in vacuum conditions to avoid attenuation from the air between sample and detector, the deposit should be stable enough and fixed to the support in order to avoid diffusion in the counting chamber. In such a case the chamber and the detector itself could be contaminated with severe consequences for sensitivity performances of the detecting system.

One of the most known techniques, applied also in this work, in order to obtain a deposit with such characteristics is the electrodeposition [41]. This process is performed in an electrolysis cell where the cathode is a metal stainless steel planchet with only one side exposed to the electrolyte and the anode is a platinum electrode. By means of the electrolysis process the radionuclide is deposited as a hydrous oxide onto the cathode. As the acidity of the solution is a critic factor in performing such process, the pH of the electrolyte solution has to be checked frequently by dipping a narrow range pH paper into the solution. At the end of the process a thin layer of the radionuclide of interest is deposited on the cathode: this will represent the radioactive sample suitable for the following alpha spectrometry analysis.

#### 2.4.1.5 *Alpha spectrometry*

The measurement of radionuclide activity in the source prepared according to the aforementioned steps is carried out with a semiconductor detector. The general bases of semiconductor physics were described in the previous section. At the present for charged particle spectrometry silicon detectors are commonly applied.

A modern version of charged particle detector for alpha spectrometry is called PIPS, an acronym for Passivated Implanted Planar Silicon [146]. The junctions of this kind of detector are realized with ion-implanted contacts that are completely buried within the Silicon wafer. In comparison with alpha detectors of older generations such as surface barrier or diffused junction detectors, the PIPS is characterized by a thin entrance window. Therefore the energy loss of alpha particles crossing the initial insensitive surface of the detector is significantly limited and the energy resolution of the detector is consequently improved. Thin windows are particularly important for the close detector-source spacing geometry that is necessary in order to achieve high efficiency performances for low level alpha spectrometry. In fact at close detector-source spacing, peak broadening occurs because many alphas enter the detector at an acute angle with higher energy loss. Therefore a thin entrance window limits the energy loss caused by such process consequently improving the energy resolution.

Further advantage of PIPS detector relates to the possibility of handling it without excessive care because the contacts are given by ion implanted surface. Therefore it can even be touched by hand and cleaned readily with a cotton ball dampened with acetone.

In order to ensure the correct identification and quantification of alpha emitting radionuclide in the sample, the detecting system must be calibrated both in energy and efficiency. In comparison to the aforementioned procedures for direct measurement systems of photon emissions, the calibration procedures of detecting system for alpha spectrometry of bioassays are generally of easier execution. This is basically due to the sample under measurement that, owing to the complex preparation procedures, is finally standardized in its geometrical and physical features. On the contrary for direct measurement the sample is the subject itself and therefore the measurements conditions are hardly reproduced in calibration phase with complex phantoms. The common and easiest way to perform energy and efficiency calibration for alpha spectrometry devices is the detection of high quality standard sources, prepared by electrodepositing a mixture of long liver alpha emitting radionuclides onto a stainless steel disc in order to reproduce the actual conditions of measurement. Therefore energy and efficiency calibrations are often simultaneously carried out in a very effective way.

Detector and sample are normally located together in a vacuum chamber. This allows limiting the energy loss of alpha particles crossing the air until the detector with significant benefit for the energy resolution of the system. For resolution purposes it would be advisable to achieve and maintain low pressure as much as possible. Yet, the vacuum conditions can create favourable conditions for contaminating detector by means of recoil effect [147, 148, 149]. Recoil energy can be imparted to the nucleus of an alpha emitting atom producing fragments that can travel from the source to the detector surface, thanks to the almost absent air absorption. The energy of such fragments may be sufficient to implant them into the detector so that they cannot be removed non-destructively. Two techniques are used to avoid recoil contamination. First, a slight negative bias is applied to the sample itself to attract the nucleus back to the sample surface, rather than allowing it to adhere to the detector or to the chamber. A second technique is based on vacuum conditions. Higher pressure than that value advisable for the best resolution performances are established to create an air layer to prevent the recoiling nucleus from reaching the detector. The recommended air barrier is about of 10 Torr cm<sup>2</sup>. It can be calculated by an empirical expression relating to chamber pressure and detector-source spacing [148]:

$$L_A = 1.6 * P * d$$

*equation 2.4.2*

where:

$L_A$  is the air layer in  $\mu\text{gcm}^{-2}$ ;

$P$  is the pressure within the vacuum chamber in Torr

$d$  is the source-detector spacing in cm.

The recoil contamination is one of the main factors affecting the background radioactivity in the vacuum chamber. Therefore it particularly influences performances of alpha spectrometry systems in terms of minimum detectable activity. Another factor that plays an important role specifically for the alpha spectrometry systems is the chemical yield in the preparation and separation process. A specific guideline gives the suitable expressions for calculating the MDA [150] but the general considerations previously introduced are still valid.

At the end of the alpha spectrometry measurement, the radionuclide activity in the sample is calculated using the tracer yield ( $Y_T$ ) given by:

$$Y_T = \frac{N_n^T}{t_M \epsilon_T A_T}$$

*equation 2.4.3*

where:

$N_n^T$  is the net area for the peak of tracer alpha;

$t_M$  is the measurement time;

$\epsilon_T$  is the efficiency factor for the tracer;

$A_T$  is the tracer activity added at the beginning of the sample manipulation.

The activity of the radionuclide of interest ( $A_R$ ) in the sample is finally evaluated as follows:

$$A_R = \frac{N_n^R}{t_M \epsilon_R Y_T}$$

*equation 2.4.4*

where:

$N_n^R$  is the net area for the peak of the radionuclide of interest;

$t_M$  is the measurement time;

$Y_T$  is the tracer yield (from equation 2.4.3)

$\epsilon_R$  is the efficiency factor for the radionuclide of interest.

## 2.4.2 MATERIALS AND METHODS

### 2.4.2.1 Description of the devices

The urine samples were collected in a vial 2 litres volume. The feces were collected in two vials: the first used just as transport container (1 litre volume); It contains the second smaller vial (0.5 litre volume) with excreta inside. This second vial is ashed together with the excreta during the chemical preparation of the sample. Samples of 100 millilitre volume were

collected for the blood. After the collection the chemical preparation of the samples is performed according to the block diagram in Figure 2.4.1.

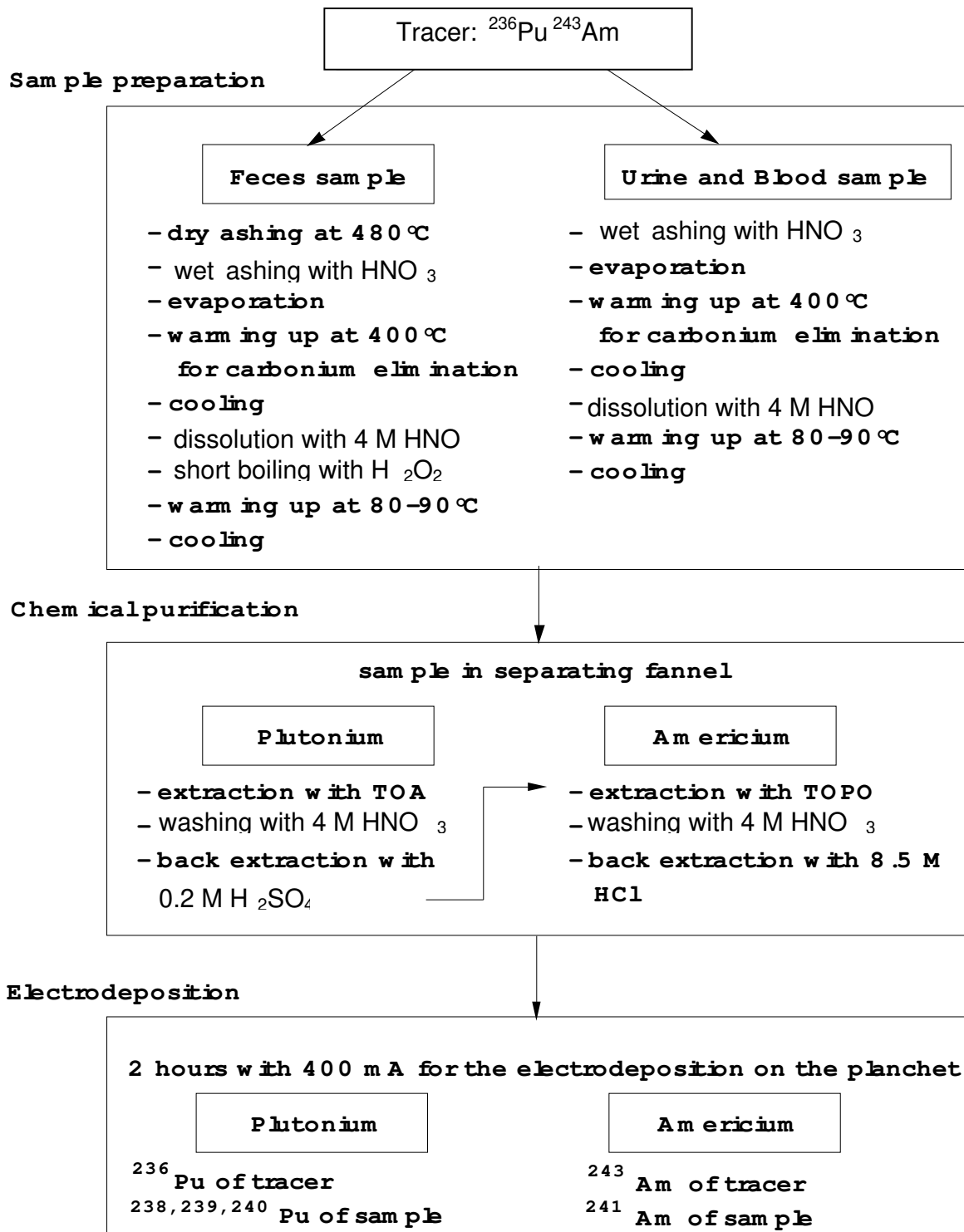


Figure 2.4.1 Diagram block for the production of a suitable sample for alpha spectrometry analysis.

The electrodeposition cell used for the production of suitable samples for the following spectroscopy analysis is shown in Figure 2.4.2. It is also shown the planchet over which the sample is electrodeposited and counted in the alpha spectroscopy phase.

The alpha spectrometry was carried out with ion implanted silicon detectors as shown in Figure 2.4.3. The entrance contact is an extremely thin boron implantation. The planchet is placed on the support and the detector is placed over the planchet. All these components are then located in the vacuum chamber for the spectrum acquisition.



**Figure 2.4.2** The main constituents of the electrodeposition cell. The planchet where the sample is electrodeposited is also shown.

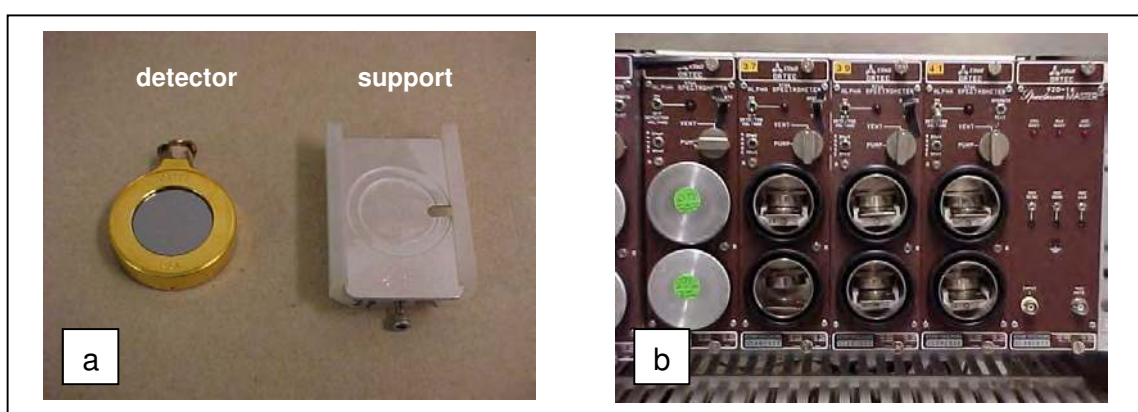


**Figure 2.4.3** The ion implanted silicon detector with the support (a) and the vacuum chambers where they are located with the sample for the measurement (b).



#### 2.4.2.2 Performances

The energy calibration of the alpha detectors was carried out using standard sources containing  $^{233}\text{U}$ ,  $^{239}\text{Pu}$ ,  $^{241}\text{Am}$  and  $^{244}\text{Cm}$ . The FWHM of the detectors used in the laboratory is about 17 keV for  $^{241}\text{Am}$  (energy resolution about 0.3 %). In the practical situations the FWHM and therefore the energy resolution depend on the thickness of the deposit on the planchet: 30-35 keV may be considered as an indicative value of FWHM for most of the actual measurement conditions [151].

At the present the routine measurements performed at the FZK Toxicological Laboratory are not able to discriminate  $^{239}\text{Pu}$  from  $^{240}\text{Pu}$ . Thus, efficiency factors and, consequently, activity measurements on such radioisotopes relate to the sum of their contributions.

Efficiency calibration is normally carried out using standard sources of  $^{241}\text{Am}$  of 523 Bq activity certified at 14.7.1989.

The FZK Toxicological Laboratory provides a value of  $5 \cdot 10^{-4}$  Bq for the MDA for each radionuclide. The value refers to the whole bioassay laboratory equipped with numerous alpha spectrometric chains: therefore it can be considered as an indication of the general performances of the laboratory.

#### 2.4.2.3 Measurements execution

A blood sample was taken from the subject in the period of staying in the Forschungszentrum Karlsruhe. Three urine and feces samples were collected by the subject himself in the following days after the return to his residence town. Therefore he was provided with the proper vials and instructed on how to handle them. The samples were sent by post to Forschungszentrum Karlsruhe. The sample collection protocol was set in order to collect samples relating to the whole excretion.

As the samples were received, they were undergone to chemical preparation in order to detect isotopes of Plutonium and Americium. Therefore for each collected sample the separation procedure has provided two further samples, according to the block diagram of Figure 2.4.1: one containing Plutonium isotopes, and the other one containing Americium.

On these samples alpha spectrometry was carried out by including them in the routine measurement programme daily carried out by the FZK Toxicological Laboratory on samples from the occupationally exposed workers.

### 2.4.3 RESULTS OF THE MEASUREMENTS

The results of the measurements for the collected blood, urine and feces samples are given in Table 2.4.1 [151]. As previously stated the activity measurements on  $^{239}\text{Pu}$  and  $^{240}\text{Pu}$  radioisotopes relate to the sum of their contributions. The activity in blood samples resulted lower than the MDA for  $^{238}\text{Pu}$  and  $^{241}\text{Am}$ . For all the other kind of measurements ( $^{239}\text{Pu} + ^{240}\text{Pu}$  in blood and any radioisotopes in urine and feces samples) the activity values resulted to be higher than the MDA.

**Table 2.4.1**  $^{238}\text{Pu}$ ,  $^{239}\text{Pu}$  and  $^{241}\text{Am}$  in blood, urine and feces samples of the investigated subject.

Date of collection	Sample	Radionuclides	Activity [Bq]	Standard deviation [%]
3.12.99	blood	$^{238}\text{Pu}$	< MDA	-
		$^{239}\text{Pu}+^{240}\text{Pu}$	$4.48 \cdot 10^{-3}$	17
		$^{241}\text{Am}$	< MDA	-
9.12.99	urine	$^{238}\text{Pu}$	$1.33 \cdot 10^{-3}$	26
		$^{239}\text{Pu}+^{240}\text{Pu}$	$1.12 \cdot 10^{-2}$	13
		$^{241}\text{Am}$	$4.46 \cdot 10^{-3}$	18
	feces	$^{238}\text{Pu}$	$1.14 \cdot 10^{-3}$	31
		$^{239}\text{Pu}+^{240}\text{Pu}$	$1.16 \cdot 10^{-2}$	13
		$^{241}\text{Am}$	$3.72 \cdot 10^{-3}$	21
10.12.99	urine	$^{238}\text{Pu}$	$1.00 \cdot 10^{-3}$	30
		$^{239}\text{Pu}+^{240}\text{Pu}$	$9.49 \cdot 10^{-3}$	13
		$^{241}\text{Am}$	$1.71 \cdot 10^{-3}$	20
	feces	$^{238}\text{Pu}$	$9.69 \cdot 10^{-4}$	27
		$^{239}\text{Pu}+^{240}\text{Pu}$	$1.32 \cdot 10^{-2}$	10
		$^{241}\text{Am}$	$3.57 \cdot 10^{-3}$	17
11.12.99	urine	$^{238}\text{Pu}$	$1.12 \cdot 10^{-3}$	30
		$^{239}\text{Pu}+^{240}\text{Pu}$	$1.64 \cdot 10^{-2}$	11
		$^{241}\text{Am}$	$4.72 \cdot 10^{-3}$	15
	feces	$^{238}\text{Pu}$	$7.77 \cdot 10^{-4}$	28
		$^{239}\text{Pu}+^{240}\text{Pu}$	$7.71 \cdot 10^{-3}$	12
		$^{241}\text{Am}$	$1.97 \cdot 10^{-3}$	21

Chapter 3  
Investigation on Plutonium metabolism



3.1.1 MATHEMATICAL TOOLS

3.1.1.1 Solution of a compartmental model

As briefly introduced in paragraph 1.3.2, the biokinetic models used in internal dosimetry are based on systems of compartments describing the kinetic of the radionuclide of interest in different organs or tissues. The amount of activity in the compartments is calculated by solving the system of differential equations which mathematically describes the compartmental model [56]. In case of a single acute intake the resulting system of differential equations with its initial conditions is given by:

$$\left\{ \begin{array}{l} \frac{dq_1(t)}{dt} = \sum_{j=2}^n r_{1,j} q_j(t) - q_1(t) \sum_{j=2}^n r_{j,1} - \lambda_R q_1(t) \\ \frac{dq_2(t)}{dt} = \sum_{j=1}^{n, j \neq 2} r_{2,j} q_j(t) - q_2(t) \sum_{j=1}^{n, j \neq 2} r_{j,2} - \lambda_R q_2(t) \\ \dots\dots \\ \frac{dq_i(t)}{dt} = \sum_{j=1}^{n, j \neq i} r_{i,j} q_j(t) - q_i(t) \sum_{j=1}^{n, j \neq i} r_{j,i} - \lambda_R q_i(t) \\ \dots\dots \\ \frac{dq_n(t)}{dt} = \sum_{j=2}^{n-1} r_{n,j} q_j(t) - q_n(t) \sum_{j=2}^{n-1} r_{j,n} - \lambda_R q_n(t) \end{array} \right. \left\{ \begin{array}{l} q_1(0) = q_0^1 \\ q_2(0) = q_0^2 \\ \dots\dots \\ q_i(0) = q_0^i \\ \dots\dots \\ q_n(0) = q_0^n \end{array} \right.$$

equation 3.1.1

where:

- $q_i(t)$  is the amount of activity in the i-th compartment at time t;
- $r_{i,j}$  is the transfer rate from j-th to i-th compartment;
- $\lambda_R$  is the physical decay constant;
- $q_0^i$  is the initial activity amount in the i-th compartment.

In the more compact matrix form, the same system of differential equations is written as:

$$\frac{d\mathbf{q}(t)}{dt} = (\mathbf{R} - \lambda_R \mathbf{I})\mathbf{q}(t) \quad \mathbf{q}(0) = \mathbf{q}_0$$

equation 3.1.2

where:

- $\mathbf{q}(t)$  is the vector of the amount of activity in the n compartments at time t;
- $\mathbf{R}$  is the matrix of the transfer rates;
- $\mathbf{I}$  is the unit matrix;
- $\mathbf{q}_0$  is the vector of initial conditions.

On the basis of the matrix form, the system can be solved by calculating the eigenvalues of the  $\mathbf{R}-\lambda_{\mathbf{R}}\mathbf{I}$  matrix. The relating eigenvectors  $\mathbf{v}_i$  will provide the solution of the system of differential equations [56]:

$$\mathbf{q}(t) = \sum_{i=1}^n c_i \mathbf{v}_i e^{\lambda_i t}$$

*equation 3.1.3*

where:

$c_i$  is the i-th coefficient;

$\lambda_i$  is the i-th eigenvalue;

$\mathbf{v}_i$  is the i-th eigenvector.

It should be pointed out that although the previous methodology is a very elegant way for solving a system of differential equations, the solution functions  $q_i(t)$  are given by a sum of exponential terms, each with its own exponent and coefficient, generally equal to the number of compartments constituting the model. For a model describing the metabolism of Plutonium isotopes after inhalation almost 50 compartments would be necessary, or even 100 if the metabolism of daughter isotopes too (as  $^{241}\text{Am}$  from  $^{241}\text{Pu}$ ) have to be modelled. The use of functions formed by a summation of 100 terms is not easy.

The previous methodology for solving a system of differential equations is appropriate when the transfer rates among the model compartments are constant, e.g. they are not depending on time. In ICRP models time dependent transfer rates are normally approximated with chains of compartments with different constant rates. Therefore the complexity of the model is increased, as a larger number of compartments is necessary, but all the transfer rates are constant, allowing to solve the model as previously described.

In the most general case, in which a compartmental model is based on time dependent transfer rates, the system of differential equations can be efficiently solved by means of numerical methods. The solution of the system is therefore given for a discrete and finite number of time points. These discrete solutions can be successively fitted to obtain an approximated function that allows calculating the solution at any time. It should be noted that the numerical functions approximating the solution are generally of a more simple and handy form than the summation of exponential terms obtained with the eigenvalues method.

In the present work the numerical methodology for solving systems of differential equations was adopted in order to consider general biokinetic models with time dependent transfer rates. For this purpose commercially available software [152] for dealing with general mathematical problems was used. Functions representing the amount of activity in the organs and tissues of the biokinetic models at any time after intake were calculated. The amount of activity calculated for the urinary bladder and the lower large intestine were multiplied by the respective clearance transfer rates to evaluate the instantaneous urinary and fecal excretion, respectively. In the practical situation the urine and fecal bioassays obviously do not refer to instantaneous rates but to a cumulative excretion over 24 hours. This is important for the first days after an initial single intake, while for times greater than about 20 days the difference among the instantaneous excretion and the 24 hours integrated function is negligible. Therefore to calculate realistic excretion values at a short time, comparable with the experimental data, the instantaneous excretion rates were integrated over a period of 24 hours for the first 20 days after exposure. The blood content of Plutonium was estimated by

calculating the amount of Plutonium activity in the blood compartment (often named transfer compartment too).

### 3.1.1.2 Target function for data vs. model comparison

The comparison of model predictions for a certain variable (e.g; activity in an organ or excreted in bioassays) with available data or empirical curves can be carried out qualitatively, as a first attempt, by plotting them. For a quantitative comparison it is necessary to select a target function that quantifies how good a certain model fits a given data set best.

An example of target function is given by Jones [111]. It is based on the assumption that bioassay data, specifically for urinary excretion, are distributed according to a lognormal distribution [153]. It is defined as:

$$L = \sum_{i=1}^n [\text{Log}d(t_i) - \text{Log}x(t_i)]^2$$

*equation 3.1.4*

where:

$d(t_i)$  is the experimental datum at time  $t_i$ ;

$x(t_i)$  is the value predicted by the model at time  $t_i$ ;

$n$  is the number of empirical data.

Other functions can be designed for such purpose, considering that the more a target function points out a disagreement between data and a curve, the more this function is appropriate. A target function was already used in a preliminary study to the present work [154]:

$$F = \sum_{i=1}^n \left[ \frac{d(t_i) - x(t_i)}{x(t_i)} \right]^2$$

*equation 3.1.5*

where the different elements have the same meaning as in Jones's target function. This target function has a similar structure to the  $\chi^2$  function. It is based on the deviation of each experimental datum from the relative value predicted by the model. The terms are then squared in order to eliminate the sign effect of the deviation. For such purpose the absolute value operation, instead of term squaring, could be also adopted and the target function would be defined as:

$$A = \sum_{i=1}^n \left| \frac{d(t_i) - x(t_i)}{x(t_i)} \right|$$

*equation 3.1.6*

By comparing the target function  $F$  and  $A$  in the equation 3.1.5 and equation 3.1.6, it can be seen that the  $F$  function will give more weight to large deviations. In fact if the experimental datum exceeds by two times the model's prediction, the squared deviation is greater than the absolute value of the deviation. On the contrary if the experimental datum

deviates from the model's prediction by less than a factor of two, the squared deviation is smaller than the absolute value of the deviation. Therefore it can be concluded that the target function F is particularly sensitive to experimental data that are significantly far (more than two times) from model's predictions.

In order to quickly compare the behavior of the different target functions, the experimental data available in the previously presented studies [80, 89-94, 98-100] were compared with the theoretical predictions of the empirical curves for the urinary excretions [80, 105, 109, 111-116,] by calculating the values of the target functions. The results for each empirical curve are given in Table 3.1.1 ordered according to the calculated values of the target functions.

**Table 3.1.1** Values of the target functions (L, F and A) calculated on the basis of the experimental data using different empirical curves..

Empirical curve	L	Empirical curve	F	Empirical curve	A
Tancock and Taylor (1993)	29	Tancock and Taylor (1993)	79	Tancock and Taylor (1993)	55
Jones (1985)	30	Jones (1985)	116	Jones (1985)	66
Leggett and Eckerman (1987)	34	Leggett and Eckerman (1987)	147	Leggett and Eckerman (1987)	72
Parkinson and Henley (1981)	44	Parkinson and Henley (1981)	197	Parkinson and Henley (1981)	89
Khokhryakov (1994)	45	Sun and Lee (1999)	197	Sun and Lee (1999)	91
Sun and Lee (1999)	57	Khokhryakov (1994)	230	Khokhryakov (1994)	93
Robertson and Cohn (1964)	61	Robertson and Cohn (1964)	340	Robertson and Cohn (1964)	114
Langham (1950)	69	Langham (1950)	436	Langham (1950)	128
Durbin (1972)	76	Durbin (1972)	508	Durbin (1972)	142

It can be seen that all the target functions yield almost the same sequence of empirical curves. Only the order of Khokhryakov's and Sun and Lee's curves are inverted when L target function is used. This means that they agree in deciding which empirical curve fits the experimental data best. However the ratios of the maximum by the minimum values calculated for each target functions are significantly different: for functions L and A it is about 2.6, whereas for F it is more than 6. As previously announced, this means that the F target function can more efficiently detect discrepancies between experimental data and model calculations. Therefore the target function F was adopted to quantify the agreement among the experimental data, empirical curves and models predictions.



### 3.1.2 ANALYSIS OF THE ICRP 67 MODEL

#### 3.1.2.1 *The reference data set*

The information available on the excretion of Plutonium is given by the experimental data and empirical curves described in the paragraphs 2.1.1 and 2.1.2 of Chapter 2. However it should be noted that the subjects, initially studied in the frame of Langham's research [80] and followed-up by Rundo et al., Moss et al., Tancock et al. [88, 89-94], were affected by various pathologies. Therefore in the present work Jones's approach [111] was followed: Only the excretion data judged by Durbin [106] to be representative of healthy subjects were used. An exception was made for some subjects with impaired kidney conditions. In these cases only the data from time periods for which Durbin showed that the impaired conditions do not influence the excretion curve were used.

The experimental data for the subjects considered in the two main 'in vivo' studies (by Langham et al., abovequoted, and by Talbot et al. [98-100]) were obtained under approximately the same experimental conditions. Therefore the data can be considered as resulting from only one group, particularly if Jones's and Durbin's method of data selection is adopted. In the following part the two data sets are briefly compared in order to point out their coherence. For each group of subjects the maximum, minimum and the geometric mean values of the Plutonium excretion were evaluated at each time point (the geometric mean as central parameter is normally adopted in such studies [111]). This was carried out only for urinary and fecal excretion data of male subjects at short time because in all the other situations (male subjects data at long time or female subjects data at any time points) only few data are available. In order to easily compare the two groups of subjects for each time, the ratios of the considered values (maximum, minimum and geometric mean) for Langham's group of subjects by the relative values for Talbot's group of subjects were calculated. The resulting ratios were finally averaged over all the time points to have an estimation of the mean discrepancies among the considered quantities of the two subjects groups. The results are given in Table 3.1.2. Several samples from Talbot's subjects were not collected exactly at 24-hours intervals as in Langham's study. Therefore, in order to have data for the same time points, samples collected in Talbot's study were corrected by means of a logarithmic interpolation to reduce them to the same sample collection intervals as in Langham's study.

**Table 3.1.2.** *Comparison of Langham's and Talbot's data sets for Plutonium daily urinary and fecal excretion: Ratios of the geometric means (RGM), maxima (Rmax) and minima (Rmin) values averaged at short time post injection.*

Parameter	Urine	Feces
RGM	0.93	1.12
Rmax	1.17	1.82
Rmin	0.74	1.50 (a)
		0.96
		0.93 (a)

(a) These values were calculated by omitting the data for the 16<sup>th</sup> day post injection.

From Table 3.1.2 it turns out that the ratio of the geometric means are very close to 1. The geometric mean of the Plutonium urinary excretion observed in Langham's subjects in the considered time period is on average 7% smaller than the same value for Talbot's subjects; for the fecal excretion a discrepancy of 12% was observed. Such percentages point out that, on average, the geometric means for the two data sets are not significantly different. The mean maximum and minimum values of the urinary excretion of Plutonium for Langham's subjects on average are +17% and -26 % of the observed values for Talbot's subjects, respectively. Only the fecal excretion of Plutonium has a maximum value that on the average is 82% greater, but a more careful analysis of the data has shown that this is due mainly to just one subject. By eliminating the excretion data of this subject, the deviation is already reduced to +50%. Large deviations of the maximum and minimum values for the two data sets can be easily found because these values relate to a single subject, and not to all the subjects of the group as the geometric mean previously calculated.

According to the previous considerations too, Langham's and Talbot's data sets can be considered as only one group of data, particularly when they are used to calculate a mean to be adopted as a reference value of Plutonium excretion. Therefore the values for the urinary excretion of Plutonium from all the subjects of the two groups were averaged by calculating the geometric mean for each time point. Analogously the geometric means of the data for Plutonium fecal excretion and blood content were calculated. From now on the term "experimental data" will refer to such geometric mean values calculated on the whole group of subjects from Langham's and Talbot's studies.

The effect of a subject's gender on the excretion of Plutonium should be also considered. Studies [100, 101] have recently pointed out slight but constant differences between the urinary excretion of Plutonium between male and female subjects. Unfortunately the small number of female subjects in Langham's study doesn't allow confirming such observation. Langham's study is based mainly on male subjects and therefore even the empirical curves available in the literature, most of which were derived from such data to evaluate the urinary and fecal excretion, primarily relate to Plutonium biokinetics in men. The few curves, calculated from data other than Langham's, as in Khokhryakhov et al. [114], relate mainly to male subjects as well.

This reflects also the most realistic situations in nuclear professional environment where most of the workers involved were and are of male gender. Therefore from now on the present work will essentially consider the biokinetics of Plutonium in male adult subjects.

In order to study and develop a model for Plutonium biokinetics in humans the experimental data we previously analyzed are of foremost importance. However, whereas for the first 4-5 months after injection a certain number of measurements is available, measurements on humans beyond this time are rare. Therefore the use of published excretion functions becomes inevitable for evaluating Plutonium urinary excretion at long time after intake. The choice of an empirical curve should comply with the following conditions:

- The number of data from which the curve was calculated should be as large as possible;
- The curve should agree with the few available experimental data for long time after injection;
- Eventual good agreement of the empirical curve provided in the same study but relating to other bioassays (such as Plutonium fecal excretion or blood contents) should be considered.

For a preliminary qualitative comparison in Figure 3.1.1 and Figure 3.1.2 the daily percentage of Plutonium excreted in the urine calculated from the various empirical curves is presented together with the available measurements. It can be already seen as the former

empirical curves given by Langham, Robertson and Cohn, Durbin, Parkinson and Hanley [80, 105, 106, 109] underestimates after 100 d post injection the few experimental data. These data agree better with the curve provided by Jones, Khokhryakov, Sun and Lee [111, 114, 116].

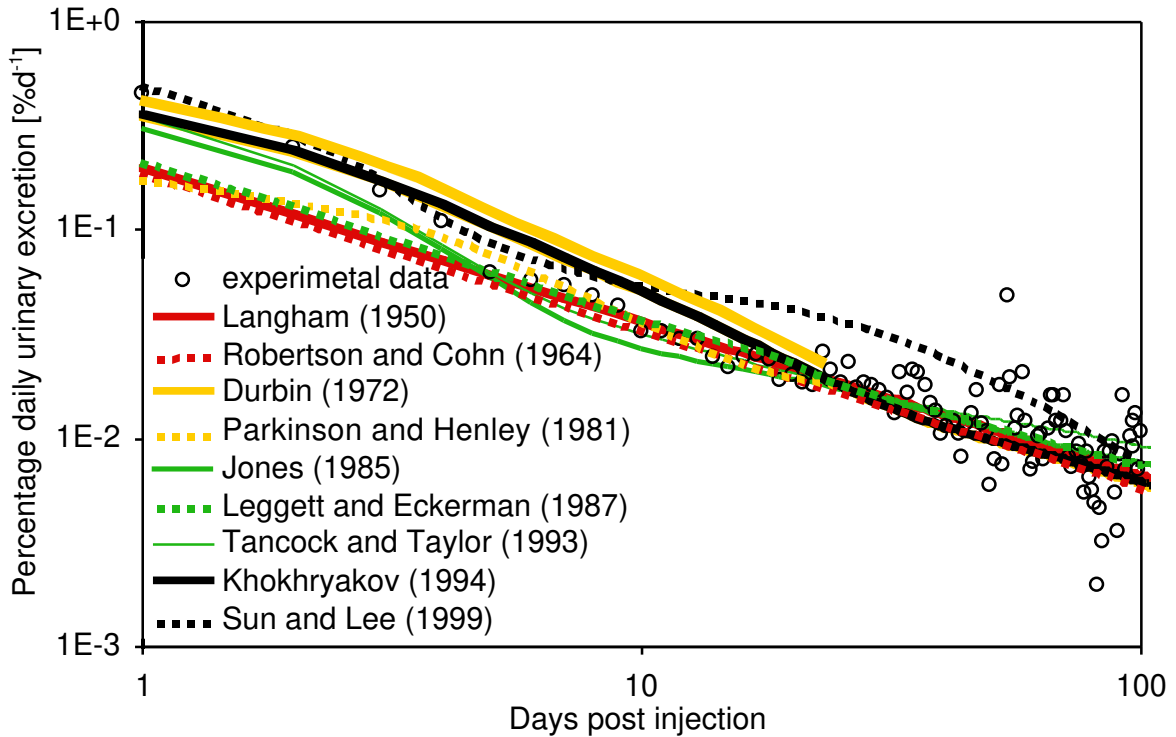


**Figure 3.1.1** Empirical curves and experimental data for Plutonium percentage daily urinary excretion up to 100 days post injection.

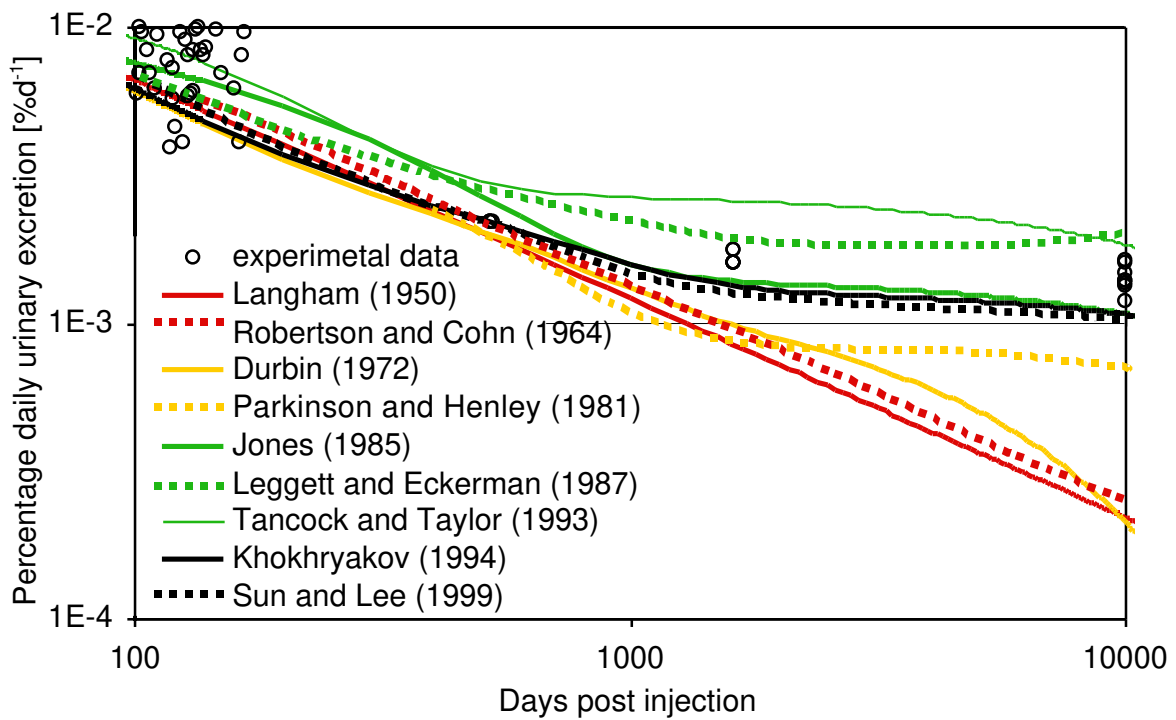


**Figure 3.1.2** Empirical curves and experimental data for Plutonium percentage daily urinary excretion after 100 days post injection.

For a more quantitative comparison the values of the F target function were calculated on the basis of the experimental data using different empirical curves. In Table 3.1.3 the empirical curves are ordered according to increasing values of the calculated F target function. As the experimental data are rare after 138 days post intake (see Langham's study), and the use of an empirical curve gets important in this time range, values of F relating only to the data after about 4 months post intake were also calculated.

**Table 3.1.3** Rank of the empirical curves for Plutonium daily percentage urinary excretion according to increasing values of the F target function. The values are calculated on the basis of both all the experimental data and the data at time greater than 4 months post injection.

All the data		Data at t > 4 months	
Rank	Curve	Rank	Curve
1	Tancock and Taylor (1993)	1	Leggett and Eckerman (1987)
2	Jones (1985)	2	Jones (1985)
3	Leggett and Eckerman (1987)	3	Khokhryakov (1994)
4	Parkinson and Henley (1981)	4	Tancock and Taylor (1993)
5	Sun and Lee (1999)	5	Sun and Lee (1999)
6	Khokhryakov (1994)	6	Parkinson and Henley (1981)
7	Robertson and Cohn (1964)	7	Robertson and Cohn (1964)
8	Langham (1950)	8	Langham (1950)
9	Durbin (1972)	9	Durbin (1972)

It can be pointed out that Tancock's and Taylor's empirical curve has the best performances when all the experimental data are considered. This should not surprise because the experimental data set is partially formed by the same data on which Tancock's and Taylor's empirical curve was developed. This confirms again that the F target function can be considered as a good indicator of the agreement between data and curves. On the opposite Langham's and Durbin's curves show the worst performances. This is due to two main reasons. Firstly the data on which these curves are based were not corrected for chemical yield, as was done later by Tancock and co-workers. Secondly Langham's and Durbin's curves were derived before the data on the urinary excretion of Plutonium by Rundo et al. were available. Therefore these curves are not able to correctly estimate the excretion at longer time, as pointed out already in Figure 3.1.2 where a significant underestimation of the real urinary excretion is shown.

If the experimental data at long times are considered, the rank of the best fitting curves changes. On the basis of the F values (not reported in the previous table), the differences among the first four curves are not greater than 50%. The next best fitting curve (Sun and Lee) has a F value that is already 2 times greater than the previous ones. All the other curves show worse performances, with F values greater by about a factor 200 or more. Among the best fitting curves, Tancock's and Taylor's curve was designed, for long time predictions, by considering only a single case of occupational contamination. Therefore it is characterized by

the worst performance of the group. Jones' curve was explicitly designed including the few available experimental data at long times and therefore a good agreement with the experimental data can be expected. The other two curves are based on partially (as in Leggett and Eckerman) or even totally different (as in Khokhryakov) data sets and therefore their agreement with the experimental data from Langham's and Talbot's subjects is even more intriguing. Furthermore Khokhryakov's curve was developed on a relatively large database of 25 subjects. According to the conditions defined above for choosing a reference empirical curve for the urinary excretion of Plutonium, Khokhryakov's curve seems to be already one of the best candidate. The fecal excretion could give further guidance.

For a qualitative comparison in Figure 3.1.3 the daily fecal Plutonium excretion calculated from the available empirical functions is presented together with the available experimental data.

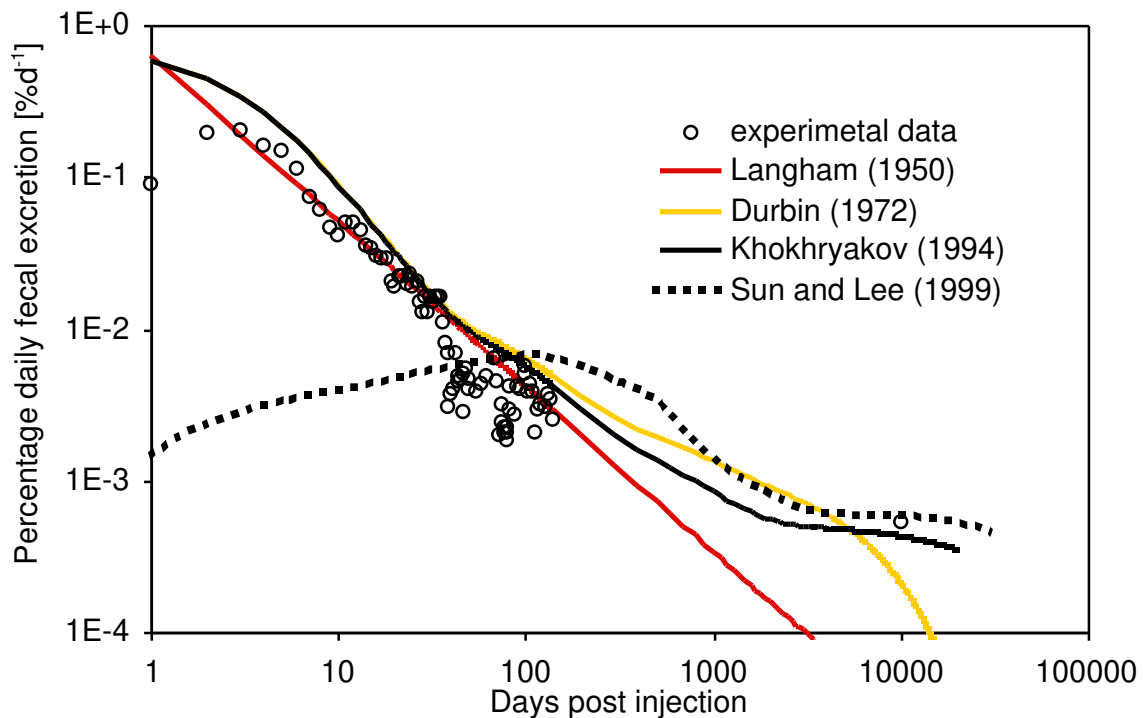


**Figure 3.1.3** Empirical curves and experimental data for Plutonium percentage daily fecal excretion.

As in the case of the urinary excretion the values of the target function  $F$  were calculated on the basis of the experimental data using the available empirical curves (Table 3.1.4). According to Table 3.1.4 Khokhryakov's curve has the best agreement with the whole experimental data set for the fecal excretion. In Figure 3.1.3 it results that Sun's and Lee's curve fits only the available data at longer times but it is characterized by the worst performance for the fecal excretion at shorter time. Langham's has a good agreement with data only at short and intermediate times while at long times it underestimates excretion. Khokhryakov's and Durbin's curves have almost the same trend at short and intermediate times (because they have the same short time exponential terms in their analytic expression) but at long times Khokhryakov's curve fits better the only available datum from one subject.

**Table 3.1.4** Rank of the empirical curves for Plutonium daily percentage fecal excretion according to increasing values of the *F* target function.

Rank	Curve
1	Khokhryakov (1994)
2	Durbin (1972)
3	Langham (1950)
4	Sun and Lee (1999)

On the basis of the previous considerations it turns out that Khokhryakov's curve seems to be the best choice for estimating the urinary excretion at long time because:

- it shows a good agreement with the few experimental data for this time period;
- it was derived from a large data set;
- the equivalent curve for the daily percentage fecal excretion has the best agreement with the experimental data.

Therefore the 'reference data set' that will be the basis for the evaluation of the model's accuracy in predicting the urinary excretion of Plutonium consists of:

- experimental data derived from systemic studies on subjects from Langham's and Talbot's subjects;
- Khokhryakov's empirical curve for estimating the urinary excretion at long time when few experimental data are available.

The experimental data for Plutonium fecal excretion and blood content were only secondarily considered because such bioassays are rarely used in the radiation protection practice. Therefore the model was tested and modified only partially on the basis of such data.

### 3.1.2.2 Model predictions compared to reference data

The estimated daily urinary excretion for the ICRP 67 model together with the reference data set (experimental data from Langham's and Talbot's studies and Khokhryakov's empirical curve beyond 4 months) are presented in Figure 3.1.4.

The plots in Figure 3.1.4 show that the ICRP 67 model overestimates the urinary excretion of Plutonium by about a factor of two for the first three days and by about 1.5 the following days of the first week. It also overshoots the experimental data and Khokhryakov's excretion curve after 100 days. At 10,000 days we have a good agreement between the experimental data, Khokhryakov's curve and ICRP 67 model. This agreement between ICRP 67 and the experimental values at around 10,000 days was achieved by introducing the aforementioned connection between ST1 soft tissue compartment and urinary bladder (as discussed in paragraph 1.4.2 of Chapter 1). The effect of this assumption was clearly demonstrated in Figure 1.4.2 where it was pointed out that the urinary excretion in the ICRP model for Plutonium biokinetics is mainly governed by a postulated excretion pathway which completely lacks justification by any known physiological process. The importance of this assumption is clearly shown in Figure 3.1.4. The curve designated ICRP67-a depicts the urinary excretion of Plutonium according to ICRP 67 model but without the connection between the soft tissue compartment ST1 and the urinary bladder. The activity previously transferred to the urinary bladder content is re-directed to the blood compartment in order to

leave the total clearance from the ST1 compartment unchanged. It turns out that the predictions underestimate the urinary excretion starting already at around 10 days and up to a factor of three at 10,000 days.

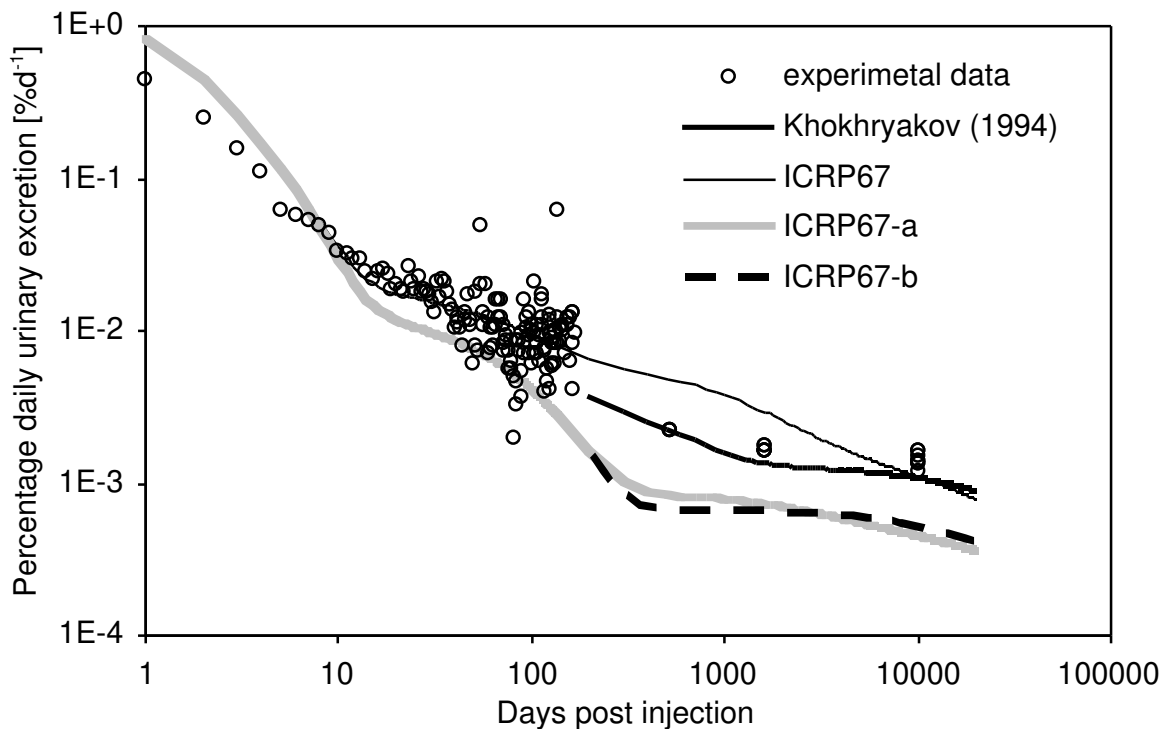


**Figure 3.1.4** Reference data set and ICRP 67 original and modified versions predictions for percentage daily urinary excretion of Plutonium.

It's well known that Plutonium is a so called "bone seeker" element because of its affinity to the bone tissues where it mainly concentrates. The model of the skeleton implemented in ICRP 67 is derived from the basic anatomical and physiological data presented in ICRP 70 [155]. In ICRP 70 age dependent bone remodelling rates are given for different age classes: From new-born until adult subjects of 60 years of age (see Table 3.1.5). For adult subjects after age 25 years, average values for both cortical and trabecular remodelling rates are given.

The skeletal model for adults implemented in ICRP 67 is based on values of 3%/year for cortical and 18%/year for trabecular remodelling rates that, at long time, are slightly smaller than the effective age related values suggested by ICRP 70. Therefore the possibility of compensating with age dependent skeleton rates the underestimation of Plutonium urinary excretion when no connection between the soft tissue compartment ST1 and the urinary bladder was tested. For this purpose in Figure 3.1.4 the curve named ICRP67-b is also depicted. It represents the Plutonium urinary excretion for an adult subject as predicted by ICRP67-a model but additionally with time dependent transfer rates for the skeletal compartments, as suggested by ICRP 70. The calculation of the urinary excretion of version ICRP67-b was carried out considering a male subject 45 years old, the age of subject HP-6 of Langham's study, from whom most of the experimental data beyond 200 days come. For this calculation the comparison with Khokhryakov's excretion curve should not be overemphasized because this curve was obtained for a group of subjects with age between 47

to 73 years, and thus does not relate to a specific age. The age dependent bone remodelling rates in the ICRP67-b model were calculated by a linear interpolation between the values suggested by the ICRP 70 for subjects 22, 35 and 60 years old. For ages greater than 60 years constant bone turnover rates were assumed. In Figure 3.1.5 the bone remodelling rates, used in the ICRP67-b model, are presented as a function of the age of an adult subject and compared with the constant remodelling rates of ICRP 67.

**Table 3.1.5** Age dependent cortical and trabecular remodelling rates for different age classes according to ICRP 70.

Age	Bone remodelling rates [%/year]	
	Cortical Bone	Trabecular Bone
0 – 3 months	300	300
1 year	105	105
5 year	56	66
10 year	33	48
15 year	19	35
22 year	9	27
35 year	2	10
60 year	4	20
Average after age 25 years	3	18

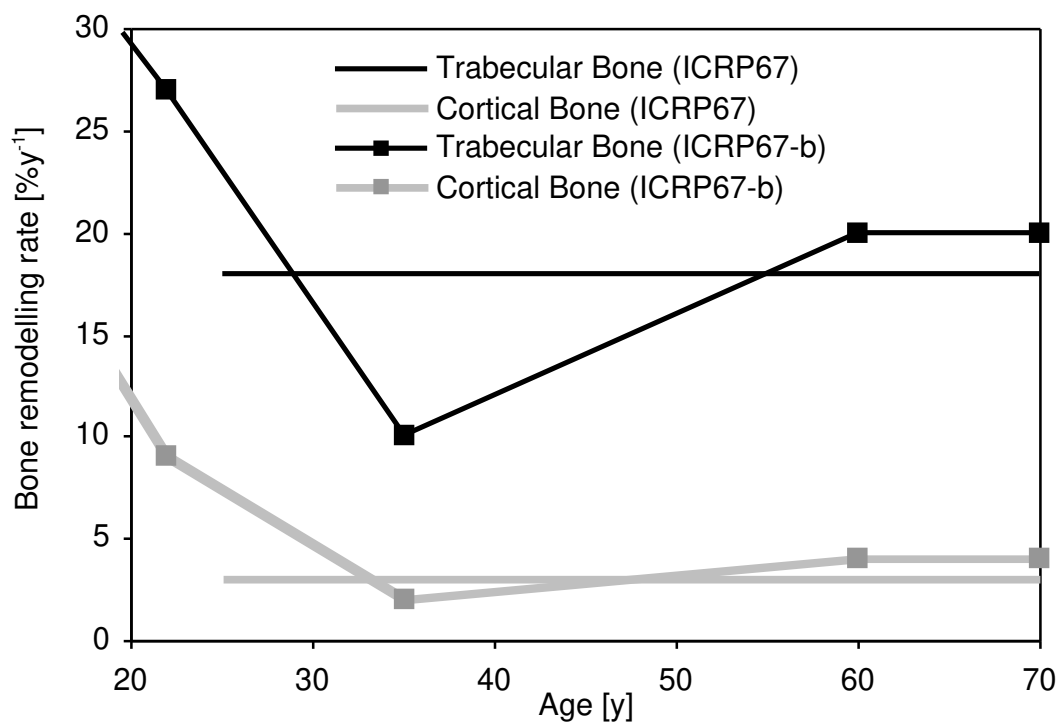


**Figure 3.1.5** Cortical and trabecular remodelling rates as functions of age.



Figure 3.1.4 shows that the use of time dependent bone turnover rates does not remedy the underestimation of the ICRP67-a model, because practically no significant lifting of the urinary excretion curve occurs. At around 10,000 days post injection the Plutonium urinary excretion is increased by about 10% relative to the value of ICRP67-a with constant bone rates, but it is still smaller by a factor of three than the experimental value at this time (0.0014 %/d on average).

The ICRP 67 model predictions for Plutonium fecal excretion and blood retention were also compared to the reference data set (Figure 3.1.6 and Figure 3.1.7). It can be pointed out that the ICRP 67 model overestimates the fecal excretion up to a factor 2 during the first week after the injection, whereas underestimates up to a factor 5 in the following twenty days. The general trend of model predictions in this time range seems to be in disagreement with experimental outcomes because the reference data shows a more gradually decrease of Plutonium activity in feces. A sufficient agreement with the reference data exists only at longer term: At around 10,000 days post injection model and experimental data differ by less than 15%. For the Plutonium activity in blood the situation is similar with an initial overestimation in the first week post injection, followed by an underestimation in the following twenty days. However in this case the ICRP 67 model underestimates the reference data up to about a factor of 20.

The effect of the deletion of the connection between the ST1 soft tissue compartment and urinary bladder on fecal excretion and blood retention was also investigated. Because of such modification the activity in the ST1 compartment is completely transferred to the blood compartment. Therefore an increase of activity in the blood compartment and consequently in the excreted activity in feces is expected. This can be seen in Figure 3.1.6 and Figure 3.1.7 (ICRP67-a curves). For the fecal excretion the effect is significant only at very long times (at 10,000 days post injection the excreted activity increases by about 30%). No effect is observable at shorter times when the model predictions and reference data are in total in disagreement. In case of the blood retention of Plutonium the activity increases at shorter times: Already at around 30 days it is increased by 50%. However the predictions of blood retention are still very far from the reference data.

Analogously to the urinary excretion analysis, the effect of age dependent bone remodelling rates according to ICRP 70 is also shown in Figure 3.1.6 and Figure 3.1.7 (ICRP67-b curves). As in the case of urinary excretion, the effect of such modification on fecal excretion and blood retention of Plutonium is quite small and, in any case, doesn't improve significantly the agreement with the reference data set.

On the basis of the previous considerations it can be summarized that:

- The Plutonium urinary excretion predicted by ICRP67 shows some disagreements with the reference data set; the fecal excretion and blood retention of Plutonium predicted by this model shows even more severe disagreement;
- If a physiologically based modelling is assumed by deleting the transfer of activity from ST1 soft tissue to urinary bladder content compartment, the ICRP 67 predictions for the Plutonium urinary excretion are significantly far from the reference data. This points out that the ICRP 67 assumption of such transfer of activity is not a minor correction of the model but essentially determines the urinary excretion of Plutonium at long times;
- Age dependent bone remodelling rates as suggested by ICRP in Publication 70 were also considered but they don't result in a significant improvement.

Therefore a general overhaul of the ICRP 67 model seems to be necessary.

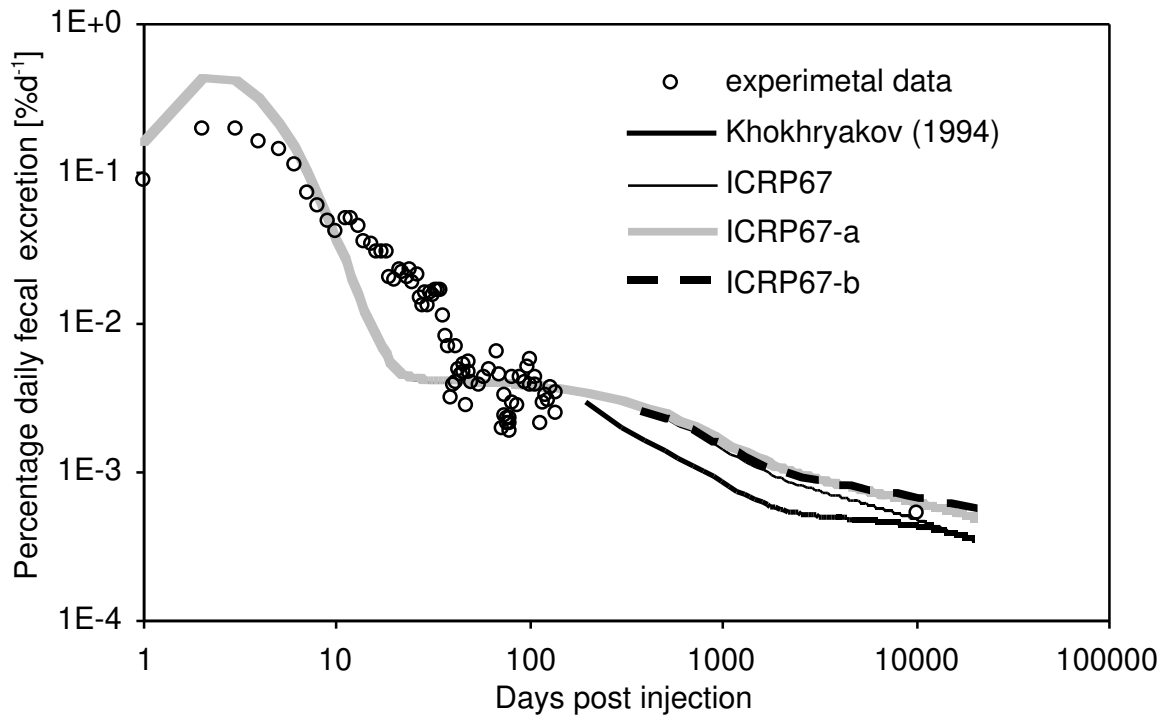


**Figure 3.1.6** Reference data set and ICRP 67 original and modified versions predictions for percentage daily fecal excretion of Plutonium.

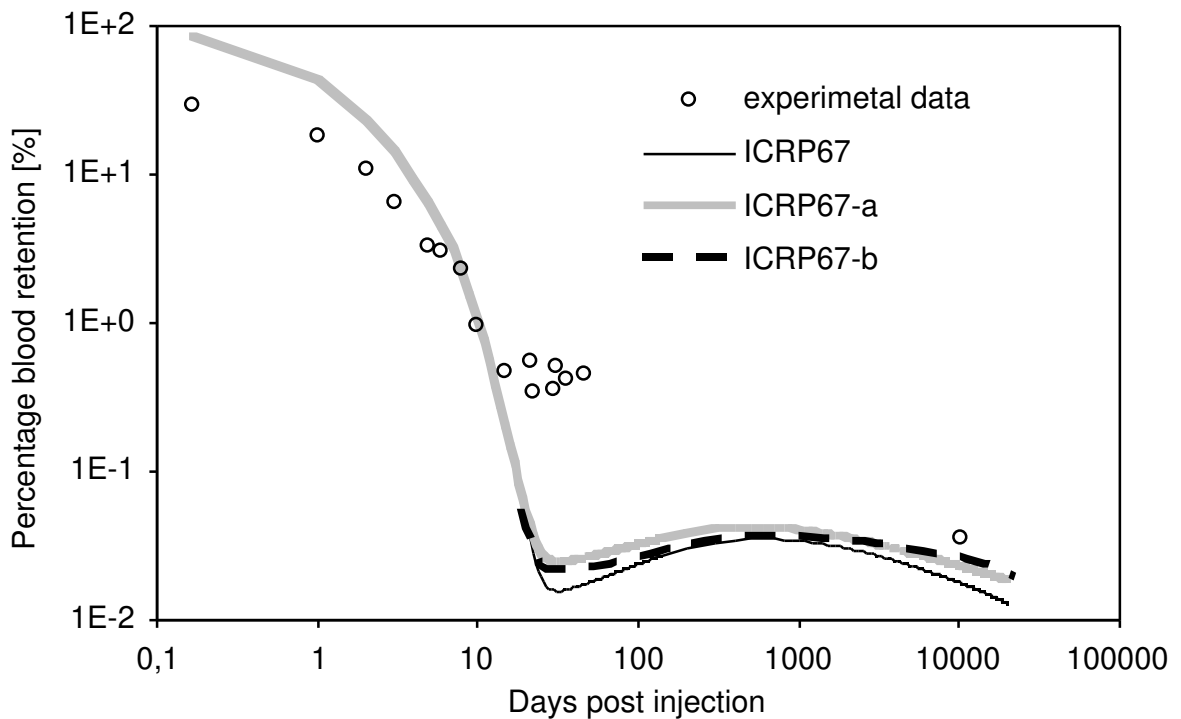


**Figure 3.1.7** Reference data set and ICRP 67 original and modified versions predictions for percentage blood content of Plutonium

### 3.1.3 MODIFICATION OF ICRP 67 MODEL

Part of the following study was already reported in recent publications [154, 156].

#### 3.1.3.1 *New concepts of skeletal remodelling*

In order to achieve a better agreement with reference data set, particularly for the urinary excretion of Plutonium, the ICRP 67 model was firstly analyzed pointing out the leading transfer processes determining the biokinetics and so the excretion of Plutonium. According to the purpose of developing a physiologically based model, the ICRP67-a model previously described was the starting point.

The activity in the central transfer compartment represents the amount of activity generally available to successive metabolising processes as urinary and fecal excretion. Therefore the contribution to the amount of activity retained in blood from the organs directly transferring activity to the blood compartment was calculated. This allows identifying which organs or tissues are of main importance to the excretion processes. At this preliminary phase of the study of the model such approach was preferred to a complete sensitivity analysis for the urinary excretion performed on all the transfer rates of the compartments present in the model. The main reasons of this approach are:

- it is not as much time-consuming as the calculation of sensitivity coefficients that should be evaluated for a number of time points covering the whole time range of interest;
- it can easily and quickly provide the contribution of whole functional systems by considering the single compartment directly connecting them to the blood compartment. This is the case of the skeletal model where the whole skeletal system transfers its activity to the blood through the marrow compartments. In a similar way the hepatic system clears its activity just through the Liver 2 compartment.

The analysis was performed for all the organs and tissues contributing to the activity content of the blood compartment: skeleton (trabecular marrow and cortical marrow), liver (compartment Liver 2), ST0, ST1 and ST2 soft tissue compartments, other kidney tissue compartment (OKT), gonads and small intestine. In Figure 3.1.8 the daily transfer of activity from those organs and tissues that mainly contribute to the blood central compartment activity is presented (daily transferred activity greater than  $10^{-5} \text{ d}^{-1}$ ).

It can be pointed out that the activity transfer from the ST0 compartment almost exclusively determines the activity content of the blood for the first 20 days after the injection. The ST1 compartment has a significant contribution just in the time range 20 – 100 days post injection. More interesting are the contributions at long term, when the disagreement between reference data set and modified version of ICRP 67 (ICRP67-a) was observed. After 100 days the contribution due to the skeleton becomes predominant. The hepatic system becomes significant at longer time: at around 8,000 days post injection it is the 80 and 66% of the contributions of ST0 soft tissue and skeleton compartments, respectively. The small intestine contributes only marginally to the activity in the blood compartments: at about 30 days its contribution is 50% of ST0 contribution and it vanishes soon from 100 days post injection.

From the previous analysis it turns out that the skeleton is the main system in determining the activity in the blood compartment at intermediate and long times. Therefore it should be considered first if ICRP 67 model predictions for biokinetics of Plutonium in this time range can be improved by considering the skeletal system. A new model for Plutonium biokinetic in skeleton recently developed was considered [157]. This model is based on available information on the microdistribution of transuranic elements in animals and humans as obtained from autoradiographic analyses. It is also based on morphometric and

histomorphometric data characterizing the human skeleton and its remodelling processes. The structure of the model is given in Figure 3.1.9 where it can be compared with the ICRP 67 original skeleton model.

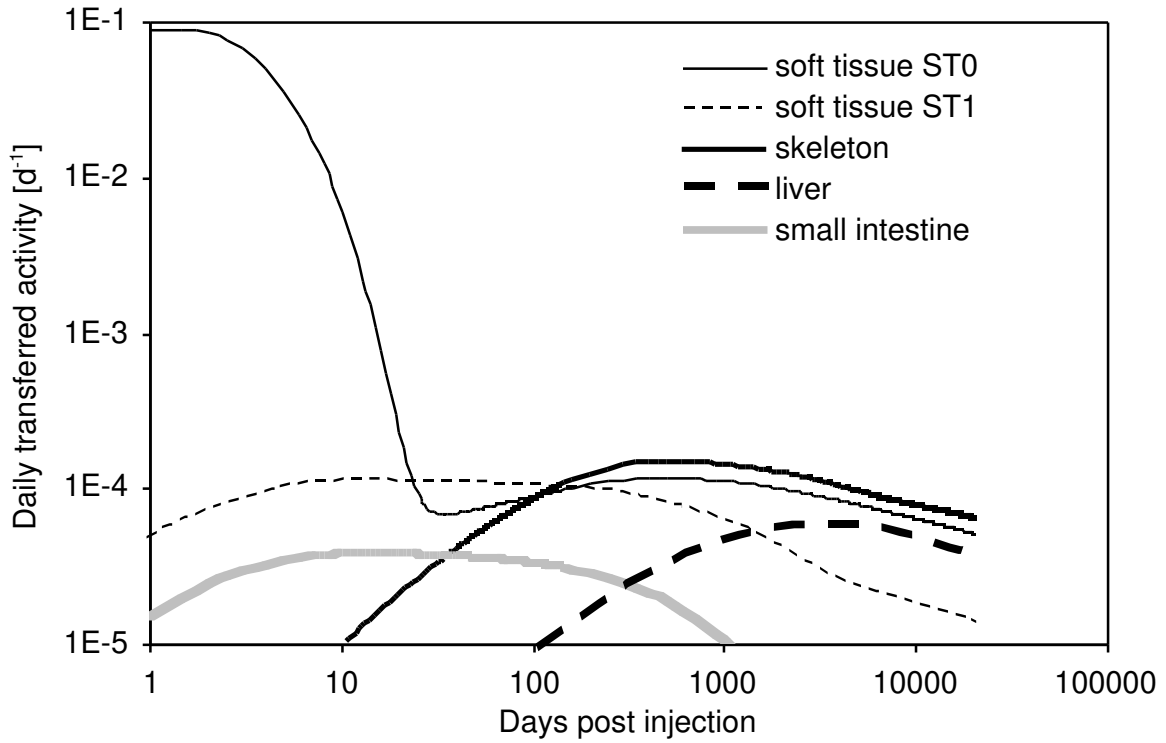


Figure 3.1.8 Fraction of Plutonium uptake transferred per unit time from the most relevant compartments to blood for the model coded ICRP67-a.

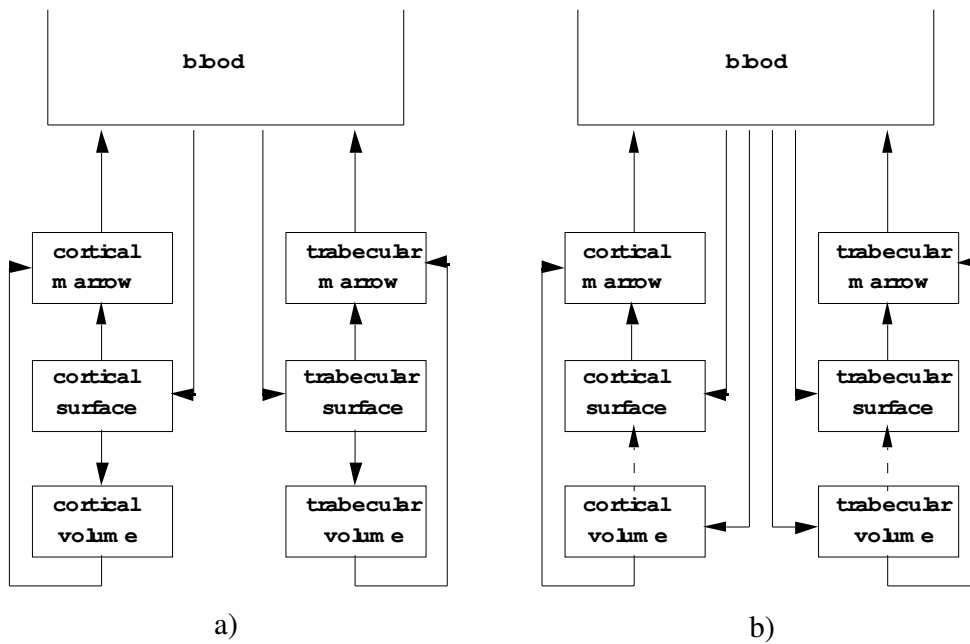


Figure 3.1.9 Structure of the skeletal models in ICRP 67 (a) and Polig [157] (b).

The structure of Polig's skeleton model is characterized by an initial deposition on both surface and volume bone compartments and not only on cortical surface as assumed in ICRP 67 model. Furthermore a transfer of activity from volume to surface compartments (dashed arrows in Figure 3.1.9) is theoretically introduced to achieve maximum generality in skeleton modelling by considering a possible local recirculation too. As presently there is no experimental evidence of such process, it was not longer considered in this skeleton model. The two models differ in the transfer rates values too, as given in Table 3.1.6.

**Table 3.1.6** Transfer rates of the skeletal models in ICRP 67 and Polig [157].

Parameter	Value [d <sup>-1</sup> ].	
	ICRP 67	Polig
Blood compartment to Trabecular surface	0.1941	0.226
Blood compartment to Trabecular volume	N.A.	0.0716
Blood compartment to Cortical surface	0.1294	0.0952
Blood compartment to Cortical volume	N.A.	0.00448
Trabecular surface to marrow	0.000493	0.00159
Trabecular volume to marrow	0.000493	0.00159
Trabecular surface to volume	0.000247	N.A.
Cortical surface to marrow	0.0000821	0.000156
Cortical volume to marrow	0.0000821	0.0000822
Cortical surface to volume	0.0000411	N.A.
Trabecular/Cortical marrow to blood compartment	0.0076	0.0076

By comparing the transfer rates for the two skeletal models it can be pointed out that Polig's model is characterized by a higher transfer of activity to the trabecular bone (+53%) and slightly smaller (-23%) to the cortical bone. The final effect is a generally higher activity transfer to the whole skeleton. Furthermore the skeletal transfer rates of Polig's model are generally higher then those ones of ICRP 67 model. On the basis of such preliminary considerations two aspects will characterize Polig's model in comparison to ICRP 67 one:

- initial higher deposition into the skeleton;
- a lower retention in the skeleton at long time with a higher transfer of activity to the blood compartment.

These considerations are confirmed by analyzing the biokinetics of Plutonium in a study compartmental model composed by just a transfer (blood) compartment connected to the skeletal model (Polig or ICRP67). The activity retention in skeleton and blood compartments was calculated and is presented in Figure 3.1.10 for both skeletal models. As preliminarily argued on the basis of the transfer rates in Table 3.1.6, the initial amount retained in the skeleton is slightly higher if Polig's model is adopted. More significantly at intermediate and long time Polig's skeletal model predicts a lower Plutonium retention than ICRP 67 and, consequently, the blood compartment contains a higher amount of activity. For example at 1,000 days post intake the use of Polig's skeletal model yields skeleton and blood

activity values by a factor of 2 smaller and by a factor 2.5 higher, respectively, than ICRP 67. At 10,000 days post intake the amount of activity in the blood compartment doesn't significantly differ in relation to the adopted skeletal model. On the basis of such considerations it can be concluded that, by predicting greater amounts of Plutonium in the transfer compartment at intermediate and long time, Polig's model seems to be able to correct the low urinary excretion of Plutonium calculated with the ICRP 67 model when no transfer of activity from ST0 soft tissue compartment to urinary bladder content is assumed (ICRP67-a curve in Figure 3.1.4). This can be verified by substituting the ICRP skeletal model in the ICRP67-a version with Polig's skeletal model and then calculating the urinary excretion of Plutonium (ICRP67-a-Polig curve in Figure 3.1.11).

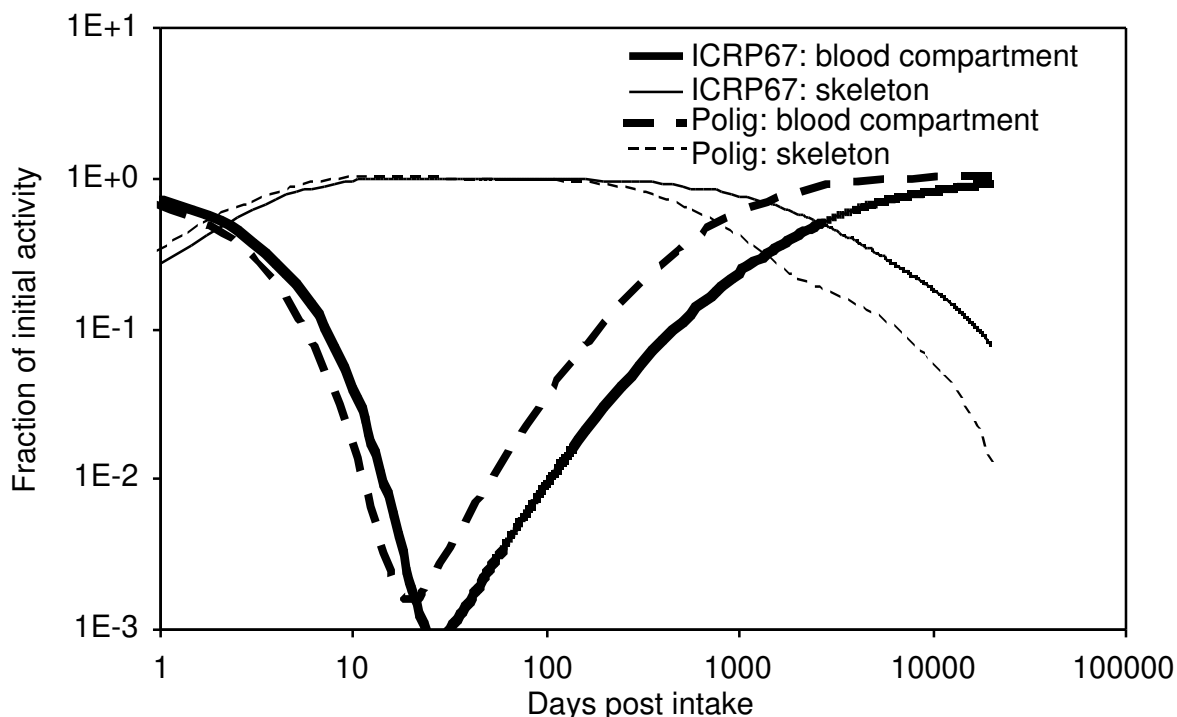


**Figure 3.1.10** Fraction of initial activity retained in blood and skeleton for a study model composed by a blood compartment connected to a skeletal model (ICRP 67 or Polig's skeletal model).

As expected from Figure 3.1.8 the substitution of the skeletal model doesn't significantly affect the activity in blood compartment up to 100 days post injection and therefore doesn't modify the urinary excretion in this time range. At long time the increase of available activity in blood compartment following the introduction of Polig's skeletal model (observed in Figure 3.1.10) enhances the urinary excretion of Plutonium: In Figure 3.1.11 the urinary excretion is closer to the reference data set up to about 2,000 days post injection. In this time range Polig's skeletal model has effected a lift of the excretion curve by a factor 2.5 in comparison with the excretion of ICRP67-a model. This seems to support the claim that Polig's skeletal model is a more realistic description of Plutonium biokinetics in skeleton than the skeletal model adopted in ICRP 67. After 2,000 days post injection the model predictions underestimate the reference data set. For example at 10,000 days the model calculations are low by nearly a factor of two, if compared to ICRP 67 (0.0011%/d<sup>-1</sup>), Khokhryakov (0.0011%/d<sup>-1</sup>) and Langham's subject HP-6 (0.0014%/d<sup>-1</sup>).

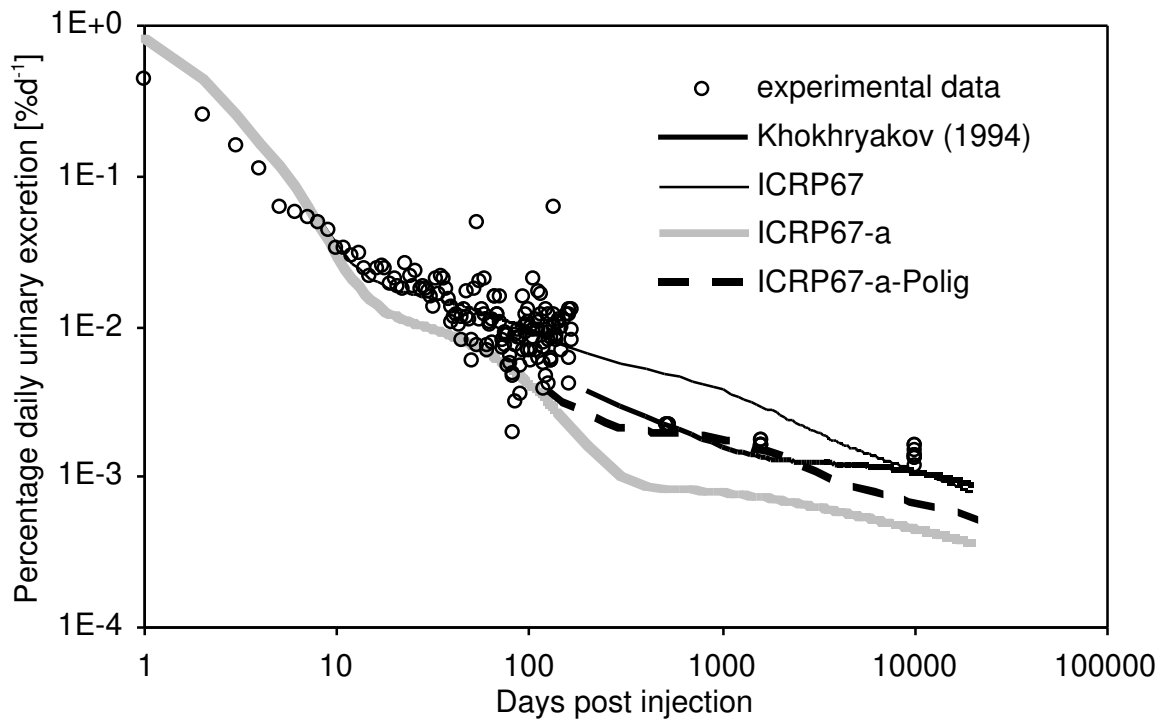


**Figure 3.1.11** Reference data set and ICRP 67 original and modified versions predictions for percentage daily urinary excretion of Plutonium.

The introduction of Polig's skeletal model does affect the Plutonium fecal excretion and retention in blood too. Particularly at long times the significantly higher availability of Plutonium in blood is confirmed by the blood retention curve that is higher than the respective curve based on ICRP67-a up to a factor 2.5 at 500 days post intake. At 10,000 days the model's predictions and the available data for one of the reference data set subject are in good agreement. The predicted higher blood content consequently affects the fecal excretion of Plutonium that tends to be higher than the ICRP67-a model predictions. However in comparison with the reference data set the calculated fecal excretion still does not agree very well.

In conclusion it should be stressed that Polig's skeletal model allows compensating the underestimation of the urinary excretion of Plutonium when no transfer of activity is assumed from ST1 soft tissue compartment to urinary bladder content. The simple introduction of this model has improved the predictions of urinary excretion up to 2,000 days post intake. Effects on secondary biokinetic curves (fecal excretion and blood retention) were considered but no significant improvement in comparison with the reference data set was observed.

### 3.1.3.2 Optimization of the parameters

On the basis of previous evaluations and preliminary calculations, optimization procedures were carried out in order to provide eventually a compartmental model that can well describe the urinary excretion of Plutonium and possibly improve ICRP 67 model predictions for Plutonium activity in feces and blood. The previously commented ICRP67-a-Polig model represents the starting point of the following optimization procedures. It is depicted in Figure 3.1.12. The numbered arrows depict the transfer rates that were modified

from the ICRP 67 model. At the top there is also a brief explanation from which experimental data (urinary excretion, fecal excretion, blood content or partitioning ratio from autopsy studies) they were estimated or calculated. The affected compartments of the gastrointestinal tract are also included.

The main characteristics of the work models that are introduced and discussed in the presented paragraph are summarized in Table 3.1.11.

- 1 Transfer rates derived from blood activity      3 Transfer rates derived from autopsy data  
 2 Transfer rates optimized on urinary excretion      4 Transfer rates derived from fecalexcretion

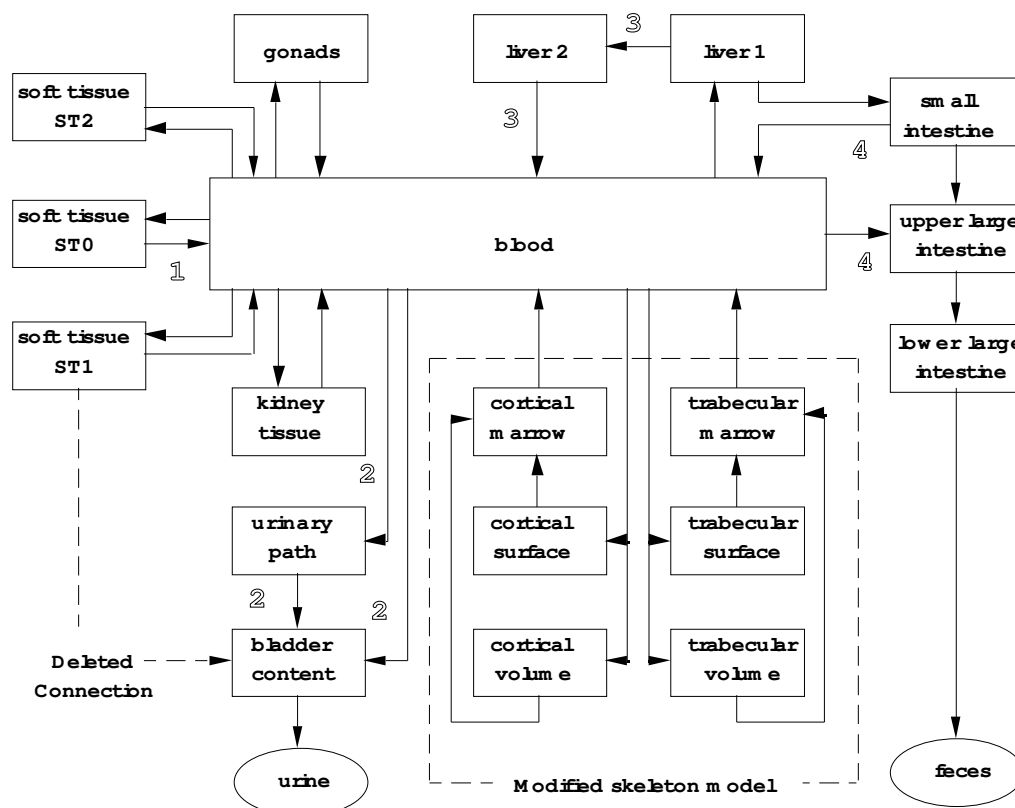


**Figure 3.1.12** The starting model in the optimization procedure (ICRP67-a-Polig) with the affected gastrointestinal tract compartments. The transfer rates successively modified are also pointed out with numbered arrows.

First of all Figure 3.1.8 suggests that the transfer rate from the ST0 soft tissue compartment almost exclusively determines the activity in the blood for the first 20 days after the injection. At longer time the effect is approximately constant and comparable to the contribution of other organs and tissues. Therefore this pathway was inspected first for the possibility of improving the model's predictions for activity in blood at short time (Figure 3.1.7) just by varying the transfer rate from ST0 compartment to the blood. For this purpose blood activity content was calculated by adopting transfer rate values uniformly distributed around the ICRP67 transfer rate assumed as central value. For each transfer rate the value of the F target function was calculated using the reference data set for blood activity content at short time. It turns out that a value of  $0.139 \text{ d}^{-1}$  (half-life 5 d) for the transfer rate from compartment ST0 to blood (arrow 1 in Figure 3.1.12) is more appropriate than the ICRP value



of  $0.693d^{-1}$ . The values of the F target function calculated for the blood reference data by adopting this new transfer rate are shown in Table 3.1.7. With the new value of the parameter implemented in the model (ICRP67-a-Polig-ST0) the function F calculated on the experimental data for blood activity decreases by a factor of about 300 of the ICRP value (second column in Table 3.1.7). This change of the ST0 clearance rate also yields a fecal excretion that is more consistent with Langham's data for the first 50 days. The function F, calculated from the experimental data for fecal excretion, reduces by factor 9 of the value calculated with the ICRP parameter (third column in Table 3.1.7). Just for comparison, the F values calculated for the other models previously introduced and discussed are also given.

The curves for Plutonium activity in feces and blood calculated on the basis of the new transfer rate are shown in Figure 3.1.13 and Figure 3.1.14, respectively, in comparison with the reference data and the predictions based on some preliminary models.

**Table 3.1.7** Values of the F target function using original and modified versions of ICRP 67 model.

Model	F value	
	Blood	Feces
ICRP67	3068	241
ICRP67-a	1285	226
ICRP67-a-Polig	461	510
ICRP67-a-Polig-ST0	11	27

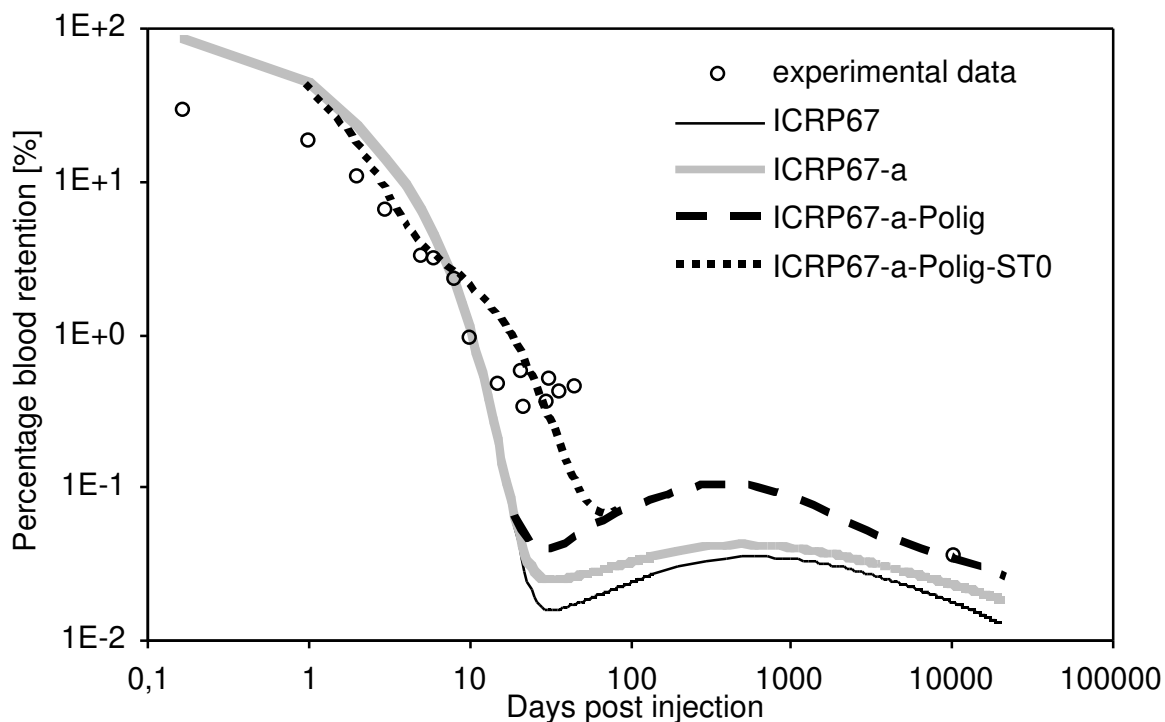


**Figure 3.1.13** Reference data set and ICRP 67 original and modified versions predictions for percentage blood content of Plutonium.

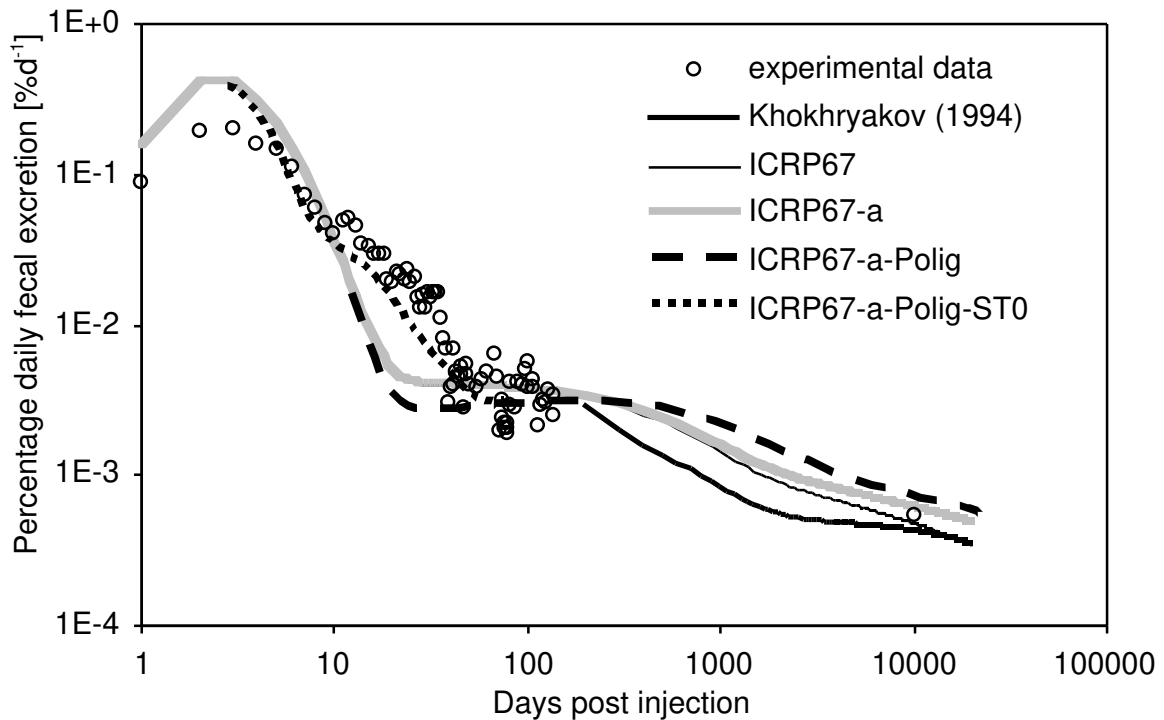


**Figure 3.1.14** Reference data set and ICRP 67 original and modified versions predictions for percentage daily fecal excretion of Plutonium.

After this first optimization step based on the reference data set for blood activity, the urinary excretion was considered. An improvement of model predictions for Plutonium urinary excretion at short times was attempted first. Specifically three transfer rates for the urinary excretion pathway system were considered (arrows 2 in Figure 3.1.12): from blood to urinary bladder content and urinary pathway compartments and from the latter to the urinary bladder content. These transfer rates determine the urinary excretion of Plutonium but, as they only affect the urinary excretion pathway, they have no influence on the retention in the remaining organs and tissues. It was therefore possible to improve the urinary excretion without significantly affecting the already good agreement between model predictions and data for blood and fecal excretion. The urinary system transfer rates were modified within a range of values uniformly distributed around ICRP67 transfer rates assumed as central values. The values of the transfer rates are distributed in a 3-dimensional grid of values: for each combination of three values the F target function was calculated using the reference data set for Plutonium urinary excretion. The values minimizing the F target are: 0.00946, 0.00992, 0.0102 d<sup>-1</sup> for the transfer rates from blood to urinary bladder content, from blood to urinary path and from urinary path to urinary bladder content compartments, respectively. Such values differ from ICRP 67 values by factors 0.73, 1.53 and 0.74, respectively.

The resulting excretion (Model-a) is presented in Figure 3.1.15. The model now predicts urinary excretion values closer to the reference data set than ICRP 67 at short and intermediate time range. However at time longer than 2000 days post injection Model-a still undershoots the reference data. Particularly at 10,000 days the model calculations are too low by nearly a factor of two, if compared with ICRP 67 (0.0011%/d-1), Khokhryakov (0.0011%/d-1) and subject HP-6 (0.0014%/d-1). Therefore the optimization of urinary pathway transfer rates was not able to significantly improve the urinary excretion at long time.

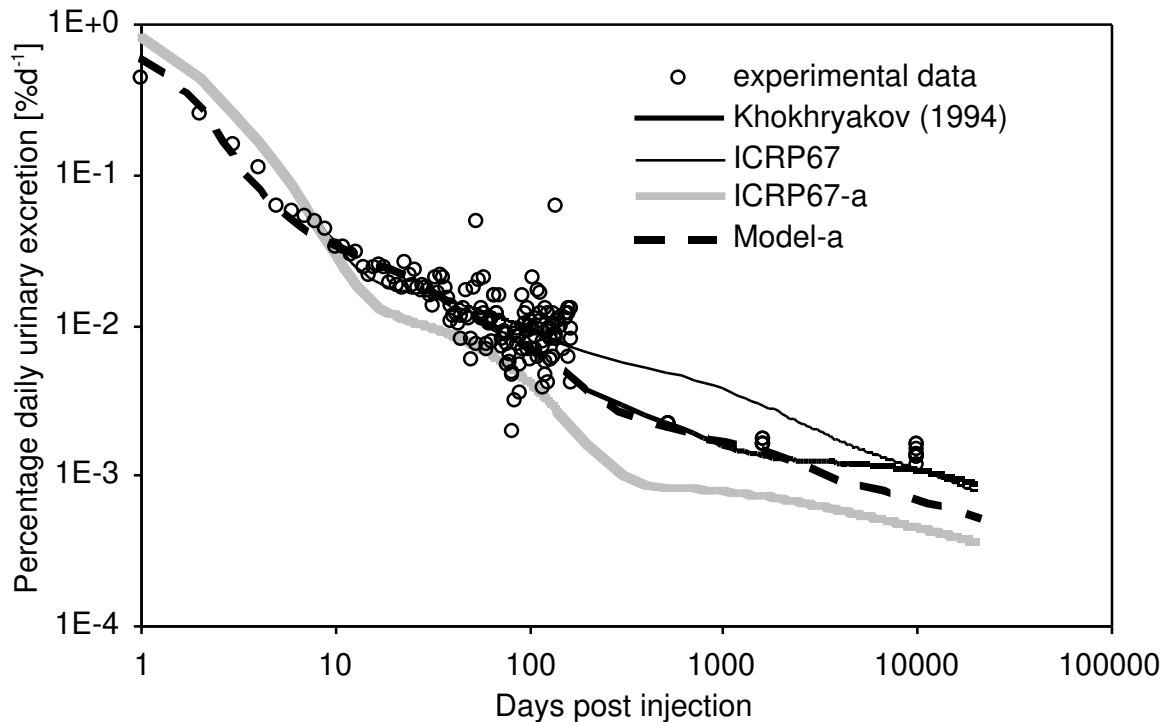


**Figure 3.1.15** Reference data set and ICRP 67 original and modified versions predictions for percentage daily urinary excretion of Plutonium.

According to Figure 3.1.8 any additional improvement of urinary excretion at long times after intake should inevitably consider the organs and tissues that affect the biokinetics at this time range, i.e. liver and skeleton. Firstly attempts for improving model predictions of Plutonium urinary excretion by considering liver transfer rates were carried out. However it turned out that the necessary variations of liver transfer rates should be so large to generate values for skeleton to liver partitioning ratios far from the findings in autopsy studies. The latter range from about 0.60 to 0.73 [158, 159, 160, 161]. Therefore a modification of Polig's skeletal model, up to now implemented into the ICRP 67 model without any adjustment, was considered.

As previously carried out in the phase of analyzing the ICRP67 model, skeletal time depending transfer rates were considered. The general rule of ICRP 70, based on physiological studies, for the age-related variation of bone turnover rates was adopted: The bone turnover rates suggested by Polig were used up to the age of 35 and from then onwards were linearly increased up to the doubled value at age 60. The trend of the skeletal transfer rates versus the age of the subjects is similar to those shown in Figure 3.1.5 even if now the values are those provided from Polig's study. It was found that introducing time-dependent skeletal turnover rates (Model-b) effects a lifting of the urinary excretion beyond about 10 years post injection. At the same time the transfers of the liver compartments (arrows 3 in Figure 3.1.12) and the fecal excretion parameters (arrows 4 in Figure 3.1.12) were changed in order to achieve a correct estimate of the skeleton to liver partitioning and the fecal excretion, respectively. The modification of these parameters was obtained by a "qualitative" fitting to the few available measurements.

The model's predictions for the urinary excretion of Plutonium are shown in Figure 3.1.16 (Model-b) together with the reference data set, Model-a, ICRP 67 model and its

modified version (ICRP67-a) (i.e. without the transfer of activity from ST0 soft tissue compartment to urinary bladder). The improvement of the long term urinary excretion of Plutonium by adopting the modification of the skeleton from Polig's studies with age depending remodelling rates is shown in Table 3.1.8. The values of the F target function based on the previous models are also presented.

**Table 3.1.8** Values of the F target function for the long term ( $t > 200$  d) urinary excretion using original and modified versions of ICRP 67 model.

Model	F value For $t > 200$ d
ICRP67	14
ICRP67-a	394
ICRP67-a-Polig	56
ICRP67-a-Polig-ST0	56
Model-a	53
Model-b	5

As discussed on the basis of Figure 3.1.8, for the previous finale stage of revisions it was not necessary to repeat the optimization of the transfer rates of the urinary pathway that provided a good agreement with the reference data set at short time. Introducing new liver transfer rates and age dependent skeletal remodelling rates had no significant influence on the urinary excretion at early times and Model-b yielded practically the same values than Model-a. The urinary excretion in Figure 3.1.16 was calculated for a subject who is 45 years old at the time of injection, the age of subject HP-6 in the reference data set for whom we have data at long times. With the current assumptions of Model-b the estimated urinary excretion of Plutonium is now higher than the predictions of Model-a. From day 200 to around 10,000 the model shows sufficient agreement with Khokhryakov's excretion curve. The deviations never exceed 30%. At day 10,000 Model-b estimates a urine excretion of  $0.0012\%/d^{-1}$ , very close to the experimental value. Therefore the modifications applied to the ICRP 67 model seem to compensate very well for the underestimation of urinary excretion caused by removing the connection between soft tissue and urinary bladder (ICRP67-a). The Model-b prediction for the skeleton-liver partitioning was also calculated (0.615) and is in good agreement with the published values [158, 159, 160, 161].

Model-b was derived with the primary goal to achieve the best estimates of urinary excretion, but estimates for fecal excretion and plutonium activity in blood were also taken into account in the optimization procedures. The calculated excretion rate in feces and the percentage of Plutonium in blood are presented in Figure 3.1.17 and Figure 3.1.18, respectively, together with the estimates from ICRP 67, its modified versions and the reference data set. The fecal excretion of Model-b is closer to the experimental data than ICRP 67. Model-b underestimates the measurements by less than 40 %, while ICRP 67 by 80 % or more. Furthermore the fecal excretion of the model has almost the same trend as the experimental data, even at short time (up to 7 days post injection) when it is characterized by an initial increase followed by a sharp decrease. The overall good performance of Model-b with regard to fecal excretion is confirmed by the values of the F target function calculated on

the basis of all the reference data set (Table 3.1.9): the F value is about 10% of the value calculated for the ICRP67 model. A similarly good agreement of Model-b predictions with the blood activity content was observed (Figure 3.1.18), and it is quantified in the third column of Table 3.1.9.

The final transfer rates adopted for Model-b are presented in Table 3.1.10. For those parameters that are unchanged from previous versions the sources are named.

**Table 3.1.9** Values of the F target function using original and modified versions of ICRP 67 model.

Model	F value	
	feces	blood
ICRP67	241	3068
ICRP67-a	226	1286
Model-b	22	10

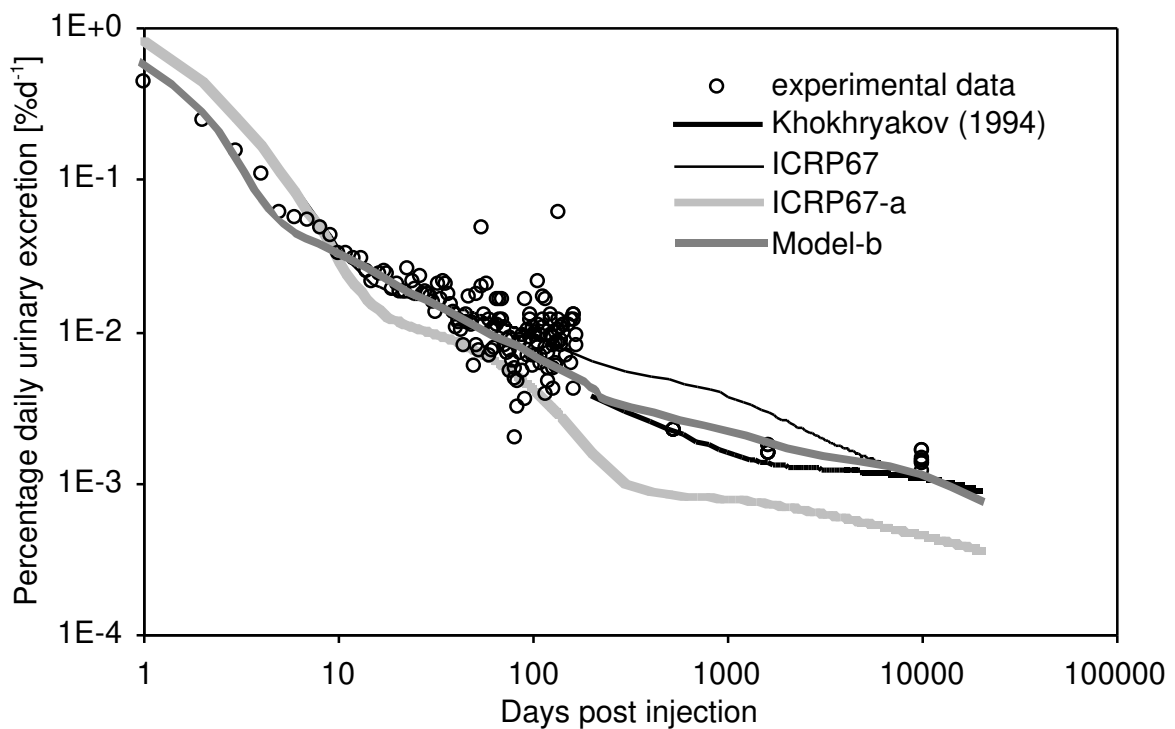


**Figure 3.1.16** Reference data set and ICRP 67 original and modified versions predictions for percentage daily urinary excretion of Plutonium.

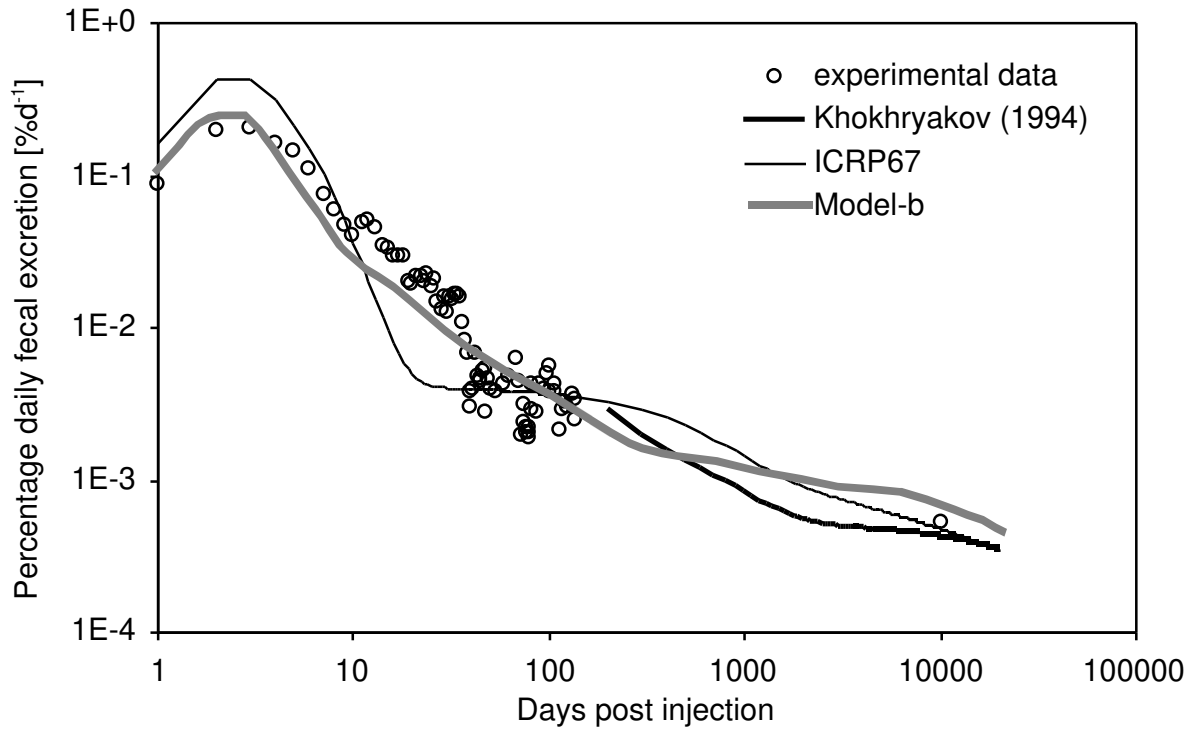


**Figure 3.1.17** Reference data set and ICRP 67 original and modified versions predictions for percentage daily fecal excretion of Plutonium.

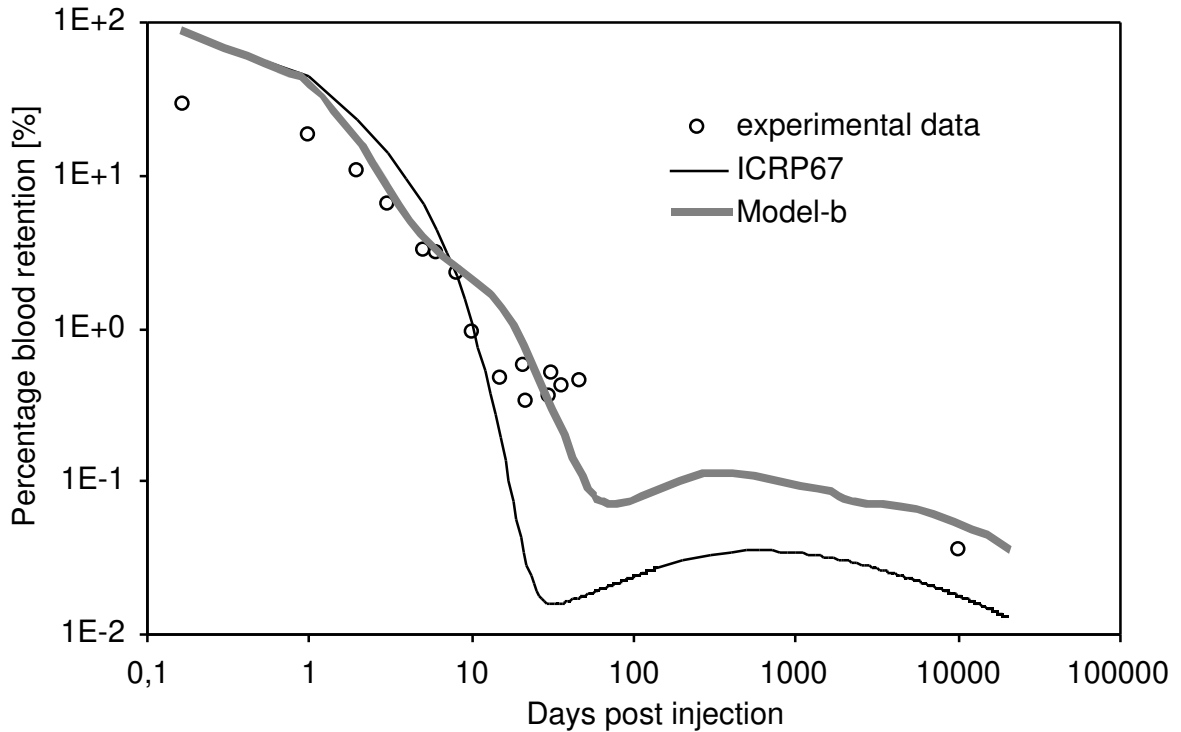


**Figure 3.1.18** Reference data set and ICRP 67 original and modified versions predictions for percentage blood content of Plutonium.

**Table 3.1.10** Transfer rates of the optimized Model-b for plutonium biokinetics.

Compartments	Transfer rates [d <sup>-1</sup> ]	Sources
Blood to liver	0.120	Polig, 1997
Blood to cortical surface	0.0952	Polig, 1997
Blood to trabecular surface	0.226	Polig, 1997
Blood to cortical volume	0.00448	Polig, 1997
Blood to trabecular volume	0.0716	Polig, 1997
Blood to urinary bladder content	0.00946	Present work
Blood to urinary path	0.00992	Present work
Blood to other kidney tissue	0.00323	ICRP 67
Blood to ULI contents	0.008	Present work
Blood to testes	0.00023	ICRP 67
Blood to ovaries	0.000071	ICRP67
Blood to ST0	0.2773	ICRP 67
Blood to ST1	0.0806	ICRP 67
Blood to ST2	0.0129	ICRP 67
ST0 to blood	0.139	Present work
Urinary path to urinary bladder content	0.0102	Present work
Urinary bladder content to excretion	12	ICRP 67
Other kidney tissue to blood	0.00139	ICRP 67
ST1 to blood	0.000950	Present work
ST1 to urinary bladder content	(deleted)	Present work
ST2 to blood	0.000019	ICRP 67
Trabecular surface to marrow	0.00159 <sup>a</sup>	Polig, 1997
Trabecular volume to marrow	0.00159 <sup>a</sup>	Polig, 1997
Cortical surface to marrow	0.000156 <sup>a</sup>	Polig, 1997
Cortical volume to marrow	0.0000822 <sup>a</sup>	Polig, 1997
Cortical marrow to blood	0.0076	Polig, 1997
Trabecular marrow to blood	0.0076	Polig, 1997
Liver 1 to Liver 2	0.01	Present work
Liver 1 to Small Intestine	0.0004	Present work
Liver 2 to Blood	0.0004	Present work
Gonads to blood	0.00019	ICRP 67
Small intest. to upper large intestine	6.0	ICRP 30
Upper large. to lower large intest.	1.8	ICRP 30
Lower large intest. to excretion (feces)	1.0	ICRP 30

<sup>a</sup> Modified from Polig. Values up to 35 years age, doubled values at 60 years age and linear interpolation in between.

**Table 3.1.11** A summary of the main characteristics of the models introduced and discussed in the present paragraph.

Model	Main characteristics
ICRP67	Model from ICRP Publication N. 67
ICRP67-a	ICRP67 model but without the transfer of activity from ST1 soft tissue to urinary bladder content
ICRP67-a-Polig	ICRP 67-a model with Polig's skeletal model
ICRP67-a-Polig-ST0	ICRP67-a-Polig model with corrected transfer rate from ST0 soft tissue to blood
Model-a	ICRP67-a-Polig-ST0 model with optimized urinary excretion transfer rates
Model-b	Final optimized model



### 3.1.4 VERIFICATION OF THE OPTIMIZED MODEL (MODEL-B)

The cases of contamination of professionally exposed subjects presented in the paragraph 2.1.3 are here used to test the optimized model (Model-b). This is the occasion to compare it to the ICRP 67 model using the data from some real cases of contamination whose intakes usually do not occur directly to the blood, as for the subjects by which the models were compared and the optimized model developed, but commonly via inhalation. The necessity of modelling the kinetics of the radionuclide in physiological systems with a larger number of organs and therefore of compartments, as those involved in a non-systemic contamination via inhalation, will generally smooth the differences in the Plutonium biokinetics predicted by the two systemic models.

The two models were compared using the F function target. For each model the intake I that minimize the F was calculated first. In the expression of F the model data  $x(t_i)$  is given by the product  $I \cdot e_u(t_i)$  where I is the intake and  $e_u(t_i)$  is the fractional urinary excretion of Plutonium at  $t_i$  predicted by the model. Therefore the F target function was expressed as:

$$F = \sum_{i=1}^n \left[ \frac{d(t_i) - I \cdot e_u(t_i)}{I \cdot e_u(t_i)} \right]^2$$

*equation 3.1.7*

The term  $d(t_i)$  represents the measured urinary excretion data and n is the number of data. The urinary excretion curves predicted by the optimized model were evaluated considering the actual age of the considered subject, owing to the age dependent bone remodelling rates.

After the calculation of the best estimation of I that minimizes the F target function for each model, the resulting values of F were compared to evaluate the agreement of models with the urinary excretion data. In Table 3.1.12 the ratio of the F values calculated with the Model-b and ICRP 67 for all the standard absorption types (M and S) and AMADs (1 and 5  $\mu$ m) are presented in the last four columns.

First of all it can be seen that the differences between the values of F are small and the resulting ratios are very close to one. This indicates that Model-b estimates the urinary excretion at least as well as ICRP 67, but avoids the unphysiological assumptions that were already commented.

Some systematic trends in F suggest further deliberations. The Model-b seems to fit better (F-ratio is slightly but systematically less than one) than the ICRP 67 model and this is particularly important for those cases with a large number of measurements. Only for two cases (10 and 18), with a smaller number of useful excretion data, does the ICRP 67 model yield a better fit than the Model-b. A close look at the data from these two cases reveals that some anomalous initial values of urinary excretion (5 times greater than the average of the values for the samples collected in the two previous and following periods) exist. Omitting just one of these outliers results in a better fit of the Model-b, than for ICRP 67.

The previous considerations are generally valid for both the absorption types and the AMAD values.

**Table 3.1.12** Testing of the Model-b using the excretion data of occupational workers. The ratios of the value of function F for the Model-b by the value for ICRP 67 model are presented for some occupationally exposed individuals and standard conditions of exposure to <sup>239</sup>Pu.

Case code	Number of data	$\frac{F(\text{Model-b})}{F(\text{ICRP 67})}$			
		AMAD = 1 $\mu\text{m}$		AMAD = 5 $\mu\text{m}$	
		Type M	Type S	Type M	Type S
242 (U)	107	0.97	0.98	0.97	0.98
193 (U)	105	0.91	0.92	0.92	0.93
4 (M)	105	0.94	0.95	0.95	0.96
208 (U)	64	0.97	0.98	0.97	0.98
25 (M)	21	0.99	0.99	0.99	0.99
10 (M)	21	1.05	1.05	1.04	1.05
18 (M)	20	1.36	1.48	1.28	1.41
7 (M)	10	0.96	0.91	0.97	0.91
21 (M)	8	0.83	0.79	0.85	0.81

(U) : case from United States Uranium and Transuranium Registries

(M) : case from Manhattan Project

Although intake estimates are not the direct goal of the verification process of this section, as they were obtained as by-product of the minimizing procedure of the function F, they are here present and commented.

In Table 3.1.13 the intakes calculated using the Model-b are presented with the percentage deviation from the ICRP 67 estimates for all the standard absorption types (M, S) and AMADs (1 and 5  $\mu\text{m}$ ). The average deviation on all the contamination cases indicates that for absorption type M the Model-b and ICRP 67 yield almost the same intakes, while for absorption type S the latter model estimates intakes to be smaller by about 10 %. This follows not only from the urinary excretion values predicted by the model, but also from the period when the considered urine samples were collected (between 1957 and 1997, i.e. 4,400 and 19,000 days post-intake). As shown in Figure 3.1.19 in case of an aerosol of 1  $\mu\text{m}$  AMAD inhaled by a forty years old subject, type M, the Plutonium urinary excretion predicted by the Model-b ranges between -11% and +7% of the ICRP 67 predictions in the period of the samples collection for the considered actual cases of contamination. Therefore on the average the final effect is that both models estimate almost the same intakes. In the same period and under the same condition of exposure, but for absorption S, the Plutonium urinary excretion predicted by the age related model ranges between -20% and +1% of the ICRP 67 predictions. Therefore the estimations of intake based on the Model-b are higher than the ICRP 67 predictions.

**Table 3.1.13** Intakes and percentage deviation from the ICRP 67 intakes calculated with the Model-b for some occupationally exposed individuals and standard conditions of exposure to  $^{239}\text{Pu}$ .

Case code	AMAD = 1 $\mu\text{m}$				AMAD = 5 $\mu\text{m}$			
	Type M $f_1 = 5 \cdot 10^{-4}$		Type S $f_1 = 1 \cdot 10^{-5}$		Type M $f_1 = 5 \cdot 10^{-4}$		Type S $f_1 = 1 \cdot 10^{-5}$	
	Intake [kBq]	$\Delta$ Intake [%]	Intake [kBq]	$\Delta$ Intake [%]	Intake [kBq]	$\Delta$ Intake [%]	Intake [kBq]	$\Delta$ Intake [%]
242	12.0	+ 4	78.3	+ 16	18.6	+ 4	178	+ 16
193	3.4	+ 4	21.8	+ 15	5.31	+ 4	49.0	+ 15
4	35.4	- 4	225.8	+ 4	50.7	- 4	457	+ 4
208	3.8	+12	24.6	+ 25	6.30	+ 12	60.4	+ 25
25	2.0	- 2	13.1	+ 7	3.00	- 2	27.3	+ 8
10	11.2	+ 3	72.5	+ 14	17.2	+ 2	162	+ 14
18	18.1	+ 3	115.9	+ 12	27.7	+ 3	253	+ 12
7	44.7	- 6	284.7	- 1	62.7	- 6	548	- 1
21	7.2	- 7	46.1	- 2	10.0	- 7	88.2	- 1

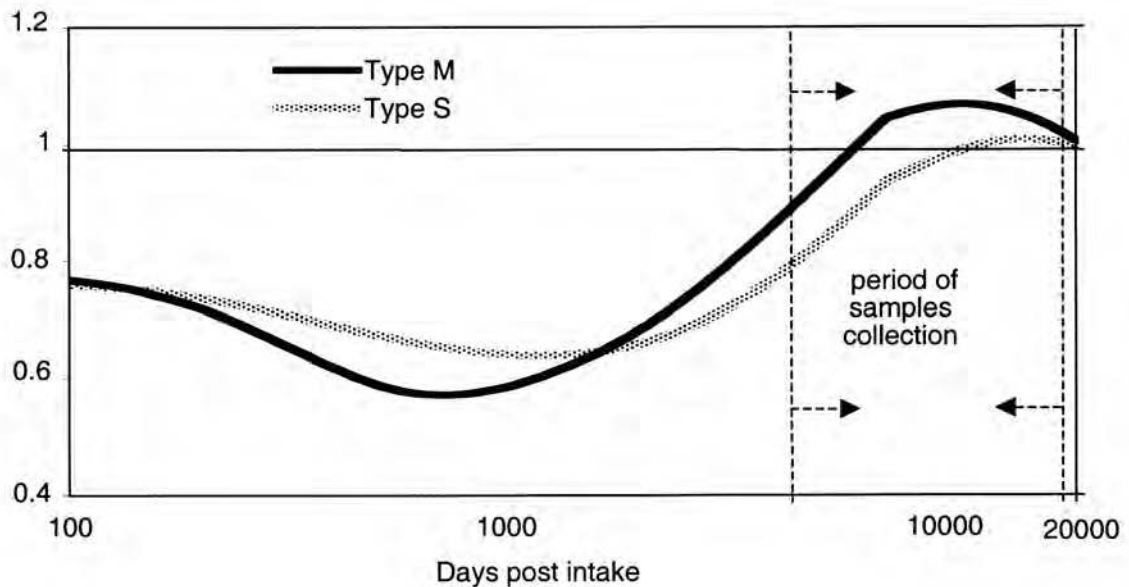


**Figure 3.1.19** Ratio of the Model-b to ICRP 67 model predictions for the urinary excretion of Plutonium in case of inhalation of 1  $\mu\text{m}$  AMAD aerosol.

### 3.1.5 CHARACTERIZATION OF THE OPTIMIZED MODEL (MODEL-B)

#### 3.1.5.1 Dose Coefficients

The committed effective dose (E(50)) (see Annex) per unit of intake (E(50) coefficient) was calculated for two main purposes:

1. to compare the new optimized model to the ICRP 67 model in terms of dose;
2. to allow using the new optimized model in the radiation protection practice, for which the E(50) is the final and legal required quantity.

As in practical situations of professionally exposed workers the major path of intake is by inhalation and the ingestion, the corresponding compartmental models proposed by ICRP [57, 58] were connected to the new systemic model Model-b. The resulting compartmental model is given in Figure 3.1.20. As currently adopted by ICRP, the part of the ICRP 66 lung model describing the kinetics of inhaled materials firmly bound in the tissues of respiratory tract were not considered (dashed lines in Figure 3.1.20).

The dose coefficients were calculated according to the ICRP method [57, 58, 162], as summarised in the Annex. For the physical characteristics of the aerosol and the conditions of exposure, the default values recommended by ICRP for standard occupational exposure via inhalation and ingestion were assumed [52, 97]. In addition to 5 µm AMAD (Activity Median Aerodynamic Diameter), considered representative of workplaces aerosols, 1 µm AMAD aerosols were considered as well, to reproduce the same set of reference dose coefficients calculated by ICRP for occupational exposure via inhalation [97]. Both absorption classes for Plutonium (M and S, i.e. moderate and slow) with the respective values of  $f_1$  ( $5.0 \cdot 10^{-4}$  for unspecified compounds and  $1.0 \cdot 10^{-5}$  for insoluble oxides) were used [52]. In case of ingestion three  $f_1$  values were assumed, as suggested by ICRP [52]:  $5 \cdot 10^{-4}$ ,  $1 \cdot 10^{-4}$  and  $1 \cdot 10^{-5}$ . The time dependent activity in the organs, as predicted by the model, was integrated over 50 years to calculate the number of transformations per bequerel of intake. The characteristics of the Plutonium physical decay were taken from Publication 38 of ICRP [9]. The radiation and tissue weighting factors are those suggested by the recent recommendations of ICRP [26].

All Plutonium radioisotopes which are encountered in the radiation protection practice were considered. In case of a contamination due to  $^{241}\text{Pu}$  the contribution to the dose from the daughter  $^{241}\text{Am}$  was also considered. The Plutonium biokinetic model was adopted also for Americium ingrowth from Plutonium decay, as assumed by ICRP. The model presented in Figure 3.1.20 was duplicated and each compartment describing Plutonium kinetics, connected to a second one through the physical decay constant of  $^{241}\text{Pu}$ , to describe the subsequent kinetics of Americium.

The radioisotope  $^{239}\text{Pu}$  was primarily considered because it is the most common Pu isotope in industrial applications. As the Model-b implements age dependent bone remodelling rates, first the time dependency of E(50) coefficients was analyzed. E(50) coefficients for  $^{239}\text{Pu}$  were calculated assuming ages at the time of intake ranging from twenty-five to sixty years and proceeding in 5 years intervals. The results are shown in Table 3.1.14 and Table 3.1.15 for inhalation and ingestion, respectively. A slight decrease of E(50) coefficients from subjects aged twenty-five to subjects aged sixty was observed. However the variation is smaller than 5% for both inhalation or ingestion. Compared to ICRP 67, the Model-b E(50) coefficients are greater by about 17-25% for these conditions of exposure: inhalation, with absorption type M; ingestion, with  $f_1 = 5 \cdot 10^{-4}$  and  $1 \cdot 10^{-4}$ . In case of intake via ingestion, with  $f_1 = 1 \cdot 10^{-5}$ , and inhalation, with absorption type S, the overestimation is around 11-14% and 4-7%, respectively. In the latter case the differences are reduced due to the higher contribution of the lung to the E(50), which is obviously not influenced by any modifications of the systemic model. Similar considerations are valid for the other Plutonium radioisotopes.

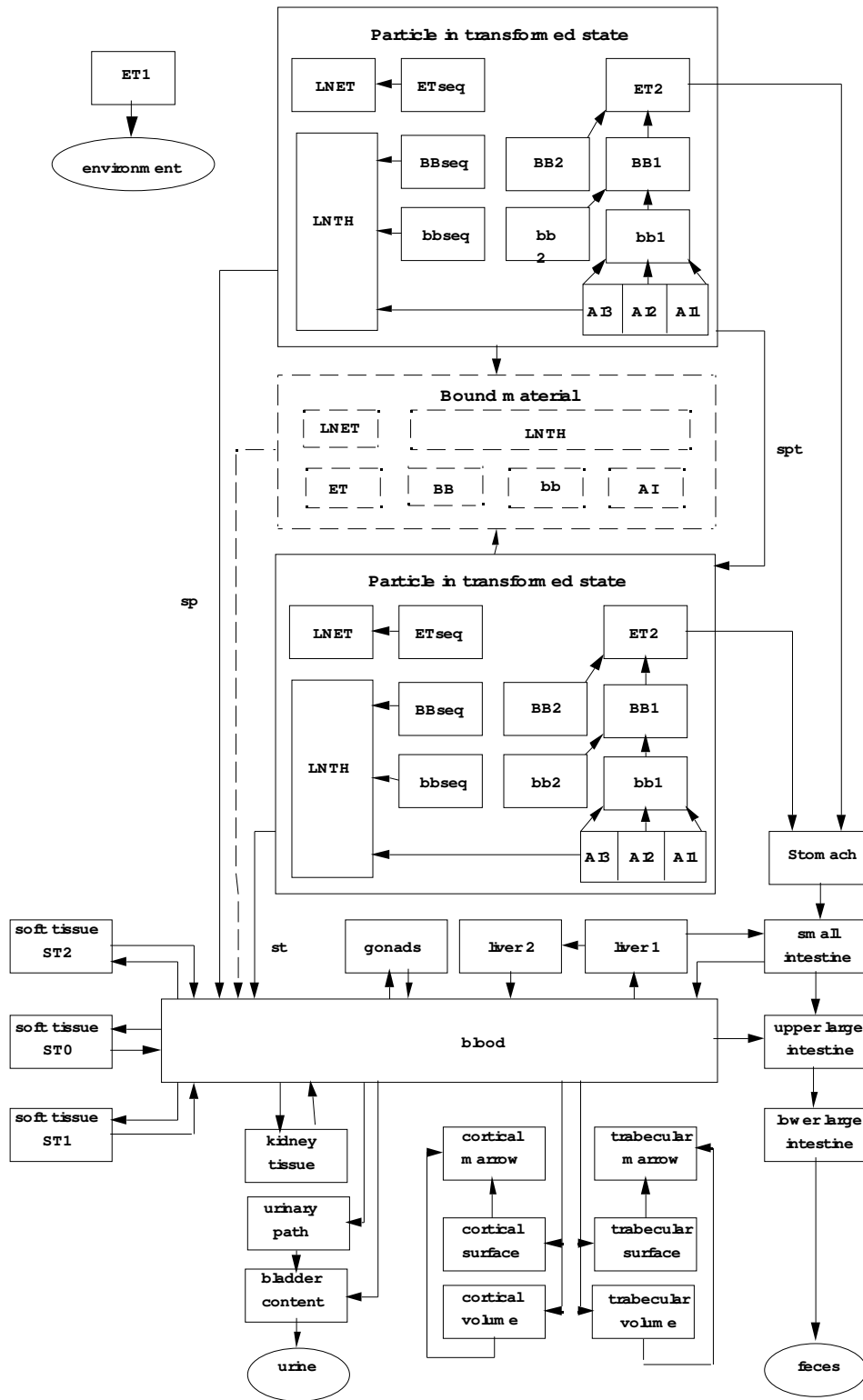


Figure 3.1.20 The Model-b connected with the gastrointestinal tract and the respiratory tract model.

**Table 3.1.14** E(50) coefficients for ICRP 67 model and the Model-b for standard conditions of exposure to  $^{239}\text{Pu}$  via inhalation. ICRP coefficients are age independent.

Type	$f_1$	Systemic model	Age at intake [y]	E(50) coefficients [Sv Bq <sup>-1</sup> ]	
				AMAD = 1 $\mu\text{m}$	AMAD = 5 $\mu\text{m}$
M	$5 \cdot 10^{-4}$	ICRP 67	-	$4.7 \cdot 10^{-5}$	$3.2 \cdot 10^{-5}$
			25	$5.7 \cdot 10^{-5}$	$4.0 \cdot 10^{-5}$
		Model-b	30	$5.7 \cdot 10^{-5}$	$3.9 \cdot 10^{-5}$
			35	$5.7 \cdot 10^{-5}$	$3.9 \cdot 10^{-5}$
			40	$5.6 \cdot 10^{-5}$	$3.9 \cdot 10^{-5}$
			45	$5.6 \cdot 10^{-5}$	$3.8 \cdot 10^{-5}$
			50	$5.5 \cdot 10^{-5}$	$3.8 \cdot 10^{-5}$
			55	$5.5 \cdot 10^{-5}$	$3.8 \cdot 10^{-5}$
S	$1 \cdot 10^{-5}$	ICRP 67	-	$1.5 \cdot 10^{-5}$	$8.3 \cdot 10^{-6}$
			25	$1.6 \cdot 10^{-5}$	$8.9 \cdot 10^{-6}$
		Model-b	30	$1.6 \cdot 10^{-5}$	$8.9 \cdot 10^{-6}$
			35	$1.6 \cdot 10^{-5}$	$8.9 \cdot 10^{-6}$
			40	$1.6 \cdot 10^{-5}$	$8.8 \cdot 10^{-6}$
			45	$1.6 \cdot 10^{-5}$	$8.8 \cdot 10^{-6}$
			50	$1.6 \cdot 10^{-5}$	$8.8 \cdot 10^{-6}$
			55	$1.6 \cdot 10^{-5}$	$8.8 \cdot 10^{-6}$
60	$1.6 \cdot 10^{-5}$	$8.8 \cdot 10^{-6}$			

**Table 3.1.15** E(50) coefficients for ICRP 67 model and the Model-b for standard conditions of exposure to  $^{239}\text{Pu}$  via ingestion. ICRP coefficients are age independent.

Systemic Model	Age at intake [y]	E(50) coefficients [Sv Bq <sup>-1</sup> ]		
		$f_1 = 5 \cdot 10^{-4}$	$f_1 = 1 \cdot 10^{-4}$	$f_1 = 1 \cdot 10^{-5}$
ICRP 67	-	$2.5 \cdot 10^{-7}$	$5.3 \cdot 10^{-8}$	$9.0 \cdot 10^{-9}$
	25	$3.1 \cdot 10^{-7}$	$6.3 \cdot 10^{-8}$	$1.0 \cdot 10^{-8}$
Model-b	30	$3.0 \cdot 10^{-7}$	$6.3 \cdot 10^{-8}$	$1.0 \cdot 10^{-8}$
	35	$3.0 \cdot 10^{-7}$	$6.2 \cdot 10^{-8}$	$9.9 \cdot 10^{-9}$
	40	$3.0 \cdot 10^{-7}$	$6.2 \cdot 10^{-8}$	$9.9 \cdot 10^{-9}$
	45	$3.0 \cdot 10^{-7}$	$6.2 \cdot 10^{-8}$	$9.9 \cdot 10^{-9}$
	50	$2.9 \cdot 10^{-7}$	$6.1 \cdot 10^{-8}$	$9.8 \cdot 10^{-9}$
	55	$2.9 \cdot 10^{-7}$	$6.1 \cdot 10^{-8}$	$9.8 \cdot 10^{-9}$
	60	$2.9 \cdot 10^{-7}$	$6.1 \cdot 10^{-8}$	$9.8 \cdot 10^{-9}$

For the routine application of Model-b in the radiation protection practice, the E(50) coefficients for a subject of age 40 at the moment of the intake can be assumed as base case values for two main reasons:

1. The E(50) coefficients are only slightly dependent on the age of the subject;
2. A subject aged forty is representing the mean age of workers.

The main contributions from organs and tissues to the E(50) coefficients for a 40 years old subject were calculated as well (Table 3.1.16) in terms of organ or tissue equivalent dose,  $H_T$  (see Annex). The values are compared with the same values using the ICRP 67 model, in order to evaluate the effect of the modification in dosimetric terms introduced by the new model. The equivalent dose to the lung is also given, because it can significantly contribute to the E(50), particularly in case of absorption type S. No difference in lung equivalent dose is expected because it just depends on the respiratory tract model. From Table 3.1.16 it can be seen that Model-b, on average for all the standard scenarios of contamination, predicts higher equivalent doses for the bone marrow (+35%,) and smaller ones for the bone surfaces and the liver (-7% and -12%, respectively) than does ICRP 67. The previous considerations relating to  $^{239}\text{Pu}$  can also be applied to the other Plutonium radioisotopes.

E(50) coefficients for a forty years old subject in case of inhalation and ingestion of the main Plutonium radioisotopes are finally given in Table 3.1.17 for standard conditions of exposure. They were partially already published in a recent publication [163]. These coefficients can be directly applied in the practical radiation protection procedures.

**Table 3.1.16** The main contributions from organs and tissues to the E(50) coefficients for a forty years old subject in term of organ or tissue equivalent dose ( $H_T(50)$ ).

Scenario: AMAD–Type or $f_1$	Organ or tissue							
	Bone Marrow		Bone Surfaces		Liver		Lung	
	Model-b. ICRP67	ICRP67	Model-b. ICRP67	ICRP67	Model-b. ICRP67	ICRP67	Model-b. ICRP67	ICRP67
<b>Inhalation</b>								
1 $\mu\text{m}$ - M	9.6•10 <sup>-5</sup>		1.4•10 <sup>-3</sup>		2.7•10 <sup>-4</sup>		2.8•10 <sup>-5</sup>	
		7.1•10 <sup>-5</sup>		1.5•10 <sup>-3</sup>		3.1•10 <sup>-4</sup>		2.8•10 <sup>-5</sup>
1 $\mu\text{m}$ - S	1.1•10 <sup>-5</sup>		1.6•10 <sup>-4</sup>		3.2•10 <sup>-5</sup>		7.9•10 <sup>-5</sup>	
		8.6•10 <sup>-6</sup>		1.7•10 <sup>-4</sup>		3.6•10 <sup>-5</sup>		7.9•10 <sup>-5</sup>
5 $\mu\text{m}$ - M	6.6•10 <sup>-5</sup>		9.7•10 <sup>-4</sup>		1.9•10 <sup>-4</sup>		1.9•10 <sup>-5</sup>	
		4.9•10 <sup>-5</sup>		1.0•10 <sup>-3</sup>		2.1•10 <sup>-4</sup>		1.9•10 <sup>-5</sup>
5 $\mu\text{m}$ - S	6.0•10 <sup>-6</sup>		8.5•10 <sup>-5</sup>		1.7•10 <sup>-5</sup>		4.7•10 <sup>-5</sup>	
		4.6•10 <sup>-6</sup>		9.1•10 <sup>-5</sup>		1.9•10 <sup>-5</sup>		4.7•10 <sup>-5</sup>
<b>Ingestion</b>								
5•10 <sup>-4</sup>	5.4•10 <sup>-7</sup>		7.9•10 <sup>-6</sup>		1.5•10 <sup>-6</sup>		~0	
		4.0•10 <sup>-7</sup>		8.2•10 <sup>-6</sup>		1.7•10 <sup>-6</sup>		~0
1•10 <sup>-4</sup>	1.1•10 <sup>-7</sup>		1.6•10 <sup>-6</sup>		3.0•10 <sup>-7</sup>		~0	
		8.1•10 <sup>-8</sup>		1.7•10 <sup>-6</sup>		3.5•10 <sup>-8</sup>		~0
1•10 <sup>-5</sup>	1.1•10 <sup>-8</sup>		1.6•10 <sup>-7</sup>		3.1•10 <sup>-8</sup>		~0	
		8.6•10 <sup>-9</sup>		1.7•10 <sup>-7</sup>		3.5•10 <sup>-8</sup>		~0

**Table 3.1.17** *E(50) coefficients based on the Model-b for standard conditions of exposure via inhalation and ingestion (NA = not applicable).*

Path of intake AMAD – Type – $f_1$	Radionuclide			
	$^{238}\text{Pu}$	$^{239}\text{Pu}$	$^{240}\text{Pu}$	$^{241}\text{Pu}$
<b>Inhalation</b>				
1 $\mu\text{m}$ – M – $5 \cdot 10^{-4}$	$5.1 \cdot 10^{-5}$	$5.6 \cdot 10^{-5}$	$5.6 \cdot 10^{-5}$	$1.1 \cdot 10^{-6}$
1 $\mu\text{m}$ – S – $1 \cdot 10^{-5}$	$3.5 \cdot 10^{-5}$	$3.9 \cdot 10^{-5}$	$3.9 \cdot 10^{-5}$	$7.2 \cdot 10^{-7}$
5 $\mu\text{m}$ – M – $5 \cdot 10^{-4}$	$1.6 \cdot 10^{-5}$	$1.6 \cdot 10^{-5}$	$1.6 \cdot 10^{-5}$	$1.9 \cdot 10^{-7}$
5 $\mu\text{m}$ – S – $1 \cdot 10^{-5}$	$1.1 \cdot 10^{-5}$	$8.8 \cdot 10^{-6}$	$8.9 \cdot 10^{-6}$	$9.5 \cdot 10^{-8}$
<b>Ingestion</b>				
NA – NA – $5 \cdot 10^{-4}$	$2.7 \cdot 10^{-7}$	$3.0 \cdot 10^{-7}$	$3.0 \cdot 10^{-7}$	$5.8 \cdot 10^{-9}$
NA – NA – $1 \cdot 10^{-4}$	$5.6 \cdot 10^{-8}$	$6.2 \cdot 10^{-8}$	$6.2 \cdot 10^{-8}$	$1.2 \cdot 10^{-9}$
NA – NA – $1 \cdot 10^{-5}$	$9.6 \cdot 10^{-9}$	$9.9 \cdot 10^{-8}$	$9.9 \cdot 10^{-8}$	$1.3 \cdot 10^{-10}$

### 3.1.5.2 Analytical functions for the urinary excretion

In order to facilitate the use of the Model-b, analytical functions were derived for the urinary excretion of Plutonium. Particular attention was paid to the urinary excretion because this type of bioassay is very common and sometimes the only feasible technique of assessment of an accidental intake

As observed for the E(50) calculations, the time dependent skeletal transfer rates of the modified model influences the urinary excretion of Plutonium in relation to the age of the subject at the time of intake. The urinary excretion of  $^{239}\text{Pu}$  for subjects aged from twenty-five to sixty years at the moment of intake was calculated for different pathways of intake and according to the usual standard scenarios of contamination. The Plutonium excreted in urine for a forty years old subject represents roughly the average of the Plutonium excreted in urine by individuals aged from twenty-five to sixty at the moment of intake. The calculations show that for inhalation of an aerosol of 5  $\mu\text{m}$  AMAD, absorption type M, the excreted Plutonium in urine is almost independent of the age of the subject at the intake up to 100 days post-intake. The greatest deviations are at 2 and 10 years post intake when the Plutonium activity excreted in urine for a forty years old subject is - 17% and +17% of the activity excreted by individuals aged sixty and twenty-five, respectively. After this the deviations become smaller and smaller until at long times post exposure the Plutonium activity excreted in urine by the reference subject aged forty is + 3% and - 9% of the Plutonium excreted by individuals aged sixty and twenty-five at the intake, respectively. The ratios of excretion curves for subjects at different ages at the moment of intake by a forty years subject excretion curve are given in Figure 3.1.21 in case of inhalation of a 5  $\mu\text{m}$  AMAD, absorption type M. For type S, the deviations are smaller. The same considerations apply for 1  $\mu\text{m}$  AMAD. In case of ingestion,  $f_1 = 5 \cdot 10^{-4}$ , the greatest deviations are at 1 and 11 years post intake when the Plutonium activity excreted in urine for a forty years old subject is - 21% and +13% of the activity



excreted by individuals aged sixty and twenty-five, respectively. For the other  $f_1$  values the deviations are even slightly smaller.

On the basis of the previous considerations a forty years old subject can be assumed as a reference subject for evaluating the average urinary excretion of occupationally exposed workers. Such an assumption also has the advantage to be coherent with the E(50) coefficients previously calculated and referring to a forty years old subject.

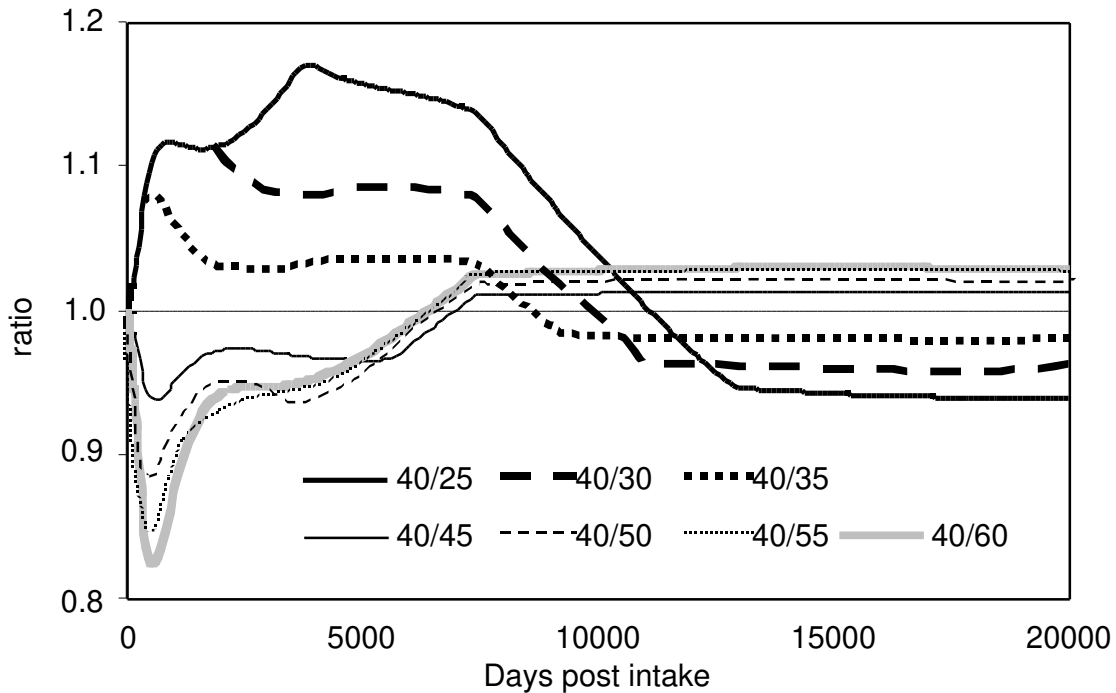


**Figure 3.1.21** Ratio of  $^{239}\text{Pu}$  urinary excretion curves for a 40 years old subject to the excretion for ages 25 to 60 years (5 years interval) (e.g. 40/25 = ratio of age 40 years to age 25 years excretion curve). Type of absorption M. AMAD = 5  $\mu\text{m}$ .

The analytical functions of the urinary excretion of Plutonium for a forty years subject were calculated in case of both inhalation and ingestion. The excretion of Plutonium in urine (equation 3.1.8) is described by a product of an exponential term, that represents the radioactive decay of the radioisotope, with a sum of seven exponential terms that follow from the biokinetic transfers of the radionuclide in the body:

$$e_u(t) = e^{-\lambda_R t} \left( \sum_{i=1}^7 c_i e^{-\lambda_i t} \right) \quad [\text{Bqd}^{-1} \text{ per Bq of intake}]$$

equation 3.1.8

where:

$e_u(t)$  is the daily urinary excretion of a Plutonium radioisotope;

$\lambda_R$  is the physical decay constant of a Plutonium radioisotope;

$\lambda_i$  and  $c_i$  are the exponents and coefficient of the exponential terms used to describe the biokinetic transfers.

The exponents relating to the physical decay are given in Table 3.1.18

**Table 3.1.18** Physical decay constants to be used in the analytical function for the urinary excretion of Plutonium ( $\exp(-\lambda_R \cdot t)$ ).

	$^{238}\text{Pu}$	$^{239}\text{Pu}$	$^{240}\text{Pu}$	$^{241}\text{Pu}$
$\lambda_R$ [ $\text{d}^{-1}$ ]	$2.17 \cdot 10^{-5}$	$7.89 \cdot 10^{-8}$	$2.91 \cdot 10^{-7}$	$1.32 \cdot 10^{-4}$

In order to calculate the other exponential terms the urinary excretion curves calculated on the basis of Model-b were plotted in a semi-logarithmic graph to reveal the conspicuous slopes that could be mathematically described with suitable exponents. A linear fitting procedure was then carried out to calculate the coefficients of the exponential terms. The whole procedure has two main advantages:

- It was avoided to using non-linear fitting procedures, as they are strongly depending on the initial values of the parameters and therefore subjected to a close local minimum;
- The preliminary graphical analysis allowed to see some common trends among the excretion curves for different scenarios of contamination. It was therefore possible to limit the variation of parameters when different scenarios were considered, making it easier to implement the analytical curves in the monitoring practice.

The coefficients and the exponents for the exponential terms relating to the biokinetic transfers of the radionuclide in the body are given in Table 3.1.19 and Table 3.1.20 in case of inhalation and ingestion, respectively. In part they were already published in a recent publication [163].

**Table 3.1.19** Exponents and coefficients of analytical functions for the urinary excretion rate of Plutonium after inhalation (Model-b ).

Index $i$	AMAD = 1 $\mu\text{m}$				AMAD = 5 $\mu\text{m}$			
	Type M		Type S		Type M		Type S	
	$f_1 = 5 \cdot 10^{-4}$		$f_1 = 1 \cdot 10^{-5}$		$f_1 = 5 \cdot 10^{-4}$		$f_1 = 1 \cdot 10^{-5}$	
	$c_i$	$\lambda_i$ [ $\text{d}^{-1}$ ]	$c_i$	$\lambda_i$ [ $\text{d}^{-1}$ ]	$c_i$	$\lambda_i$ [ $\text{d}^{-1}$ ]	$c_i$	$\lambda_i$ [ $\text{d}^{-1}$ ]
1	$3.03 \cdot 10^{-4}$	$8.8 \cdot 10^{-1}$	$2.94 \cdot 10^{-6}$	$8.8 \cdot 10^{-1}$	$3.60 \cdot 10^{-4}$	$8.8 \cdot 10^{-1}$	$3.57 \cdot 10^{-6}$	$8.8 \cdot 10^{-1}$
2	$8.81 \cdot 10^{-6}$	$91 \cdot 10^{-2}$	$5.07 \cdot 10^{-8}$	$9 \cdot 10^{-2}$	$1.20 \cdot 10^{-5}$	$9 \cdot 10^{-2}$	$1.03 \cdot 10^{-7}$	$9 \cdot 10^{-2}$
3	$-2.18 \cdot 10^{-6}$	$11 \cdot 10^{-2}$	$3.91 \cdot 10^{-9}$	$1 \cdot 10^{-2}$	$1.61 \cdot 10^{-6}$	$1 \cdot 10^{-2}$	$2.84 \cdot 10^{-8}$	$1 \cdot 10^{-2}$
4	$1.06 \cdot 10^{-5}$	$6 \cdot 10^{-3}$	$-1.34 \cdot 10^{-7}$	$1.5 \cdot 10^{-3}$	$4.81 \cdot 10^{-6}$	$6 \cdot 10^{-3}$	$-7.36 \cdot 10^{-8}$	$1.5 \cdot 10^{-3}$
5	$1.69 \cdot 10^{-6}$	$1 \cdot 10^{-3}$	$1.89 \cdot 10^{-7}$	$8 \cdot 10^{-4}$	$1.12 \cdot 10^{-6}$	$1 \cdot 10^{-3}$	$1.03 \cdot 10^{-7}$	$8 \cdot 10^{-4}$
6	$1.71 \cdot 10^{-5}$	$1 \cdot 10^{-5}$	$-8.91 \cdot 10^{-8}$	$2 \cdot 10^{-4}$	$1.17 \cdot 10^{-5}$	$1 \cdot 10^{-5}$	$-5.11 \cdot 10^{-8}$	$2 \cdot 10^{-4}$
7	$-1.56 \cdot 10^{-5}$	$8 \cdot 10^{-6}$	$2.44 \cdot 10^{-7}$	$4 \cdot 10^{-5}$	$-1.07 \cdot 10^{-5}$	$8 \cdot 10^{-6}$	$1.30 \cdot 10^{-7}$	$4 \cdot 10^{-5}$

**Table 3.1.20** Exponents and coefficients of analytical functions for the urinary excretion rate of Plutonium after ingestion (Model-b).

Index i	$f_1 = 5 \cdot 10^{-4}$		$f_1 = 1 \cdot 10^{-4}$		$f_1 = 1 \cdot 10^{-5}$	
	$c_i$	$\lambda_i [d^{-1}]$	$c_i$	$\lambda_i [d^{-1}]$	$c_i$	$\lambda_i [d^{-1}]$
1	$4.77 \cdot 10^{-6}$	$7.5 \cdot 10^{-1}$	$9.54 \cdot 10^{-7}$	$7.5 \cdot 10^{-1}$	$9.54 \cdot 10^{-8}$	$7.5 \cdot 10^{-1}$
2	$3.06 \cdot 10^{-7}$	$9.5 \cdot 10^{-2}$	$6.12 \cdot 10^{-8}$	$9.5 \cdot 10^{-2}$	$6.12 \cdot 10^{-9}$	$9.5 \cdot 10^{-2}$
3	$5.63 \cdot 10^{-8}$	$8.2 \cdot 10^{-3}$	$1.13 \cdot 10^{-8}$	$8.2 \cdot 10^{-3}$	$1.13 \cdot 10^{-9}$	$8.2 \cdot 10^{-3}$
4	$-4.18 \cdot 10^{-9}$	$1.2 \cdot 10^{-3}$	$-8.36 \cdot 10^{-10}$	$1.2 \cdot 10^{-3}$	$-8.36 \cdot 10^{-11}$	$1.2 \cdot 10^{-3}$
5	$8.55 \cdot 10^{-9}$	$8 \cdot 10^{-4}$	$1.71 \cdot 10^{-9}$	$8 \cdot 10^{-4}$	$1.71 \cdot 10^{-10}$	$8 \cdot 10^{-4}$
6	$9.06 \cdot 10^{-8}$	$1 \cdot 10^{-5}$	$1.81 \cdot 10^{-8}$	$1 \cdot 10^{-5}$	$1.81 \cdot 10^{-9}$	$1 \cdot 10^{-5}$
7	$-8.24 \cdot 10^{-8}$	$8 \cdot 10^{-6}$	$-1.65 \cdot 10^{-8}$	$8 \cdot 10^{-6}$	$-1.65 \cdot 10^{-9}$	$8 \cdot 10^{-6}$

For an intake via inhalation the exponents of the first three terms describing the short-term excretion are equal under all the conditions of exposure. The exponents of the last four terms depend on the type of absorption, but turn out to be almost independent on the AMAD of the aerosol. The exponential expression deviates from the exact analytical solution of the model by less than 5% for the first 10 days post-intake and less than 2% up to 20,000 days post-intake. In case of ingestion it was possible to obtain reasonably good fitting using the same exponents for all the standard  $f_1$  values. The coefficients of the exponential terms were firstly calculated for the analytical function of the Plutonium urinary excretion relating to  $f_1 = 5 \cdot 10^{-4}$ . The same coefficients can be used for the analytical functions relating to the other two  $f_1$  values ( $1 \cdot 10^{-4}$  and  $1 \cdot 10^{-5}$ ). In the latter cases the coefficients for  $f_1 = 5 \cdot 10^{-4}$  should be multiplied by factors derived from the  $f_1$  values ( $1 \cdot 10^{-4} / 5 \cdot 10^{-4} = 0.2$  and  $1 \cdot 10^{-5} / 5 \cdot 10^{-4} = 0.02$ ). Even with this extreme simplification the exponential expression deviates from the exact analytical solution of the model by less than 15% for the first 10 days post-intake and less than 10% up to 20,000 days post-intake.

### 3.1.5.3 Sensitivity analysis

A sensitivity analysis was applied to the optimized model in order to pick out the most significant parameters for the urinary excretion of Plutonium. To a lesser extent fecal excretion and activity in blood were also considered. Respiratory tract and gastrointestinal compartmental models connected to the systemic model were considered as well, and the sensitivity analysis was applied to their parameters too, in order to consider real cases of contamination via ingestion or inhalation. The results of the present sensitivity analysis have two main applications. First of all it allows to identify the transfer rates and in a certain way the physiological processes whose alteration could explain possible significant deviations of the measurements of the excreted activity from the model predictions. Secondly they will be used as a screening method to reduce the number of model parameters that must be considered in the subsequent analysis of the uncertainty of the model predictions for Plutonium excretion in urine. As usual great importance was placed on the urinary excretion of Plutonium because the monitoring of the internal contamination following an intake of a Pu-radioisotope is mainly based on measurements of activity in biological samples, more

commonly in urine. The methodology and the results of the present analysis were in part already published in a recent publication [164].

Many of the methods available for conducting sensitivity analysis have been described and compared in the general context of models development [165]. One of the most common methods is the differential sensitivity analysis, based on partial differentiation of the equations mathematically describing the model. The sensitivity coefficient for an independent variable is calculated from the partial derivative of the dependent variable with respect to the independent variable. In the specific case of the present work the dependent variable is the excreted Plutonium activity and the independent variables are the rates of transfer of activity among the compartments. As a rule the derivatives are multiplied by the ratio of the transfer rate value to the model predictions of excreted activity for the base-case scenario in order to normalize the results and avoiding the effects of the units.

Concerning the interpretation of the sensitivity coefficients as defined above, an independent variable to which a dependent variable is particular sensitive has a sensitivity coefficient that tends to be unity or larger; on the contrary with low sensitivity the coefficient will tend to zero. For example a sensitivity coefficient of + 0.1 (- 0.1) indicates that an increase of +1% in the independent variable results in a + 0.1% (- 0.1%) variation in the dependent variable.

In the sensitivity studies for the first order biokinetic models the differential analysis has been often used because the differential equations that describe the model can be easily recasted to provide a set of equations by which to calculate the sensitivity coefficients [166]. This method can be efficiently applied when exact solutions of the system of differential equations are available. As time-dependent transfer rates are assumed in the optimized model (Model-b), only a numerical solution can be obtained. Therefore the sensitivity coefficients were calculated by numerical partial differentiation. The sensitivity coefficient for the daily urinary excretion of Plutonium activity ( $e_u$ ) with respect to the  $i$ -th transfer rate ( $\lambda_i$ ) is defined as:

$$S_i = \frac{\Delta e_u}{\Delta \lambda_i} \frac{\lambda_i}{e_u}$$

*equation 3.1.9*

Similar expressions were used for the sensitivity coefficients relating to fecal excretion and blood content of Plutonium. The ratio  $\Delta e_u / \Delta \lambda_i$  was evaluated by changing the rate constant  $\lambda_i$  only by 1% and calculating the resulting increment  $\Delta e_u$  of the daily excretion in urine. Some preliminary calculations of  $S_i$  with respect to some transfer rates for different increments (0.1%, 0.5%, 1%, 5% and 10%) were carried out. It was found that the increment of 1% is small enough to represent a valid approximation of the derivative and, at the same time, is large enough to avoid rounding problems [164].

The sensitivity coefficients so determined are time dependent through both the function  $e_u$ , which depends on the time post intake, and the transfer rates of the skeletal system, for which the new model has introduced an age-related dependency. In order to consider the sensitivity over a large period, the coefficients  $S_i$  were calculated at 10, 100, 1,000 and 10,000 days post intake.

The sensitivity analysis was carried out for the Model-b parameters both for a direct uptake into blood (i.e. injection) and for ingestion or inhalation. In the latter two cases a sensitivity analysis for the parameters that describes the non-systemic phase of the contamination was carried out as well. As in previous analyses, the systemic model (Model-b) was connected to the ICRP models for the gastrointestinal tract [58] and for the respiratory

tract [57] to consider a contamination via ingestion and inhalation, respectively. The usual standard scenarios of contamination were considered.

The results relating to the sensitivity analysis for the systemic parameters are discussed first. The sensitivity coefficients for the urinary excretion of Plutonium calculated following a contamination via injection are presented in Figure 3.1.22. The coefficients are given up to a minimum value of  $10^{-3}$  but only those parameters whose sensitivity coefficients have an absolute value greater than 0.1 at least for one time point are presented and considered to be significant for the Plutonium excretion in urine [166]. Besides the transfer rates related to the urinary system, only the transfer rates from blood to the first compartment of liver (Liver 1) and to the cortical surface have significant sensitivity coefficients at any time point after injection. At short time (10 and 100 days after injection) the urinary excretion of Plutonium is sensitive to the transfer rates for the ST0 (in- and outgoing flux) and ST1 (incoming flux) soft tissue compartments, and to the transfer of activity from blood to the trabecular bone. At long time (1,000 and 10,000 days after injection) it turns out that the most significant sensitivity coefficients are for the outgoing flux from ST1 and the incoming flux into ST2 soft tissue compartments, the transfer rate from the second compartment of the liver (Liver 2) to blood and the remodelling rate for the cortical bone. The trabecular remodelling rate seems to play a major part at intermediate times only (100 and 1,000 days post injection).

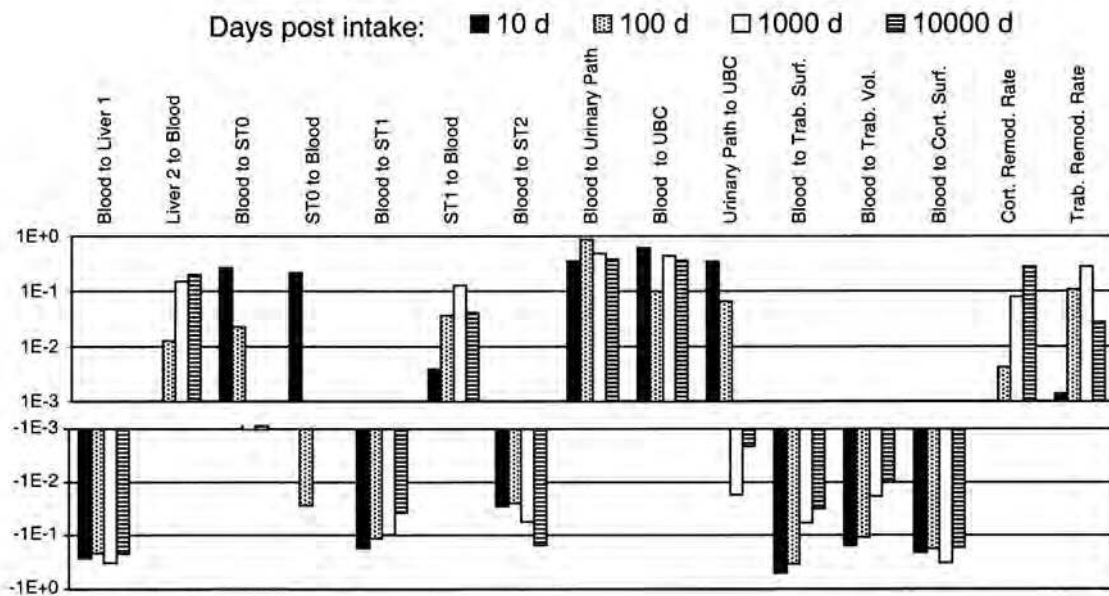


**Figure 3.1.22** Systemic sensitivity coefficients  $S_i$  for the urinary excretion of Plutonium assessed with the Model-b following an intake via injection. Only the transfer rates with  $|S_i| > 0.1$  at least for one time point are shown.

The sensitivity coefficients for the systemic parameters of the Model-b in case of contamination via ingestion or via inhalation are summarized in a semi-quantitatively way in Table 3.1.21. This permits one to easily find out the variation in the significance in relation to the path of intake. Only the parameters whose sensitivity coefficients have an absolute value greater than 0.1, at least for one time point, are presented. The letters  $p$  and  $n$  indicate that the sensitivity coefficient is greater than + 0.1 and smaller than - 0.1, respectively. It can be generally stated that the slower the transfer of activity is from the non-systemic to the

systemic part, the more the sensitivity coefficients for the systemic transfer rates deviate from the values calculated in case of a direct uptake into the blood. For example if the first column of Table 3.1.21, relating to the sensitivity in case of ingestion, is compared with Figure 3.1.22, relating to a case of injection, it is seen that the same systemic transfer rates are significant for the same time points. And this also is obvious for the sensitivity coefficients of the systemic parameters in case of inhalation, absorption type M, as well. The only considerable variation is for the trabecular remodelling rate that is significant only at 1,000 days after inhalation. In case of inhalation of a compound of absorption type S, that is characterized by a much slower transfer of activity from the respiratory tract to the systemic organs, several variations in the significance of the sensitivity coefficients for the systemic transfer rates occur. The transfer rates from blood to the soft tissue compartment ST1 and to trabecular surface extend their significance up to 1,000 days post intake. Furthermore in comparison with the absorption type M the transfer rates from blood to ST0 and from ST1 to blood are not significant any more, while the transfer rate from Liver 2 to blood limits its significance only to 10,000 days post intake. Generally it can be concluded that the sensitivity analysis for inhalation or ingestion does not reveal any new significant parameters compared to direct systemic intake. The latter is therefore an appropriate scenario for determining the transfer rates of interest for the subsequent uncertainty analysis.

**Table 3.1.21** Systemic parameters whose sensitivity coefficients for the urinary excretion of Plutonium are greater than +0.1 (indicated by p) or smaller than -0.1 (indicated by n). Standard paths and conditions of exposure were assumed.

Parameter	Ingestion				Inhalation (M)				Inhalation (S)			
	Days after intake:				Days after intake:				Days after intake:			
	10 <sup>1</sup>	10 <sup>2</sup>	10 <sup>3</sup>	10 <sup>4</sup>	10 <sup>1</sup>	10 <sup>2</sup>	10 <sup>3</sup>	10 <sup>4</sup>	10 <sup>1</sup>	10 <sup>2</sup>	10 <sup>3</sup>	10 <sup>4</sup>
Blood to Liver 1	n	n	n	n	n	n	n	n	n	n	n	n
Liver 2 to Blood			p	p			p	p				p
Blood to ST0	p				p							
ST0 to Blood	p				p				p			
Blood to ST1	n	n			n	n			n	n	n	
ST1 to Blood			p				p					
Blood to ST2				n				n				n
Blood to Urin. Path	p	p	p	p	p	p	p	p	p	p	p	p
Blood to UBC	p	p	p	p	p	p	p	p	p	p	p	p
Urin. Path to UBC	p				p				p			
Blood to Trab. Surf.	n	n			n	n			n	n	n	
Blood to Trab. Vol.	n	n			n	n			n	n		
Blood to Cort. Surf.	n	n	n	n	n	n	n	n	n	n	n	n
Cort. Remod. Rate				p				p				p
Trab. Remod. Rate		p	p				p				p	

The sensitivity coefficients for the fecal excretion of Plutonium calculated following a contamination via injection are presented in Figure 3.1.23. Most of the transfer rates with high sensitivity for the urinary excretion, are also significant for fecal excretion, such as the transfer rates of the soft tissue compartments and those relating to the skeleton. Among the latter the transfer from trabecular marrow to blood should now be added even though it is significant only at 100 days post intake. As expected, the parameters of the urinary system are now less important: They are significant only at long times (10,000 days post injection). The transfer rate from the urinary path to the urinary bladder content obviously can have no any effect at all. All the parameters relating to the Plutonium biokinetics in liver are now significant. Particularly important is the transfer of activity from the Liver 1 compartment to the small intestine whose sensitivity coefficient is significant at all the time points considered. This is true also for the transfer of activity from blood to the upper large intestine (ULI).

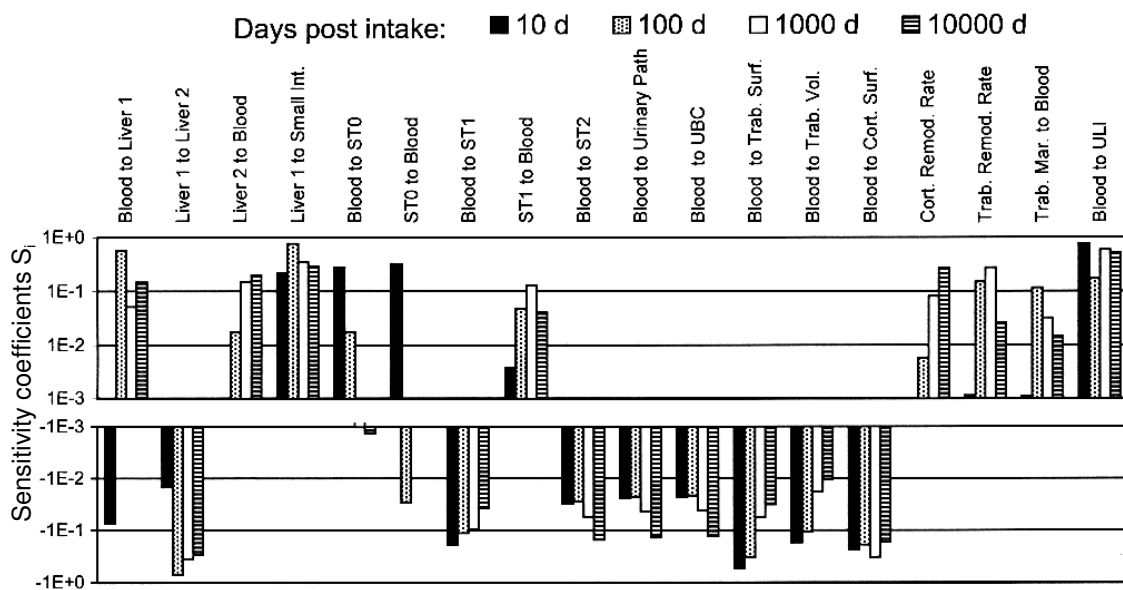


**Figure 3.1.23** Systemic sensitivity coefficients  $S_i$  for the fecal excretion of Plutonium assessed with the Model-b. Only the transfer rates with  $|S_i| > 0.1$  at least for one time point are shown.

The sensitivity coefficients for Plutonium in blood following an injection are presented in Figure 3.1.24. Almost all the transfer rates that were significant for the urinary excretion are still relevant in determining the amount of Plutonium in the blood. This confirms also the validity of using the transfer of activity to the blood for identifying the parameters and processes that are important in determining the urinary excretion, as carried out by means of Figure 3.1.8 in the phase of model developing (see paragraph 3.1.3.1). In comparison to the results of sensitivity analysis for the urinary excretion, the transfer rate from the urinary path to the urinary bladder content can not obviously have any effect. In addition two further transfer rates are now significant: the trabecular remodelling rate and the rate from blood to the upper large intestine (ULI). These parameters now turn out to be significant for the fecal excretion too.

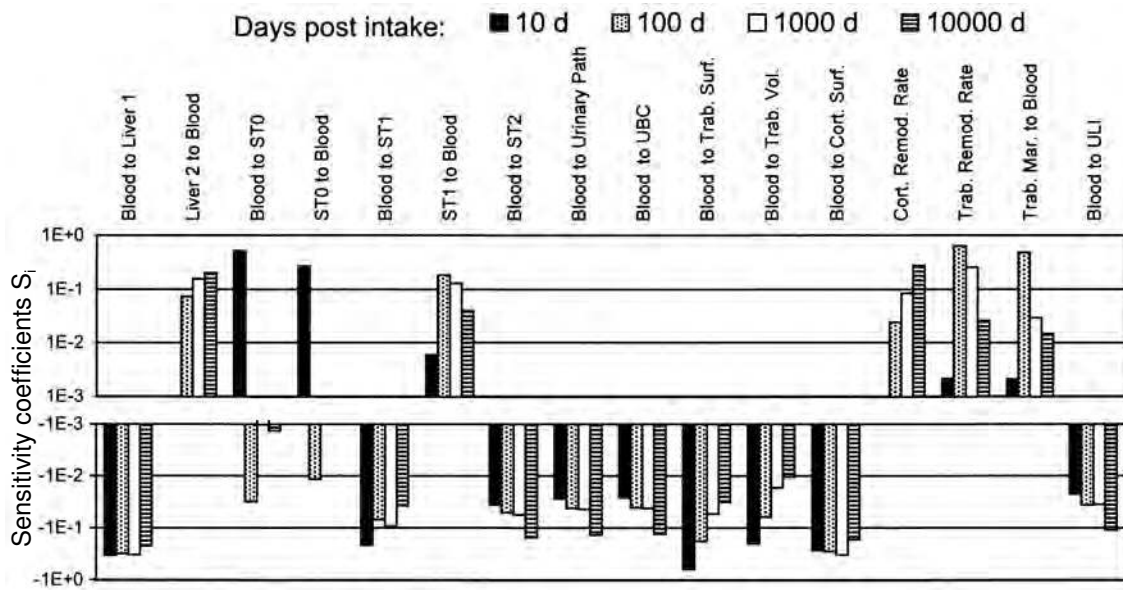


**Figure 3.1.24** Systemic sensitivity coefficients  $S_i$  for the Plutonium activity in blood assessed with the Model-b. Only the transfer rates with  $|S_i| > 0.1$  at least for one time point are shown.

The sensitivity analysis of the parameters of respiratory tract and gastrointestinal models was performed just for the most important and common bioassay, i.e. the activity in urine. In case of contamination via ingestion it turns out that the most important parameter is the uptake factor  $f_1$ , whose sensitivity coefficient is always equal to +1.0 at any time point. This was observed in similar sensitivity analysis [166]. The transfer rate from the small intestine to the upper large intestine (ULI) is also significant for some time points because it affects the value of the  $f_1$ .

In case of inhalation the sensitivity coefficients for the transfer rates of the respiratory tract model that have an absolute value greater than 0.1, at least for one time point and for one absorption type, are presented in Figure 3.1.25 and Figure 3.1.26 for type M and S, respectively. It turns out that for type M the only significant parameters are the absorption parameters  $s_p$ ,  $s_{pt}$  and  $s_t$  and the transfer rate from the ET2 extrathoracic compartment to the gastrointestinal tract. In case of inhalation of a compound with a slow rate of absorption into blood (type S) the transfer rates from the three compartments of the alveolar-interstitial region to the bb1 compartment of the bronchiolar region become significant, particularly at long time after inhalation. In any case the sensitivity analysis seems to indicate that the urinary excretion of Plutonium is not particularly sensitive to the clearance rates of all the other compartments related to the particle transport in the bronchial and bronchiolar regions.



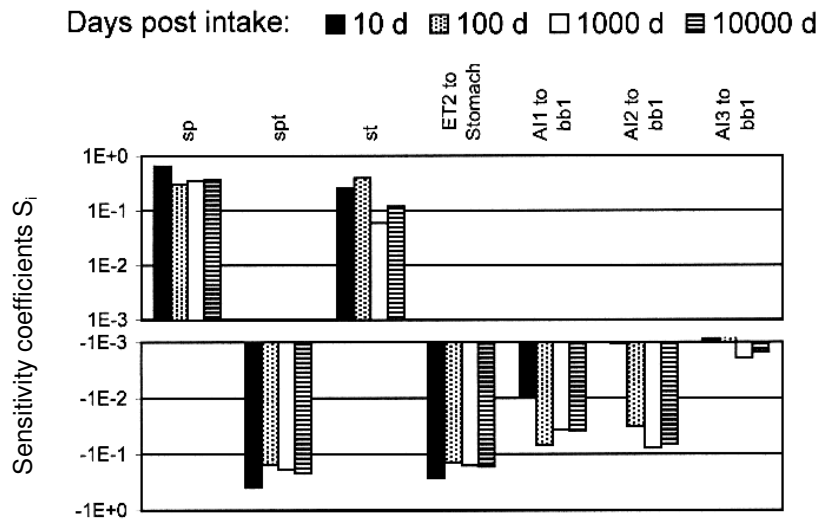


**Figure 3.1.25** Pre-systemic sensitivity coefficients  $S_i$  for the urinary excretion of Plutonium assessed with the Model-b connected to ICRP 66 respiratory model (type M). Only the transfer rates with  $|S_i| > 0.1$  at least for one time point and one absorption type are shown.

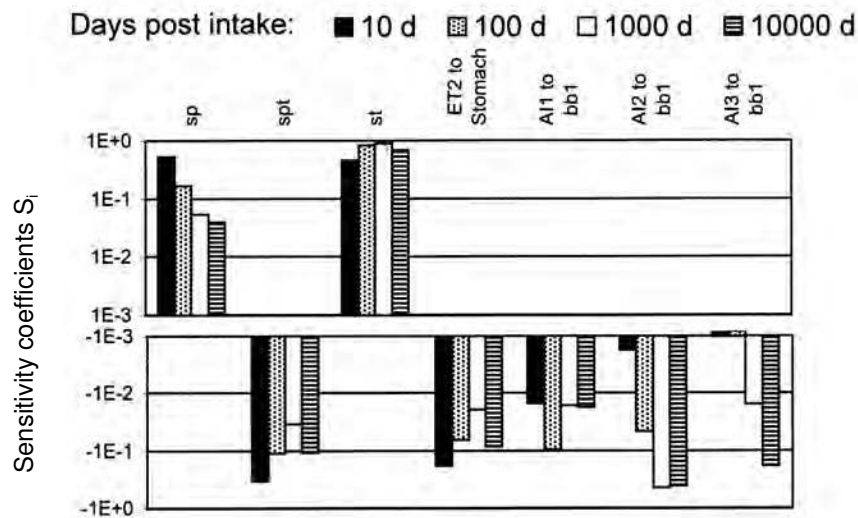


**Figure 3.1.26** Pre-systemic sensitivity coefficients  $S_i$  for the urinary excretion of Plutonium assessed the Model-b connected to ICRP 66 respiratory model (type S). Only the transfer rates with  $|S_i| > 0.1$  at least for one time point and one absorption type are shown.

As an example a practical application of the previous sensitivity analysis is shown in the following. The results of the sensitivity analysis for the respiratory tract allow to evaluate the effects of the modifying factors proposed by ICRP for the parameters describing the particle transport in the human respiratory tract. In the Annexe E of Publication 66 of ICRP [57] modifying factors  $\Phi_m$  are recommended by which the parameters of the respiratory model should be multiplied in order to consider alterations in the particle transport model due to factors such as age, smoking, pollutants, disease or pharmacological agents. The respiratory model parameters that are supposed to be altered are the clearance from the BB1 bronchial compartment and the bb1 bronchiolar compartment, for almost all the causes of clearance alteration, and the clearance from the two alveolar-interstitial compartments AI2 and AI3 together with the fraction deposited in AI1, for the effects of cigarette smoking. As suggested by the sensitivity analysis, only the cigarette smoking, affecting the clearance from the alveolar-interstitial compartments, would significantly alter the urinary excretion of Plutonium. Assuming the modifying factors proposed by ICRP and using the Model-b for Plutonium, it was calculated that smoking would cause an enhancement of the urinary excretion of type S Plutonium by 17 %, 43 % and 44 % at 100, 1,000 and 10,000 days post inhalation, respectively (see Figure 3.1.27).

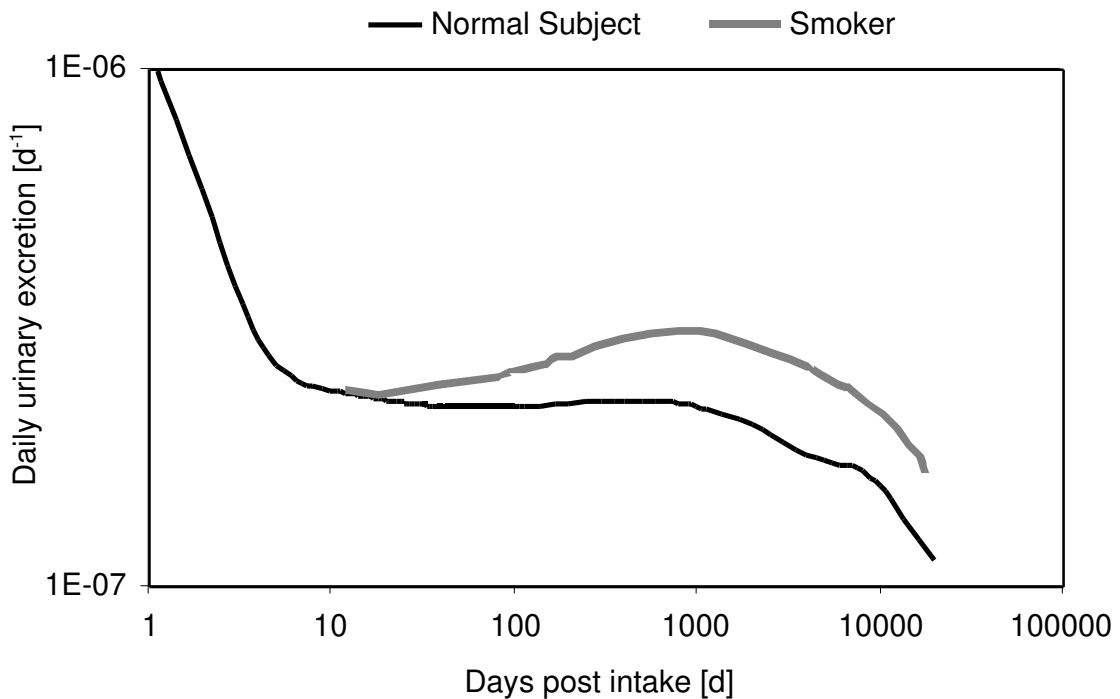


**Figure 3.1.27** Daily percentage urinary excretion of type S Plutonium for a smoker compared to a normal subject using the Model-b and the ICRP 66 respiratory tract model.

#### 3.1.5.4 Uncertainty analysis

Uncertainty analyses of models are generally performed in order to determine the uncertainty of a model's predictions that results from imprecisely known input variables. In the specific context of the present work, the effects of incomplete knowledge [167] of the

transfer rates on the Plutonium urinary excretion and, to a lesser extent, on the fecal excretion and blood content are investigated.

Nowadays different methods are available for performing an uncertainty analysis. Monte Carlo techniques are among the most common and effective procedures. This technique is based on performing a model's multiple evaluations with probabilistically selected input, and then using the results of these evaluations to determine the uncertainty. In a more detailed way, Monte Carlo analysis involves four steps.

1. Selection of the range and distribution for each input variable. These selections will be used in the next step for generating a sample of values of the variable. The main problem in this step is the choice of the distribution. If the analysis is just of exploratory nature, then rather crude but easily implemented statistical distributions can be considered (e.g. uniform, log-uniform or triangular). However if more realistic results are expected from the uncertainty analysis, then other distributions should be considered as well.
2. In a second step values must be sampled from the chosen distribution and for each input variable. The most widely used sampling procedures are random sampling, importance sampling and Latin hypercube sampling [168]. The result of this step is a n-dimensional vector of the form:

$$\mathbf{x}_i = [x_{i1}, x_{i2}, x_{i3}, \dots, x_{in}] \quad i = 1, 2, 3, \dots, n$$

*equation 3.1.10*

where n is the number of input variables (i.e. the number of transfer rates considered in the uncertainty analysis) and m is the size of the sample (i.e. the number of values sampled for each input variable).

3. In a third step the model is evaluated for a large number of sampling vectors and a sequence of results ( $y_i$ ) is generated in the following form:

$$y_i = f(x_{i1}, x_{i2}, x_{i3}, \dots, x_{in}) = f(\mathbf{x}_i) \quad i = 1, 2, 3, \dots, n$$

*equation 3.1.11*

4. In the last step the results of the previous evaluations are used as basis for the uncertainty analysis. One of the most common methods to represent the uncertainty is the mean value and a variance of the distribution of the generated values. In the particular case in which the output variable is described by a log-normal distribution, the geometric mean ( $\langle y \rangle$ ) as central parameter and the geometric standard deviation ( $S_g(y)$ ) as indicator of variability should be estimated according to the following expressions:

$$\langle y \rangle = \text{Exp} \left[ \frac{\sum_i^m \text{Log} y_i}{m} \right] = \sqrt[m]{\prod_i y_i}$$

*equation 3.1.12*

$$S_g(y) = \text{Exp} \left[ \frac{\sum_i^m (\text{Log} y_i - \text{Log} \langle y \rangle)^2}{m-1} \right]$$

*equation 3.1.13*

The use of such values allows to characterize the uncertainty of the output variable by two numbers.

In comparison to other uncertainty analysis techniques [169] (such as Taylor series based differential analysis, response surface methodology or Fourier amplitude test), Monte Carlo procedures have some important advantages:

- The full range of each input variable is sampled and then used as input for calculating model predictions;
- The uncertainty is evaluated without using surrogate models, i.e. an approximating model that resembles the original model under study and on which the uncertainty analysis can be performed more effectively;
- The full stratification over the range of each input variable facilitates the identification of non-linearities, thresholds and discontinuities;
- The approach is conceptually simple and can be easily implemented in iterative procedures.

The most relevant drawback of using Monte Carlo techniques for uncertainty analyses is the fact that a large number of model evaluations are required. Therefore if the model is computationally expensive to evaluate or many input variables are considered and for each variable many values are sampled, the time and cost for performing the required calculations may be too large. In this context results of the above sensitivity analysis can be used for screening purposes in order to reduce the number of input variables that are considered in the uncertainty analysis [170]. Only those input variables that significantly affect model predictions for a certain output variable should be considered. Furthermore computational time and cost needs for uncertainty analysis can be reduced by adopting an effective procedure for the generation of the random values of the input variables. The Latin Hypercube Sampling (LHS) procedure [170] rather than random sampling techniques will improve the efficiency of random values generation. The LHS procedure is a stratified sampling technique that generates a sample of size  $m$  for each of the  $n$  input parameters in the following way:

- The range of each input variable is divided into  $m$  non-overlapping intervals on the basis of equal probability. Such a division will therefore depend on the statistical distribution assumed for the input variable;
- One value from each interval is randomly generated according to the statistical distribution in this interval;
- The previous two steps are repeated for each of the  $n$  input variables;
- The  $m$  values obtained for the  $x_1$  input variable are paired in random manner with the  $m$  values of the  $x_2$  input variable. These  $m$  pairs are combined in a random manner with the  $m$  values of the  $x_3$  input variable and so on until all the  $n$  input variables are considered.

The main advantage of the LHS procedure is that the full range of input parameters is sampled, whereas in a simple random sampling scheme, combinations of input parameter values could easily come from the same subintervals.

In adopting the LHS procedure the choice of the sample size  $m$  should be carefully considered in relation to the number  $n$  of input variables. It is preferable that  $m$  (the size of the sample, i.e. the number of values sampled for each input variable) be greater than or equal to  $(4/3) \cdot n$  [171]. Of course, if the model is simple and can be run quickly, then  $m$  could even be larger.

The sensitivity analysis has already pointed out the main significant transfer rates for the urinary excretion, fecal excretion and blood content of Plutonium predicted by the optimized model (Model-b). These parameters represent the input variables of the uncertainty analysis. In accordance with similar recent studies [166] a log-normal distribution for the input variable was assumed. The range of variation of the transfer rates was set at the 1<sup>st</sup> and 99<sup>th</sup> percentile of the log-normal distribution centred around the base case values.

Geometric standard deviations ranging from 1.25 to 2.25 (at 0.25 intervals) were preliminarily assumed for the log-normal distribution of the input variables. The aim was to find out the geometric standard deviation (GSD) for the input variable distribution that would determine a urinary excretion of Plutonium (or fecal excretion or blood content) predicted by the model with an uncertainty comparable to the observed uncertainty of data from different human subjects. Therefore, assuming a certain geometric standard deviation for the transfer rates, the variance and the mean of Plutonium urinary excretion (or fecal excretion or blood content) predicted by the model were compared to the corresponding variance and mean for the experimental data. A variance comparison test was firstly performed by considering the ratio of the two estimates of variance, one calculated on the basis of the experimental data and the second one on model's predictions. If the variances turn out to be statistically equal, a mean comparison test was successively performed to test if the mean too can be considered statistically equal [172].

In order to use the previous statistical test a normal distribution of the data should be assumed. As model predictions of activity in urine, feces and blood (tested with a  $\chi^2$  test, [172]) and the bioassays (as reported in literature [111]) can be considered log-normally distributed, the statistical tests were performed on the logarithm of the values.

Sufficient experimental data for calculating variances and means at each time point after injection are only available up to about 100 days post intake. Therefore only the most significant transfer rates in determining the activity in urine, feces and blood at short time (10 and 100 days post injection, in Figure 3.1.22, Figure 3.1.23 and Figure 3.1.24) were considered. They are summarized in Table 3.1.22. The results of the statistical analysis of means and variances are given in Table 3.1.23. It turns out that, in case of transfer rates with a GSD = 1.50, for 98% of the considered time points the model predicts a variance for the urinary excretion of Plutonium that doesn't significantly differ from the variance based on the experimental data. Furthermore for 88% of all time points the means do not significantly differ as well. In case of a GSD = 1.75, the agreement is a little worse for the urinary excretion, but the fecal excretion and the blood activity predicted by the model significantly improve their agreement with experimental data. For 94% of the considered time points, the model predicts a variance for the fecal excretion of Plutonium that doesn't significantly differ from the variance based on the experimental data. For 39% of the time points the mean doesn't significantly differ as well. The corresponding values for the activity in blood are 57% and 50%, respectively. For higher values of the GSD the urinary excretion predicted by the model agrees less and less with the variance and the mean values based on the experimental data. Therefore a GSD = 1.75 can be reasonably assumed as a realistic parameter for the geometric standard deviation of the Model-b transfer rates, to reproduce the dispersion of the subjects' values experimentally observed at short time. It is particularly interesting to point out that this choice is coherent with the factors suggested by ICRP 66 in Annex E [57] to estimate the uncertainty of several respiratory tract model parameters.

For the remaining transfer rates affecting the model's predictions at longer time, the aforementioned GSD (1.75) was assumed. The final Model-b predictions for the daily percentage urinary and fecal excretion and for the blood percentage content are presented in Figure 3.1.28, Figure 3.1.29 and Figure 3.1.30, respectively, with the relating uncertainties: the 16<sup>st</sup> and 84<sup>th</sup> percentiles (1 GSD) and the 1<sup>st</sup> and 99<sup>th</sup> percentiles. It turns out that the geometric mean of the values calculated on the basis of model's predictions for log-normally distributed transfer rates coincide with the model's predictions when basic values of the transfer rates are assumed. This was observed in all the following evaluations based on different scenarios of contamination.

**Table 3.1.22** Most significant transfer rates for the Plutonium urinary excretion, fecal excretion and blood content at short time (10 and 100 days post intake).

System Parameter	Urine	Feces	Blood
<i>Liver</i>			
Blood to Liver 1	X	X	X
Liver 1 to Liver 2		X	
Liver 1 to Small Intestine		X	
<i>Soft Tissue</i>			
Blood to ST0 soft tissue	X	X	X
ST0 soft tissue to Blood	X	X	X
Blood to ST1 soft tissue	X	X	X
ST1 soft tissue to Blood			X
<i>Urinary system</i>			
Blood to Urinary Path	X		
Blood to Urinary Bladder Content	X		
Urinary Path to Urinary Bladder Content	X		
<i>Skeletal system</i>			
Blood to Trabecular Surface	X	X	X
Blood to Trabecular Volume	X	X	X
Blood to Cortical Surface	X	X	X
Trabecular Remodelling Rate	X	X	X
Trabecular Marrow to Blood	X	X	X
<i>Gastrointestinal tract</i>			
Blood to Upper Large Intestine		X	

**Table 3.1.23** Variance Comparison: percentage of data failing to reject the statistical hypothesis  $\sigma_1=\sigma_2$ . Mean Comparison: percentage of data failing to reject the statistical hypothesis  $\mu_1=\mu_2$  when  $\sigma_1=\sigma_2$ .

$\sigma_g$	Urine		Feces		Blood	
	Variance Comparison [%]	Mean Comparison [%]	Variance Comparison [%]	Mean Comparison [%]	Variance Comparison [%]	Mean Comparison [%]
1.25	20	15	9	3	0	0
1.50	98	88	55	30	21	21
1.75	85	80	94	39	57	50
2.00	63	59	97	39	64	64
2.25	44	44	85	39	71	64
2.50	41	41	73	36	71	64
2.75	34	34	48	33	71	64
3.00	34	34	42	33	71	71

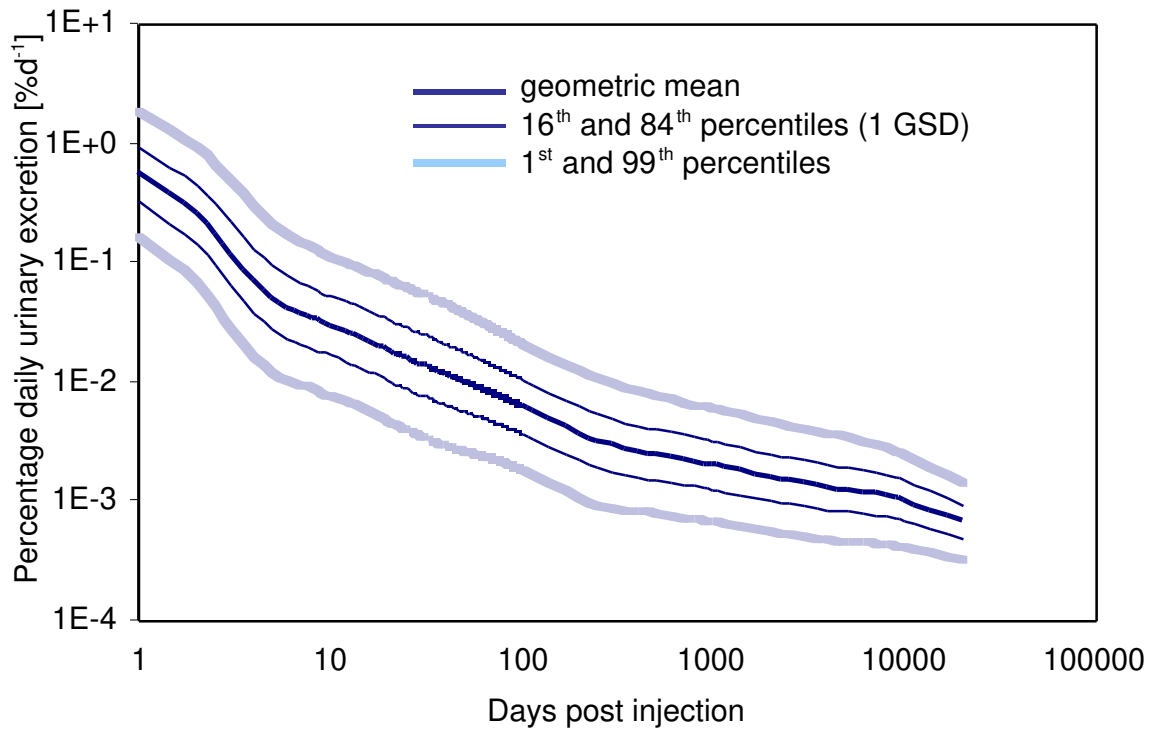


**Figure 3.1.28** Mean values and range of the daily percentage urinary excretion of Plutonium predicted by the Model-b after an injection (Geometric Standard Deviation, GSD, of model transfer rates = 1.75).

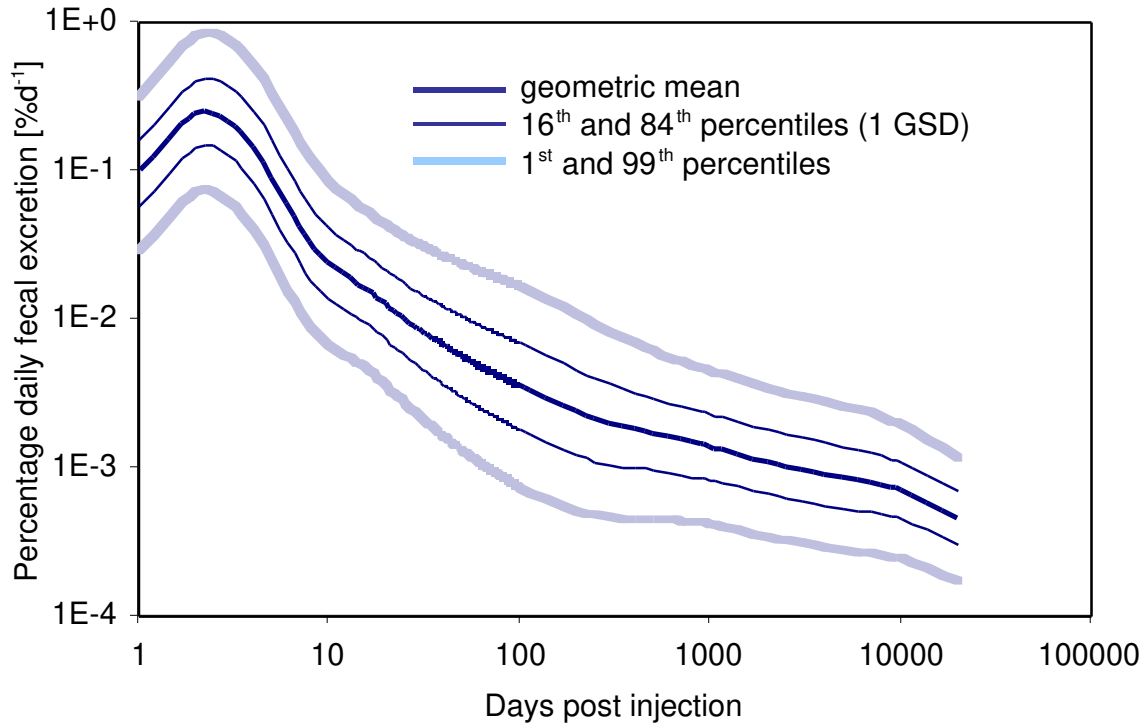


**Figure 3.1.29** Mean values and range of the daily percentage fecal excretion of Plutonium predicted by the Model-b after an injection (Geometric Standard Deviation, GSD, of model transfer of model transfer rates = 1.75).

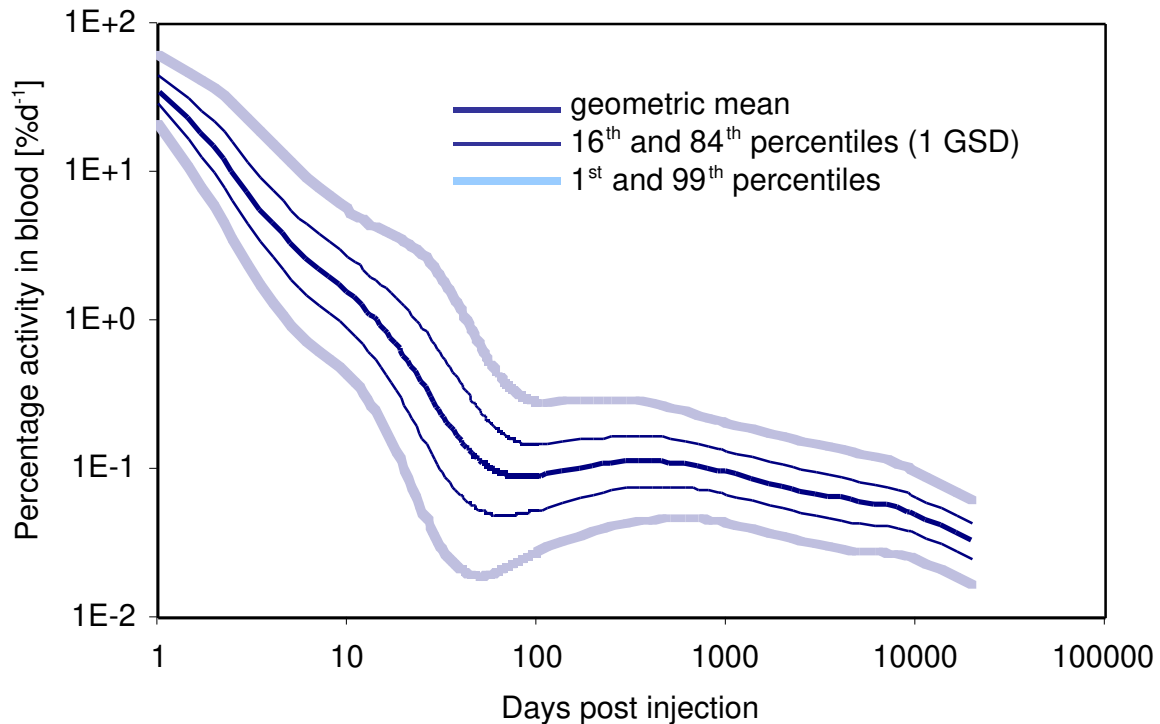


**Figure 3.1.30** Mean values and range of the percentage blood content of Plutonium predicted by the Model-b model after an injection (Geometric Standard Deviation, GSD, of model transfer = 1.75).

In order to evaluate the uncertainty of model's predictions in the practical cases of contamination, similar calculations were performed for the daily percentage urinary excretion in case of inhalation and ingestion. For the uncertainty of the not-systemic parameters, resulted significant in the previous sensitivity analysis, further assumptions were done. For the  $f_1$  gut uptake a distribution (GSD = 2.60) as suggested by Khursheed was assumed [166]. For the respiratory parameters of Figure 3.1.25 and Figure 3.1.26, the uncertainties suggested by the ICRP 66 were assumed. Otherwise, if ICRP doesn't provide any indication about the uncertainty of the respiratory tract model parameters, a GSD = 1.75 was assumed, analogously to the outcomes of uncertainty analysis for the systemic parameters.

As example Figure 3.1.31 shows the results of the model's predictions with the relating uncertainties (the 16<sup>st</sup> and 84<sup>th</sup> percentiles, 1 GSD, and the 1<sup>st</sup> and 99<sup>th</sup> percentiles) in case of an inhalation of a compound type S, AMAD = 5 $\mu$ m by a standard worker. In comparison to the uncertainties for the urinary excretion of Plutonium following a systemic contamination, a contamination via inhalation (or other not-systemic path) will determine a greater range in the uncertainties of model's predictions because a larger number of varying transfer rates are considered. The values of GSD of the model's predictions for the daily percentage urinary excretion are summarized in Figure 3.1.32 for the main standard conditions of exposure. The GSD of Model-b predictions of Plutonium urinary excretion after ingestion are significantly greater than the GSD relating to an inhalation event, even if a smaller number of transfer rates were varied in the former case. This is due to two main reasons:

- The sensitivity analysis has pointed out the greatest sensitivity coefficients for the  $f_1$  gut uptake factor (+1);
- The greatest GSD (2.60) was assumed for the  $f_1$  gut uptake factor [166].



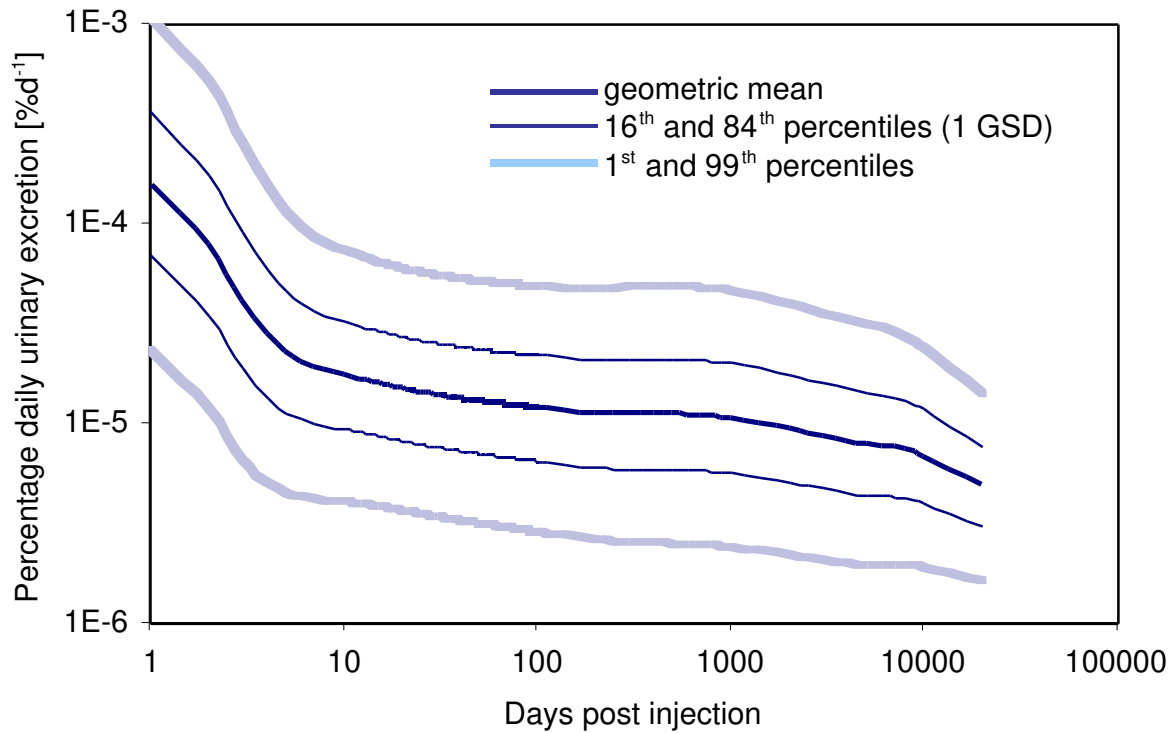


**Figure 3.1.31** Mean values and range of the daily percentage urinary excretion of Plutonium predicted by the Model-b after inhalation of a compound type S, AMAD = 5 $\mu$ m by a standard worker.

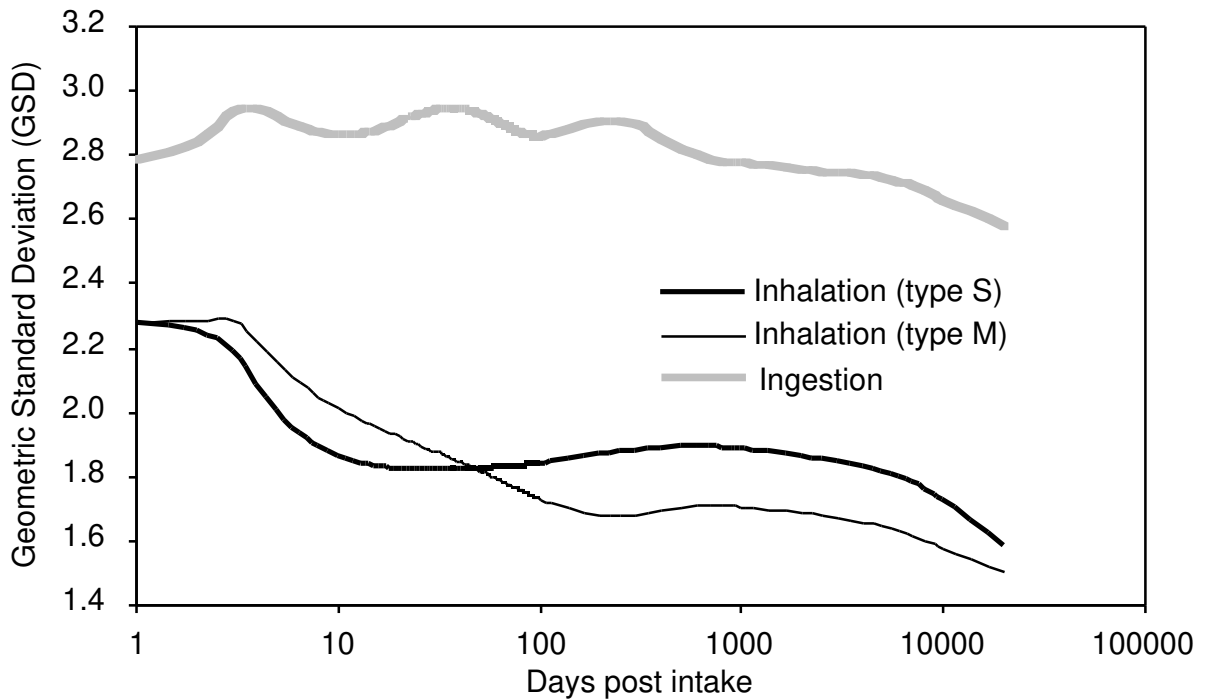


**Figure 3.1.32** GSD of Model-b predictions for the daily percentage urinary excretion of Plutonium assuming different standard conditions of exposure.

By means of Figure 3.1.32 it is possible to calculate the uncertainties associated to Model-b predictions for the daily urinary excretion rate. The plot relating to an exposure via ingestion was calculated with a gut uptake factor  $f_1 = 5 \cdot 10^{-4}$ , but it well approximates the plots for all the  $f_1$  factor values. A  $5 \mu\text{m}$  AMAD aerosol was considered for the inhalation case. The curves in Figure 3.1.32 enable to estimate whether a certain experimental measurement is statistically in good agreement with the model predictions and their uncertainty.

## 3.2 APPLICATION OF THE OPTIMIZED MODEL TO A CASE OF CONTAMINATION

---

### 3.2.1 HARMONIZATION OF THE ACTIVITY MEASUREMENTS IN BIOASSAYS

The contamination case was presented in the paragraph 2.2 of Chapter 2. The results of the Plutonium and Americium measurements on organs and bioassays performed in the frame of the present work are provided in paragraphs 2.3.3 and 2.4.3, respectively. The data from previous measurements campaign carried out on the subject are available from previous studies presented in paragraph 2.2.2.

The results of the measurements for the radionuclides content in the urine and feces samples often relate to the total activity of different combinations of Americium and Plutonium radioisotopes. Up to 3902 days post intake the available measurements relate to the total activity of  $^{239}\text{Pu} + ^{240}\text{Pu}$  and to  $^{238}\text{Pu} + ^{241}\text{Am}$ ; at 2528 and 2923 days to  $^{238}\text{Pu} + ^{239}\text{Pu} + ^{240}\text{Pu}$  and to the only  $^{241}\text{Am}$  activity (Table 2.2.3). Finally the measurements performed in occasion of the present work (about 6000 days post intake) relates to the total activity of  $^{239}\text{Pu} + ^{240}\text{Pu}$  and to the activity of the only  $^{238}\text{Pu}$  and  $^{241}\text{Am}$  (Table 2.4.1).

In order to have the same kind of measurements over all the observation time (from the intake up to the present), the measurements from previous studies relating to the total activity of different radionuclides were recast to reproduce the same kind of results provided in the frame of the present work. For such purpose the ratios of the initial activity of the Plutonium radionuclides present in the inhaled material (see paragraph 2.2.1) were corrected on the basis of the physical decay time of each radionuclide and assuming that all the Plutonium radioisotopes have the same biokinetics (as currently assumed by ICRP). This was carried out particularly for the measurements relating to the total activity of the  $^{238}\text{Pu} + ^{239}\text{Pu} + ^{240}\text{Pu}$  in order to provide them in the form of  $^{238}\text{Pu}$  and  $^{239}\text{Pu} + ^{240}\text{Pu}$ .

Such approach is not applicable in order to discriminate the single radionuclide contribution (Plutonium or Americium) to the total activity of  $^{238}\text{Pu} + ^{241}\text{Am}$  because the initial ratio changes with the time not only in relation to the different physical decay times, but also to the different metabolism of the radionuclides in human body. Therefore for the measurements available up to 3902 days post intake the urine and feces content of the single  $^{238}\text{Pu}$  and  $^{241}\text{Am}$  can be evaluated only after the adoption of the appropriate biokinetic model for both Plutonium and Americium.

### 3.2.2 CLASSIFICATION OF THE AVAILABLE MEASUREMENTS

On the basis of the available data in scientific literature and the measurements performed in the frame of the present work, a significant number of data is now available for the considered case of contamination. Data relating to  $^{241}\text{Am}$  activity in lung, liver and bone, and of all the contaminating radioisotopes in urine, feces and blood are available for a time range covering almost 16 years after the contamination event.

Apart the accuracy and precision characterizing each type of measurements in relation to the adopted technique, not all the measurements can be considered of the same reliability

when they are used for internal dosimetry purposes as model verification, intake estimations and dose calculations.

According to these purposes fairly reliable measurements are:

- The lung burden of Americium;
- The urinary excretion of Plutonium.

The former data are considered reliable because it can be analyzed using only the respiratory tract model and therefore avoiding assumptions about the systemic metabolism: therefore the final model is simpler and a smaller number of parameters must be considered. The only drawback is that this kind of data comprises two sources of intake (Americium directly inhaled and such originating from the  $^{241}\text{Pu}$  decay). Therefore it's necessary to model the ingrowth of Americium following the Plutonium decay by connecting each compartment of Plutonium biokinetic model to the relative compartment for Americium biokinetics.

The latter kind of data can be considered fairly reliable for two main reasons. Firstly, no decay product is involved as only the parent radionuclide, Plutonium, is considered. Secondly, the model at hand (Model-b) was optimized basically for predicting urinary excretion of Plutonium, whereas the other kinds of bioassays (feces and blood) were considered only at a lesser extent. The only drawback of such group of data is given by the necessity of using both the respiratory tract and systemic models. Therefore a great number of parameters may influence the model's predictions of urinary excretion of Plutonium, making difficult a modification of the model for improving the agreement with experimental data.

The remaining measurements (Americium activity in bone, liver, urine, feces and blood, Plutonium activity in feces and blood) can be considered less reliable for the purposes they are here used for. Specifically they are:

- The bone and liver burden of Americium;
- The urinary and fecal excretion and the blood content of Americium;
- The fecal excretion and the blood content of Plutonium.

In fact all these kinds of measurements need the use of both non-systemic and systemic models. Furthermore, for the measurements relating to Americium, both sources of intake (the fraction directly inhaled and the fraction due to the parent Plutonium decay) must be considered. For measurements relating to Plutonium the systemic modelling for fecal excretion and blood activity is less reliable than for urinary excretion.

Further considerations about the data and their classification in the previous two groups (reliable and less reliable for internal dosimetry purposes) must be pointed out.

Urinary excretion of  $^{238}\text{Pu}$  only at long time was considered in the set of the reliable data because the available data at shorter time are provided together with the Americium activity data considered less reliable for modelling purposes on the basis of the previous considerations.

The lymph nodes burden of Americium could be theoretically classified in the group of more reliable measurements because it is characterized by the same qualities and drawbacks of the lung retention of Americium. However care should be taken in the practical situation when measurements are compared to model's predictions. In fact the evaluation of lymph nodes burden is based on the use of specific efficiency factors for lymph nodes located in the mediastinum, according to the morphometric characteristics of the LLNL phantom used for the calibration. This configuration is slightly different from the real morphology of respiratory tract because lymphatic tissues are spread all over the thoracic region. Furthermore ICRP respiratory tract model includes general compartments to represent the draining action carried out by all the lymphatic tissues in the thoracic region and not only by the mediastinal

lymph nodes, as in the LLNL phantom. For such reasons the results for the measurements of Americium burden in mediastinal lymph nodes can be only partially compared to the model's predictions.

According to the previous classification, the priority goal in dealing with all the available measurements was to fit the group of more reliable measurements (urinary excretion of Plutonium and the lung burden of Americium). Particular care was taken in modelling Plutonium urinary excretion, according to the specific aim at the basis of present work. On the basis of this first group of measurements the main assumptions about the conditions of exposure were set and the intakes were evaluated. The fits to the second group of less reliable measurements were assigned a lower priority and they were used just to get an idea about the general validity of the assumptions based on the more reliable measurements even for this second group of data.

### 3.2.3 ANALYSIS OF THE SET OF RELIABLE MEASUREMENTS

An inhalation of a polydisperse aerosol with 10  $\mu\text{m}$  AMAD was assumed with standard physical characteristics (geometric standard deviation 2.5, particle density 3  $\text{gcm}^{-3}$ , shape factor 1.5). This value is approximately the geometric mean of the extreme diameters (from 3 to 40  $\mu\text{m}$ ) of Plutonium containing particles, as evaluated with SEM exposure and qualitative X-ray analysis of dust samples by the laboratory where the accident occurred [123, 124].

Different initial hypotheses can be assumed for the absorption type of the inhaled compound. According to ICRP [52] two absorption type for Plutonium are possible for a contamination event in working areas: Moderate and Slow (type M and S). In ICRP [173] Fast (F) absorption type are even considered, but only for member of the population and, therefore, this type of absorption is here not considered. Furthermore, the fast absorption rate into the blood is not coherent with the slow urinary excretion rate of Plutonium, as suggested by a first look at the urinary excretion measurements. For Americium only M absorption type is considered by ICRP for occupational exposition. However, the lung content of Americium is due to not only the amount directly inhaled, but also to the ingrowth from  $^{241}\text{Pu}$  decay. Therefore, if S type absorption is assumed for Plutonium, absorption rate into the blood slower than default M type could be reasonably assumed for Americium from  $^{241}\text{Pu}$  decay.

On the basis of these considerations the only default absorption type (M) provided by ICRP was assumed for Americium directly inhaled into the lung. The reference biokinetic model provided by ICRP [2] was assumed. For Americium ingrowth from Plutonium two absorption types can be initially assumed. Therefore different approaches were considered for this fraction of Americium.

On a first approach the same absorption type of the father Plutonium radionuclide can be assumed, according to a common default assumption of ICRP. This means that Americium is firmly bound in the inhaled compound of Plutonium and therefore it shows the same biokinetic behaviour. Under such hypotheses the same absorption types (S or M) are assumed for both Plutonium and Americium (scenario 1 and scenario 2 in Table 3.2.1, respectively). Consequently Plutonium systemic model, as previously obtained with the optimization procedures (Model-b), was assumed for Americium too.

On the second approach an absorption type for Americium different from that one for the father Plutonium was considered. Therefore when the S absorption type is assumed for Plutonium, M absorption type is assumed for Americium (scenario 3 in Table 3.2.1). This means that Americium, after its formation following  $^{241}\text{Pu}$  decay, behaves according to its

own biokinetic. Therefore Americium own systemic model, as provided by ICRP [2], was assumed in this scenario of contamination.

**Table 3.2.1** Different possible assumptions for the absorption types and systemic models for Plutonium and Americium (directly inhaled and due to the ingrowth from  $^{241}\text{Pu}$  decay).

Radionuclide	Scenario 1		Scenario 2		Scenario 3	
	Type	Model	Type	Model	Type	Model
Pu, all the isotopes	S	Model-b	M	Model-b	S	Model-b
$^{241}\text{Am}$ from $^{241}\text{Pu}$ decay	S	Model-b	M	Model-b	M	ICRP 67
$^{241}\text{Am}$ directly inhaled	M	ICRP 67	M	ICRP 67	M	ICRP 67

Predictions of Americium activity in lungs were calculated for each of the considered scenarios of Table 3.2.1. On the basis of the experimental data for Americium activity retained in lungs, intakes were evaluated first. The intake was evaluated by minimizing the value of the F target function, written according to equation 3.1.7, where the model's predictions for  $e_u(t)$  are now substituted by the Americium activity retained in lungs per unit of intake and the experimental values are given now by the measurements of Americium in lungs. The evaluated intakes were then multiplied by the model's predictions of Americium retained in lung per unit of intake. The resulting values are presented with the available measurements for comparison purposes in Figure 3.2.1, Figure 3.2.2 and Figure 3.2.3 for the scenarios of contamination number 1, 2 and 3, respectively (Table 3.2.1). In the same figures the single contributions to Americium burden in lung (Americium directly inhaled and from  $^{241}\text{Pu}$  decay) are also plotted.

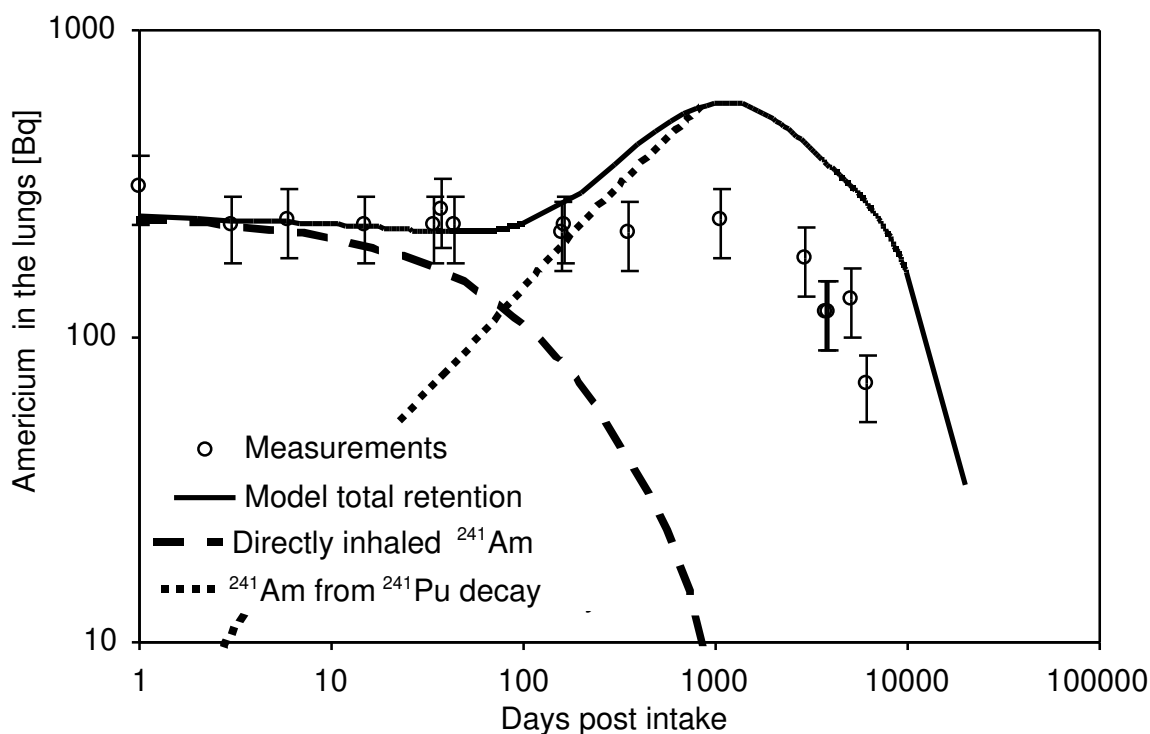


**Figure 3.2.1** Measurements and model predictions for Americium activity retained in lungs for the scenario 1 (see Table 3.2.1).

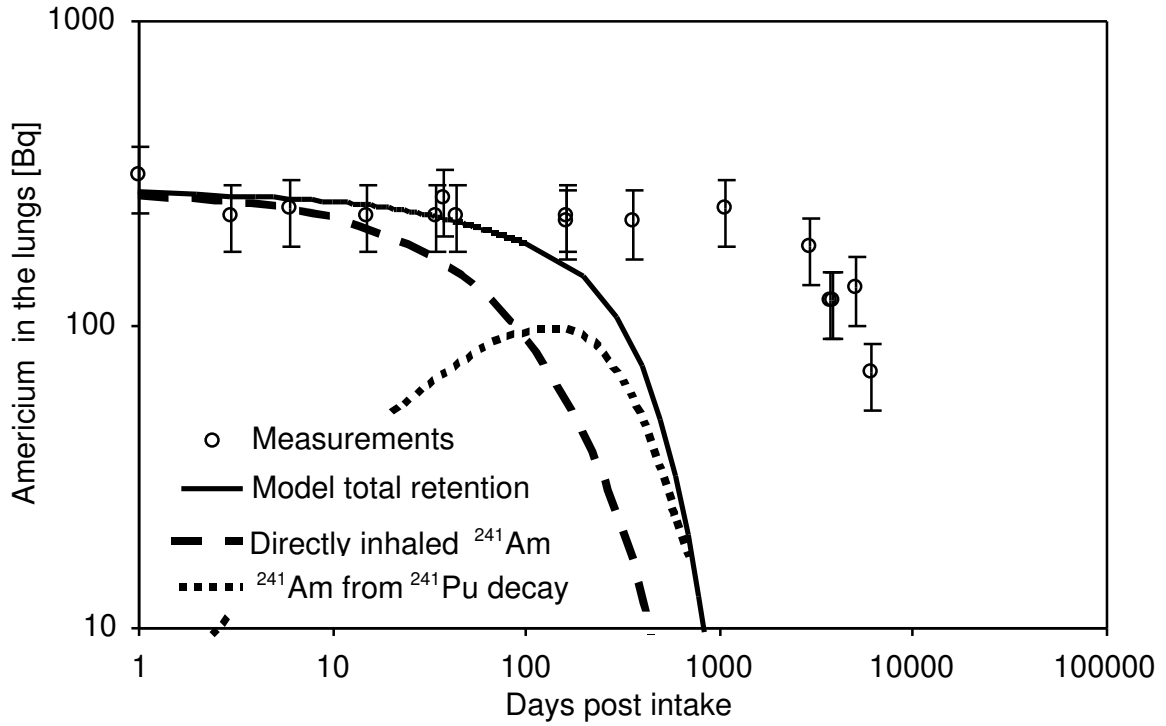


**Figure 3.2.2** Measurements and model predictions for Americium activity retained in lungs for the scenario 2 (see Table 3.2.1).

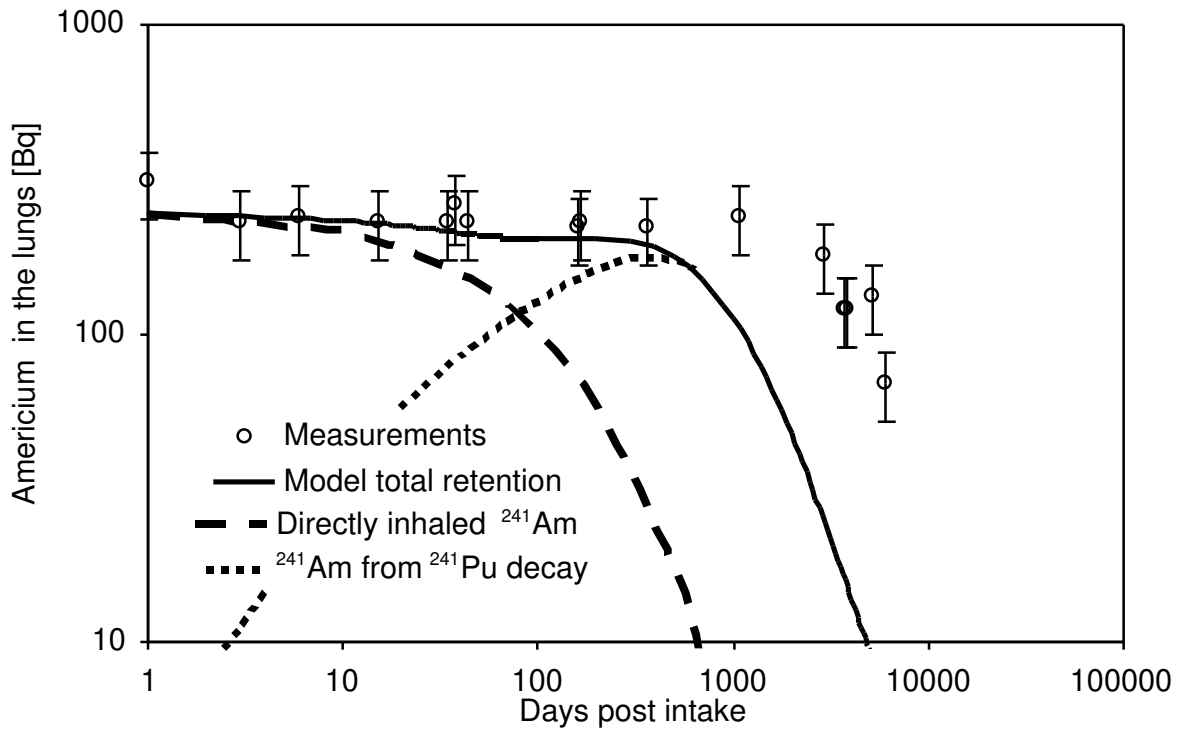


**Figure 3.2.3** Measurements and model predictions for Americium activity retained in lungs for the Scenario 3 (see Table 3.2.1).

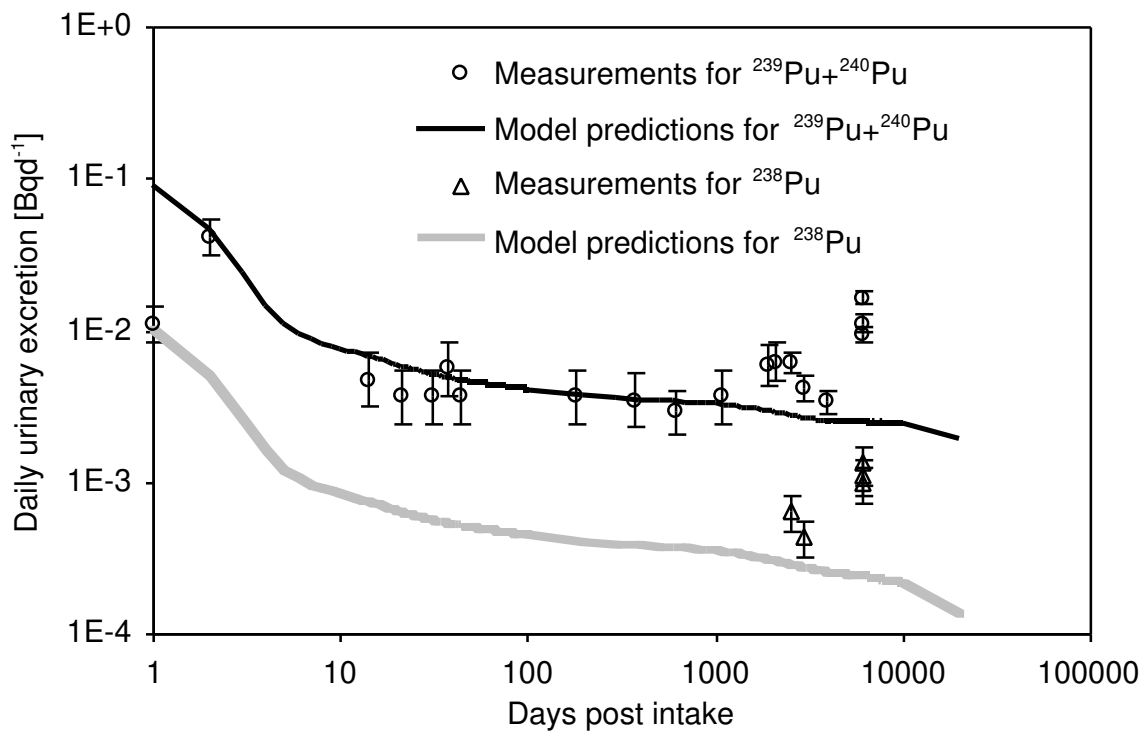


**Figure 3.2.4** Measurements and model predictions for Plutonium activity excreted in urine for the Scenario 1 of contamination (see Table 3.2.1).

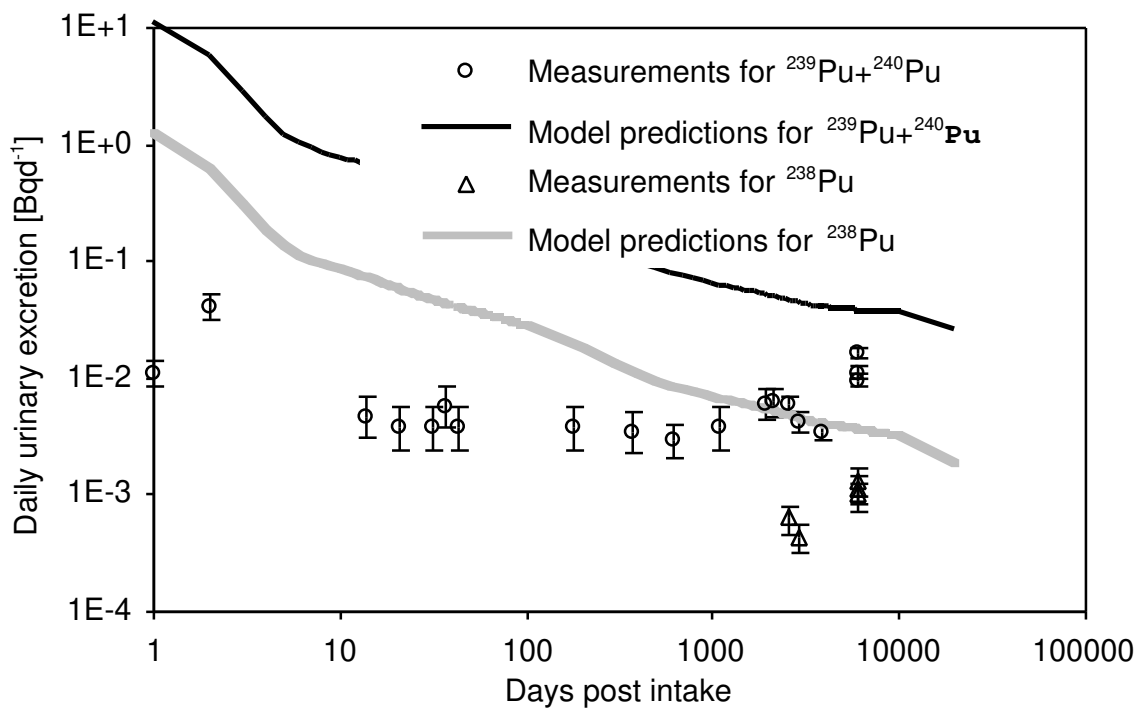


**Figure 3.2.5** Measurements and model predictions for Plutonium activity excreted in urine for the Scenario 2 of contamination (see Table 3.2.1).



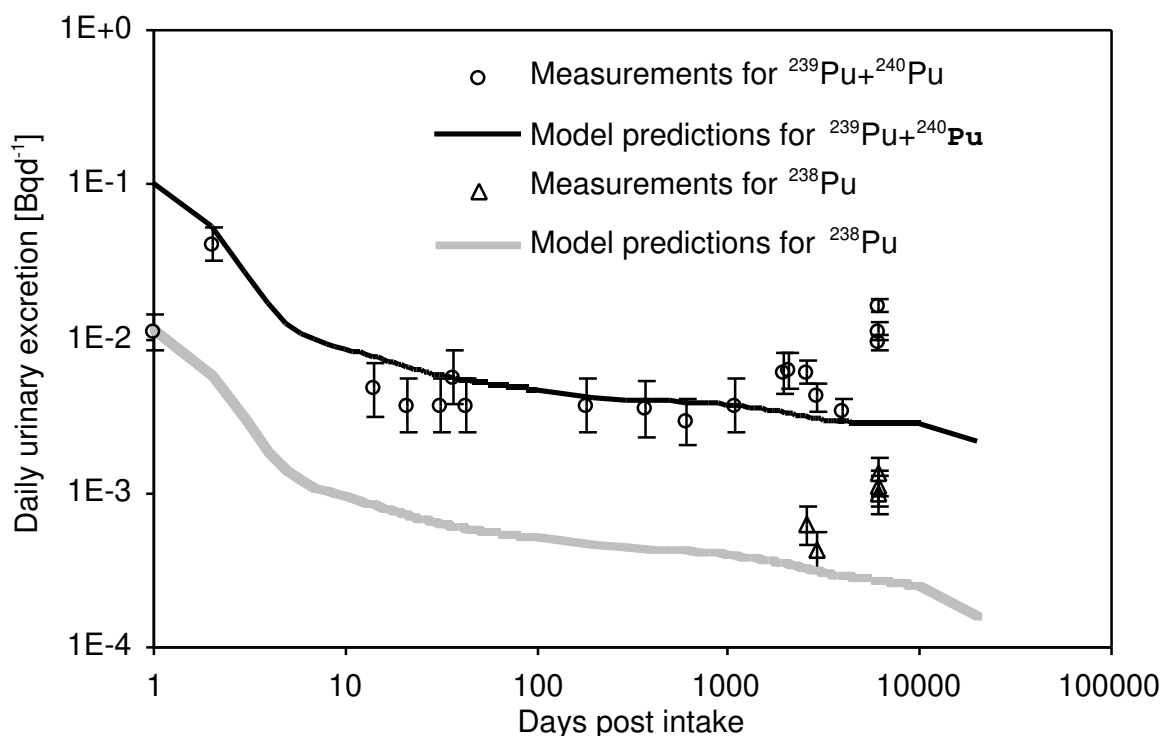


**Figure 3.2.6** Measurements and model predictions for Americium activity excreted in urine for the Scenario 3 of contamination (see Table 3.2.1).

Model's predictions for the urinary excretion of Plutonium were also evaluated for the same previous scenarios. The intakes calculated on the basis of the Americium activity retained in the lungs were multiplied by the model's predictions for the urinary excretion per unit of intake ( $e_u(t)$ ). The resulting values are presented with the available measurements for comparison purposes in Figure 3.2.4, Figure 3.2.5 and Figure 3.2.6 for the scenarios of contamination number 1, 2 and 3, respectively (Table 3.2.1).

Model's predictions for Americium in the lungs and the urinary excretion of Plutonium clearly point out that the basic assumption characterizing the scenario 2 of the contamination (absorption type M for Plutonium) is not realistic. The predicted Americium retention in lungs considerably underestimates the experimental data already after 100 days post intake (Figure 3.2.2). Furthermore the intake evaluated from Americium lung retention data at short time (for which model's predictions are still good) determine a model's urinary excretion of Plutonium in disagreement with the relating experimental findings (Figure 3.2.5). Therefore such scenario of contamination was not considered anymore and all the attention was then focalised on the scenarios 1 and 3.

From the plots relating to the Americium burden in the lungs it can be pointed out that the retained activity at short time (up to about 100 days post intake) is mainly due to directly inhaled Americium. On the contrary, at long time, the activity in lungs is mainly due to the Americium ingrowth from  $^{241}\text{Pu}$  decay. For both the scenarios 1 and 3 model's predictions for the Americium lung retention at short time and the urinary excretion of Plutonium up to 2,000 days post intake fit the experimental findings. Therefore the assumptions on the absorption type for the Plutonium (type S) and for the Americium directly inhaled (type M), common to both scenarios, seems to be appropriate. It should be pointed out that only the Plutonium

excretion at long time (after 2,000 days post intake) predicted by the model still underestimates the experimental results. In this time range the subject's excretion is characterized by the enhancement that made this case a particularly interesting contamination event.

The Americium burden in lungs at long time, due to the  $^{241}\text{Pu}$  decay, overestimates the experimental findings in the scenario 1 (up to a factor 4) and underestimates them in the scenario 3 (by about a factor 12). Therefore such fraction of Americium seems to behave in the respiratory tract with an absorption type ranging from the type S (the absorption type for the father Plutonium in the scenario 1) and the type M (the reference absorption type for Americium adopted in the scenario 3). In order to improve model's predictions of Americium lung retention, the absorption parameter determining the Americium retention in lungs at long time ( $s_l$ ) was varied in the range from  $0.0001 \text{ d}^{-1}$  (the reference value for absorption type S) to  $0.005 \text{ d}^{-1}$  (the reference value for absorption type M). It was found that model's predictions for the Americium burden in lungs significantly improve their agreement with the experimental findings at long time if a value  $0.001 \text{ d}^{-1}$  is assumed for  $s_l$  (Figure 3.2.7). The other absorption parameters ( $s_p$  and  $s_{pt}$ ) were set to the default values for the absorption type S.

Such modification may have a reasonable physiological explanation:

- The Americium just formed after Plutonium decay behaves at short time in the respiratory tract as the father (Plutonium default values of  $s_p$  and  $s_{pt}$  for the absorption type S are therefore assumed);
- At longer time Americium own specific metabolic characteristics gets more and more evident (therefore the value of  $s_l$  has reasonably a value between the default values for S and M absorption types).

Therefore such approach can be considered more realistic in comparison to the assumption of an Americium ingrowth with all the same absorption parameters of the father Plutonium (as usually assumed by ICRP and here in the scenario 1) or with its own default absorption characteristics (as in case of a direct inhalation).

On the basis of the previous assumed value of  $s_l$  for Americium ingrowth from  $^{241}\text{Pu}$  decay, the intake of  $^{241}\text{Am}$  directly inhaled was evaluated as 9 kBq. The intakes of all the other involved radionuclides are easily evaluated by means of their ratio at the moment of the intake. The relating value of the F target function calculated on lung measurements is 50% and 1% of the value calculated in case of the scenarios 1 and 3 respectively. This quantitatively points out the improvement of the model's predictions of Americium lung retention when the absorption parameters are changed according to the previous assumptions.

The model's predictions for the urinary excretion of Plutonium are equal to those ones evaluated in case of the scenario 1 (Figure 3.2.4) because only the default  $s_l$  absorption parameter for Americium ingrowth was modified and no parameter relating to Plutonium was modified.

Model's predictions for the lymph nodes burden of Americium were compared to few available measurements too and a good agreement was found even for this set of data.

At conclusion of the analysis of the most reliable measurements for modelling and testing purposes, a good agreement of model's predictions with the experimental data was obtained. Furthermore the considered modification (the change of the  $s_l$  absorption parameter for Americium ingrowth from Plutonium decay) seems to be reasonably acceptable from a physiological point of view too. However the enhancement of Plutonium urinary excretion at

long time is not yet described by the considered assumption in the previous model. A specific paragraph is dedicated to this issue (see paragraph 3.2.5).

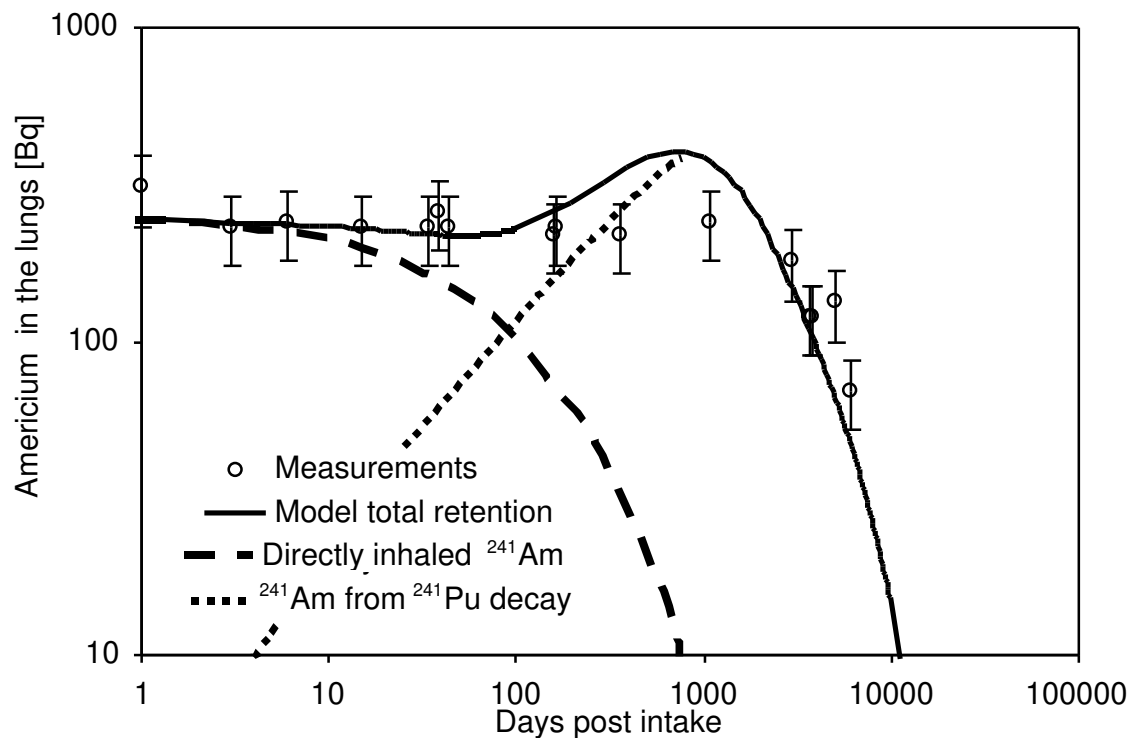


**Figure 3.2.7** Measurements and model predictions for Americium activity retained in lungs based on  $s_l = 0.001 d^{-1}$  for the lung absorption of <sup>241</sup>Am ingrowth from <sup>241</sup>Pu decay.

It should be pointed out also that according to the approach followed by some participants to the IAEA intercomparison exercise, where this case of contamination was already proposed [123], a mixture of soluble (M) and insoluble compounds (S) could be also considered. In the frame of the present work it was found that an inhaled compound formed by about 30% of Plutonium of S type (as in Scenario 1) and 70% of M type (as in Scenario 2) determine a retention of Americium in the lungs in a very good agreement with the experimental findings. Unfortunately it was also observed that the consequent urinary excretion of Plutonium would not agree with the available measurements: as the excreted Plutonium is mainly given (about 70%) by the inhaled compound of type M, the urinary excretion curve will not significantly differ from the plot in Figure 3.2.5, relating to scenario 2.

### 3.2.4 ANALYSIS OF THE SET OF LESS RELIABLE MEASUREMENTS

By adopting the assumptions based on the lung burden of Americium and the urinary excretion of Plutonium, the data set formed by the less reliable groups of measurements was also analyzed.

Among the less reliable measurements a good agreement of Plutonium fecal excretion at long time after exposure was achieved (Figure 3.2.8). Significant discrepancies (an order of magnitude) were pointed out only for the samples collected between 10 and 40 days post intake. Model's predictions for the Plutonium retention in blood significantly deviate from the available measurements: they overestimates the measurements by about an order of magnitude. However, only two measurements, relating to  $^{238}\text{Pu}$  and  $^{239}\text{Pu}+^{240}\text{Pu}$  activity, are available for such kind of bioassays. They were carried out just in occasion of the present work and no other measurement is available from the previous measurements campaigns on the same subject. Furthermore only one of the available measurements for the blood content of Plutonium resulted to be greater than the MDA of the detecting system. Owing to these issues no further consideration can be reasonably done on such kind of bioassay.

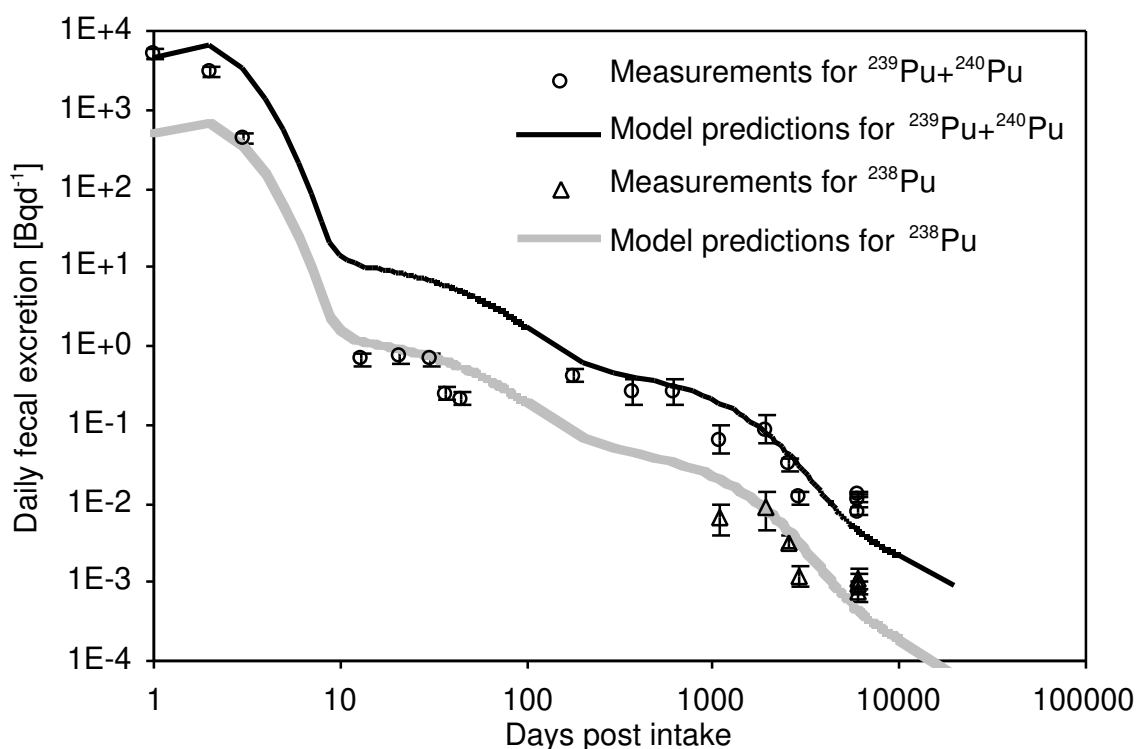


**Figure 3.2.8** Measurements and model predictions for Americium activity excreted in feces on the basis of the model developed on the most reliable set of data.

In order to analyze the measurements relating Americium activity in organs (liver and bone) and bioassays (urine, feces and blood) further considerations about Americium systemic biokinetics should be done. The analysis of the lung burden of Americium pointed out that the biokinetic of Americium ingrowth from Plutonium decay can be modelled with a value of the absorption parameter ( $s_i$ ) between the default values for the father Plutonium (S type) and the Americium (M type).

According to this consideration the biokinetics of Americium ingrowth in the systemic phase of the contamination after the absorption from the respiratory tract into blood should be described by a “hybrid” systemic model between the systemic model of the father (the optimized model here developed) and Americium own systemic model (as provided by ICRP). Such issue strictly interests the systemic model adopted for Americium ingrowth from Plutonium decay. Therefore it has no effect on the biokinetics of Plutonium in the respiratory tract and in the systemic phase of the contamination and, in conclusion, on its urinary

excretion that is one of the main issue of the present work. For such reasons it was not more analyzed here. It should be just mentioned that two extreme approaches were briefly considered for the systemic behaviour of Americium ingrowth: one based on the same systemic behaviour of Plutonium and a second one on Americium own systemic model. The results showed that in the first case a pretty good agreement of model's predictions for the Americium fecal excretion was found; in the second case the model's predictions don't fit anymore the measurements for this bioassay but significantly improve their agreement with the measurements for Americium blood content. Similar effects were observed if bone and liver burden of Americium are considered. This seems to confirm the idea that the Americium ingrowth is characterized by a biokinetics that is in between the two possible extreme assumptions, i.e. its own biokinetics and the father Plutonium biokinetics.

### 3.2.5 PLUTONIUM URINARY EXCRETION ENHANCEMENT

In the frame of the analysis of the reliable measurements group, a deviation of model's predictions from experimental findings for the urinary excretion of Plutonium was pointed out after 2,000 days post intake. In fact the urinary excretion of the studied subject is characterized by a continuous enhancement of the urinary excretion of Plutonium that is getting more and more significant with time. This phenomenon was already observed by previous measurements campaigns and it is confirmed by the last measurements, carried out at about 6,000 days post intake in occasion of the present work (Table 2.4.1). The urinary excretion of Plutonium for the studied subject resulted to be higher by up to about a factor 6 and by about an average factor 3.5 in comparison to the urinary excretion observed at about 1,000 days post intake.

A similar excretion enhancement seems to be present, at a lesser extent, even for the Plutonium fecal excretion (Figure 3.2.8).

Such enhancement of the urinary excretion of Plutonium was recently also observed in other subjects [122] too that were accidentally contaminated long time ago (ten years ago or more). However the enhancement of Plutonium urinary excretion observed in those subjects is less significant than what was observed for the subject investigated here.

#### 3.2.5.1 *The effect of the uncertainty of the transfer rates*

The hypothesis of further internal contamination events that could explain the enhancement of Plutonium urinary excretion can be neglected on the basis of the typology of working activity in which the subject was engaged after the main contamination event occurred in 1983. Such enhancement can't be described by the available biokinetic models for the Plutonium metabolism in humans. According to the optimized model (Model-b), that can be reasonably considered now the most recent updated model for Plutonium biokinetics, the urinary excretion of Plutonium from 1000 days to 6000 days post intake should decrease by a factor 1.5. ICRP 67 model for Plutonium metabolism would predict even a more significant decrease (a factor 2.6) in the same time period, therefore more in disagreement with the experimental findings that, on the contrary, pointed out for this subject an enhancement by an average factor 3.5.

The biokinetic model developed here, as all the biokinetic models generally used in radiation protection dosimetry, describe the metabolism of a radionuclide for a standard subject, representing the average of the morphometric and physiological characteristics of the

subjects of a population of healthy adult men. The possible deviation of model's predictions for a certain quantity (as the activity in bioassays) from the experimental findings could be attributed to individual parameters that deviate from the default values used for a general standard subject. In the paragraph 3.1.5.4 the uncertainty for the urinary excretion of Plutonium due to transfer rate values varying according to a certain distribution was investigated. The variation of Plutonium urinary excretion due to possible individual variations of biokinetic parameters from the default values for a standard subject were evaluated (see Figure 3.1.10 and Figure 3.1.13).

The methodology and the results obtained in the uncertainty analysis carried out for the optimized model were here used in order to analyze the enhancement of Plutonium urinary excretion observed for the considered subject.

The uncertainty analysis pointed out that the variability of the urinary excretion measurements observed for the subjects excretion available in literature can be realistically modelled by adopting model's systemic transfer rates with a lognormal distribution centred on the default value with a geometric standard deviation  $GSD = 1.75$ . On the basis of this result and using the indications available in literature for the uncertainty of the parameters of the respiratory tract model [57] the uncertainty of the urinary excretion of Plutonium was calculated. This is the basic methodology used for plotting the curves in Figure 3.1.13 for in case of conditions of standard exposition conditions of exposure. The curves specifically evaluated for the exposure conditions of the here-investigated subject are given in Figure 3.2.9 together with the measurements for the urinary excretion of  $^{239}\text{Pu}+^{240}\text{Pu}$ .

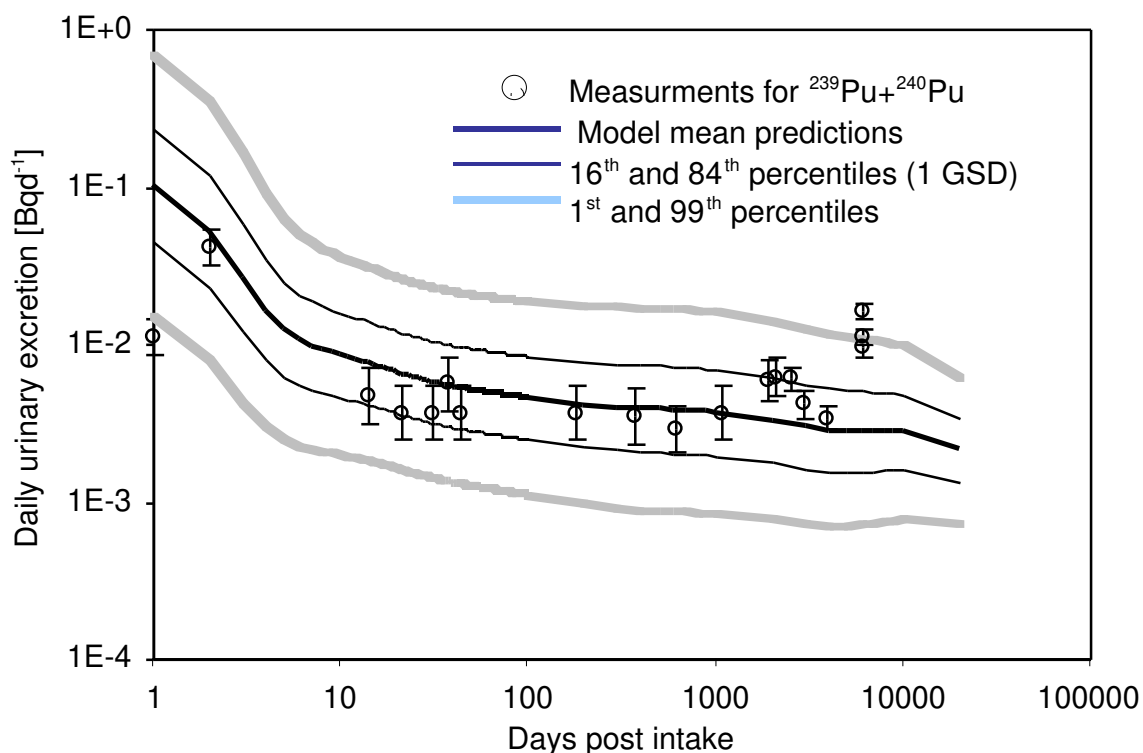


**Figure 3.2.9** Comparison of the mean values and range of the daily percentage urinary excretion of Plutonium predicted by the Model-b after inhalation of a compound type S, AMAD =  $10\mu\text{m}$  with measurements of the urinary excretion  $^{239}\text{Pu}+^{240}\text{Pu}$  for the investigated subject.

The comparison of model's predictions with the available measurements points out that the experimental data for the urinary excretion of Plutonium are fitted quite well, up 1000 days post intake, by the central curve representing the mean Plutonium urinary excretion for a population of subjects characterized by different Plutonium biokinetics. At intermediate time (about 2,000 days post intake) the measurements are characterized by an enhancement of the excretion that is at the limit of the confidence interval for the 16<sup>th</sup> and 84<sup>th</sup> percentiles. Finally, at 6,000 days post intake, the measurements for the urinary excretion of Plutonium are on average out of the confidence interval for the 16<sup>th</sup> and 84<sup>th</sup> percentiles and at the limits of the confidence interval for the 1<sup>st</sup> and 99<sup>th</sup> percentiles.

This seems to point out that it can be still theoretically possible to find a combination of transfer rates, in the range of the values representing possible inter-subject differences, that can describe the observed trend of Plutonium urinary excretion measurements observed for the subject here analyzed.

### 3.2.5.2 *The research of the best fitting individual parameters*

The search of which transfer rates and the evaluation of those values that could explain the Plutonium urinary excretion of the investigated subject was performed by complying with a main constraint: only transfer rates values in the range that turned out to be representative for inter-subject biokinetic differences were considered. In fact the assumption of a particularly great, or small, value for certain specific transfer rates could easily generate almost whatever desired trend for the activity distribution of Plutonium in the compartments of the model. However if the assumed value of the transfer rate is out of the realistic range of values expected considering the possible differences in the individual biokinetics, it should be concluded that the model can not describe the radionuclide metabolism in this specific subject. Therefore extensive modification of the model should be considered.

For the purpose of the present paragraph the results of the sensitivity analysis for Plutonium biokinetics performed in the paragraph 3.1.5.3 were extensively applied.

The transfer rates determining Plutonium urinary excretion specifically at long time with a scarce importance for the excretion at shorter time were firstly considered because they are the best candidates for simulating a long-term enhancement of Plutonium urinary excretion. On the basis of the sensitivity analysis performed for the systemic and the respiratory tract transfer rates, type S, (Figure 3.1.22 and Figure 3.1.26), the leading parameters are:

- for the systemic model: The transfer from the Liver 2 compartment; the transfer from blood to the ST2 soft tissue compartment; the cortical remodelling rate;
- for the respiratory tract model: The clearance from the alveolar-interstitial compartments.

These transfer rates were modified on the basis of the results of the sensitivity analysis in order to generate always an enhancement of the urinary excretion. Therefore the transfer rates for which an increase of the value causes an enhancement of Plutonium excretion (i.e. with a positive sensitivity coefficient  $S_i$ ) were increased, whereas those for which an increase of the value causes a diminution of Plutonium excretion (i.e. with a negative sensitivity coefficient  $S_i$ ) were decreased.

Quantitatively the modification of the value of such transfer rates was carried out respecting the constraint presented at the beginning of the paragraph. The systemic transfer rates were increased or decreased by multiplying or dividing them by a factor 3. As the uncertainty analysis showed that the variation range of the systemic transfer rates can be realistically described by a lognormal distribution with a GSD = 1.75, the variation by a factor

3 is equivalent to assume a value for a certain transfer rate within the interval of the 1<sup>st</sup> - 99<sup>th</sup> percentile.

The transfer rates of the respiratory tract model were varied on the basis of the factor suggested by the ICRP 66 [57]. Values relating to the extremes of the accepted range of variation were assumed. However a decrease of the transfer rates describing the clearance of Plutonium from the alveolar-interstitial compartments would have modified not only the urinary excretion of Plutonium (determining the observed enhancement), but also the lung retention of Americium from Plutonium decay. In the previous paragraph a good fitting was already achieved for this group of measurements. Therefore the  $s_i$  parameter for Americium ingrowth (previously set to 0.001 d<sup>-1</sup> just on the basis of the <sup>241</sup>Am lung burden measurements) was re-evaluated in order that the decrease of the Plutonium clearance rates from the alveolar interstitial did not significantly change the achieved good fitting of the measurements for the lung burden of Americium.

It turned out 0.0025 d<sup>-1</sup> as best value of the absorption parameter  $s_i$  for Americium ingrowth if the long term measurements for Plutonium urinary excretion, characterized by the observed enhancement, are also considered.

The calculated urinary excretion of Plutonium is presented in Figure 3.2.10.

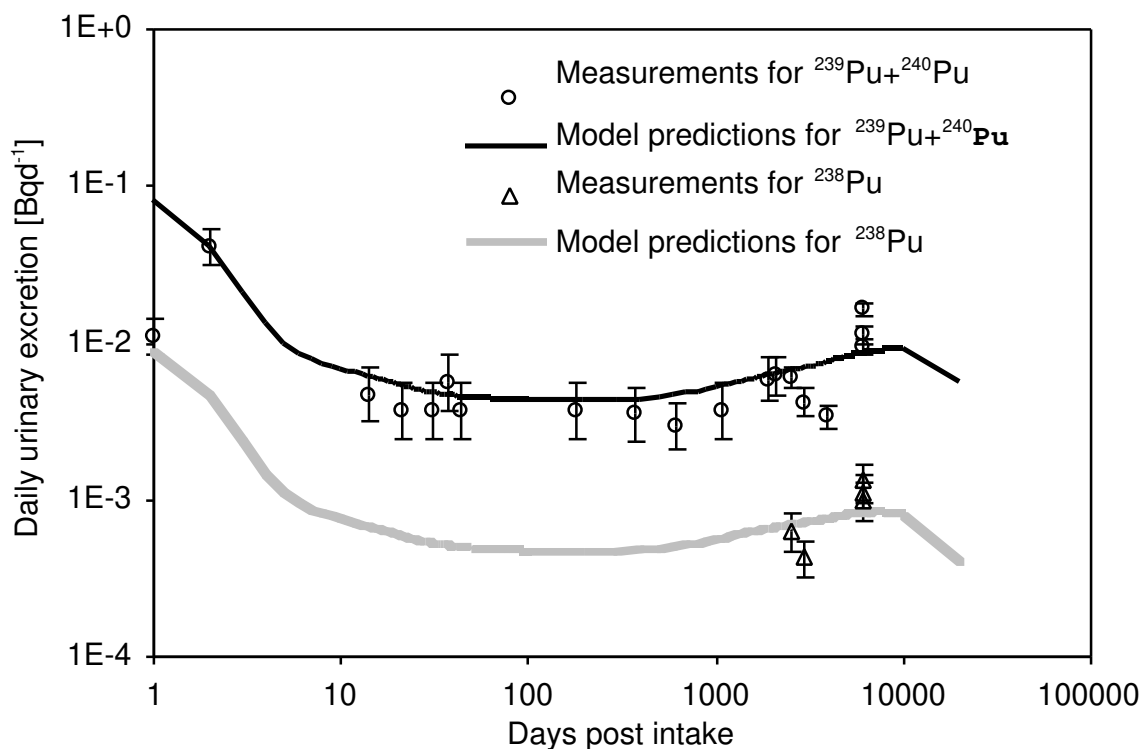


**Figure 3.2.10** Measurements and model predictions for Americium activity excreted in urine using individual parameters for the investigated subjects.

The relating model's predictions for lung burden of Americium are presented in Figure 3.2.11.



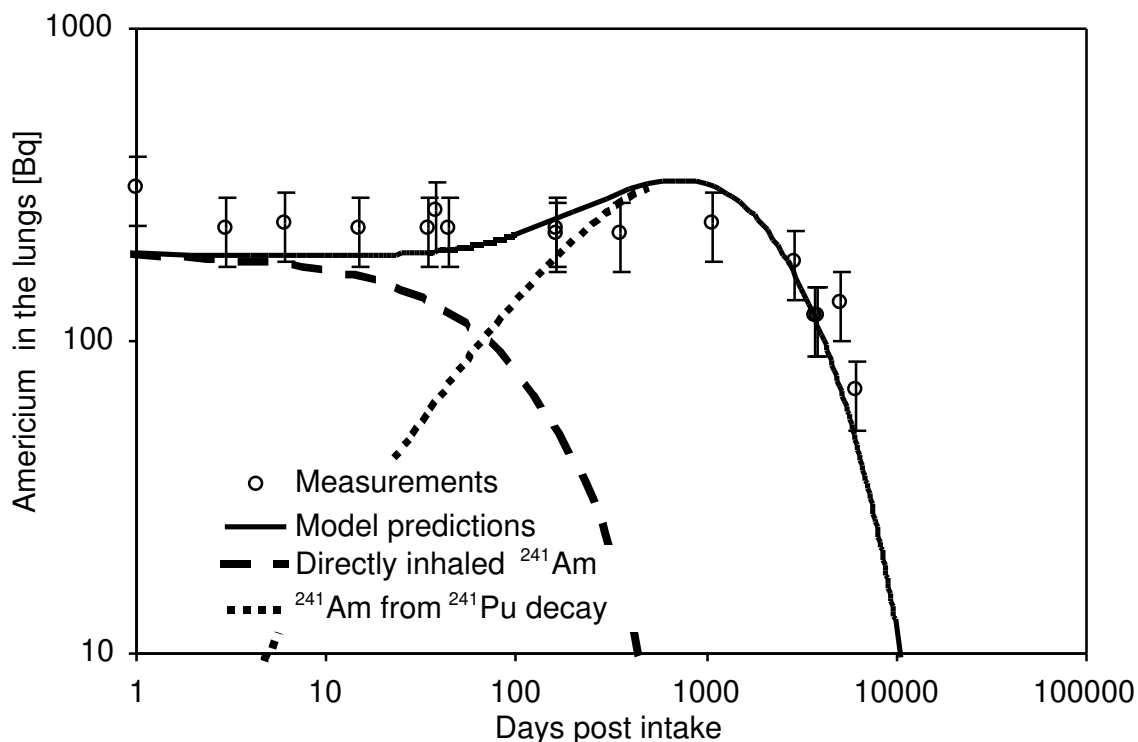


**Figure 3.2.11** Measurements and model predictions for Americium activity retained in lungs using individual parameters for the investigated subjects.

A very good agreement between model's predictions and measurements of the urinary excretion of Plutonium was found. Particularly at long time the model predicts an enhancement of the urinary excretion of Plutonium that seems to be comparable with the enhancement experimentally observed. A good agreement of model's predictions for the lung burden of Americium with the experimental findings was still kept.

All the measurements previously classified in the most reliable groups of data for testing and modelling purpose are now well fitted over all the time of observation of the subject.

On the basis of the previous last assumptions the intake of  $^{241}\text{Am}$  directly inhaled was evaluated as 7 kBq. The intakes of all the other involved radionuclides were calculated by means of the their ratio at the moment of the intake (second column of Table 3.2.2).

It should be pointed out that experimental data were fitted by adopting assumptions always oriented to develop each time a realistic and physiologically based model. In this frame, as already underlined, the factors, by which the transfer rates were modified in order to adapt the model to this specific subject, were chosen in the range of values as estimated on the basis of the uncertainty analysis. Furthermore all the assumptions were kept very simple and somewhat "rough" as much as it was possible: for example only the transfer rates determining Plutonium urinary excretion mainly at long time were considered in order to model the observed enhancement of urinary excretion. Other combination of transfer rate parameters could have been considered too. For example even parameters significantly influencing the urinary excretion not only at long time could be used for such purpose, by compensating their effect at short time with other parameter with opposite effect in the same time period. This suggests that different other approaches, even if more complicated but always acceptable in the frame of likely inter-individual differences, could be possible in order to describe the enhancement of Plutonium urinary excretion at long time.

In a preliminary analysis of the present case of contamination [174], when not all the results from sensitivity and uncertainty analysis were available, another approach to fit the data set of the most reliable measurements and to explain the long-term enhancement of Plutonium urinary excretion was followed. A good agreement of Americium burden in lungs with experimental findings was achieved by adopting the scenario 1 but with increased values of the clearance parameters from the alveolar-interstitial regions. As such modification determines a decrease of urinary excretion of Plutonium, as pointed out now by the sensitivity analysis, the adoption of transfer rates time depending and with values out of a realistically acceptable range, as suggested by uncertainty analysis, was necessary. Therefore the methodology presented here seems to describe the phenomenon of the urinary excretion enhancement in a simpler way on the basis of all the information provided by the complete sensitivity and uncertainty analyses carried out in the previous paragraphs and in the frame of acceptable inter-individual differences of Plutonium biokinetics.

### 3.2.6 DOSE ASSESSMENTS

Committed effective doses for the studied case of contamination were eventually calculated. The intakes for all the inhaled radionuclides were evaluated by means of their ratio at the moment of the intake with the  $^{241}\text{Am}$  directly inhaled, for which the intake was previously calculated (7 kBq). It was necessary to calculate new E(50) coefficients for two main reasons:

- The scenario of contamination differs from the usual standard conditions, as an aerosol with AMAD = 10  $\mu\text{m}$  was assumed;
- The systemic model was modified from the optimized model Model-b, as specific transfer rate parameters were assumed for the studied subject;
- The respiratory tract model was modified as a different values of Plutonium clearance rates from alveolar interstitial and of  $s_l$  for Americium ingrowth were assumed.

For these reasons the E(50) coefficients are different from the values provided for the optimized model with default transfer rates and for standard conditions of exposure (Table 3.1.17).

The results of the E(50) assessments are given in Table 3.2.2 together with the intakes and the E(50) coefficients for each radionuclide inhaled by the studied subject. A final total E(50) value of  $6.4 \cdot 10^{-1}$  Sv was calculated.

**Table 3.2.2** Intakes, E(50) coefficients and final E(50) values for each radionuclide inhaled by the studied subject. The contribution of  $^{241}\text{Am}$  from  $^{241}\text{Pu}$  decay is also included.

Radionuclide	Intake [Bq]	E(50) Coefficient [Sv/Bq]	E(50) [Sv]
$^{238}\text{Pu}$	$6.3 \cdot 10^3$	$7.0 \cdot 10^{-6}$	$4.4 \cdot 10^{-2}$
$^{239}\text{Pu}$	$3.9 \cdot 10^4$	$7.1 \cdot 10^{-6}$	$2.8 \cdot 10^{-1}$
$^{240}\text{Pu}$	$1.8 \cdot 10^4$	$7.1 \cdot 10^{-6}$	$1.3 \cdot 10^{-1}$
$^{241}\text{Pu}$	$5.3 \cdot 10^5$	$1.1 \cdot 10^{-7}$	$5.8 \cdot 10^{-2}$
$^{241}\text{Am}$	$7.0 \cdot 10^3$	$1.9 \cdot 10^{-5}$	$1.3 \cdot 10^{-1}$
Total			$6.4 \cdot 10^{-1}$

The optimized model (Model-b) derived from the ICRP 67 can describe the metabolism of Plutonium in humans providing realistic estimations of the urinary excretion of Plutonium. It avoids the assumptions that were part of ICRP model and that have not a clear physiological explanation. These assumptions were introduced by ICRP in order to correct the predictions for the long term urinary excretion, diverging from the available experimental data. Furthermore the optimized model predictions for Plutonium fecal excretion and blood burden are in a better agreement with the available data from experiments on humans than ICRP 67 model's predictions.

Furthermore, for the first time, it was implemented a recently developed model for Plutonium biokinetics in the skeleton: it was shown that this model provides a more realistic description of Plutonium biokinetics than the currently adopted ICRP skeleton model.

As urine bioassays is the most common technique used for monitoring the internal exposure to Plutonium for occupationally exposed workers, the optimized model predictions for the urinary excretion were tested on some experimental data sets from actual cases of contamination: the optimized model fits the considered data sets at least as well the ICRP 67 model, but without the necessity of adopting physiologically unrealistic assumptions.

The optimized model was eventually used in order to analyze a well documented case of contamination via inhalation from a mixture of Plutonium and Americium, characterized by a significant enhancement of Plutonium urinary excretion after 16 years post intake. The sensitivity analysis, carried out on the transfer rates of the optimized model and ICRP 66 respiratory tract model, pointed out the main parameters in determining the urinary excretion of Plutonium. The uncertainty analysis performed on such parameters allowed evaluating their range of variation that can be considered as due to the inter-subjectual differences in the Plutonium biokinetics. It turned out that no variation of a single parameter in the range of the values occurring in healthy subjects can alone determine the enhancement of Plutonium urinary excretion observed in the studied subject. Particularly the bone remodelling rates, considered as the ones of the main parameters for the biokinetics of Plutonium, were found to be not able to explain the observed enhancement of the urinary excretion.

However it was found that it is possible to describe the enhancement of Plutonium excretion by adopting specific-subject values for the group of parameters determining the urinary excretion of Plutonium at long term. The values were set in a way that they are always in the range of physiological variation, as estimated by means of the uncertainty analysis.

The enhancement of the urinary excretion of Plutonium for the studied subject can be consequently considered as due to a subject-specific Plutonium biokinetics, but still coherent with the possible variations estimated for the general population.

The present work was mainly oriented to the improvement of the available Plutonium biokinetic model and to the analysis of a particular case of contamination, but it should be pointed out that different by-products were obtained from such analyses:

- Analytical functions were developed in order to estimate the urinary excretion of Plutonium after inhalation and ingestion in common standard conditions of exposure without solving the whole system of differential equations mathematically describing the biokinetic compartmental model. Such functions, together with the calculated dose coefficients, allow implementing the present model in the easiest way in the routine monitoring of internal exposure to Plutonium;

- Executable files in a ‘user friendly’ format are available for the estimation of any further observable quantity other than the urinary excretion for standard conditions of exposure, as predicted by the above-mentioned analytical functions. These executable files easily allow any further research on the Plutonium biokinetics using the optimized model.
- Methodologies as the sensitivity and the uncertainty analysis, not so commonly used in the frame of the internal dosimetry studies, were widely applied. The complete sensitivity analysis performed on the optimized model has provided a deep knowledge about such model, enabling to perform any further studies in an easier and more efficient way. The uncertainty analysis provided an important indication about the range of variation of the transfer rates of Plutonium biokinetic models; up to now such information was available only in few cases (as for the ICRP 66 respiratory tract model) despite the increasing interest on the uncertainty of the parameters used in the biokinetic models [175, 176].

Furthermore the uncertainty analyses has provided the uncertainty associated to the excretion curves. This will allow estimating an intake with its own uncertainty. The same methodology developed here and applied for the excretion curves can be used to evaluate the uncertainty associated to the dose coefficients. This enables us to calculate the committed effective dose  $E(50)$ , as the intake multiplied by the dose coefficient, with an indication about the final uncertainty of the dose, that is not yet possible in the present ‘state of the art’ of the internal dosimetry. This issue is now under study and it will be the subject of further works.

# Annex

## Quantities used in Radiological Protection and Internal Dosimetry

The interaction of the ionizing radiations with the biological matter determine a release of energy that changes the physical characteristics of atoms and molecules and may thus sometimes damage cells and tissues. When a damage to cells occurs two effects are possible:

1. The cell can get unable to survive or to reproduce;
2. It can be able to live and reproduce but in a modified form.

These two different effects of the interaction of ionizing radiation have important consequences for the whole organism the cells belong to.

In the first case if the damage has caused a significant loss of cells the relating tissue will be likely characterized by a decrease of its own functions. The probability of causing such harm will be zero at small doses but will increase quickly above a certain level of dose, called dose threshold. Above such threshold the severity of the damage too will increase with the dose. This type of effect due to the ionizing radiation is currently called “deterministic”.

In the second case the clone produced by the cell, still alive but subdued to modification owing to the ionizing radiation interaction, may show malignant consequences, after a variable delay called latency period. The probability of a cancer increases with the dose but the severity of the cancer is not affected by the level of the dose. This kind of effect is called “stochastic”. It is currently assumed that the stochastic effect have no dose threshold and that the probability of occurrence is roughly proportional to the dose, particularly for doses smaller than the dose threshold for deterministic effect. In the particular case in which the damage occurred in a cell for the transmission of the genetic information, the effect may result in defects in the progeny of the exposed persons. This particular type of stochastic effect is called “hereditary”.

The system of radiation protection has the primary goal of preventing the occurrence of deterministic effects and of limiting the effect of the stochastic effects to an acceptable level; this means that professional activities with exposure to ionizing radiations should not be characterized by a risk higher than other professional activities currently considered “safe”.

In order to control the exposure to ionizing radiation quantities have been expressively designed and developed by ICRP for radiation protection purposes. The quantities were developed by ICRP since different years [58] up to a wide and deep review and update work presented in the Publication 60 [26].

The fundamental quantity in radiation protection is the absorbed dose  $D$  given by:

$$D = \frac{d\varepsilon}{dm}$$

*equation A.1*

where  $d\varepsilon$  is the energy of the ionizing radiations absorbed by the matter of mass  $dm$ . The SI unit for the absorbed dose is  $\text{J kg}^{-1}$  and its special name is “gray” (Gy). The absorbed dose is defined

to be specified at a point but it is normally used to express the average dose absorbed by an organ or a tissue:

$$D_T = \frac{\varepsilon_T}{m_T}$$

*equation A.2*

where  $\varepsilon_T$  is the average dose absorbed by the organ or tissue of  $m_T$ .

The probability of occurrence of stochastic effects depends linearly on the absorbed dose over the low dose range. The dose response relationship is not linear for deterministic effects; therefore the absorbed dose is not indicative of the severity of such effects, unless the dose is uniformly absorbed over the organ or tissue of interest.

However the probability of stochastic effects depends not only on the absorbed dose, but also on the type and energy of the radiation causing delivering the dose to the biological matter. In order to take into account of this effect radiation weighting factors,  $w_R$ , have been set up. The radiation weighting factors are given in Table A.1.

**Table A.1** Radiation weighting factors.

Type and energy range	Radiation weighting factor, $w_R$
Photons, all energies	1
Electrons and muons, all energies	1
Neutrons, energy $E_n < 10$ keV	5
$10 \text{ keV} \leq E_n < 100 \text{ keV}$	10
$100 \text{ keV} \leq E_n < 2 \text{ MeV}$	20
$2 \text{ MeV} \leq E_n < 20 \text{ MeV}$	10
$E_n \geq 20 \text{ MeV}$	5
Protons, other than recoil protons, energy $> 2 \text{ MeV}$	5
Alpha particles, fission fragments, heavy nuclei	20

The absorbed dose weighted by the radiation weighting factors is called equivalent dose and it is expressed as following:

$$H_T = \sum_R w_R D_{T,R}$$

*equation A.3*

where  $D_{T,R}$  is the absorbed dose averaged over a tissue or organ T due to the radiation R and  $w_R$  is the relating radiation weighting factor. The summation is introduced in order to account of a radiation field where particles of types and energy with different radiation weighting factors are

present. As the radiation weighting factors are dimensionless, the SI unit for the equivalent dose is still  $\text{J kg}^{-1}$ , as the absorbed dose. The special name for this quantity is “sievert” (Sv).

The probability of occurring stochastic effects relating to the absorption of a certain equivalent dose is however depending on the specific irradiated organ or tissue as well. Therefore the equivalent dose is corrected in order to obtain a quantity better correlated to the probability of stochastic effects. The factor by which the equivalent dose absorbed by an organ or a tissue T is weighted is called tissue weighting factor,  $w_T$ , and the resulting quantity is called effective dose, E, expressed as following:

$$E = \sum_T w_T H_T$$

*equation A.4*

The effective dose can be easily expressed in terms of absorbed dose:

$$E = \sum_T w_T H_T = \sum_T w_T \sum_R w_R D_{T,R}$$

*equation A.5*

As the tissue weighting factors are dimensionless, the SI unit for the effective dose is still  $\text{J kg}^{-1}$ , as the absorbed dose and its special name is still sievert (Sv).

The values of the tissue weighting factors represents the proportion of the detriment from stochastic effects resulting from tissues to the total detriment from stochastic effects when the body is irradiated uniformly. The tissue weighting factors recommended by ICRP are given in Table A.2.

**Table A.2** Tissue weighting factors.

Tissue or organs	Tissue weighting factor, $w_T$
Gonads	0.20
Bone marrow	0.12
Colon	0.12
Lung	0.12
Stomach	0.12
Bladder	0.05
Breast	0.05
Liver	0.05
Oesophagus	0.05
Thyroid	0.05
Bone surface	0.01
Skin	0.01
Remainder	0.05

The group of remainder organs is composed of the following ten additional tissues and organs: adrenals, brain, small intestine, upper large intestine, kidney, muscle, pancreas, spleen, thymus and uterus.

It should be pointed out that the absorbed dose is a dosimetric quantity that is generally used in physics to express the energy absorbed in the matter, not necessarily organs and tissues, owing to the interaction of ionizing radiation. The equivalent dose and the effective dose are typically radiation protection quantities because they are corrected by dimensionless factors, the radiation and tissue weighting factors, in order to reflect the probability of occurrence of stochastic effects.

The presented radiation protection quantities can be considered as an indicator of the risk associated to the exposition to ionizing radiations. In case of exposure from external radiation sources (external dosimetry) such quantities are evaluated by means of operational quantities connected to measurable quantities as the absorbed dose and fluxes. In case of internal dosimetry the radiation protection quantities are calculated by means of the biokinetics models. The dose is delivered to the organs and tissue for all the time the radionuclides is retained in the body, but for radiation protection purposes of professionally exposed workers a period of 50 years is considered. The radiation protection quantities used in internal dosimetry and calculated on a time period of 50 years are conventionally named as “committed”. The committed equivalent dose to a certain target organ T, due to the radionuclide retained in the organ source S, is expressed, according to ICRP methodology, as the product of two factors:

- The total number of transformations of the radionuclide in the source organ;
- the energy absorbed per grams in the target organ per transformation of the radionuclide in the source organ .

Therefore the committed equivalent dose is given by:

$$H(50)(T \leftarrow S) = k U_S \sum_R SEE(T \leftarrow S)_R$$

*equation A.6*

where:

$U_S$  is the number of nuclear transformations of the radionuclide in source organ S over a conventional period of 50 years;

$SEE(T \leftarrow S)_R$  is the specific effective energy, i.e. the energy, modified by the radiation weighting factor for radiation type R, absorbed in the target organ T from each transformation in the source organs S; it is expressed in  $\text{MeV g}^{-1}$ ;

k is a constant due to the units used for the previous quantities in order to get the committed equivalent dose expressed in sievert.

The number of transformations of the radionuclide  $U_S$  is calculated by means of the biokinetic models. The specific effective energy is calculated as:

$$SEE(T \leftarrow S)_R = \frac{Y_R E_R W_R AF(T \leftarrow S)_R}{m_T}$$

*equation A.7*

where:

$Y_R$  is the yield of the radiation type R per transformation of the radionuclide;

$E_R$  (in MeV) is the average or unique energy of the radiation R;

$AF(T \leftarrow S)_R$  is the fraction of energy absorbed in the target organ T per emission of radiation type R in the source organ S;



$w_R$  is the radiation weighting factor for the radiation type R;  
 $m_T$  (in grams) is the mass of the target organ T.

The total committed equivalent dose to the target organ T from all the source organs S, over which the introduced radionuclide is distributed, is given by the summation over source organs S:

$$H_T(50) = \sum_S H(50)(T \leftarrow S) = k \sum_S U_S \sum_R SEE(T \leftarrow S)_R = k \sum_S U_S \sum_R \frac{Y_R E_R w_R AF(T \leftarrow S)_R}{m_T}$$

*equation A.8*

The committed effective dose is calculated on the basis of the committed equivalent dose analogously to the expression in equation A.4:

$$E(50) = \sum_T w_T H_T(50)$$

*equation A.9*

The ICRP, in the Publication 61, provides an expression to evaluate the committed effective dose where a way to weight committed equivalent dose for the organs or tissues of the remainder group is also given:

$$E(50) = \sum_{T=1}^{12} w_T H_T(50) + w_{\text{remainder}} \frac{\sum_{T=13}^{22} m_T H_T(50)}{\sum_{T=13}^{22} m_T}$$

*equation A.10*

where T ranging from 1 to 12 represents the main organs of Table A.2, T ranging from 13 to 22 represents the ten remainder organs with tissue weighting factor  $w_{\text{remainder}} = 0.05$  and  $m_T$  is the respective mass.

In those exceptional cases in which a single one of the remainder tissues or organs receives an equivalent dose in excess of the highest dose absorbed by any of the twelve main organs or tissues for which a weighting factor is specified (Table A.2), half of  $w_{\text{remainder}}$  (0.025) must be applied to this tissue or organ and half of  $w_{\text{remainder}}$  to the average dose in the rest of the remainder organs group. Therefore in such case the committed effective dose must be calculated as:

$$E(50) = \sum_{T=1}^{12} w_T H_T(50) + 0.025 \frac{\sum_{T=13}^{22} m_T H_T(50) - m_{T^*} H_{T^*}(50)}{\sum_{T=13}^{22} m_T - m_{T^*}} + 0.025 H_{T^*}(50)$$

*equation A.11*

where  $T^*$  relates to the organ or tissue of the remainder group that has the highest committed equivalent dose in comparison to the main organs or tissues.



1. **Plutonium.** W. Koelzer (Editor), Forschungszentrum Karlsruhe, KfK Report 4516, 1989.
2. International Commission on Radiological Protection. **Age-dependent doses to members of the public from intake of radionuclides: Part 2 Ingestion dose coefficients.** ICRP Publication 67. Pergamon Press, Oxford; Ann. ICRP 23(3/4); 1993.
3. Milkukova, M. S., Gusev, N. I., Sentyurin, I. G. and Sklarenko, I. S. **Analytical chemistry of plutonium.** A. P. Vinogradov Editor, Ann Arbor-Humphrey Science Publishers, London, 1969.
4. Leonard, B.R. Jr. **Properties of plutonium isotopes.** In **Plutonium handbook – A guide to technology** Volume I. Edited by Wick, O.J., Gordon and Breach Science Publishers, New York, 1967.
5. Bruzzi, L., Cicognani, G. and Dominici, G. **Il ciclo del combustibile dei reattori nucleari.** CNEN (ENEA), Rome, 1981.
6. **McGraw-Hill Encyclopedia of Energy,** McGraw-Hill Inc., USA, 1981.
7. Pfennig, G., Klewe-Nebenius, H. and Seelmann-Eggebert, W. **Karlsruher Nuklidkarte,** Forschungszentrum Karlsruhe, 1998.
8. Pacific National Northwest Laboratory. **Hanford Internal Dosimetry Technical Basis Manual.** PNNL Manual, PNNL-MA-860, Richland, WA, 2000.
9. International Commission on Radiological Protection. **Radionuclide transformations: energy and intensity of emissions.** ICRP Publication 38. Pergamon Press, Oxford; Ann. ICRP 11–13; 1983.
10. Taylor, D. M. **Chemical and physical properties of plutonium.** In **Uranium, Plutonium, Transplutonic elements** H. C. Hodge, J. N. Stannard, J. B. Hirsch (Eds), Springer – Verlag, Heidelberg, 323-347, 1973.
11. International Commission on Radiological Protection. **The metabolism of plutonium and related elements.** ICRP Publication 48. Pergamon Press, Oxford; Ann. ICRP 16(2/3), 1986.
12. O’Boyle, N. C., Nicholson, G. P., Piper, T. J., Taylor, D. M., Williams, D.R. and Williams, G. **A review of Plutonium(IV) selective ligands.** Appl. Radiat. Isot., 48(2):183-200, 1997.
13. Taylor, D. M. **Environmental plutonium in humans.** Appl. Rad. Isot. 46(11):1245-1252, 1995.

14. Baskaran, M., Asbill S., Santschi, P., Davis, T., Brooks, J., Champ, M., Makeyev, V. and Khlebovich, V. **Distribution of  $^{239,240}\text{Pu}$  and  $^{238}\text{Pu}$  concentrations in sediments from the Ob and Yenisey Rivers and the Kara Sea.** Appl. Rad. Isot. 46(11):1109-1119, 1995.
15. Stradling, G. N. **Decorporation of actinides: a review of recent research.** Journal of alloys and compounds, (271-273):772-777, 1998.
16. Domingo, J. L. **Developmental toxicity of metal chelating agents.** Reproductive toxicology, 12(5):499-510, 1998.
17. Boocock, G. and Popplewell, D.S. **Distribution of plutonium in human blood serum proteins.** Nature, 208:282-283.
18. Boocock, G., Danpure, C.J., Popplewell, D.S. and Taylor, D.M. **The subcellular distribution of plutonium in rat liver.** Radiat. Res. 42:381-396, 1970.
19. Paquet, F., Ramounet, B., Métivier, H. and Taylor, D. M. **The bioinorganic chemistry of Np, Pu and Am in mammalian liver.** Journal of alloys and compounds, 271-273:85-88, 1998.
20. Taylor, D. M. **The bioinorganic chemistry of actinides in blood.** Journal of alloys and compounds, 271-273:6-10,1998.
21. Chipperfield, A.R. and Taylor, D.M. **Binding of plutonium and americium to bone glycoproteins.** Nature, 219:609-610, 1968.
22. Chipperfield, A.R. and Taylor, D.M. **The binding of plutonium and americium to bone glycoproteins.** Eur. J. Biochem. 17:581-585, 1970.
23. Chipperfield, A.R. and Taylor, D.M. **The binding of thorium(IV), plutonium(IV), americium(IV) and curium(IV) to the constituents of bovine cortical bone *in vitro*.** Radiat. Res. 51:15-30, 1972.
24. Turner, G.A. and Taylor, D.M. **The transport of plutonium, americium and curium in the blood rats.** Phys. Med. Biol. 13:535-546, 1968.
25. Stannard, J.N. **Biomedical aspects of plutonium.** In Uranium, Plutonium, Transplutonic elements H. C. Hodge, J. N. Stannard, J. B. Hirsch (Eds), Springer – Verlag, Heidelberg, 309-322, 1973.
26. International Commission on Radiological Protection. **1990 Recommendations of the International Commission on Radiological Protection.** ICRP Publication 60. Pergamon Press, Oxford; Ann. ICRP 21(1-3), 1990.
27. Thompson, R.C. (Ed) **Proceedings of the Hanford Symposium on the Biological implications of Transuranic Elements.** Richland, Washington, Health Phys. 8 (6):561-780, 1962.
28. Bair, W.J. **Toxicity of plutonium.** In Advances in Radiation Biology, 4:255-425, J.T. Lett, H. Adler and M. Zelle Editors, New York, 1974.

29. Nenot, J.-C. and Stather, J. W. **The toxicity of plutonium, americium and curium.** Report prepared for the European Communities Commission, Pergamon Press, Oxford, 1979.
30. United Nations Scientific Committee on the Effects of Atomic Radiation (UNSCEAR), **Genetic and somatic effects of ionizing radiation.** Report to the General Assembly, United Nations, New York, 1986.
31. United Nations Scientific Committee on the Effects of Atomic Radiation (UNSCEAR), **Sources and effects of ionizing radiation.** Report to the General Assembly, United Nations, New York, 1994.
32. Clarke, R.H., Dunster, J., Nenot, J.-C., Smith, H. and Voelz, G.L. **The environmental safety and health implications of plutonium.** *J. Radiol. Prot.*, 16(2): 91-105, 1996.
33. Humphreys, E.R., Loutit, J.F. and Stones, V.A. **The induction by <sup>239</sup>Pu of myeloid leukaemia and osteosarcoma in female CBA mice.** *Int. J. Radiat. Biol.* 51(2):331-339, 1987.
34. Wilkinson, G.S., Tietjen, G.L., Wiggs, L.D., Galke, W.A., Acquavella, J.F., Reyes M., Yoelz, G.L. and Waxweiler, R.J. **Mortality among plutonium and other radiation workers at a plutonium weapons facility.** *Am. J. Epidemiol.* 125(2):231-250, 1987.
35. Wiggs, L.D., Johnson, E.R., Cox-DeVore, C.A. and Voelz, G.L. **Mortality through 1990 among white males workers at the Los Alamos National Laboratory: considering exposures to plutonium and external ionizing radiation.** *Health Phys.* 67(6):577-588, 1994.
36. Voelz, G.L. and Lawrence, J.N.P. **A 42-year medical follow-up of Manhattan Project plutonium workers.** *Health Phys.* 61(2):181-190, 1991.
37. Hohryakov, V.F. and Romanov, S.A. **Lung cancer in radiochemical industry workers.** *Sci. Total Environ.* 142:25-28, 1994.
38. Claycamp, H.G., Okladnikova, N.D., Azivova, T.V., Belyaeva, Z.D., Boecker, B.B., Pesternikova, V.S., Scott, B.R., Shekhter-Levin, S., Sumina, M.V., Sussman, N.B., Teplyakov, I.I. and Wald, N. **Deterministic effects from occupational radiation exposures in a cohort of Mayak PA workers: data base description.** *Health Phys.* 79(1):48-54, 2000.
39. Okladnikova, N.D., Pesternikova, V.S., Sumina, M.V. and Doschenko, V.N. **Occupational diseases from radiation exposure at the first nuclear power plant in USSR.** *Sci. Total Environ.* 142:9-17, 1994.
40. Nuclear Energy Agency (NEA), **The environmental and biological behaviour of plutonium and some other transuranium elements.** Report by a NEA Group of experts. Nuclear Energy Agency, OECD, Paris, 1981.
41. Singh, N. P. **Thorium, uranium and plutonium in human tissues of world-wide general population.** *J. Radioanal. Nuc. Chem.*, 138(2):347-364, 1990.

42. Mayall, A., Thomas, S., and Cooper, J. **Radioactive effluents from nuclear power stations and nuclear fuel reprocessing plants in the European community. 1977-1986. Part 2 Radiological Aspects.** EUR15928EN, European Commission, Bruxelles, 1994.
43. Hohryakov, V.F., Syslova, C.G. and Skryabin, A.M. **Plutonium and the risk of cancer. A comparative analysis of Pu-body burdens due to releases from nuclear plants (Chelyabinsk-65, Gomel area) and global fallout.** Sci. Total Environ. 142:101-104, 1994.
44. Kossenko, M.M., Hoffman, D.A., and Thomas, T.L. **Stochastic effects of environmental radiation exposure in populations living near the Mayak industrial association: preliminary report on study of cancer morbidity.** Health Phys. 79(1):55-62, 2000.
45. Schneider, M. and Coeytaux, X. **L'industrie du plutonium: de l'effriment d'un mythe à l'urgence d'une reconversion.** In Controle – La Revue de l'Autorité de Sûreté Nucléaire, 138:94-98, 2001.
46. Oi, N. **Plutonium challenges: changing dimension of global cooperation.** IAEA Bulletin, International Atomic Energy Agency, Vienna, 40(1):12-16, 1998.
47. Murray, R.L. **Nuclear Energy: an introduction to the concepts, systems and applications of nuclear process.** Fourth Edition, Pergamon Press, Oxford, 1993.
48. Albright, D., Berkhout, F. and Walker, W. **World inventory of plutonium and highly enriched uranium - 1992.** Stockholm International Peace Research Institute (SIPRI), Oxford University Press, Oxford, 1993.
49. Pelliccioni, M. **Fondamenti fisici della radioprotezione.** Pitagora Editrice, Bologna, 1989.
50. Melandri, C. **Fondamenti di dosimetria interna.** ENEA, Roma, 1992.
51. Le Guen, B. **Intakes routes and biological bases.** In the Proceedings of Assessments of doses from occupational intakes of radionuclides, 6 – 10 October 1997, Mol, Belgium, 1997.
52. International Commission on Radiological Protection. **Individual monitoring for internal exposure of workers: replacement of ICRP 54.** ICRP Publication 78. Pergamon Press, Oxford; Ann. ICRP 27(3-4); 1998.
53. Hinds, W.C. **Aerosol Technology – Properties, behaviour and measurement of airborne particles.** Ed. John Wiley & Sons, New York, 1982.
54. International Commission on Radiological Protection. **Radiation dose to patients from radiopharmaceuticals.** ICRP Publication 80. Pergamon Press, Oxford; Ann. ICRP 28(3); 1998.

55. International Atomic Energy Agency (IAEA). **Assessment of occupational exposure due to intakes of radionuclides**. Safety Standard Series, No. RS-G-1.2, IAEA, Vienna, 1999.
56. Jacquez, J.A. **Compartmental analysis in biology and medicine**. Elsevier Publishing Company, Amsterdam, 1972.
57. International Commission on Radiological Protection. **Human respiratory tract model for radiological protection**. Oxford: Pergamon Press; ICRP Publication 66, 24(1-3), 1994.
58. International Commission on Radiological Protection. **Limits for intakes of radionuclides by workers**. Oxford: Pergamon Press; ICRP Publication 30, 2(3/4) 1979.
59. Piechowski, J., Cavadore, D., Tourte, J., Cauquil, M.H., Raynaud, P., Harduin, J.C. and Chaptinel, Y. **Model and practical information concerning the radiotoxicological assessment of a wound contaminated by Plutonium**. Rad. Prot. Dosim. 26(1/4):265-270, 1989.
60. Piechowski, J. **Wound models and effects of therapy**. In the Proceedings of Assessments of doses from occupational intakes of radionuclides, 6 – 10 October 1997, Mol, Belgium, 1997.
61. Culot, J.-P. **In vivo techniques for monitoring radionuclides**. In the Proceedings of Assessments of doses from occupational intakes of radionuclides, 6 – 10 October 1997, Mol, Belgium, 1997
62. International Commission on Radiological Protection. **General principles for the radiation protection of workers**. ICRP Publication 75. Pergamon Press, Oxford; Ann. ICRP 27(1); 1997.
63. International Atomic Energy Agency (IAEA). **Direct methods for measuring radionuclides in the human body**. Safety Series No. 114, IAEA, Vienna, 1996.
64. Vickers, L.R. **The gender-specific chest wall thickness prediction equations for routine measurements of <sup>239</sup>Pu and <sup>241</sup>Am within the lung using HPGe detectors**. Health Phys. 70(3):346-357, 1996.
65. Sumerling, T.J. and Quant, S.P. **Measurements of the human anterior chest wall by ultrasound and estimates of chest wall thickness for use in determination of transuranic nuclides in the lung**. Rad. Prot. Dosim. 3(4):203-210, 1982.
66. Krutchen, D.A. and Anderson, A.L. **Improved ultrasonic measurement techniques applied to assay of Pu and other transuranics in lung**. Health Phys. 59(1):117-123, 1990.
67. Toohey, R.T., Palmer, E., Anderson, L., Berger, C., Cohen, N., Eisele, G., Wachholz, B. and Burr, W. Jr. **Current status of whole-body counting as a means to detect and quantify previous exposures to radioactive materials**. Health Phys. 60, Sup. 1:7-42, 1991.

68. **Council Directive 96/29/Euratom of 13 May 1996 laying down basic safety standards for the protection of the health of workers and the general public against the dangers arising from ionizing radiation.** Official Journal of the European Communities, Vol. 39, 29 June 1996.
69. Hurtgen, C. **Bioassay techniques for the analysis of excreta.** In the Proceedings of Assessments of doses from occupational intakes of radionuclides, 6 – 10 October 1997, Mol, Belgium, 1997
70. Boecker, B., Hall, R., Inn, K., Lawrence, J., Ziemer, P., Eisele, G., Wachholz, B. and Burr, W. **Current status of bioassay procedures to detect and quantify previous exposure to radioactive material.** Health. Phys. 60, Suppl. 1: 45-100, 1991.
71. Moorthy, A. R., Schopfer, C. J. and Bannerjee, S. **Plutonium from atmospheric weapons testing: fission track analysis of urine samples.** Anal. Chem. 60:857-860, 1988.
72. Wrenn, M. E., Singh, N. P. and Xue, Y. H. **Urinary excretion of <sup>239</sup>Pu by the general population: measurement techniques and results.** Rad. Prot. Dosim. 53(1-4):81-84, 1994.
73. Wyse, E.T. and Fisher, D. R. **Radionuclide bioassay by inductively coupled plasma mass spectrometry (ICP-MS).** Rad. Prot. Dosim. 55(3):199-206, 1994.
74. International Commission on Radiological Protection. **Age-dependent doses to members of the public from intake of radionuclides: Part 2 Ingestion dose coefficients.** ICRP Publication 67. Pergamon Press, Oxford; Ann. ICRP 23(3/4); 1993.
75. International Commission on Radiological Protection. **Age-dependent doses to members of the public from intake of radionuclides: Part 1.** ICRP Publication 56. Pergamon Press, Oxford; Ann. ICRP 20(2); 1989.
76. Leggett, R.W. **A retention-excretion model for americium in humans.** Health Phys. 62:288-310; 1992.
77. Leggett, R.W., Bouville, A. and Eckermann, K.F. **Reliability of the ICRP's systemic biokinetic models.** Radiat. Prot. Dosim. 79(1-4):335-342.
78. Taylor, D.M., Lehman, F., Planas-Bohne, F. and Seidel, F. **The metabolism of radiohafnium in rats and hamsters: a possible analog of plutonium for metabolic studies.** Radiat. Res. 95:339-358, 1983.
79. Popplewell, D.S. **Biokinetics and absorption of actinides in human volunteers: A review.** Appl. Radiat. Isot. 46(5):279-286, 1995.
80. Langham, W.R., Bassett, S.H., Harris, P.S. and Carter, R.E. **Distribution and excretion of plutonium administered intravenously to man.** Los Alamos Scientific Laboratory; LASL Report LA-1151; 20 September 1950. Reprinted in Health Phys. 38(June):1031-1060, 1980.



81. Crowley, J., Lanz, H., Scott, K. and Hamilton, J.H. **A comparison of the metabolism of plutonium (<sup>238</sup>Pu) in man and the rat.** Argonne National Laboratory, Argonne, Illinois, Report CH-3589, 1946.
82. Russell, E. R. and Nickson, J. J. **The distribution and excretion of plutonium in two human subjects.** Argonne National Laboratory, Argonne, Illinois, Report CH-3607, 1946.
83. Nickson, J.J. and Rose, J. E. **Report for month of January 1946.** Medical Industrial Hazards Section, Metallurgical Laboratory, University of Chicago, Report MUC-HG-1187, 1946.
84. Nickson, J.J. and Rose, J. E. **Report for month of February 1946.** Medical Industrial Hazards Section, Metallurgical Laboratory, University of Chicago, Report MUC-HG-1184, 1946.
85. Nickson, J.J. and Rose, J. E. **Report for month of March & April 1946.** Medical Industrial Hazards Section, Metallurgical Laboratory, University of Chicago, Report MUC-HG-1203, 1946.
86. Russell, E. R. **Report for month of May 1946.** Biochemical Survey Section, Metallurgical Laboratory, University of Chicago, Report MUC-ERR-206, 1946.
87. Russell, E. R. **Report for month of June 1946.** Biochemical Survey Section, Metallurgical Laboratory, University of Chicago, Report MUC-ERR-211, 1946.
88. Rundo, J., Starzyk, P.M. and Sedlet, J. **The excretion rate and retention of plutonium 10,000 days after acquisition.** In the Proceedings of IAEA International seminar on diagnosis and treatment of incorporated radionuclides, 8 December 1975, Vienna, International Atomic Energy Agency (IAEA), 15-22, 1976.
89. Rundo, J., Starzyk, P.M., Sedlet, J., Larsen, R.P., Oldham, R.D. and Robinson, J.J. **Plutonium in the excreta of three subjects 104 days after injection.** Argonne National Laboratory, Radiological and Environmental Research Division Annual Report, July 1973 – June 1974, Report ANL-75-3, 136-141, 1974.
90. Rundo, J., Larsen, R.P. and Ilcewicz, F.H. **Plutonium in the blood of two subjects 104 days after injection.** Argonne National Laboratory, Radiological and Environmental Research Division Annual Report, July 1974 – June 1975, Report ANL-75-60, 86-88, 1975.
91. Rundo, J., Starzyk, P.M., Larsen, R.P., Oldham, R.D., Sedlet, J. and Robinson, J.J. **The excretion rate and retention of plutonium 104 days after injection.** Argonne National Laboratory, Radiological and Environmental Research Division Annual Report, July 1974 – June 1975, Report ANL-75-60, 89-91, 1975.
92. Rundo, J. and Ilcewicz, F.H. **Plutonium content and excretory plasma clearance of plutonium 104 days after injection.** Argonne National Laboratory, Radiological and Environmental Research Division Annual Report, July 1977 – June 1978, Report ANL-78-65, 142-144, 1978.

93. Moss W.D. and Guatier, M.A. **Additional short-term plutonium urinary excretion data from the 1945-1947 plutonium injection studies.** In Occupational Health and Environment Research 1983: Health, Safety and Environment Division, Compiler G.L. Voelz, Los Alamos National Laboratory, Report LA-10365-PR, 29-34, 1985.
94. Tancock, N. P. and Taylor, N. A. **Plutonium excretion data from 1945-1947 human injection study: correction fro recovery losses and derivation of rate constant for long-term elimination.** Rad. Prot. Dosim. 46(4):241-246, 1993.
95. Lloyd, R.D., Atherton, D. R., McFarland, S. S., Mays, C. W., Stevens, W., Williams, J: L. and Taylor, G. N. **Studies of injected  $^{237}\text{Pu}(\text{IV})$  citrate in beagles.** Health Phys. 30(January):47-52, 1976.
96. Talbot, R. J., Knight, D. A. and Morgan, A. **Biokinetics of  $^{237}\text{Pu}$  citrate and nitrate in rat: implications for Pu studies in man.** Health Phys. 59(2):183-187, 1990.
97. International Commission on Radiological Protection. **Dose Coefficients for intakes of radionuclides by workers – Replacement of ICRP Publication 61.** Oxford: Pergamon Press; ICRP Publication 68, Ann. ICRP 24(4); 1995.
98. Talbot, R. J., Newton, D. and Warner, A. J. **Metabolism of injected plutonium in two healthy men.** Health Phys. 65(1):41-46, 1993.
99. Talbot, R. J. and Newton, D. **Blood retention and renal clearance of  $^{237}\text{Pu}$  in man.** In the Proceedings of The International Seminar on health effects of internally deposited radionuclides, Heidelberg, Germany, 18-21 April, 1994.
100. Talbot, R. J., Newton, D. and Dmitriev S. N. **Sex-related differences in the human metabolism of plutonium.** Rad. Prot. Dosim. 71(2):107-121, 1997.
101. Taylor, D. M. **Gender-specific differences in the biokinetics of plutonium and other actinides.** Rad. Prot. Dosim. 79(1-4):359-362, 1998.
102. Newton, D., Talbot, R. J., Kang, C. and Warner, A. J. **Uptake of plutonium by the human liver.** Rad. Prot. Dosim. 80(4):385-395, 1998.
103. Warner, A. J., Talbot, R. J. And Newton, D. **Deposition of plutonium in human testes.** Rad. Prot. Dosim. 55(1):61-63, 1994.
104. Beach, S. A. and Dolphin, G. W. **Determination of plutonium body burdens from measurements of daily urine excretion.** In Assessment of radioactivity in man, Vienna, Internatinal Atomic Energy Agency, Vol. II: 603-615, 1964.
105. Robertson, J. S. and Cohn, S. H. **Evaluation of plutonium exposures in man.** Health Phys. 10(June):373-390,1964.
106. Durbin, P.W. **Plutonium in man: a new look at the old data.** In Radiobiology of Plutonium, edited by B.J. Stover and W.S.S. Jee, J W Press; 469-530, Salt Lake City, 1972.

107. Hempelmann, L.H., Langham, W.H., Richmond, C.R. and Voelz, G.L. **Manhattan project Plutonium workers: a twenty-seven year follow-up of selected cases.** Health Phys. 25(November):461-479; 1973.
108. Voelz, G.L., Hempelmann, L.H., Lawrence, J.N.P. and Moss, W.D. **A thirtytwo year medical follow-up of Manhattan project Plutonium workers.** Health Phys. 37(October):445-485, 1979.
109. Parkinson, W. Jr. and Henley, L. C. **A proposed long-term excretion equation for Plutonium.** Health Phys. 40(March):327-331, 1981.
110. International Commission on Radiological Protection. **The metabolism of compounds of Plutonium and other actinides.** Oxford: Pergamon Press; ICRP Publication 19; 1972.
111. Jones, S.R. **Derivation and validation of a urinary excretion function for Plutonium applicable over tens of years post uptake.** Radiat. Prot. Dos. 11(1):19-27; 1985.
112. Leggett, R. W. and Eckerman, K. F. **A method for estimating the systemic burden of Pu from urinalyses.** Health Phys. 52(3):337-346, 1987.
113. Tancock, N. P. and Taylor, N. A. **Derivation of a new expression to describe the urinary excretion of plutonium by man.** Rad. Prot. Dosim. 46(4):229-239, 1993.
114. Khokhryakhov, V.F., Menshikh, Z.S., Suslova, K.G., Kudryavtseva, Z.B., Tokarskaya, Z.B. and Romanov, S.A. **Plutonium excretion model for the healthy man.** Radiat. Prot. Dos. 53(1-4): 235-239; 1994.
115. Leggett, R.W. **A model of the retention, translocation and excretion of systemic Pu.** Health Phys. 49(6):1115-11137; 1985.
116. Sun, C. and Lee, D. **Plutonium fecal and urinary excretion functions: derivation from a systemic whole-body retention function.** Health Phys. 76(6):619-627, 1999.
117. Voelz, G.L., Grier, R.S. and Hempelmann, L.H. **A 37-year medical follow-up of Manhattan project Pu workers.** Health Phys. Vol. 48(3): 249-259, 1985.
118. Voelz, G.L. and L.H., Lawrence. **A 42-year medical follow-up of Manhattan project plutonium workers.** Health Phys. Vol. 61(2): 181-190, 1991.
119. Voelz, G.L., Lawrence, L.H., and Johnson, E. R. **Fifty years of plutonium exposure to Manhattan Project plutonium workers: an update.** Health Phys. Vol. 73(4): 611-619, 1997.
120. Voelz, G.L. **Private communication.** Los Alamos National Laboratory, Los Alamos, NM, USA, 1998.
121. United States Transuranium and Uranium Registries. **Annual Report of the United States Transuranium and Uranium Registries.** April 1992 - September 1993, 1993.

122. Dilger, H. **Private Communication**. Forschungszentrum Karlsruhe, Karlsruhe, Germany, 1998.
123. International Atomic Energy Agency (IAEA). **Intercomparison and biokinetic model validation of radionuclide intake assessment**. Report of a co-ordinated project 1996-1998, IAEA-TECDOC-1071, Vienna, 1999.
124. Dörfel, H., Andrasi, A., Bailey, M.R., Birchall, A., Castellani, C.-M., Hurtgen, C., Jarvis, N., Johansson, L., LeGuen, B. and Tarroni, G. **Third European intercomparison exercise on internal dose assessment**. Forschungszentrum Karlsruhe, Wissenschaftliche Berichte, FZKA 6457, Karlsruhe, 2000.
125. Wernli, C. **Private Communication**. Paul Scherrer Institut, Villigen, Switzerland, 1995.
126. Doerfel, H. **Private Communication**. Forschungszentrum Karlsruhe, Karlsruhe, 1998.
127. Melandri, C. **Metodi diretti per la determinazione della contaminazione interna**. Rapporto Tecnico ENEA, RT/PAS/85/14, ENEA, Roma, 1985.
128. Knoll, G. F. **Radiation detection and measurement**. John Wiley & Sons, Inc. (Eds), New York, 1979.
129. Tsoufanidis, N. **Measurement and detection of radiation**. Hemisphere Publishing Corporation (Eds), New York, 1983.
130. Marinelli, L.D. **The use of NaI(Tl) crystal spectrometers in the study of g-ray activity in vivo**. Brit. Journal Radiol. Supp. 7:38-43, 1957.
131. International Commission on Radiation Units and Measurements. **Phantoms and computational models in therapy, diagnosis and protection**. ICRU, Report 48, ICRU Publications, Bethesda, USA, 1992.
132. Deutsches Institut für Normung. **Nachweisgrenze und Erkennungsgrenze bei Kernstrahlungsmessungen**. DIN 25 482, Teil 2, September 1992.
133. Currie, L.A. **Limits for qualitative detection and quantitative determination – Application to Radiochemistry**. Anal. Chem. 40(3):586-593, 1968.
134. International Standard Organization. **Determination of the lower limits of detection and decision for ionising radiation measurements**. Part 1, 2, 3. ISO/11929, Geneva, 1994.
135. Michel, R., Mende, O. and Kirchoff, K. **On the determination of decision thresholds, detection limits and confidence intervals in nuclear radiation measurements**. Kerntechnik, 62(2-3):104-108, Carl Hanser Verlag, München, 1997.
136. Doerfel, H. **Private Communication**. Forschungszentrum Karlsruhe, Karlsruhe, 1998.

137. Breitestein, B.D., Newton, C.E., Norris, H.T., Heid, K.R., Robinson, B., Palmer, H.E., Rieksts, G.A., Spitz, H.B., McInroy, J.F., Boyd, H.A., Eutsler, B.C., Romero, D., Durbin, P.W. and Schmidt, C.T. **The U.S. Transuranium Registry report on the <sup>241</sup>Am content of a whole body**. Health Phys. 49(4): 559-661, 1985.
138. **EMCA Plus – MCA Emulation Software. Instruction Manual**. Silena – Società per l'Electronica Avanzata, Milano, 1993.
139. Draper, N.R. and Smith, H. **Applied Regression Analysis**. John Wiley & Sons, Inc. New York, 1966.
140. Dean, P.N. **Estimation of the chest wall thickness in lung counting for Plutonium**. Health Phys. 24(4): 439-441, 1973.
141. Garg, S.P. **Ultrasonic measurements of the chest wall thickness**. Health Phys. 32(1): 34-39, 1977.
142. Fry, F.A. and Sumerling, T. **Measurement of the chest wall thickness for assessment of Plutonium in human lungs**. Health Phys. 39(7):89-92, 1980.
143. Anderson, A.L. **Personal Communication**, Lawrence Livermore National laboratory, Livermore, CA, USA. Quoted in Berger, C.D. and Lane, B.H. **Biometric estimation of chest wall thickness of females**. Health Phys. 49(3):419-424, 1985.
144. **Sample Preparation for Alpha Spectroscopy**. Technical Brief in Canberra – Product Catalog & Reference Guide, Edition Eleven. Canberra Industries, Meriden Connecticut, USA, 1998.
145. Caldini, M. and Valenza, T. **Analitica Strumentale**. In Diagnostica e tecniche di laboratorio Vol. 1, Chimica Clinica, Parte Prima. Filippo Pasquinelli (Editor), Rosini editrice S.r.L., Firenze, 1990.
146. **PIPS Detectors**. In Canberra – Product Catalog & Reference Guide, Edition Eleven. Canberra Industries, Meriden Connecticut, USA, 1998.
147. Sill, C.W. and Olsen, D.G., **Sources and prevention of recoil contamination of solid-state detectors**. Analytical Chemistry, 42:1596-1607, 1970.
148. **A Practical Guide To Successful Alpha Spectroscopy**. Application Note in Canberra – Product Catalog & Reference Guide, Edition Eleven. Canberra Industries, Meriden Connecticut, USA, 1998.
149. **Maintaining Low Detector Backgrounds in Alpha Spectrometry**. Technical Brief in Canberra – Product Catalog & Reference Guide, Edition Eleven. Canberra Industries, Meriden Connecticut, USA, 1998.
150. Bundesministerium für Umwelt, Naturschutz und Reaktorsicherheit. **Richtlinie über Anforderungen an Inkorporationmeßstellen vom 4/9/1996**. GMBI Nr. 46, 1996.
151. Stuhlfauth, H. **Private Communication**. Forschungszentrum Karlsruhe, Karlsruhe, 2000.

152. Stephen Wolfram, **The Mathematica Book**. Fourth Edition. Wolfram Media/Cambridge University Press, 1999.
153. Beach, S.A., Dolphin, G.W., Duncan, K.P. and Dunster, H.J. **A basis for routine urine sampling of workers exposed to Plutonium 239**. Health Phys. 12(July):1671-1682; 1966.
154. Luciani, A. and Polig E. **Verification and modification of the ICRP67 model for plutonium dose calculation**. Health Phys. 78(3):303-310; 2000.
155. International Commission on Radiological Protection. **Basic anatomical and physiological data for use in Radiological Protection: The Skeleton**. ICRP Publication 70. Pergamon Press, Oxford; Ann. ICRP 25(2); 1995.
156. Luciani, A. **Ein optimiertes biokinmetisches Modell für Plutonium**. Forschungszentrum Karlsruhe, Jahresbericht 1998 der Haptabteilung Sicherheit, FZKA 6230; 1999.
157. Polig, E. **Labels of surface-seeking radionuclides in the human skeleton**. Health Phys. 72(1): 19-33; 1997.
158. Thomas, R.G., Healy, J.W. and McInroy, J.F. **Plutonium partitioning among internal organs**. Health Phys. 46(April):839-844; 1984.
159. Kathren, R.L. McInroy, J.F., Reichert, M.M. and Swint, M.J. **Partitioning of Pu238, Pu239 and Am241 in skeleton and liver of U.S. Transuranium Registry autopsy cases**. Health Phys. 54(February):181-188, 1988.
160. McInroy, J.F., Kathren, R.L. and Swint, M.J. **Distribution of Plutonium and Americium in whole bodies donated to the United States Transuranium Registry**. Radiat. Prot. Dos. 26(1/4):151-158; 1989.
161. Popplewell, D.S. and Ham, G.J. **Distribution of Plutonium and Americium in tissues from a human autopsy case**. J. Radiol. Pro. 9(3):159-164, 1989.
162. International Commission on Radiological Protection. **Annual limits of intake of radionuclides by workers based on the 1990 Recommendations**. ICRP Publication 61. Pergamon Press, Oxford; Ann. ICRP 21(4); 1991.
163. Luciani, A. **Plutonium dose assessments based on a new model derived from ICRP 67**. Health Phys. 80(6):618-619; 2001.
164. Luciani, A., Doerfel, H. and Polig, E. **Sensitivity analysis of the urinary excretion of Plutonium**. Radiat. Prot. Dosim. 93(2):179-183; 2001.
165. Hamby, D.M. **A comparison of sensitivity analysis techniques**. Health Phys. 68(2):195-204; 1995.
166. Khursheed, A. and Fell, T.P. **Sensitivity analysis for the ICRP Publication 67 biokinetic model for Plutonium**. Radiat. Prot. Dos. 74(1/2):63-73; 1997.

167. Harrison, J.D., Khursheed, A., Phipps, A.W., Goosses, L., Kraan, B. and Harper, F. **Uncertainties in biokinetic parameters and dose coefficients determined by expert judgement.** Radiat. Prot. Dosim. 79(1-4):355-358; 1998.
168. McKay, M.D., Conover, W.J. and Beckman, R.J. **A comparison of the three methods for selecting values of input variables in the analysis of output from a computer code.** Technometrics, 21:239-245; 1979.
169. Helton, J.C. **Uncertainty and sensitivity analysis techniques for use in performance assessment for radioactive waste disposal.** Reliability Engineering and System Safety, 42:327-367; 1993.
170. Khatib-Rahbar, M., Cazzoli, E., Lee, M., Nourbakhsh, H., Davis, R. and Schmidt, E. **A probabilistic approach to quantifying uncertainties in the progression of severe accidents.** Nuclear Science and Engineering, 102:219-259; 1989.
171. Iman, R. and Helton, J. **A comparison of uncertainty and sensitivity analysis techniques for computer codes.** NUREG/CR-3904, United States Nuclear Regulatory Commission; 1985.
172. Armitage, P. and Berry, G. **Statistical methods in medical research. Second Edition.** Blackwell Scientific Publications, Oxford, 1987.
173. International Commission on Radiological Protection. **Age-dependent doses to members of the Public from intake of radionuclides: Part 4 Inhalation Dose Coefficients.** Oxford: Pergamon Press; ICRP Publication 71, Ann. ICRP 25(3-4); 1996.
174. Luciani, A., Polig, E., Doerfel, H. **An age-related model derived from ICRP 67 model for Plutonium dose assessments: application to an updated case of contamination.** Oral Presentation at the 8th International Conference on Low level measurements of actinides and long-lived radionuclides in biological and environmental samples, Oarai, Japan, 16-20 October 2000, Proceedings of the Conference, Journal of Radioanalytical and Nuclear Chemistry 252(2):301-307, 2002.
175. National Council on Radiation protection and Measurements. **Evaluating the reliability of biokinetic and dosimetric models and parameters used to assess individual doses for risk assessment purposes.** NCRP Commentary N. 5, NCRP Publications, Bethesda, MD, USA, 1998.
176. Leggett, R.W. **Reliability of the ICRP's dose coefficients for members of the public. 1. Sources of uncertainty in the biokinetic models.** Rad. Prot. Dosim. 95(3):199-213, 2001.





## OWN PUBLICATIONS RELATED TO THE SUBJECT

---

### JOURNALS

- Luciani, A., Polig, E., Doerfel, H. **An age-related model derived from ICRP 67 model for Plutonium dose assessments: application to an updated case of contamination**, Oral Presentation at the **8th International Conference on Low level measurements of actinides and long-lived radionuclides in biological and environmental samples**, Oarai, Japan, 16-20 October 2000, Proceedings of the Conference, Journal of Radioanalytical and Nuclear Chemistry 252(2):301-307, 2002.
- Luciani, A. **Plutonium dose assessments based on a new model derived from ICRP 67**, Health Phys. 80(6):618-619, 2001
- Luciani, A., Doerfel, H., Polig, E. **Sensitivity analysis of the urinary excretion of Plutonium**, Rad. Prot. Dosim. 93(2):179-183, 2001.
- Luciani, A., Polig, E. **Verification and modification of the ICRP-67 model for plutonium dose calculation**, Health Phys. 78(3):303-310, 2000.

### TECHNICAL AND ANNUAL REPORTS

- Luciani, A. and Castellani, C.M. **Biocinetica del Plutonio nell'organismo umano: analisi e modifica del modello ICRP 67**. Rapporto Tecnico ENEA, RT/AMB/PRO/2001/5, ENEA, Roma, 2001.
- Luciani, A. **Dosisabschätzungen mit einem neuen altersabhängigen Modell für Plutonium**, In Jahresbericht 1999 der Hauptabteilung Sicherheit, Forschungszentrum Karlsruhe, Redaktion W. Kölzer, Wissenschaftliche Berichte, FZKA 6430, 2000.
- Luciani, A. **Ein optimiertes biokinetisches Modell für Plutonium**, In Jahresbericht 1998 der Hauptabteilung Sicherheit, Forschungszentrum Karlsruhe, Redaktion W. Kölzer, Wissenschaftliche Berichte, FZKA 6230, 1999.

### WORK IN PROGRESS

- Luciani, A. Doerfel, H. And Polig, E. **Uncertainty analysis of the Plutonium urinary excretion**. Accepted as contribution to the **Workshop on Internal Dosimetry of Radionuclides – Occupational, Public and Medical Exposure**, Oxford, United Kingdom, 9-12 September 2002, Proceedings of the Conference will be published in Radiation Protection Dosimetry.



## ACKNOWLEDGEMENTS

---

Special thanks to Prof. Dr. Olaf Dössel who honoured me to be the main referee of the present work providing important suggestions for a successful execution.

I thank Dr. Hans-Richard Doerfel who offered me the possibility of working on this project and who, as co-referee, always gave me suggestions of great importance for addressing the goals of the work. I likewise thank Dr. Scott Miller who honoured me to be the co-referee and who provided a critical review of the whole work. I am grateful to Dr. Erich Polig for the helpful discussions we had about modelling theory, without which the present work would have not been successfully completed.

I thank Ms. Andrea Zieger and Dr. Heike Stuhlfauth for their support in providing the basic issues relating to the experimental techniques. Many thanks to Dr. Horst Dilger as well who gave me useful information about the available cases of contamination with interesting suggestions.

I'm particularly indebted to Dr. Giuseppe Tarroni who, since my employment at its Institute of ENEA, has always encouraged me with enthusiasm in completing the present work. Special thanks to Dr. Carlo-Maria Castellani who addressed me to internal dosimetry studies since my graduation and who looked over the work with keen comments. Thanks to Dr. Elena Fantuzzi too for her support and friendship.

Finally I would like to remember here all the people that made my staying in Forschungszentrum Karlsruhe a very pleasant period: Mrs. Ilona Hofmann for her help in everyday problems for which she found always, smiling, a solution; Mrs. Gabriele Nagel and Mrs. Karin Burkhard for their patience during our conversations in German.

I would take the chance here to thank all the people that I met in Karlsruhe and particularly Frederic and Nancy for their friendly spontaneity, Patrice for his kind support, Marta and Leena for their invaluable cheerfulness.



Name: Andrea Luciani  
 Date and place of birth: 12/05/1970 Ferrara, Italy  
 Nationality: Italian

## Education

- March 1998**      **Qualified Expert for Ionizing Radiation** (according to the Directive 96/29/EURATOM, Title 1, Art. 1). Certification of Ministry of Labour – Rome.
- 1994-1996**      **Specialization School on Health Physics, with honours – University of Bologna, Italy**  
Dissertation: Atmospheric aerosol in urban area: granulometric analysis for pulmonary deposition assessments.  
 Referee: Prof. Giuseppina Maltoni Giacomelli.
- 1989-1994**      **Graduation in Physics (“Laurea in Fisica”) with honours – University of Bologna, Italy**  
Dissertation: Internal dose assessments with Whole Body Counter: a methodology for hospital work routine.  
 Referee: Prof. Giuseppina Maltoni Giacomelli.

## Experiences

- Since May 2000**      **Researcher at ENEA – Institute for Radiation Protection, Bologna (Italy)**  
Subject: Internal dosimetry, radiation protection.  
Activities: Characterization of the new developed model for plutonium metabolism in humans: dose factors, sensitivity and uncertainty analysis. Implementation of other ICRP models (e.g. for further transuranium elements, radium, etc.) according to the needs of the institute as Italian leading centre for radiation protection problems; courses of internal dosimetry for professionally exposed workers in ENEA; dose evaluations for the Italian military contingent dislocated in Kosovo exposed to the risk of Depleted Uranium intake.
- February 1998 - April 2000**      **Doctorand at Forschungszentrum Karlsruhe – Institut für Strahlenschutz, Karlsruhe (Germany)**  
Subject: Biokinetic modelization, activity measurements.  
Activities: Optimization of ICRP biokinetic models for transuranium to better fit the available data of plutonium activity in urine, faeces and blood. Development of a new model for plutonium biokinetics. Analysis of the measurements of the americium and plutonium activity “*in vivo*” and “*in vitro*”, respectively, carried out for a case of contamination.
- January 1997 - December 1998**      **Fellowship holder at ENEA – Institute for Radiation Protection, Bologna (Italy)**  
Subject: Internals dosimetry, activity measurements  
Activities: Calibration of High-purity Ge detector for “*in vivo*” measurements of low energy photon emitters with the LLNL phantom. Dose assessments for the Italian participation to the IAEA intercomparison “Interpretation of Internal Contamination Monitoring Data”. Assessments of doses to testes after <sup>131</sup>I therapy for ablation of thyroid post surgical remnants in patients with differentiated thyroid cancer.
- December 1994 - November 1995**      **Fellowship holder at ENEA – Institute for Radiation Protection, Bologna (Italy).**  
Subject: Internal and external dosimetry, decontamination actions, physics of aerosols  
Activities: Analysis of radioactive aerosol (<sup>137</sup>Cs) generated during the decontamination works in a goods-station of a city of north Italy. Dose assessments for the workers exposed to the risk of inhalation and external exposition. Characterization of aerosols (number and mass distribution vs. aerodynamic diameter) for pulmonary deposition assessments.
- July 1993 – June 1994**      **Undergraduate apprentice at Maggiore Hospital – Health Physics Section, Bologna (Italy)**  
Subject: Internal dosimetry  
Activities: : Calibration of NaI(Tl) detector for “*in vivo*” measurements of high energy photon emitters. Implementation of a control routine methodology of “*in vivo*” activity measurements and dose assessments for Nuclear Medicine Section workers in the frame of the hospital radiation protection system.

## Main Publications

---

- Luciani, A., Polig, E., Doerfel, H. "An age-related model derived from ICRP 67 model for Plutonium dose assessments: application to an updated case of contamination", Oral Presentation at the "8th International Conference on Low level measurements of actinides and long-lived radionuclides in biological and environmental samples", Oarai, Japan, 16-20 October 2000, Proceedings of the Conference, Journal of Radioanalytical and Nuclear Chemistry 252(2):301-307, 2002.
- Luciani, A. "Plutonium dose assessments based on a new model derived from ICRP 67", Health Phys. 80(6):618-619, 2001
- Luciani, A., Doerfel, H., Polig, E. "Sensitivity analysis of the urinary excretion of Plutonium", Rad. Prot. Dosim. 93(2):179-183, 2001.
- Luciani, A., Polig, E. "Verification and modification of the ICRP-67 model for plutonium dose calculation", Health Phys. 78(3):303-310, 2000.
- Luciani, A. "Dosisabschätzungen mit einem neuen altersabhängigen Modell für Plutonium", In Jahresbericht 1999 der Hauptabteilung Sicherheit, Forschungszentrum Karlsruhe, Redaktion W. Kölzer, Wissenschaftliche Berichte, FZKA 6430, 2000.
- Luciani, A. "Ein optimiertes biokinetisches Modell für Plutonium", In Jahresbericht 1998 der Hauptabteilung Sicherheit, Forschungszentrum Karlsruhe, Redaktion W. Kölzer, Wissenschaftliche Berichte, FZKA 6230, 1999.
- Ceccarelli, C., Battisti, P., Gasperi, M., Fantuzzi, E., Pacini, F., Gualdrini, G.F., Pierantoni, M.C., Luciani, A., Diokich, D., Pinchera, A. "Radiation Dose to the Testes after <sup>131</sup>I Therapy for Ablation of Postsurgical Thyroid Remnants in patients with Differentiated Thyroid Cancer", The Journal of Nuclear Medicine, 40(10):1716-1721, 1999.
- Luciani, A., Castellani, C.M., Olivero, L., Donato, R. "Caratterizzazione Granulometrica e Valutazione di Dose da Inalazione per un Aerosol Contaminato da Cs 137" IV Congresso di protezione radiologica dei paesi Europei del mediterraneo occidentale - Barcellona, Spagna. 27-29 Maggio 1998 Proceedings in "RADIOPROTECCION" (Sociedad Espanola de Proteccion Radiologica. 1998) - Senda Editorial, S.A., Special Issue Maggio 1998, pagg.224-227, 1998.
- Berico, M., Luciani, A., Formignani, M. "Atmospheric aerosol in an urban area: measurements of TSP and PM10 standards and pulmonary deposition assessment", Atmospheric Environment, 31:3659-3665, 1997.